



**Green synthesis, characterisation and application of metal nanoparticles using chemical constituents of selected South African plants**

by

**UMAR BADEGGI, MUHAMMAD**

**Thesis submitted in fulfilment of the requirement for the degree**

**Doctor of Philosophy: Chemistry**

**in the**

**Faculty of Applied Sciences**

**at the Cape Peninsula University of Technology**

**Supervisor: Prof. Ahmed Mohammed**

**Co-Supervisor: Dr. Subelia Botha**

**Bellville (September, 2020)**

**CPUT copyright information**

**The dissertation/thesis may not be published either in part (in scholarly, scientific or technical journals), or as a whole (as a monograph), unless permission has been obtained from the University.**

## DECLARATION

I, Umar Badeggi Muhammad, declare that the contents of this dissertation/thesis represent my own unaided work, and that the dissertation/thesis has not previously been submitted for academic examination towards any qualification. Furthermore, it represents my own opinions and not necessarily those of the Cape Peninsula University of Technology.



25/09/2020

---

Signed

Date

## ABSTRACT

Diabetes mellitus and bacterial infections are among the leading health challenges facing the world. These challenges are not restricted by age or gender as it affects every individual, causing a great deal of burden not only on health but also on the world's economy. Concerted efforts, therefore, have been continuously made to find other alternatives (including the trials of medicinal plants). *Leucosidea sericea* and *Hypoxis hemerocallidea* are probably the most popular medicinal plants used by many ethnic groups in South Africa. These plants have played a significant role in the management of many diseases, including diabetes and bacterial infections. Scientific investigations have confirmed the traditional uses of the plants. In the modern-day nanotechnology advancement, nanoscale materials have continued to gain more attention as "smart" alternatives due to numerous advantages. In the biomedical sector, nanomaterials made from gold and silver have demonstrated interesting abilities in the management of many diseases. However, their methods of synthesis dictate their application. Gold and silver nanoparticles synthesized using the physical and chemical methods suffer several setbacks. These include longer reaction time, use of sophisticated instruments, and harsh chemicals. The toxic chemicals may also cause environmental pollution. Green synthesis is, therefore, a better alternative.

In this study, *Leucosidea sericea* and *Hypoxis hemerocallidea* were exhaustively extracted and partitioned into hexane, dichloromethane, ethyl acetate, methanol and water extracts. Preliminary screening showed that only the ethyl acetate, methanol and aqueous extracts formed gold and silver nanoparticles. Therefore, the ethyl acetate and methanol extracts were chromatographed using both silica gel and Sephadex column chromatography to further purify the extracts. Subsequent use of High-Performance Liquid Chromatography and Liquid Chromatography-Mass spectrometry led to the identification/isolation of the compounds. These techniques were corroborated by nuclear magnetic resonance spectroscopy.

The individual total extracts and fractions/compounds were then used in the green synthesis of gold and silver nanoparticles which were fully characterized using various spectroscopic, optical and microscopic techniques. *In vitro* stability studies were also conducted using various media and buffers. The properties and behaviour of the nanoparticles (between those of the total extract and fractions/compounds) from the above characterization and studies were compared.

Thereafter, their potential biological applications were evaluated. First, the nanoparticles were diluted to various concentrations to confirm that they still retain their characteristic features even at lower concentrations. The *in vitro* antioxidant, antidiabetic and antibacterial activities were then examined at low concentrations.

The antioxidant activities were done using three assays. 2, 2'-Azino-bis (3-ethylbenzo thiazoline-6-sulfonic acid), Ferric Reducing Antioxidant Power and the total phenolic content. The total extract and fractions/compounds were evaluated alongside the nanoparticles for comparison. The results were expressed based on the standard curve of the standard antioxidant compounds employed in the case of each assay. The antidiabetic activity was conducted using alpha-glucosidase and alpha-amylase enzymatic assays. Like the antioxidant studies, a comparison was made between the total extract, fractions/compounds, and the standard antidiabetic drug, acarbose. In the case of antibacterial studies, the aqueous solutions of the total extracts and fractions/compounds did not show activity even at high concentrations (>2000 µg/mL). The nanoparticles displayed activity against six bacterial species, consisting of both Gram-positive and Gram-negative types. The results were compared to those of the standard antibiotics.

Having identified the chemical structure of the compounds (phytochemicals), the study confirmed the involvement of the functional groups in the green synthesis of gold and silver nanoparticles. The fact that individual phytochemical and fractions successfully formed stable nanoparticles also showed their reducing and capping abilities. In addition to the above, the comparison of the nanoparticles with those of the total extracts revealed that procyanidins and hypoxoside were the major compounds contributing to the easy formation of nanoparticles in the respective extracts.

This study has avoided the use of toxic chemicals, external stabilizers, and have resulted in the production of bioactive gold and silver nanoparticles. However, toxicity concerns remained a challenge even in the green synthesis. This should, therefore, be further explored for better applications in the biomedical field.

## ACKNOWLEDGEMENTS

This work would not have seen the light of the day if not for the mentorship of my supervisors Prof. Ahmed Mohammed and Dr. Subelia Botha. A great deal of knowledge and skills have been acquired under your guidance. Your time, commitment and unflinching supports throughout this journey cannot be forgotten. I truly have no right words to use in expressing my sincere gratitude to you two but I am sure that almighty God will reward you immensely. Thank you.

Dr. Abdulrahman Elbagory, you are my small mentor after my supervisors. You introduced me to the green synthesis and did not stop giving me assistance and support. May you go to high places in life.

Dr. Enas Ismail of both CPUT and Al Ahzahr University, Cairo, Egypt has tremendously assisted me in this journey. Your guidance and support is highly appreciated.

Prof J. L. Marnewick, Dr. J. A. Badmus and Mr. Fanie Rautenbasch of Oxidative Stress Research Centre, CPUT. The space and resources at the centre made it easier, thank you. Dr. J. A. Badmus, your time, patience and coaching will be remembered.

Words have sincerely failed me to properly thank Dr. A. B. Mohammed, the current director of academic planning (DAP) of IBB University, Lapai, Nigeria. Your constant checks on both myself and my family back home cannot be undervalued. Your frequent counseling, support, kindness, prayers and encouragement were always timely. May Allah continue to uplift you.

Abdulkadir Mohammed always look after my old parents, even at difficult times. May almighty Allah love you too.

Mrs. Mthembu, Adonis, Jellian, Dawn, Mr. Spies, Dr. Le Roux and all other members of staff of Chemistry CPUT, thank you so much for your care, concern and assistance.

My bosom friends, Dr. M. O. Akhrame, Dr. Toyin Alabi, Dr. Mekin Mohammed, Dr. Kasim Badmus and "Drs to be" Y.O. Ayipo, B. A. Lawal, W.O Afolabi were in constant touch with me. Your advice, support and guidance have not gone in vain. I will continue to appreciate them. Thank you.

My colleagues in the lab Dr. Nino, Abobaker, Akeem, Eloge, Khadidiatou, Aliwa, Bongiwe, Selena, Rondo, Sulafa, and Ali were wonderful. I appreciate our time together.

The UWC, UCT and Dua'a group brothers are equally appreciated. I thank Saba and Muhammad Bello Ladan (MBL) for their company. MBL (soon to be Dr.) is appreciated for many assistances. You have been there for me since the beginning, throughout the times and you are still there, financially, morally and spiritually. May God be sufficient for you.

I would also like to appreciate senior colleagues of the department of Chemistry IBB University, especially Associate Profs: I. I. Lakan, U. U. Elele, Y. B. Paiko, and Drs: Y. Azeh, M. J. Adisa and M. D. Zago. Thank you all for your support and prayers.

Dr. Jimoh Oladejo of FUT, Minna set the ball rolling and made sure all was well. Your time and efforts are highly appreciated. Dr. Isah Lawal (BUK) and Dr. Bashir of FUT, thank you all.

Barr. Babazduru M. Badeggi, you were the brain behind the whole journey. You inspired me all through and I will continue to remember that. May you successfully complete your Ph.D. soon too.

Abubakar Gimba, Abdullahi Usman, Yaba, Alhaji Musa Sharu, Abdullahi Gimba, Musa Umar have always found time to visit my family. I am highly grateful.

My heartfelt appreciation goes to my father, Alhaji Muhammad Kwombo. You sacrificed a lot for me to be where I am today. Thank you for always believing in education even when you did not get the opportunity. Thank you for the support, patience, prayers and love.

To my brothers, Isah and Ahmad and my sisters, I thank you so much for being there for me. I appreciate the support and prayers. Thank you all.

To my wife and special friend Fatima Bintu Umar, I owe you a lot. I want to thank you for holding my hand, for the prayers, for the understanding and for the love and care. I want to specially thank you for taking good care of the kids even at difficult times. I also appreciate the understanding of my little angels (Khadijah, Sayyida and Husna). I love you all.

Finally, I would like to thank Ibrahim Badamasi Babangida University, Lapai, Nigeria for giving me the opportunity, SANZAF and CPUT for financial assistance towards this study.

## **DEDICATION**

To the memory of my late mother, Halima Muhammad

## PREFACE

This thesis is made up of **6 chapters**, written in the article-based format according to the guidelines of the respective journal where the articles were either published or submitted to.

**Chapter one:** Briefly introduces the study by giving relevant information on green nanotechnology, green chemistry, green synthesis of metallic nanoparticles and their advantages over other methods, characterization techniques and applications of gold and silver nanoparticles. The rationale, hypothesis, aims and objectives were also stated in this chapter.

**Chapter two:** Reviews both *Leucosidea sericea* and *Hypoxis hemerocallidea*, including traditional uses, biological properties, and compounds isolated from them. It also dwells into nanotechnology, types of nanoparticles, green synthesis using extracts and the phytochemicals involved. The use of pure phytochemicals as reducing and capping agents as well as their applications was also highlighted. This chapter also detailed biomedical applications of gold and silver nanoparticles and explains the techniques in the characterization of metallic nanoparticles. A review article "**Uni-capped metal nanoparticles: synthesis, mechanism and applications**" is in preparation.

**Chapter three:** Focuses on the green synthesis, characterization, and applications of gold nanoparticles using the chemical constituents of *L. sericea*. It explains the involvement of procyanidins in the green synthesis process and evaluated the antidiabetic and antioxidant properties of the extracts as well as for the nanoparticles. This was published in **biomolecules**.

**Chapter four:** Presents the biosynthesis, characterization and biological applications of procyanidin capped silver nanoparticles. The mechanism of reaction in the formation of the silver nanoparticles was also proposed. The antioxidant, antidiabetic and antibacterial activities were also examined. This was published by the **Journal of Functional biomaterials**.

**Chapter five:** Relates biofabrication, characterization and applications of *Hypoxis hemerocallidea* and hypoxoside mediated silver nanoparticles. The chapter compares the optical, chemical and crystal properties of the two silver nanoparticles. It also examined the involvement of hypoxoside as the main reducing and capping agent responsible for the formation of spherical nanoparticles. The variation of their biological activities was also evaluated. The manuscript has been prepared to be submitted to **nanomaterials**.

**Chapter six:** Is the general discussion of all the findings in summary and conclusions. Brief recommendations for future work was also given.





Article

# Green Synthesis of Gold Nanoparticles Capped with Procyanidins from *Leucosidea sericea* as Potential Antidiabetic and Antioxidant Agents

Umar M. Badeggi <sup>1</sup>, Enas Ismail <sup>1</sup>, Adewale O. Adeloye <sup>1</sup>, Subelia Botha <sup>2</sup>,  
 Jelili A. Badmus <sup>3</sup>, Jeanine L. Marnewick <sup>3</sup>, Christopher N. Cupido <sup>4</sup> and  
 Ahmed A. Hussein <sup>1,\*</sup>

<sup>1</sup> Chemistry Department, Cape Peninsula University of Technology, Symphony Rd., Bellville 7535, South Africa; 217064221@mycput.ac.za (U.M.B.); enas.ismail4@yahoo.com (E.I.); aowale@gmail.com (A.O.A.)

<sup>2</sup> Electron Microscope Unit, University of the Western Cape, Bellville 7535, South Africa; subotha@uwc.ac.za

<sup>3</sup> Oxidative Stress Research Centre, Institute of Biomedical and Microbial Biotechnology, Cape Peninsula University of Technology, Symphony Rd., Bellville 7535, South Africa; jabadmus@lautech.edu.ng (J.A.B.); Marnewickj@cput.ac.za (J.L.M.)

<sup>4</sup> Department of Botany, University of Fort Hare, Private Bag X1314, Alice 5700, South Africa; ccupido@ufh.ac.za

\* Correspondence: mohammedam@cput.ac.za; Tel.: +27-21-959-6193; Fax: +27-21-959-3055







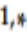
Received: 5 January 2020; Accepted: 2 March 2020; Published: 13 March 2020



**Abstract:** In this study, procyanidins fractions of dimers and trimers (F1–F2) from the *Leucosidea sericea* total extract (LSTE) were investigated for their chemical constituents. The total extract and the procyanidins were employed in the synthesis of gold nanoparticles (Au NPs) and fully characterized. Au NPs of 6, 24 and 21 nm were obtained using LSTE, F1 and F2 respectively. Zeta potential and in vitro stability studies confirmed the stability of the particles. The enzymatic activity of LSTE, F1, F2 and their corresponding Au NPs showed strong inhibitory alpha-amylase activity where F1 Au NPs demonstrated the highest with IC<sub>50</sub> of 1.88 µg/mL. On the other hand, F2 Au NPs displayed

Article

# Biosynthesis, Characterization, and Biological Activities of Procyanidin Capped Silver Nanoparticles

Umar M. Badeggi <sup>1,†</sup>, Jelili A. Badmus <sup>2,‡</sup>, Subelia S. Botha <sup>3</sup>, Enas Ismail <sup>1,§</sup>,  
 Jeanine L. Marnewick <sup>2</sup>, Charlene W. J. Africa <sup>4</sup> and Ahmed A. Hussein <sup>1,\*</sup>

<sup>1</sup> Department of Chemistry, Cape Peninsula University of Technology, Symphony Rd., Bellville 7535, South Africa; 217064221@mycput.ac.za (U.M.B.); enas.ismail4@yahoo.com (E.I.)

<sup>2</sup> Applied Microbial and Health Biotechnology Institute, Cape Peninsula University of Technology, Symphony Rd., Bellville 7535, South Africa; jabadmus@lautech.edu.ng (J.A.B.); marnewickj@cput.ac.za (J.L.M.)

<sup>3</sup> Electron Microscope Unit, University of the Western Cape, Bellville 7535, South Africa; subotha@uwc.ac.za

<sup>4</sup> Department of Medical Biosciences, University of the Western Cape, Bellville 7535, South Africa; cafrica@uwc.ac.za

\* Correspondence: mohammedam@cput.ac.za; Tel.: +27-21-959-6193; Fax: +27-21-959-3055

† Permanent address: Department of Chemistry, Ibrahim Badamasi Babangida University Lapai, PMB 11, Minna 4947, Nigeria.

‡ Permanent address: Department of Biochemistry, Ladoke Akintola University of Technology, Ogbomoso 210214, Nigeria.

§ Permanent address: Physics Department, Faculty of Science (Girls Branch), Al Azhar University, Nasr city, Cairo 11884, Egypt.

Received: 17 July 2020; Accepted: 31 August 2020; Published: 19 September 2020



**Abstract:** In this study, procyanidin dimers and *Leucosidea sericea* total extract (LSTE) were employed in the synthesis of silver nanoparticles (AgNPs) and characterized by ultraviolet-visible (UV-Visible) spectroscopy, high-resolution transmission electron microscopy (HRTEM), selected area electron

## TABLE OF CONTENTS

DECLARATION .....	ii
ABSTRACT.....	iii
ACKNOWLEDGEMENTS .....	v
DEDICATION.....	vii
PREFACE.....	viii
RESEARCH ARTICLE 1 .....	ix
RESEARCH ARTICLE 2.....	x
LIST OF FIGURES .....	xvi
LIST OF TABLES .....	xix
LIST OF SCHEMES.....	xx
LIST OF APPENDECES.....	xxi
GLOSSARY .....	xxii
CHAPTER ONE .....	1
1.1 Introduction .....	1
1.2 <i>Leucosidea sericea</i> and <i>Hypoxis hemerocallidea</i> .....	2
1.3 Green synthesis of gold and silver nanoparticles .....	3
1.4 Characterization of gold and silver nanoparticles .....	4
1.5 Applications of gold and silver nanoparticles .....	5
1.6 Problem statement and rationale .....	6
1.7 Hypothesis .....	7
1.8 Research aim.....	7
1.9 Research objectives.....	7
References .....	9
CHAPTER TWO .....	16
LITERATURE REVIEW .....	16
2.1 Plants and their importance.....	16
2.1.1 Phytochemicals in plant .....	17
2.2 <i>Hypoxis hemerocallidea</i> .....	22
2.2.1 Occurrence and uses .....	22
2.2.2 The chemistry and biology of <i>Hypoxis hemerocallidea</i> and its isolated compounds .....	24
2.3 <i>Leucosidea sericea</i> .....	25
2.3.1 Occurrence and uses .....	25
2.3.2 The chemistry and biology of <i>L. sericea</i> and its isolated compounds .....	27
2.3.3 Identification of other compounds in <i>L. sericea</i> extract based on LC-MS analysis .....	31
2.3.2.1 Procyanidins .....	33

2.4 Characterization of isolated compounds.....	34
2.4.1 Nuclear Magnetic Resonance (NMR) spectroscopy.....	34
2.4.2 Liquid Chromatography-Mass Spectrometry (LC-MS) .....	35
2.5 Nanotechnology.....	36
2.5.1 Classification of nanostructured materials (NSMs) .....	36
2.5.2 Synthesis of metallic nanoparticles .....	43
2.5.2.1 Green synthesis of nanomaterials using plant resources.....	46
2.5.2.1.1 Reducing and stabilising ability of plant extracts and its phytoconstituents” .....	48
2.5.2.1.2 Factors affecting nanoparticle formation and stability using phytochemicals .....	50
2.5.2.1.3 Synthesis of biologically active nanoparticles using isolated phytochemicals.....	57
2.5.3 Physicochemical properties of metallic nanoparticles.....	73
2.5.3.1 Optical properties of gold and silver nanoparticles.....	73
2.5.3.2 Fluorescence quenching properties of gold and silver nanoparticles .....	75
2.5.3.3 Shape and size related activities .....	75
2.5.3.4 Stability studies of gold and silver nanoparticles.....	76
2.6 Characterization of gold and silver nanoparticles .....	80
2.6.1 Ultra-Violet Visible spectroscopy .....	80
2.6.2 X-Ray Diffraction (XRD).....	81
2.6.3 Transmission Electron Microscopy (TEM).....	82
2.6.4 Energy-dispersive X-ray spectroscopy.....	83
2.6.5 Dynamic Light Scattering (DLS).....	84
2.7 Biological applications of gold and silver nanoparticles .....	85
2.7.1 Antioxidants.....	85
2.7.2 Antidiabetic activities .....	88
2.7.3 Antibacterial activities .....	90
2.8 Other potential biomedical applications of gold and silver nanoparticles .....	106
2.8.1 Photodynamic therapy (PDT) .....	106
2.8.2 Photothermal therapy (PTT) .....	106
2.8.3 Drug delivery carriers .....	107
References .....	108
CHAPTER THREE.....	134
Green Synthesis of Gold Nanoparticles Capped with Procyanidins from <i>Leucosidea sericea</i> as Potential Antidiabetic and Antioxidant Agents .....	134
Abstract .....	135
3.1 Introduction.....	135
3.2 Materials and Methods.....	137
3.2.1 Chemicals and materials .....	137

3.2.2 Characterisation .....	138
3.2.2 Extraction and Purification of F1 and F2 from LSTE .....	139
3.2.3. Liquid Chromatography–Mass Spectrometry (LC–MS) Analysis.....	139
3.2.4. Green Synthesis of Gold Nanoparticles .....	140
3.2.5. Stability Study.....	140
3.2.6. Dilution Study .....	140
3.2.7 In-Vitro Methods Employed in Antidiabetic Studies.....	140
3.2.7.1 Alpha-Amylase Inhibitory Activity .....	140
3.2.7.2 Alpha-Glucosidase Inhibitory Activity .....	141
3.2.8. Antioxidant Activity .....	141
3.2.8.1. Ferric Reducing Antioxidant Power (FRAP) Assay .....	141
3.2.8.2. Total Phenolic Content.....	142
2.8.3. 2'-Azino-Bis-3-Ethylbenzotiazolin-6- Sulfonic Acid (ABTS) Assay.....	142
3.3 Results and Discussion.....	142
3.3.1 The <i>L. sericea</i> Constituents and Gold Nanoparticle Formation .....	142
3.3.2. UV-Visible Spectroscopic Analysis .....	148
3.3.3 High-Resolution Transmission Electron Microscopy (HR-TEM) .....	149
3.3.4 X-Ray Diffraction (XRD) Analysis .....	153
3.3.5 Dynamic Light Scattering (DLS) Measurement of AuNPs .....	153
3.3.6 In Vitro Stability Study .....	156
3.3.7 Dilution Study .....	158
3.3.8 In-Vitro Antidiabetic Studies.....	159
3.3.9 Antioxidant Activity/Total Phenolic Content.....	161
3.3.10 Quantification of the Total Phenolic Content in the AuNPs from the FC Assay ....	162
3.3.11 Conclusions.....	163
Author Contributions .....	163
Supplementary Materials .....	164
Funding .....	164
Acknowledgments.....	164
Conflicts of Interest.....	164
References .....	165
CHAPTER FOUR .....	175
Biosynthesis, Characterization, and Biological Activities of Procyanidin Capped Silver Nanoparticles.....	175
Abstract .....	176
4.1 Introduction .....	176
4.2 Materials and Methods.....	178

4.2.1 Materials and chemicals .....	178
4.2.2 Characterisation .....	179
4.2.3 Extraction of phytochemicals and formation of Silver nanoparticles .....	179
4.2.3.1 Extraction and purification of chemical constituents .....	179
4.2.3.2 Biosynthesis of silver nanoparticles.....	179
4.3 Stability Evaluation of AgNPs.....	180
4.4 Dilution study .....	180
4.5 In-vitro Enzymatic assay .....	180
4.5.1 Alpha-amylase inhibitory activity.....	180
4.5.2 Alpha-glucosidase inhibitory activity .....	181
4.6 Antibacterial activity .....	181
4.7 Antioxidant activity .....	181
4.7.1 Ferric Reducing Antioxidant Power (FRAP) assay.....	181
4.7.2 Folin–Ciocalteu (FC) assay .....	182
4.7.3 2,2'-azino-bis-3-ethylbenzotiazolin-6- sulfonic acid (ABTS) assay .....	182
4.8 Statistical analysis.....	182
4.9. Results and discussion .....	182
4.9.1 Identification and mechanism of procyanidin-AgNPs formation.....	182
4.9.2 UV-Visible Analysis .....	185
4.9.3 HRTEM Analysis .....	186
4.9.4 XRD Analysis .....	187
4.9.5 DLS measurement.....	188
4.9.6 In vitro stability study .....	190
4.9.7 Dilution study.....	190
4.9.8 In-vitro Enzyme inhibition.....	191
4.9.9 Antioxidant activity.....	194
4.9.10 The antibacterial assay of AgNPs.....	196
4.10 Conclusions .....	198
Supplementary Materials .....	198
Author Contributions .....	199
Funding .....	199
Acknowledgments.....	199
Conflicts of Interest .....	199
References .....	200
CHAPTER FIVE.....	209
Biofabrication, characterization and applications of <i>Hypoxis hemerocallidea</i> and hypoxoside mediated silver nanoparticles.....	209

Abstract .....	209
5.1 Introduction .....	210
5.2 Materials and Methods.....	212
5.2.1 Materials and chemicals .....	212
5.2.2 Isolation of hypoxoside .....	212
5.2.3 Biofabrication of HHE-AgNPs and HPX-AgNPs.....	213
5.2.4 Characterisation .....	213
5.2.5 In-vitro Enzymatic assay.....	213
5.2.5.1 Alpha-amylase inhibitory activity .....	213
5.2.5.2 Alpha-glucosidase inhibitory activity .....	214
5.2.6 Antioxidant activity.....	214
5.2.6.1 Ferric Reducing Antioxidant Power (FRAP) assay .....	214
5.2.6.2 Total Phenolic Content (TPC) .....	214
5.2.6.3 2,2'-azino-bis-3-ethylbenzotiazolin-6- sulfonic acid (ABTS) assay.....	215
5.2.7 Antimicrobial activity of silver nanoparticles.....	215
5.2.8 Statistical analysis.....	215
5.3 Results and discussion .....	216
5.3.1 Isolation, characterization and properties of hypoxoside.....	216
5.3.2. Biofabrication of HHE-AgNPs and HPX-AgNPs.....	217
5.3.3. Morphology and size of HHE-AgNPs and HPX-AgNPs.....	218
5.3.4. The crystallinity of HHE-AgNPs and HPX-AgNPs.....	220
5.3.5. Dynamic Light Scattering.....	221
5.3.6. Biological activities .....	223
5.3.6.1. Antidiabetic activities of HHE-AgNPs and HPX-AgNPs.....	223
5.3.6.3. Antimicrobial studies of HHE-AgNPs and HPX-AgNPs .....	226
5.4 Conclusions .....	227
Author Contributions .....	228
Funding .....	228
Acknowledgments.....	228
Conflicts of Interest.....	228
References .....	229
CHAPTER SIX.....	236
General discussion .....	236
Conclusion.....	240
Recommendations.....	240
References .....	242

## LIST OF FIGURES

Figure 2. 1: Basic structures of major flavonoids that are found in plants .....	18
Figure 2. 2: Chemical structures of some flavonols, flavones, and isoflavones found in plants .....	19
Figure 2. 3: Examples of flavanols, flavanones and anthocyanidins found in plants .....	21
Figure 2. 4: Chemical structures of some naturally occurring non-flavonoids. ....	21
Figure 2. 5: Map of South Africa showing the Cape Floristic Region. One of the world richest plant kingdoms with certain plant species peculiar to it alone.....	22
Figure 2. 6: The aerial part of <i>Hypoxis Hemerocallidea</i> with the (A) star-like yellow flowers and the (B) underground tuberous corm with root-like attachments .....	23
Figure 2. 7: Structure of (A) $\beta$ -sitosterol, (B) $\beta$ -sitosterol glucoside, (C) Campesterol, and (D) Hypoxoside isolated from <i>Hypoxis Hemerocallidea</i> .....	255
Figure 2. 8: Images of <i>Leucosidea sericea</i> showing (A) whole plant, (B) leaves are alternatively arranged and covered with silver hairs (C) rough dark-brown bark on the surface and reddish inner bark, (D) greenish yellow flowers that brings forth young shoots in spring	26
Figure 2. 9: Newly identified compounds from the LC-MS analysis of <i>L. sericea</i> .....	32
Figure 2. 10: Demonstration of linkages and types of procyanidin molecules. (A) depicts monomeric (-)-epicatechin with labelled carbon 4 and 8 as the sites for linkage, n=1; when n=2, it's a dimer up to -50. (B) is a procyanidin B2 dimer, showing a B-type (4 $\rightarrow$ 8) linkage. (C) shows an example of B-type (4 $\rightarrow$ 6) linkage, specifically a procyanidin B5 dimer. (D) represents an A-type dimer, showing (2 $\rightarrow$ 7, 4 $\rightarrow$ 8) linkages. It is a procyanidin A2 dimer ...	34
Figure 2. 11: Classification of nanostructured materials based on dimensionality .....	38
Figure 2. 12: Structures of C20, C36, C60, C70 and C84 .....	39
Figure 2. 13: Scheme showing hydrophilic fullerene organic derivatives .....	40
Figure 2. 14: Structures of graphene (left), (A) single-walled carbon nanotubes and (B) multi-walled carbon nanotubes .....	41
Figure 2. 15: Functionalization and applications of CNTs .....	42
Figure 2. 16: Scheme representing (A) Solid Lipid Nanoparticle (SLNPs) and (B) Nanostructured lipid carrier (NLC) .....	43
Figure 2. 17: A scheme showing the top-down and bottom-up procedure for synthesis of nanoparticles .....	44
Figure 2. 18: Different top-down and bottom-up synthesis methods of nanoparticles .....	45
Figure 2. 19: A scheme representing the oscillation of the free electrons around a nanoparticle .....	733
Figure 2. 20: UV-Visible spectra and colour variation of gold nanorods with different aspect ratios .....	744
Figure 2. 21: Different shapes and colours of silver NPs .....	766



Figure 3. 1: LC–MS profile of the <i>L. sericea</i> aerial part extract. 1: ferulic acid; 2: quinic acid; 3: luteolin 4: procyanidin dimer; 5: caffeic acid; 6: hyperoside, 7: kaempferol galactoside; 8: quercetin; 9: kaempferol rutinoside; 10: hydroxyferulic acid .....	1433
Figure 3. 2: LC–MS profile of F1. 1: procyanidin dimer (type B); 2: procyanidin trimer (type B); 3: coumaric acid .....	1444
Figure 3. 3: LC–MS profile of F2. 1: procyanidin dimer (type B), 2: procyanidin trimer (type B) .....	1455
Figure 3. 4: Absorption spectra of (a) gold solution, (b) aqueous solution of the <i>Leucosidea sericea</i> total extract (LSTE), aqueous solution of (c) F1 and (d) F2 and the corresponding AuNPs of (e) LSTE, (f) F1 and (g) F2.....	1499
Figure 3. 5: HRTEM images for LSTE, F1 and F2 AuNPs are represented as (a,b,c) and the corresponding particle size distributions as (d,e,f) respectively. The inset in a, b and c, showing the bright rings are the SAED of the respective TEM images .....	15151
Figure 3. 6: EDS spectra of (a) blank, (b) LSTE AuNPs, (c) F1 AuNPs and (d) F2 AuNPs .....	1522
Figure 3. 7: XRD patterns of the (a) LSTE AuNPs, (b) F1 AuNPs and (c) F2 AuNPs .....	1533
Figure 3. 8: Hydrodynamic size of (a) LSTE, (c) F1, (e) F2 and zeta potential of (b) LSTE, (d) F1 and (f) F2 AuNPs measured using Dynamic Light Scattering (DLS).....	1555
Figure 3. 9: Stability of gold nanoparticles at given time intervals.....	<b>Error! Bookmark not defined.8</b>
Figure 3. 10. Surface plasmon resonance wavelength ( $\lambda_{max}$ ) of diluted concentrations of LSTE-, F1- and F2- AuNPs, while (Q) represents a plot of absorbance against various concentrations, showing the linear proportionality of intensity with increasing concentration. R2 = 0.9455 (LSTE AuNPs), R2 = 0.9908 (F1 AuNPs) and R2 = 0.9848 (F2 AuNPs).....	159
Figure 4. 1: Absorption spectra of (A) <i>Leucosidea sericea</i> total extract-, (B) F1-, and (C) F2-mediated silver nanoparticles. The cuvettes labelled A-C (inset) represent the colour of the respective AgNPs while the clear solution (D) shows the colour of 1 mM AgNO <sub>3</sub> solution used for the biosynthesis .....	1855
Figure 4. 2: High-Resolution transmission electron microscopy images for <i>Leucosidea sericea</i> total extract -, F1-, and F2-mediated silver nanoparticles are represented as A, D, G and the corresponding particle size distributions as B, E, H respectively. The corresponding selected area electron diffraction pattern of the respective HRTEM images are represented as C, F, I.....	187
Figure 4. 3: X-ray Diffraction patterns of the silver nanoparticles formed from <i>Leucosidea sericea</i> total extract (A), F1 (B), and F2 (C) showing the crystalline nature of the particles	188
Figure 4. 4: Surface Plasmon Resonance ( $\lambda_{max}$ ) of (A) <i>Leucosidea sericea</i> total extract mediated silver nanoparticles, (B) F1-mediated silver nanoparticles, and (C) F2-mediated	

silver nanoparticles showing the retention of properties by the particles even at low concentrations. ....	191
Figure 4. 5: Antidiabetic activities with regards to alpha-amylase (A) and alpha-glucosidase (B) inhibition by <i>Leucosidea sericea</i> total extract (LSTE), procyanidin fractions (F1 and F2), and their respective silver nanoparticles (LSTE-, F1-, and F2-AgNPs).....	1933
Figure 4. 6: Antioxidant activity in terms of the ABTS (2,2'-azino-bis-3-ethylbenzotiazolin-6-sulfonic acid), FRAP (Ferric Reducing Antioxidant Power), and FC (Folin–Ciocalteu) scavenging activity by <i>L. sericea</i> total extract (LSTE), procyanidin fractions (F1 and F2), and their respective silver nanoparticles (LSTE-, F1- and F2-AgNPs). The antioxidant activities were measured based on the equivalence of standard antioxidants Trolox, vitamin C (ascorbic acid), and gallic acid .....	1955
Figure 5. 1: UV-Vis spectra of (C) HHE-AgNPs and (D) HPX-AgNPs. The insets (i) and (ii) represents the colour of the HHE-AgNPs and HPX-AgNPs respectively. ....	2176
Figure 5. 2: High-Resolution transmission electron microscopy images showing the morphology of (A, C) HHE-AgNPs and (B, D) HPX-AgNPs. The C represents irregular, hexagonal, and rod-like shapes of the HHE-AgNPs .....	21919
Figure 5. 3: Histogram displaying the particle size distribution of (A) HHE-AgNPs and (B) HPX-AgNPs.....	22020
Figure 5. 4: X-Ray Diffraction patterns showing the diffraction peaks of (A) HHE-AgNPs (A) and (B) HPX-AgNPs. C and D shows the selected area electron diffraction of the respective HHE-AgNPs and HPX-AgNPs .....	221
Figure 5. 5: Hydrodynamic size (HDS) and polydispersity index (PDI) showing the population of particles in (A) HHE-AgNPs, and (B) HPX-AgNPs .....	22222
Figure 5. 6: Zeta potential of (A) HHE-AgNPs, and (B) HPX-AgNPs. The zeta potential values indicate the surface of the nanoparticles were covered with negative ions.....	2233

## LIST OF TABLES

Table 2.1: Compounds isolated from <i>L. sericea</i> and their biological activities .....	288
Table 2.2: The 12 principles of green chemistry .....	47
Table 2.3: Recent literature on the green synthesis of silver and gold nanoparticles using plant extracts, depicting the phytochemicals (functional groups) involved .....	56
Table 2.4: The use of single compounds in the green synthesis of MNPs, the size and functional group involved, the reaction time, stability and applications .....	60.60
Table 2.5: Recent literature on the application of silver and gold nanoparticles as antioxidant agents.....	877
Table 2.6: Recent literature on the application of silver and gold nanoparticles as antidiabetic agents.....	899
Table 2.7: Recent literature on the application of silver and gold nanoparticles with antibacterial activities. The size of the nanoparticles, the inhibitory concentration and the bacterial species studied are included.....	922
Table 3.1: Particle size and zeta potential for AuNPs obtained from DLS. ....	1566
Table 3.2: Inhibitory activities of LSTE, F1, F2 and AuNPs on alpha-glucosidase and alpha-amylase. ....	160
Table 3.3: Antioxidant activities of LSTE, F1, F2 and the corresponding AuNPs.....	161
Table 4.1: Particle size and zeta potential for AgNPs obtained from DLS .....	1899
Table 4.2: The enzymatic inhibitory activity, expressed as IC <sub>50</sub> of the <i>L. sericea</i> total extract (LSTE), the intact fractions (F1 and F2), and those of their corresponding silver nanoparticles (LSTE-, F1- and F2-AgNPs) using two assays (µg/mL).....	1944
Table 4.3: The antioxidant activity of the <i>L. sericea</i> total extract (LSTE), the intact fractions (F1 and F2), and those of their corresponding silver nanoparticles (LSTE-, F1- and F2-AgNPs) using three assays (ABTS, FRAP, and FC). The percentage phenolic content (FC) of the silver nanoparticles is also presented in the last column of the table.....	1955
Table 4.4. The minimum inhibitory concentration (MIC, µg/mL) values of the <i>L. sericea</i> total extract (LSTE), the intact fractions (F1 and F2), and their corresponding silver nanoparticles (LSTE-, F1- and F2-AgNPs) using six bacterial species.....	1977
Table 5.1: The IC <sub>50</sub> values of the antidiabetic activities of HHE- AgNPs and HPX-AgNPs in micro gram per litre (µg/mL).....	22424
Table 5.2: The antioxidant activities of HHE-AgNPs and HPX-AgNPs. The three assays compared the antioxidant properties of the two silver nanoparticles.....	22525
Table 5.3: Minimum inhibitory concentration of the antimicrobial activities of AgNPs using six bacterial species. The activity of Ceftazidime as the standard was also included (µg/mL)	2277

## LIST OF SCHEMES

Scheme 2.1: Structure of Hypoxoside (D) and the aglycon, Rooperol (E) after conversion using $\beta$ -glucosidase enzyme.....	25
Scheme 2.2: Schematic diagram showing various components of a typical nuclear magnetic resonance spectrometer .....	35
Scheme 2.3: Schematic representation of a typical Liquid Chromatography-Mass Spectrometry flow chart .....	36
Scheme 2.4: Schematic representation showing beam of light, sample and reference as well as the detector in a modern UV-Visible spectroscopy. ....	811
Scheme 2.5: Schematic representation of a typical powder X-ray diffractometer .....	822
Scheme 2.6. Different components of a typical transmission electron microscopy .....	833
Scheme 2.7: Showing the incidence of beam of electrons on an electron, the subsequent excitation and ejection of inner electron and the replacement of an electron from a higher energy in the vacant hole of the electron.....	844
Scheme 2.8: Showing the zeta potential of colloidal solutions.....	855
Scheme 3.1: The proposed reduction of gold salt and encapsulation of the hybrid gold NPs in the F1 and F2 matrix. In addition to the chelating power of the oxygen atom to the metal surface, the intermolecular hydrogen bonding between procyanidins can also make double and triple capping shells and contributing to the stability of the NPs. The reduction power of the phenolic structures with <i>ortho</i> -OH, can be facilitated by the formation of stable <i>ortho</i> -quinone structure .....	1477
Scheme 4.1: Proposed mechanism of procyanidin-AgNPs formation.....	1834
Scheme 5.1: Structure of Hypoxoside (A) and the aglycon, Rooperol (B) after conversion using $\beta$ -glucosidase enzyme.....	2166

## LIST OF APPENDECES

Appendix A: The proton ( <sup>1</sup> H) Nuclear Magnetic Resonance spectra of Fraction F1 .....	243
Appendix B: The carbon 13 ( <sup>13</sup> C) Nuclear Magnetic Resonance spectra of Fraction F1 .....	244
Appendix C: The carbon 13 (DEPT-135) Nuclear Magnetic Resonance spectra of Fraction F1 .....	245
Appendix D: The proton ( <sup>1</sup> H) Nuclear Magnetic Resonance spectra of Fraction F2 .....	246
Appendix E: The carbon 13 ( <sup>13</sup> C) Nuclear Magnetic Resonance spectra of Fraction F2 .....	247
Appendix F: The carbon 13 (DEPT-135) Nuclear Magnetic Resonance spectra of Fraction F2 .....	248
Appendix G: Other HRTEM images (A-F) of the <i>Leucosidea sericea</i> total extract-mediated gold nanoparticles. The images were taken at various points on the gold coated carbon grid. ....	249
Appendix H: Continued with other HRTEM images (G-J) .....	250
Appendix I: Other HRTEM images (A-F) of the F1-mediated gold nanoparticles. The images were taken at various points on the gold coated carbon grid .....	253
Appendix J: Other HRTEM images (A-F) of the <i>Leucosidea sericea</i> total extract-mediated silver nanoparticles. The images were taken at various points on the silver coated carbon grid indicating agglomerates of the nanoparticles. These were taken alongside the image represented in figure 4.2 A .....	255
Appendix K: Hydrodynamic size of (a) F1, (c) F2-, (e) <i>Leucosidea sericea</i> total extract-mediated silver nanoparticles and zeta potential of (b) F1, (d) F2- and (f) <i>Leucosidea sericea</i> total extract- mediated silver nanoparticles as measured by Dynamic Light Scattering technique .....	256
Appendix L: Stability of <i>Leucosidea sericea</i> total extract-mediated silver nanoparticles for (A1) 0 h, (A2) 24 h, (A3) 48 h, F1- mediated silver nanoparticles for (B1) 0 h, (B2) 24 h and (B3) 48 h and F2- mediated silver nanoparticles for for (C1) 0 h, (C2) 24 h, (C3) 48 h in different solutions and buffers .....	245
Appendix M: HRTEM images used in evaluating the size and shape of HHE-AgNPs. The images were taken at various points of the nanoparticles on the carbon grid .....	245
Appendix N: ADDENDUM .....	246

## GLOSSARY

ABTS	2, 2'-Azino-bis (3-ethylbenzo thiazoline-6-sulfonic acid)
AgNO <sub>3</sub>	Silver nitrate
AgNPs	Silver nanoparticles
AAE/g	Ascorbic acid per gram
AuNPs	Gold nanoparticles
BHI	Brain-Heart infusion
BSA	Bovine serum albumin
CTD	Ceftazidime
<sup>13</sup> C-NMR	Carbon-13 nuclear magnetic resonance
CuSO <sub>4</sub>	Copper sulphate
CNPs	Ceramic nanoparticles
CNTs	Carbon nanotubes
CYS	Cysteine
<sup>1</sup> D-NMR	One-dimensional nuclear magnetic resonance
<sup>2</sup> D-NMR	Two-dimensional nuclear magnetic resonance
DMSO	Dimethyl sulfoxide
DCM	Dichloromethane
DI	Deionized water
DLS	Dynamic light scattering
DEPT 135	Distortionless enhancement by polarization transfer
DPPH	2, 2'-diphenyl-1-picrylhydrazyl
DNS	3,5-dinitro salicylic acid
EDX	Energy dispersive x-ray spectroscopy
EtOAc	Ethyl acetate
FCC	Face-centered cubic
F1	Procyanidins fractions of dimers and trimers
F2	Procyanidins fraction of trimers
FRAP	Ferric Reducing Antioxidant Power
FTIR	Fourier transforms infrared spectroscopy
FC	Folin–Ciocalteu's phenol reagent
GA	Gallic acid
G	Gram
GLY	Glycine

HAT	Hydrogen atom transfer
HAuCl <sub>4</sub> .XH <sub>2</sub> O	Tetrachloroauric acid
HCl	Hydrochloric acid
HEX	Hexane
HDS	Hydrodynamic size
HH	<i>Hypoxis hemerocallidea</i>
HHE-AgNPs	<i>Hypoxis hemerocallidea extract</i> -mediated silver nanoparticles
HPEA	Ethanesulphonic acid
HPLC	High-performance liquid chromatography
HPX	Hypoxoside
HPX-AgNPs	Hypoxoside-mediated silver nanoparticles
HR-TEM	High-Resolution Transmission Electron Microscopy
H <sub>2</sub> SO <sub>4</sub>	Sulphuric acid
<sup>1</sup> H-NMR	Proton nuclear magnetic resonance
IC <sub>50</sub>	Half maximal inhibitory concentration
INT	Iodonitrotetrazolium chloride
LC–MS	Liquid Chromatography–Mass Spectrometry
LSPR	Localised surface plasmon resonance
LSTE	<i>Leucosidea sericea</i> total extract
μL	Microlitre
MS	Mass spectrometry
MNPs	Metallic nanoparticles
MeOH	Methanol
mg	Milligram
mL	Millilitre
MIC	minimum inhibitory concentration
min	Minutes
MWCNTs	Multi-walled carbon nanotubes
NaCl	Sodium Chloride
Na <sub>2</sub> CO <sub>3</sub>	Sodium carbonate
NaH <sub>2</sub> PO <sub>4</sub>	Sodium dihydrogen phosphate
Na <sub>2</sub> HPO <sub>4</sub>	Disodium hydrogen phosphate
NA	Not active at the tested concentration
N/Av	Information not available in the literature cited

NLC	Nanostructured lipid carrier
NMs	Nanomaterials
NMR	Nuclear magnetic resonance
NPs	Nanoparticles
NSMs	Nanostructured materials
PBS	Phosphate buffered saline
PDI	Polydispersity index
PDT	Photodynamic therapy
PNPs	Polymer nanoparticles
PTT	Photothermal therapy
p-NPG	<i>P</i> -nitrophenyl- $\alpha$ -D-glucopyranoside
QTOF	Quadrupole time-of-flight
ROS	Reactive oxygen specie
SAED	Selected area electron diffraction
SET	Single electron transfer
SPR	Surface plasmon resonance
SLNPs	Solid lipid nanoparticles
SCNPs	Semiconductors nanoparticles
SWCNTs	Single-walled carbon nanotubes
SD	Standard deviation
TEM	Transmission electron microscopy
TE/g	Trolox equivalent per gram
TLC	Thin layer chromatography
TPC	Total Phenolic Content
TPTZ	2,4,6-tri[2-pyridyl]-s-triazine, Iron (III) chloride hexahydrate
T2DM	Type II diabetes mellitus
TMS	Tetramethylsilane
UV-VIS	Ultra-Violet Visible spectroscopy
UHPLC	Ultra-high-performance liquid chromatography
v/v	Volume by volume
WHO	World Health Organization
XRD	X-ray diffraction
XPS	X-ray photoelectron spectroscopy
ZP	Zeta potential



## CHAPTER ONE

### 1.1 Introduction

Nanotechnology has emerged as a multidisciplinary field of research that can be defined as "the science, engineering, and technology of design, production, characterization, and application of structures, devices and systems of the range of 1-100 nm" (Balachandar et al., 2019). The past few decades had witnessed a significant progress as nanotechnology develops into diverse fields such as biology, physics, engineering, material science and chemistry (Bayda et al., 2020). As the technology advances, environmental safety and other concerns in the production processes of nanoscale materials led to the birth of green nanotechnology and green chemistry (Anastas, 1999). The green nanotechnology has to do with deliberate development of reasonable and meaningful procedures to produce materials as well as their related processes in an environmentally friendly manner to reduce the use of harsh and hazardous chemicals (Wong & Karn, 2012). "Green chemistry is the design, development and implementation of chemical products and processes to reduce or eliminate the use and generation of substances hazardous to human health and the environment" (Anastas, 1999). One of the rational ideas of the green chemistry is that "prevention is better than cure", that is, it is better to avoid the production of toxic substances than try to solve the problems that might result from the use of harmful chemicals (Anastas, 1999). Through the green chemistry principles, materials are now designed and formed from natural resources with greater efficiency and minimal hazards, and the materials also tend to be biocompatible, biodegradable and renewable (Kumar & Kaur, 2020). Consequently, green chemistry as an interdisciplinary approach is expected to improve the quality of nanomaterials and environmental health and contribute to the world's economic growth (Ali et al., 2020). For instance, there is an increasing global demand for safe and portable drinking water, leaving over 800 million people without access to quality water. Additionally, there is a projected increase in the total energy requirement of more than 30 % by the year 2035 (Ali et al., 2020). Moreover, environmental pollution occasioned by the release of millions of tons of waste into the environment had continued to rise (Sarong et al., 2020). The more worrisome is the incessant emergence of deadly diseases challenging the wellbeing of the world population (Loste et al., 2020). These are among the reasons for an urgent need for cleaner and safer materials and environment. Green chemistry and green nanotechnology may pave ways to resolving these problems as the principles can be applied in many fields including the preparation and application of novel gold and silver nanoparticles (Sarong et al., 2020).

A lot of recent research activities across various fields have been focused on the preparation of gold and silver nanoparticles due to their numerous application potentials (Ashraf et al., 2019). They are synthesized by physical and chemical methods such as laser ablation and evaporation-condensation (Magnusson et al., 1999), ball milling (Ayoman & Hosseini, 2016), sonication and hydrothermal (Muneer et al., 2015), chemical reduction (Dang et al., 2011), supercritical fluid deposition (Erkey, 2009) and spinning (Janas & Koziol, 2016). However, these methods involve the use of sophisticated instruments and require a high amount of energy which is costly (Maddinedi et al., 2017). Also, they involve the use of hazardous chemicals which do not only have a negative impact on the environment but also limit their applicability in some fields like biomedical (Lee et al., 2014). To mitigate these challenges, the biological or green synthesis methods serve as a better alternative. In the green synthesis procedure, microorganisms such as fungi (Clarance et al., 2020), bacteria (Lee et al., 2020), algae (Venkatraman et al., 2018), yeasts (Narayanan & Sakthivel, 2010) and actinomycetes (Hamed et al., 2020) have been employed to form gold and silver nanoparticles. They are, however, associated with various difficulties including tedious workup, handling of cell cultures and long incubation time (Nath & Banerjee, 2013). Hence, plants are considered the most preferred candidates because they are abundantly available, easily accessible, non-toxic, easy to handle and most importantly possess chemical constituents (Saratale et al., 2018). Several plants have been used in the preparation of gold and silver nanoparticles (Alomar et al., 2020; Biswal & Misra, 2020; Esmaili et al., 2020; Kalimuthu et al., 2020). Quite a number of South African plants such as *Cynanchum africanum*, *Dicerotheramnus rhinocertis*, *Eriocephalus africanus* and *Hermannia alnifolia* have been used in the synthesis of gold nanoparticles. The phytochemicals in these plants enabled successful reduction of gold and subsequent formation of the nanoparticles (Elbagory et al., 2016).

### **1.2 *Leucosidea sericea* and *Hypoxis hemerocallidea***

*Leucosidea sericea* and *Hypoxis hemerocallidea* are two important medicinal plants that are native to South Africa. They have been widely used by different tribes in South Africa to cure many diseases including cancer, urinary infections, skin-related disorders, as astringent and vermifuge, ophthalmia and worm infections (Naidoo et al., 2013; Asong et al., 2019; Nair et al., 2012; van Wyk, 2008). Other reported biological activities of the plants include antibacterial, antioxidant, anti-inflammatory, anti-acne and anthelmintic (Keneilwe et al., 2018; Mwinga et al., 2019; Nair et al., 2012; Sharma et al., 2014; Aremu et al., 2010; Moteetee et al., 2019). A few chemical constituents associated with these interesting bioactivities have been identified and isolated from the plants (Drewes et al., 2008; Sharma

et al., 2014). Some of the compounds include aspidinol, phytol,  $\beta$ -sitosterol and hypoxoside (Adamu et al., 2019; Bosman et al., 2004; Laporta et al., 2007; Sharma et al., 2014). Since the phytoconstituents in the extracts of plant generally account for their reducing and capping abilities (Ovais et al., 2018), these bioactive ingredients may be useful in the green synthesis of gold and silver nanoparticles.

### **1.3 Green synthesis of gold and silver nanoparticles**

“Green chemistry is the design, development and implementation of chemical products and processes to reduce or eliminate the use and generation of substances hazardous to human health and the environment.” (Anastas, 1999). The protocols of green synthesis are simple, facile, environmentally friendly, cost-effective and can be carried out on a large scale (Maddinedi et al., 2017). Through the protocols, some bioactive and biocompatible materials such as the gold and silver nanoparticles have been developed for biomedical applications (Vijilvani et al., 2020). Several studies have reported the green synthesis and characterization of gold nanoparticles (Kalimuthu et al., 2020; Unal et al., 2020; Chellapandian et al., 2019; Patil et al., 2019; Hemmati et al., 2019) and silver nanoparticles (Ravichandran et al., 2019; Alomar et al., 2020; Biswal & Misra, 2020; Esmaili et al., 2020) using different plant extracts. Furthermore, different plant parts such as leaves, fruits, seeds, stem bark, flowers and roots were used for the green synthesis of MNPs (Kalimuthu et al., 2020).

With the aid of Fourier transform Infra-red spectroscopy (FTIR), the phytochemicals responsible for the reduction and/or stabilization may be grouped into phenols and amides (Isaac et al., 2013), amino and carboxylic group (Zhang et al., 2020), polysaccharides and proteins (Abbasi et al., 2015), phenolics, amines and nitriles (Dzimitrowicz et al., 2019), proteins, alcohols, ketones and aldehydes (Song et al., 2009), carbohydrates, peptides and proteins (Francis et al., 2014), flavonoids (Wang et al., 2018), carbonyl compounds (Franco-Romano et al., 2014), flavonoids and polyphenols (Das & Velusamy, 2014), and amines (Anuradha et al., 2015). What is common in all the classes is the presence of nitrogen-containing functional group in the case of amines, amides and nitriles while others have carbonyl and/or hydroxyl groups in them. It may imply that possession of lone pairs of electrons is a key factor since all groups possess at least one and that may be the determining factor for reducing and capping abilities of the class of phytochemicals.

More recently, single phytochemicals isolated from plant such as quercetin (Lee & Park, 2019), escin (Shamprasad et al., 2019), phloridzin (Payne et al., 2018), isoimperatorin (Mavaei et al., 2020), resveratrol (Dong et al., 2019) and several flavonoids (Švecová et al.,

2018) have been used to synthesize green gold and silver nanoparticles with interesting activities. The advantages include the production of cleaner gold and silver nanoparticles with enhanced physicochemical properties. Secondly, since their chemical structures are known, it is easier to predict the functional groups involved in the reduction and stabilization of the gold and silver nanoparticles unlike crude extracts where many phytochemicals are involved.

#### **1.4 Characterization of gold and silver nanoparticles**

Another important aspect of green synthesis is the determination of the physicochemical properties of the synthesized gold and silver nanoparticles. Understanding the characteristic features such as the size, shape, surface charge and morphology is of utmost importance as most applications rely on this information (Clarance et al., 2020). The Ultra-Violet Visible (UV-Vis) Spectroscopy, Transmission Electron Microscopy (TEM), Selected Area Electron Diffraction (SAED), X-Ray Diffraction (XRD), Dynamic Light Scattering (DLS), Energy-Dispersive X-Ray Spectroscopy (EDX) are among the techniques that have been employed to determine absorbance, size and morphology, crystallinity, polydispersity, hydrodynamic size and zeta potential of gold and silver nanoparticles (Ahmad et al., 2019; Khoobchandani et al., 2020; Alshehddi & Bokhari, 2020; Ibrahim et al., 2020). The surface plasmon resonance of nanoparticles may depend on the metal involved among other factors. For instance, while silver nanoparticles possess surface plasmon resonance at about 320-500 nm, the gold counterparts appear at 500-600 nm (Soni & Sosa, 2013; Unal et al., 2020).

From the TEM micrographs, the morphology and size of gold and silver nanoparticles can be determined. Gold or silver nanoparticles synthesized from plant extracts or pure phytochemicals often show predominantly spherical shapes in the nanoscale range of 1-100 nm (Elbagory et al., 2017; Alle et al., 2020). Although, the measured size is usually bigger than that measured by the TEM analysis, the DLS measurement also provides information on the size alongside polydispersity index (PDI). The PDI is used to determine the degree of homogeneity of the particles in colloidal solutions (Danaei et al., 2018).

The zeta potential (ZP) shows the extent of stability of the colloidal solutions. ZP values could be positive or negative depending on the type of ions surrounding the surface of the nanoparticles. However, the degree of stability depends on the magnitude of the ZP value and not the charge (Danaei et al., 2018). Several studies have employed XRD in conjunction with SAED to confirm the crystallinity of both silver and gold nanoparticles (Vijilvani et al., 2020).

EDX has been used to further confirm the type of MNPs that has been synthesized since it can detect heavy metals like gold and silver (Govindappa et al., 2018).

### **1.5 Applications of gold and silver nanoparticles**

Gold and silver nanoparticles are emerging nanoscale entities with applications in various fields such as photocatalytic, electrochemical (Mavaei et al., 2020), catalytic (Vijilvani et al., 2020), agriculture (Alshehddi & Bokhari, 2020) and degradation of pollutants (Garg et al., 2020). Additionally, these nanoparticles have more biomedical applications such as wound healing (Augustine, 2018), drug delivery, tissue engineering, pharmaceutical, as antibiofilm, antimicrobial, anticancer (Hamed et al., 2020; Alle et al., 2020), antibacterial, antifungal (Alomar et al., 2020; Ashraf et al., 2019), tumour therapeutic (Al-Yasiri et al., 2017), antiviral, antioxidant, plasmodial, anti-inflammatory, larvicidal, anti-angiogenic, antiplatelet, antibacterial (Balachandar et al., 2019; Biswal & Misra, 2020; Saravanan et al., 2018), antidiabetic (Ponnanikajamideen & Rajeshkumar, 2019) and as photothermal therapeutic agents (Grabowska-Jadach et al., 2019).

The microbial infections have been a burden to the world such that a recent estimate suggested that by 2050, it will become the cause of 10 million deaths (Lysy et al., 2016). Although the mechanisms of action are still poorly understood, several studies have reported the activities of silver and gold nanoparticles on bacterial species, on enzymes such as alpha-amylase and alpha-glucosidase and their scavenging properties (Ponnanikajamideen & Rajeshkumar, 2019; Hamed et al., 2020; Balachandar et al., 2019).

Among the most important physicochemical properties of gold and silver nanoparticles is their surface area, surface charge, morphology and size which have allowed them to interact in biological systems and react freely at cellular levels (Sathishkumar et al., 2016). Because of these, gold and silver nanoparticles are believed to inhibit bacterial species by disrupting the cell walls. As nanoparticles are internalized, metal ions like those of gold and silver are released, causing the activation of reactive oxygen species which would cause cell death (Kumar et al., 2019). Silver nanoparticles have shown excellent bactericidal activities on the Gram-negative species because they are able to easily penetrate their cell walls better than those of the Gram-positive species (Singh et al., 2018).

Up to 425 million youths suffered from diabetes in a recent report (Renner et al., 2020). Gold and silver nanoparticles are also being evaluated in search of alternative remedies for this disease (Ponnanikajamideen & Rajeshkumar, 2019; Govindappa et al., 2018). The antidiabetic properties of gold and silver nanoparticles have been associated with their

increased surface area to volume ratio among other properties compared to their precursor bulk materials (Shamprasad et al., 2019).

The scavenging abilities of gold and silver nanoparticles have also been extensively reported (Govindappa et al., 2018). Nanoparticles have been used as carriers of antioxidant agents with better efficiency (Kumar et al., 2015). The antioxidant properties of gold and silver nanoparticles have been linked to their enhanced properties in synergy with the phytochemicals, serving as capping agents.

### **1.6 Problem statement and rationale**

The conventional physical and chemical methods of synthesis of gold and silver nanoparticles have suffered many drawbacks. While the physical protocols have disadvantages such as the need for sophisticated instruments, high cost and consumption of higher amount of energy, the chemical methods are associated with the use of chemicals that are considered toxic. Chemicals such as sodium borohydrides, sodium citrate and hydrazine have limited the application of gold and silver nanoparticles, especially for biomedical. Apart from the limited applicability occasioned by harmful precursors, the remnants from these chemicals are also released into the environment, causing another threat to the ecosystem. Gold nanoparticles synthesized from sodium citrate for example, have been found to be extremely toxic in both *in vitro* and *in vivo* studies (Freese et al., 2012). Therefore, the use of safer materials becomes advantageously essential. The green synthesis protocols take care of many of the shortcomings in accordance with the principles of green chemistry. Several factors such as the use of eco-friendly solvents, cost-effectiveness, short reaction time, low energy consumption are among the key benefits of green synthesis. However, the most beneficial is the use of phytochemicals in plants as reducing as well as capping agents. Most literature reports relied on FTIR spectroscopy to identify the phytochemicals responsible for reduction and stabilization which may need to be further studied because FTIR only speculates the phytochemicals based on functional group identification. Unfortunately, many phytochemicals, especially polyphenols, share similar functional groups. As such, other forms of characterization may be necessary to arrive at the exact phytochemicals.

Upon identification, there may also be the need to isolate the chemical constituents (compounds) and evaluate their ability to synthesize and possibly cap the MNPs. Recently, single phytochemicals have been used to synthesize gold and silver nanoparticles with interesting characteristics (Payne et al., 2018; Shamprasad et al., 2019). Limited reports, however, exist on the comparative studies between the MNPs of the extracts and those of

the isolated compounds, which will bring about a better understanding of the involvement of the phytochemicals and/or the functional groups.

Furthermore, renewed attention has been given to silver nanoparticles as a promising chemotherapeutic agent for overcoming the continuous resistance of bacteria to many antibiotics (Stiufiuc et al., 2013). In addition, since oxidative stress is linked to other diseases such as diabetes, gold and silver nanoparticles with dual potential will be of immense benefit.

### **1.7 Hypothesis**

The chemical constituents in the aqueous extracts of plant (phytoconstituents) can reduce both gold and silver precursors into their corresponding nanoparticles with potential biomedical applications. The phytoconstituents are mainly polyphenols and are responsible for the reduction as well as stabilization of the nanoparticles, working in synergy to enhance the capping ability of the plant extracts. Upon isolation, individual phytochemicals with certain functional groups can also reduce and cap gold and silver nanoparticles.

### **1.8 Research aim**

The aim of this study was to carry out the green synthesis of gold and silver nanoparticles using the chemical constituents of both *L. sericea* and *H. hemerocallidea*, characterize the nanoparticles and evaluate their antidiabetic, antioxidant and antibacterial activities.

### **1.9 Research objectives**

- ❖ Collection of plant samples from Afriplex, Limited, South Africa.
- ❖ Extraction of each plant extract and preparation of the crude extract.
- ❖ Column chromatography using both silica gel and Sephadex for fractionation and purification of the extracts.
- ❖ Identification and isolation of compounds using different spectroscopic techniques.
- ❖ Green synthesis of gold and silver nanoparticles using the crude extracts, fractions, and compounds from the two plants
- ❖ Characterization of the nanoparticles using various microscopic, spectroscopic, and optical techniques.
- ❖ Comparative studies of the physicochemical properties between the nanoparticles of the crude extracts, fractions and compounds
- ❖ Investigation of the stability of the nanoparticles in different biological buffers and media.

- ❖ Evaluation of the antioxidant activities of the nanoparticles using three different assays.
- ❖ Examination of the antidiabetic properties of the nanoparticles using alpha-amylase and alpha-glucosidase enzymes.
- ❖ Investigation of the antibacterial activities of the nanoparticles on three Gram-positive and three Gram-negative species known to cause many diseases.



## References

- Abbasi, T., Anuradha, J., Ganaie, S.U. & Abbasi, S.A. 2015. Gainful utilization of the highly intransigent weed *Ipomoea* in the synthesis of gold nanoparticles. *Journal of King Saud University - Science*, 27(1): 15–22.
- Abdulla Abdulaziz Alshehddi, L. & Bokhari, N. 2020. Influence of gold and silver nanoparticles on the germination and growth of *Mimusops laurifolia* seeds in the South-Western Regions in Saudi Arabia. *Saudi Journal of Biological Sciences*, 27(1): 574–580.
- Adamu, M., Mukandiwa, L., Awouafack, M.D., Ahmed, A.S., Eloff, J.N. & Naidoo, V. 2019. Ultrastructure changes induced by the phloroglucinol derivative agrimol G isolated from *Leucosidea sericea* in *Haemonchus contortus*. *Experimental Parasitology*, 207:107780.
- Ahmad, S., Munir, S., Zeb, N., Ullah, A., Khan, B., Ali, J., Bilal, M., Omer, M., Alamzeb, M., Salman, S.M. & Ali, S. 2019. Green nanotechnology: A review on green synthesis of silver nanoparticles — An ecofriendly approach. *International Journal of Nanomedicine*, 14: 5087–5107.
- Al-Yasiri, A.Y., Khoobchandani, M., Cutler, C.S., Watkinson, L., Carmack, T., Smith, C.J., Kuchuk, M., Loyalka, S.K., Lugão, A.B. & Katti, K. V. 2017. Mangiferin functionalized radioactive gold nanoparticles (MGF-198AuNPs) in prostate tumor therapy: Green nanotechnology for production: In vivo tumor retention and evaluation of therapeutic efficacy. *Dalton Transactions*, 46(42): 14561–14571.
- Ali, S., Perveen, S., Ali, M., Jiao, T., Sharma, A.S., Hassan, H., Devaraj, S., Li, H. & Chen, Q. 2020. Bioinspired morphology-controlled silver nanoparticles for antimicrobial application. *Materials Science and Engineering C*, 108:110421.
- Alle, M., G. B. reddy, Kim, T.H., Park, S.H., Lee, S.H. & Kim, J.C. 2020. Doxorubicin-carboxymethyl xanthan gum capped gold nanoparticles: Microwave synthesis, characterization, and anti-cancer activity. *Carbohydrate Polymers*, 229: 115511.
- Alomar, T.S., AlMasoud, N., Awad, M.A., El-Tohamy, M.F. & Soliman, D.A. 2020. An eco-friendly plant-mediated synthesis of silver nanoparticles: Characterization, pharmaceutical and biomedical applications. *Materials Chemistry and Physics*, 249: 123007.
- Anastas, P.T. 1999. Green Chemistry and the role of analytical methodology development. *Critical Reviews in Analytical Chemistry*, 29(3): 167–175.
- Anuradha, J., Abbasi, T. & Abbasi, S.A. 2015. An eco-friendly method of synthesizing gold nanoparticles using an otherwise worthless weed pistia (*Pistia stratiotes* L.). *Journal of Advanced Research*, 6(5): 711–720.
- Aremu, A.O., Ndhlala, A.R., Fawole, O.A., Light, M.E., Finnie, J.F. & Van Staden, J. 2010. In vitro pharmacological evaluation and phenolic content of ten South African medicinal plants used as anthelmintics. *South African Journal of Botany*, 76(3): 558–566.
- Ashraf, A., Zafar, S., Zahid, K., Salahuddin Shah, M., Al-Ghanim, K.A., Al-Misned, F. & Mahboob, S. 2019. Synthesis, characterization, and antibacterial potential of silver nanoparticles synthesized from *Coriandrum sativum* L. *Journal of Infection and Public Health*, 12(2): 275–281.
- Asong, J.A., Ndhlovu, P.T., Khosana, N.S., Aremu, A.O. & Otang-Mbeng, W. 2019. Medicinal plants used for skin-related diseases among the Batswanas in Ngaka Modiri Molema District Municipality, South Africa. *South African Journal of Botany*, 126: 11–20.

- Augustine, R. 2018. Skin bioprinting: A novel approach for creating artificial skin from synthetic and natural building blocks. *Progress in Biomaterials*, 7(2): 77–92.
- Ayoman, E. & Hosseini, S.G. 2016. Synthesis of CuO nanopowders by high-energy ball-milling method and investigation of their catalytic activity on thermal decomposition of ammonium perchlorate particles. *Journal of Thermal Analysis and Calorimetry*, 123(2): 1213–1224.
- Balachandar, R., Gurumoorthy, P., Karmegam, N., Barabadi, H., Subbaiya, R., Anand, K., Boomi, P. & Saravanan, M. 2019. Plant-mediated synthesis, characterization and bactericidal potential of emerging silver nanoparticles using stem extract of *Phyllanthus pinnatus*: A recent advance in phytonanotechnology. *Journal of Cluster Science*, 30(6): 1481–1488.
- Bayda, S., Adeel, M., Tuccinardi, T., Cordani, M. & Rizzolio, F. 2020. The history of nanoscience and nanotechnology: From chemical-physical applications to nanomedicine. *Molecules*, 25(1): 1–15.
- Biswal, A.K. & Misra, P.K. 2020. Biosynthesis and characterization of silver nanoparticles for prospective application in food packaging and biomedical fields. *Materials Chemistry and Physics*, 250: 123014.
- Bosman, A.A., Combrinck, S., Roux-Van Der Merwe, R., Botha, B.M. & McCrindle, R.I. 2004. Isolation of an anthelmintic compound from *Leucosidea sericea*. *South African Journal of Botany*, 70(4): 509–511.
- Chellapandian, C., Ramkumar, B., Puja, P., Shanmuganathan, R., Pugazhendhi, A. & Kumar, P. 2019. Gold nanoparticles using red seaweed *Gracilaria verrucosa*: Green synthesis, characterization and biocompatibility studies. *Process Biochemistry*, 80: 58–63.
- Clarance, P., Luvankar, B., Sales, J., Khusro, A., Agastian, P., Tack, J.C., Al Khulaifi, M.M., AL-Shwaiman, H.A., Elgorban, A.M., Syed, A. & Kim, H.J. 2020. Green synthesis and characterization of gold nanoparticles using endophytic fungi *Fusarium solani* and its in-vitro anticancer and biomedical applications. *Saudi Journal of Biological Sciences*, 27(2): 706–712.
- Danaei, M., Dehghankhold, M., Ataei, S., Hasanzadeh Davarani, F., Javanmard, R., Dokhani, A., Khorasani, S. & Mozafari, M.R. 2018. Impact of particle size and polydispersity index on the clinical applications of lipidic nanocarrier systems. *Pharmaceutics*, 10(2): 1–17.
- Dang, T.M.D., Le, T.T.T., Fribourg-Blanc, E. & Dang, M.C. 2011. Synthesis and optical properties of copper nanoparticles prepared by a chemical reduction method. *Advances in Natural Sciences: Nanoscience and Nanotechnology*, 2(1).
- Das, J. & Velusamy, P. 2014. Catalytic reduction of methylene blue using biogenic gold nanoparticles from *Sesbania grandiflora* L. *Journal of the Taiwan Institute of Chemical Engineers*, 45(5): 2280–2285.
- Dong, Y., Wan, G., Yan, P., Qian, C., Li, F. & Peng, G. 2019. Fabrication of resveratrol coated gold nanoparticles and investigation of their effect on diabetic retinopathy in streptozotocin induced diabetic rats. *Journal of Photochemistry & Photobiology, B: Biology*, 195(1): 51–57.
- Drewes, S.E., Elliot, E., Khan, F., Dhlamini, J.T.B. & Gcumisa, M.S.S. 2008. *Hypoxis hemerocallidea*- Not merely a cure for benign prostate hyperplasia. *Journal of Ethnopharmacology*, 119(3): 593–598.

- Dzimitrowicz, A., Jamróz, P., diCenzo, G.C., Sergiel, I., Kozlecki, T. & Pohl, P. 2019. Preparation and characterization of gold nanoparticles prepared with aqueous extracts of *Lamiaceae* plants and the effect of follow-up treatment with atmospheric pressure glow microdischarge. *Arabian Journal of Chemistry*, 12(8): 4118–4130.
- Elbagory, A.M., Cupido, C.N., Meyer, M. & Hussein, A.A. 2016. Large scale screening of southern African plant extracts for the green synthesis of gold nanoparticles using microtitre-plate method. *Molecules*, 21(11).
- Elbagory, A.M., Meyer, M., Cupido, C.N. & Hussein, A.A. 2017. Inhibition of bacteria associated with wound infection by biocompatible green synthesized gold nanoparticles from South African plant extracts. *Nanomaterials*, 7:417.
- Erkey, C. 2009. Preparation of metallic supported nanoparticles and films using supercritical fluid deposition. *Journal of Supercritical Fluids*, 47(3): 517–522.
- Esmaili, F., Koohestani, H. & Abdollah-Pour, H. 2020. Characterization and antibacterial activity of silver nanoparticles green synthesized using *Ziziphora clinopodioides* extract. *Environmental Nanotechnology, Monitoring and Management*, 14: 100303.
- Francis, G., Thombre, R., Parekh, F. & Leksminarayan, P. 2014. Bioinspired synthesis of gold nanoparticles using *Ficus benghalensis* (Indian Banyan) leaf extract. *Chemical Science Transactions*, 3(1): 470–474.
- Franco-Romano, M., Gil, M.L.A., Palacios-Santander, J.M., Delgado-Jaén, J.J., Naranjo-Rodríguez, I., Hidalgo-Hidalgo De Cisneros, J.L. & Cubillana-Aguilera, L.M. 2014. Sonosynthesis of gold nanoparticles from a *geranium* leaf extract. *Ultrasonics Sonochemistry*, 21(4): 1570–1577.
- Freese, C., Uboldi, C., Gibson, M.I., Unger, R.E., Weksler, B.B., Romero, I.A., Couraud, P.O. & Kirkpatrick, C.J. 2012. Uptake and cytotoxicity of citrate-coated gold nanospheres: Comparative studies on human endothelial and epithelial cells. *Particle and Fibre Toxicology*, 9: 1–11.
- Garg, N., Bera, S., Rastogi, L., Ballal, A. & Balaramakrishna, M. V. 2020. Synthesis and characterization of L-asparagine stabilised gold nanoparticles: Catalyst for degradation of organic dyes. *Spectrochimica Acta - Part A: Molecular and Biomolecular Spectroscopy*, 232: 118126.
- Govindappa, M., Hemashekhar, B., Arthikala, M.K., Ravishankar Rai, V. & Ramachandra, Y.L. 2018. Characterization, antibacterial, antioxidant, antidiabetic, anti-inflammatory and antityrosinase activity of green synthesized silver nanoparticles using *Calophyllum tomentosum* leaves extract. *Results in Physics*, 9: 400–408.
- Grabowska-Jadach, I., Kalinowska, D., Drozd, M. & Pietrzak, M. 2019. Synthesis, characterization and application of plasmonic hollow gold nanoshells in a photothermal therapy—New particles for theranostics. *Biomedicine and Pharmacotherapy*, 111: 1147–1155.
- Hamed, A.A., Kabary, H., Khedr, M. & Emam, A.N. 2020. Antibiofilm, antimicrobial and cytotoxic activity of extracellular green-synthesized silver nanoparticles by two marine-derived actinomycete. *RSC Advances*, 10(17): 10361–10367.
- Hemmati, S., Rashtiani, A., Zangeneh, M.M., Mohammadi, P., Zangeneh, A. & Veisi, H. 2019. Green synthesis and characterization of silver nanoparticles using *Fritillaria* flower extract and their antibacterial activity against some human pathogens. *Polyhedron*, 158: 8–14.
- Ibrahim, H.M., Reda, M.M. & Klingner, A. 2020. Preparation and characterization of green

- carboxymethylchitosan (CMCS) – Polyvinyl alcohol (PVA) electrospun nanofibers containing gold nanoparticles (AuNPs) and its potential use as biomaterials. *International Journal of Biological Macromolecules*, 151: 821–829.
- Isaac, R.S.R., Sakthivel, G. & Murthy, C. 2013. Green synthesis of gold and silver nanoparticles using *Averrhoa bilimbi* fruit extract. *Journal of Nanotechnology*, 2013: 906590.
- Janas, D. & Koziol, K.K. 2016. Carbon nanotube fibers and films: Synthesis, applications and perspectives of the direct-spinning method. *Nanoscale*, 8(47): 19475–19490.
- Kalimuthu, K., Cha, B.S., Kim, S. & Park, K.S. 2020. Eco-friendly synthesis and biomedical applications of gold nanoparticles: A review. *Microchemical Journal*, 152: 104296.
- Keneilwe, M., Saramma, G. & Kelvin, C. 2018. An in-vitro antioxidant and antidiabetic evaluation of traditional medicinal plants of Botswana. *Journal of Pharmaceutical Research International*, 22(6): 1–12.
- Khoobchandani, M., Katti, K.K., Karikachery, A.R., Thipe, V.C., Srisrimal, D., Mohandoss, D.K.D., Darshakumar, R.D., Joshi, C.M. & Katti, K. V. 2020. New approaches in breast cancer therapy through green nanotechnology and nano-ayurvedic medicine– Pre-clinical and pilot human clinical investigations. *International Journal of Nanomedicine*, 15: 181–197.
- Kumar, A. & Kaur, H. 2020. Sprayed in-situ synthesis of polyvinyl alcohol/chitosan loaded silver nanocomposite hydrogel for improved antibacterial effects. *International Journal of Biological Macromolecules*. 145: 950–964.
- Kumar, S.P., Birundha, K., Kaveri, K. & Devi, K.T.R. 2015. Antioxidant studies of chitosan nanoparticles containing naringenin and their cytotoxicity effects in lung cancer cells. *International Journal of Biological Macromolecules*, 78: 87–95.
- Kumar, V., Singh, S., Srivastava, B., Bhadouria, R. & Singh, R. 2019. Green synthesis of silver nanoparticles using leaf extract of *Holoptelea integrifolia* and preliminary investigation of its antioxidant, anti-inflammatory, antidiabetic and antibacterial activities. *Journal of Environmental Chemical Engineering*, 7(3): 103094.
- Laporta, O., Pérez-Fons, L., Mallavia, R., Caturla, N. & Micol, V. 2007. Isolation, characterization and antioxidant capacity assessment of the bioactive compounds derived from *Hypoxis rooperi* corm extract (African potato). *Food Chemistry*, 101(4): 1425–1437.
- Lee, Jaewook, Park, E.Y. & Lee, Jaebeom. 2014. Non-toxic nanoparticles from phytochemicals: Preparation and biomedical application. *Bioprocess and Biosystems Engineering*, 37(6): 983–989.
- Lee, K.X., Shameli, K., Yew, Y.P., Teow, S.Y., Jahangirian, H., Rafiee-Moghaddam, R. & Webster, T.J. 2020. Recent developments in the facile bio-synthesis of gold nanoparticles (AuNPs) and their biomedical applications. *International Journal of Nanomedicine*, 15: 275–300.
- Lee, Y.J. & Park, Y. 2019. Green synthetic nanoarchitectonics of gold and silver nanoparticles prepared using quercetin and their cytotoxicity and catalytic applications. *Journal of Nanoscience and Nanotechnology*, 20(5): 2781–2790.
- Loste, N., Roldán, E. & Giner, B. 2020. Is green chemistry a feasible tool for the implementation of a circular economy? *Environmental Science and Pollution Research*, 27(6): 6215–6227.
- Lysy, P.A., Corritore, E. & Sokal, E.M. 2016. New insights into diabetes cell therapy. *Current*

*Diabetes Reports*.16: 38-48.

- Maddinedi, S. babu, Mandal, B.K. & Maddili, S.K. 2017. Biofabrication of size controllable silver nanoparticles – A green approach. *Journal of Photochemistry and Photobiology B: Biology*, 167: 236–241.
- Magnusson, M.H., Deppert, K., Malm, J., Bovin, J. & Samuelson, L. 1999. Size- selected gold nanoparticles by aerosol technology. *Nanostructured Materials*. 12: 45–48.
- Mavaei, M., Chahardoli, A., Shokoohinia, Y., Khoshroo, A. & Fattahi, A. 2020. One-step synthesized silver nanoparticles using isoimperatorin: Evaluation of photocatalytic, and electrochemical activities. *Scientific Reports*, 10(1): 1–12.
- Moteetee, A., Moffett, R.O. & Seleteng-Kose, L. 2019. A review of the ethnobotany of the Basotho of Lesotho and the Free State province of South Africa (South Sotho). *South African Journal of Botany*, 122: 21–56.
- Muneer, I., Farrukh, M.A., Javaid, S., Shahid, M. & Khaleeq-Ur-Rahman, M. 2015. Synthesis of Gd<sub>2</sub>O<sub>3</sub>/Sm<sub>2</sub>O<sub>3</sub> nanocomposite via sonication and hydrothermal methods and its optical properties. *Superlattices and Microstructures*, 77: 256–266.
- Mwinga, J.L., Asong, J.A., Amoo, S.O., Nkadimeng, S.M., McGaw, L.J., Aremu, A.O. & Otang-Mbeng, W. 2019. In vitro antimicrobial effects of *Hypoxis hemerocallidea* against six pathogens with dermatological relevance and its phytochemical characterization and cytotoxicity evaluation. *Journal of Ethnopharmacology*, 242: 112048.
- Naidoo, D., Van Vuuren, S.F., Van Zyl, R.L. & De Wet, H. 2013. Plants traditionally used individually and in combination to treat sexually transmitted infections in northern Maputaland, South Africa: Antimicrobial activity and cytotoxicity. *Journal of Ethnopharmacology*, 149(3): 656–667.
- Nair, J.J., Aremu, A.O. & Van Staden, J. 2012. Anti-inflammatory effects of *Leucosidea sericea* (Rosaceae) and identification of the active constituents. *South African Journal of Botany*, 80: 75–76.
- Narayanan, K.B. & Sakthivel, N. 2010. Biological synthesis of metal nanoparticles by microbes. *Advances in Colloid and Interface Science*, 156(1–2): 1–13.
- Nath, D. & Banerjee, P. 2013. Green nanotechnology- A new hope for medical biology. *Environmental Toxicology and Pharmacology*, 36(3): 997–1014.
- Ovais, M., Khalil, A.T., Islam, N.U., Ahmad, I., Ayaz, M., Saravanan, M., Shinwari, Z.K. & Mukherjee, S. 2018. Role of plant phytochemicals and microbial enzymes in biosynthesis of metallic nanoparticles. *Applied Microbiology and Biotechnology*, 102(16): 6799–6814.
- Patil, M.P., Seo, Y.B., Lim, H.K. & Kim, G. Do. 2019. Biofabrication of gold nanoparticles using *Agrimonia pilosa* extract and their antioxidant and cytotoxic activity. *Green Chemistry Letters and Reviews*, 12(3): 208–216.
- Payne, J.N., Badwaik, V.D., Waghwan, H.K., Moolani, H. V., Tockstein, S., Thompson, D.H. & Dakshinamurthy, R. 2018. Development of dihydrochalcone-functionalized gold nanoparticles for augmented antineoplastic activity. *International Journal of Nanomedicine*, 13: 1917–1926.
- Ponnanikajamideen, M. & Rajeshkumar, S. 2019. In vivo type 2 diabetes and wound-healing effects of antioxidant gold nanoparticles synthesized using the insulin plant *Chamaecostus cuspidatus* in albino rats. *Canadian Journal of Diabetes*, 43(2): 82-89.
- Ravichandran, V., Vasanthi, S., Shalini, S., Shah, S.A.A., Tripathy, M. & Paliwal, N. 2019.

- Green synthesis, characterization, antibacterial, antioxidant and photocatalytic activity of *Parkia speciosa* leaves extract mediated silver nanoparticles. *Results in Physics*, 15: 102565.
- Renner, S., Blutke, A., Clauss, S., Deeg, C.A., Kemter, E., Merkus, D., Wanke, R. & Wolf, E. 2020. Porcine models for studying complications and organ crosstalk in diabetes mellitus. *Cell and Tissue Research*, 380(2): 341–378.
- Saratale, R.G., Saratale, G.D., Shin, H.S., Jacob, J.M., Pugazhendhi, A., Bhaisare, M. & Kumar, G. 2018. New insights on the green synthesis of metallic nanoparticles using plant and waste biomaterials: Current knowledge, their agricultural and environmental applications. *Environmental Science and Pollution Research*, 25(11): 10164–10183.
- Saravanan, M., Asmalash, T., Gebrekidan, A., Gebreegziabiher, D., Araya, T., Hilekiros, H., Barabadi, H. & Ramanathan, K. 2018. Nano-medicine as a newly emerging approach to combat human immunodeficiency virus (HIV). *Pharmaceutical Nanotechnology*, 6: 17–27.
- Sarong, M.M., Orge, R.F., Eugenio, P.J.G. & Monserate, J.J. 2020. Utilization of rice husks into biochar and nanosilica: For clean energy, soil fertility and green nanotechnology. *International Journal of Design and Nature and Ecodynamics*, 15(1): 97–102.
- Sathishkumar, G., Jha, P.K., Vignesh, V., Rajkuberan, C., Jeyaraj, M., Selvakumar, M., Jha, R. & Sivaramakrishnan, S. 2016. Cannonball fruit (*Couroupita guianensis*, Aubl.) extract mediated synthesis of gold nanoparticles and evaluation of its antioxidant activity. *Journal of Molecular Liquids*, 215: 229–236.
- Shamprasad, B.R., Keerthana, S., Megarajan, S., Lotha, R., Aravind, S. & Veerappan, A. 2019. Photosynthesized escin stabilized gold nanoparticles exhibit antidiabetic activity in L6 rat skeletal muscle cells. *Materials Letters*, 241: 198–201.
- Sharma, R., Kishore, N., Hussein, A. & Lall, N. 2014. The potential of *Leucosidea sericea* against *Propionibacterium acnes*. *Phytochemistry Letters*, 7(1): 124–129.
- Singh, J., Dutta, T., Kim, K.H., Rawat, M., Samddar, P. & Kumar, P. 2018. 'Green' synthesis of metals and their oxide nanoparticles: Applications for environmental remediation. *Journal of Nanobiotechnology*: 1–24.
- Song, J.Y., Jang, H.K. & Kim, B.S. 2009. Biological synthesis of gold nanoparticles using *Magnolia kobus* and *Diopyros kaki* leaf extracts. *Process Biochemistry*, 44(10): 1133–1138.
- Soni, A. & Sosa, S. 2013. Phytochemical analysis and free radical scavenging potential of herbal and medicinal plant extracts. *Journal of Pharmacognosy and Phytochemistry JPP*, 22(24): 22–29.
- Stiufiuc, R., Iacovita, C., Lucaciu, C.M., Stiufiuc, G., Dutu, A.G., Braescu, C. & Leopold, N. 2013. SERS-active silver colloids prepared by reduction of silver nitrate with short-chain polyethylene glycol. *Nanoscale Research Letters*, 8(1): 1–5.
- Švecová, M., Ulbrich, P., Dendisová, M. & Matějka, P. 2018. SERS study of riboflavin on green-synthesized silver nanoparticles prepared by reduction using different flavonoids: What is the role of flavonoid used? *Spectrochimica Acta - Part A: Molecular and Biomolecular Spectroscopy*, 195: 236–245.
- Unal, I.S., Demirbas, A., Onal, I., Ildiz, N. & Ocsoy, I. 2020. One step preparation of stable gold nanoparticle using red cabbage extracts under UV light and its catalytic activity. *Journal of Photochemistry and Photobiology B: Biology*, 204: 111800.
- Venkatraman, A., Yahoob, S.A.M., Nagarajan, Y., Harikrishnan, S., Vasudevan, S. &

- Murugasamy, T. 2018. Pharmacological activity of biosynthesized gold nanoparticles from brown algae- Seaweed *Turbinaria conoides*. *NanoWorld Journal*, 4(1): 17–22.
- Vijilvani, C., Bindhu, M.R., Frincy, F.C., AlSalhi, M.S., Sabitha, S., Saravanakumar, K., Devanesan, S., Umadevi, M., Aljaafreh, M.J. & Atif, M. 2020. Antimicrobial and catalytic activities of biosynthesized gold, silver and palladium nanoparticles from *Solanum nigurum* leaves. *Journal of Photochemistry and Photobiology B: Biology*, 202: 111713.
- Wang, L., Lu, F., Liu, Y., Wu, Y. & Wu, Z. 2018. Photocatalytic degradation of organic dyes and antimicrobial activity of silver nanoparticles fast synthesized by flavonoids fraction of *Psidium guajava L.* leaves. *Journal of Molecular Liquids*, 263: 187–192.
- Wong, S. & Karn, B. 2012. Ensuring sustainability with green nanotechnology. *Nanotechnology*, 23(29): 22–24.
- van Wyk, B.E. 2008. A broad review of commercially important southern African medicinal plants. *Journal of Ethnopharmacology*, 119(3): 342–355.
- Zhang, L., Mazouzi, Y., Salmain, M., Liedberg, B. & Boujday, S. 2020. Antibody-gold nanoparticle bioconjugates for biosensors: Synthesis, characterization and selected applications. *Biosensors and Bioelectronics*, 165:112370.

## CHAPTER TWO

### LITERATURE REVIEW

#### 2.1 Plants and their importance

Plants have been of great significance, providing many needs such as food in the form of vegetables, corn, nuts, cereals, and tubers for both animals and man. Economically, plant products such as timber have been the source of income for some individuals as they are made into different furniture and are also used as part of roofing material for houses. Ornamental plants have also been used for decoration and beautifications (Brandon, 1991).

Plants could be in the form of trees, shrubs, herbs and climbers. Shrubs are medium-sized woody plants that are not as tall as trees but taller than herbs. The woody hard stem is known as the trunk which gives rise to many branches bearing leaves, fruits and flowers. A good example of a shrub is *Leucosidea sericea* (Aremu et al., 2010). Different parts of plant such as leaves, tubers, bark, rhizome, aerial part and seed have also been employed for many purposes. A tuber is more or less the stem and partly the root, usually a swollen structure that is found underground (Nair and Kanfer, 2008). *Hypoxis hemerocallidea* (Hypoxis) is a well-known tuberous plant.

Although certain plants were the chief source of primary health care for some up to now, very little was known about the bioactive components that are present in them, let alone their properties. Research activities by scientists to understand these began much later (Halberstein, 2005). Indeed, research results demonstrated the link between the traditional use of plant for treatment of many diseases. However, it was not until the 19th century that the isolation of biologically active compound (quinine) took place from the bark of the Cinchona tree (Phillipson, 1995). The work of phytochemists, among other scientists, led to the identification of various phytochemicals. Thus, alkaloids, flavonoids, polyphenols, acids, sugars and terpenoids were believed to be present in plants and so responsible for many of their pharmacological activities. In a 1996 study, six out of the top 20 pharmaceutical prescriptions were natural products from plants. The discovery of artemisinin, taxol, and etoposide attracted more attention towards plants as a source of novel drugs. Vincristine and paclitaxel have also been discovered as anticancer drugs with plant origin (Phillipson, 1999).

The use of plant, especially as traditional medicines, cannot be overemphasized. Many nations, including the developed ones, have and are still using plant either in combination with modern treatments or as the main source of primary health care provision. The reasons may be cultural, pharmacological properties, accessibility, cost-saving and lesser side



effects. One plant, for instance, may possess antioxidant, antibacterial, and/or antidiabetic properties that have been associated with the combination of different phytochemicals in it (Halberstein, 2005).

### **2.1.1 Phytochemicals in plant**

The secondary metabolites from plants can be classified into three major groups: (a) terpenoids, (b) sulfur-containing compounds and nitrogen-containing alkaloids, and (c) flavonoids and polyphenolic compounds. Phenolic compounds have found interesting biological activities and thus attracted considerable attention (Tsao, 2010).

Phenolics are widely spread in the plant kingdom as over 8000 different types have been identified in various plant species. They form an important part of the human diet and are essential to the plant in several ways; they protect plants from herbivores and microbial infection, protection against Ultra-Violet radiation, pigmentation and stimulation of nitrogen-fixing nodules. Phenolics are characterized by having at least one aromatic ring and one or more hydroxyl groups attached. They range from simple, low molecular-weight, single aromatic-ringed compounds to large and complex compounds such as tannins and derived polyphenols. Phenolics can be further classified into two groups: flavonoids and non-flavonoids (Tsao, 2010).

#### **Flavonoids**

Flavonoids are the most abundant of the phenolic compounds and are found throughout the plant kingdom. They comprise fifteen carbons with two aromatic rings connected by a three-carbon-bridge. They are found in high concentrations in leaves and the skin of fruits and play crucial roles as secondary metabolites (Martins et al., 2011). The main subclasses of flavonoids are flavones, flavonols, flavan-3-ols, flavanones, isoflavones and anthocyanidins (figure 2.1).

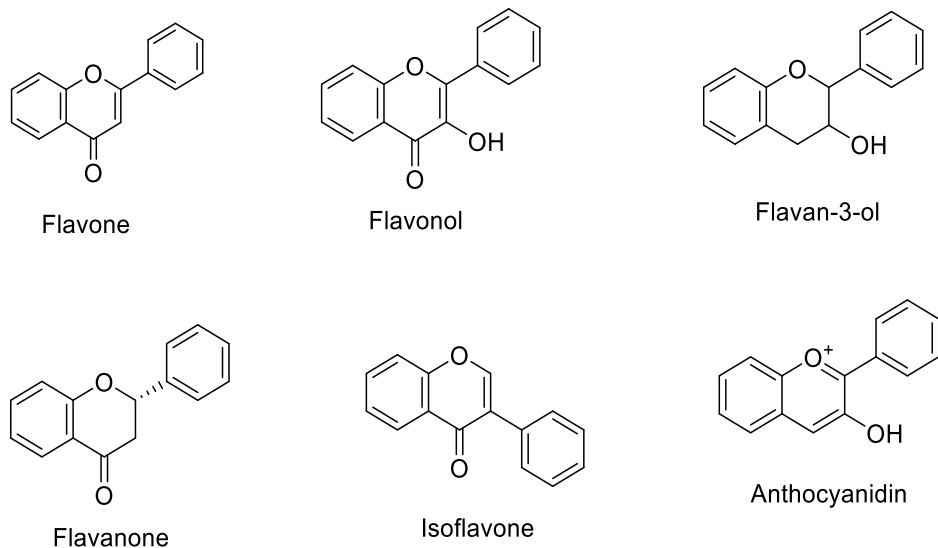


**Figure 2. 1: Basic structures of major flavonoids that are found in plants**

The basic skeleton of flavonoids can have many substituents, hydroxyl groups being present at positions 4', 5, and 7. Often, sugars are found with flavonoids, existing naturally as glycosides. The presence of sugars and several hydroxyl groups usually enhance the solubility of flavonoids in water, whereas other substituents like alkyl groups make them lipophilic.

Of the flavonoids, flavonols are the most widely distributed all over the plant kingdom. Structural variations and distribution of flavonols are extensive. Much information is available about their presence in most of the vegetables, fruits and beverages. Flavonols such as quercetin, kaempferol and myricetin (figure 2.2) mostly exist as O-glycosides. Conjugation occurs at position 3 of the C-ring but can also occur at positions 5, 7, 4', 3' and 5' of the carbon ring (Tsao, 2010).

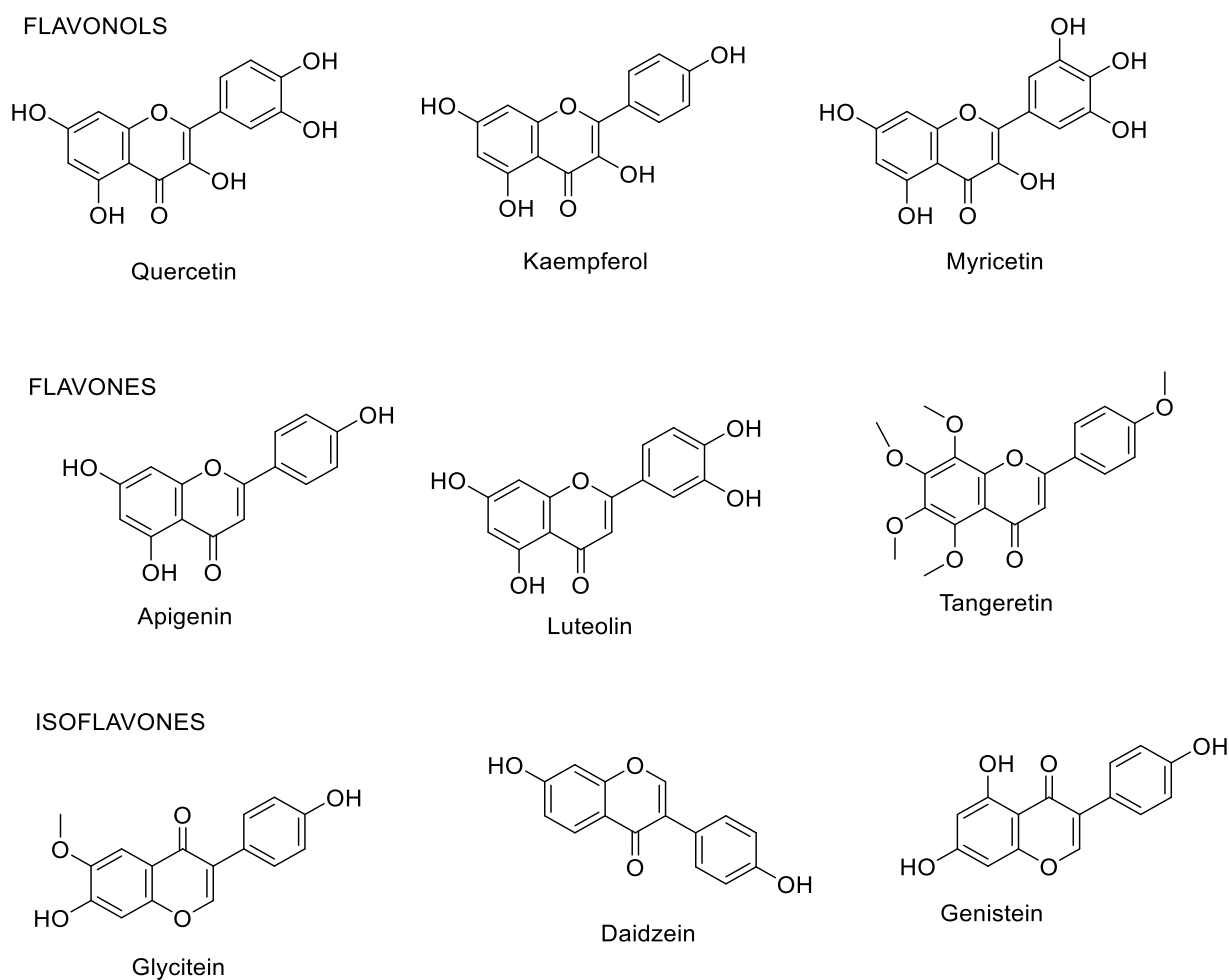


**Figure 2. 2: Chemical structures of some flavonols, flavones and isoflavones found in plants**

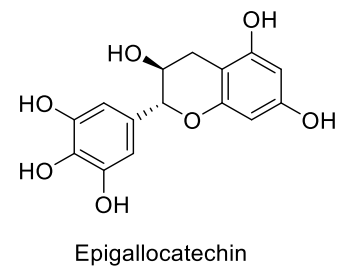
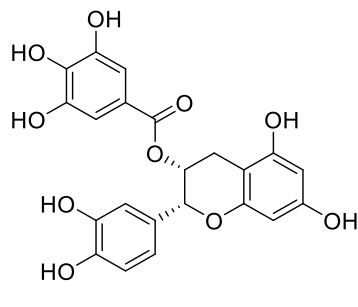
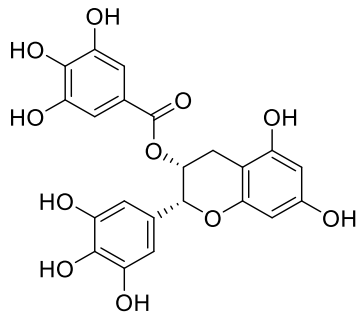
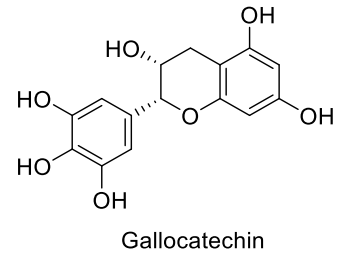
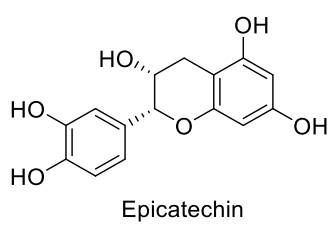
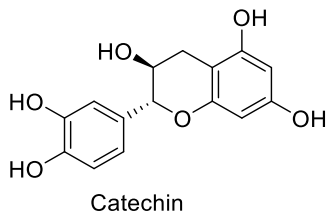
Structurally, flavones are much related to the flavonols (figure 2.2) except in cases of apigenin and luteolin having C- and A- ring substituents. Although they do not have oxygenation at C-3, a few substitutions are possible with flavones. These include O- and C-alkylation, glycosylation, hydroxylation and methylation. They occur as 7-O-glycosides and are not as widely distributed as the flavonols.

Isoflavones are predominantly found in leguminous plants and their characteristic is the possession of a B-ring at C3. Some examples are shown in figure 2.2.

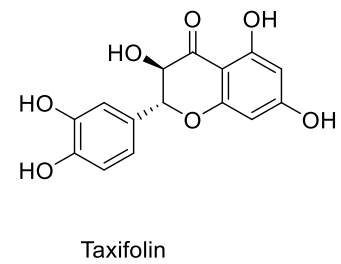
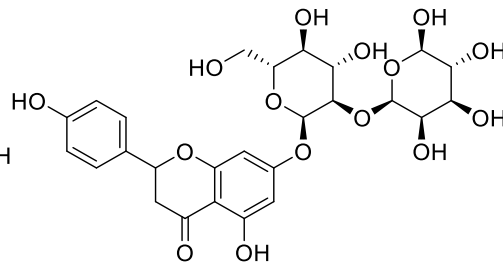
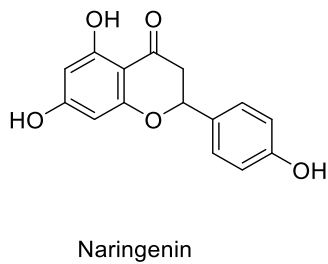
Flavan-3-ols are a diverse subclass of flavonoids ranging from simple monomers like catechin to very complex polymers. Other structurally related flavonoids to flavan-3-ol are

the anthocyanidins and flavanones. They are non-planer and have a saturated C3 in the heterocyclic C-ring (figure 2.3) (Tsao, 2010; Martins et al., 2011).

#### FLAVANOLS



#### FLAVANONES



#### ANTHOCYANIDINS

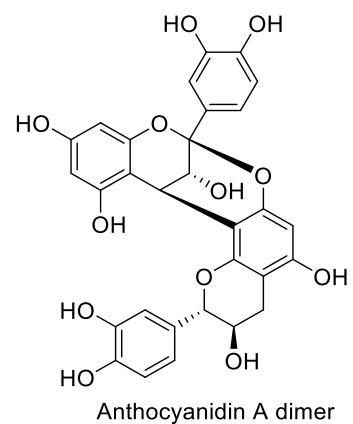
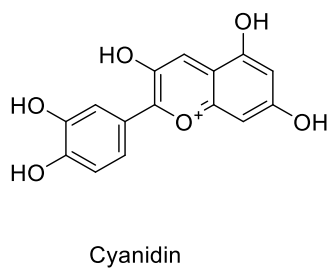
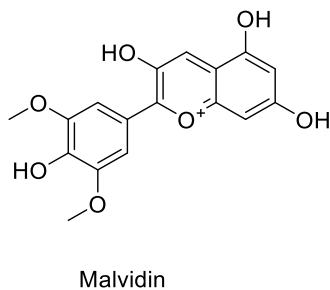


**Figure 2. 3: Examples of flavanols, flavanones and anthocyanidins found in plants**

### Non-flavonoids

Phenolic acids, stilbenes and hydrocinnamates are also found in fruits, vegetables and other plant sources, and can be classified as non-flavonoids according to their structure. They have been equally reported to have several benefits as they play a role in promoting human health such as in the reduction of some degenerative diseases like cancer and diabetes (Yoon et al., 2011). Some examples are shown in figure 2.4.

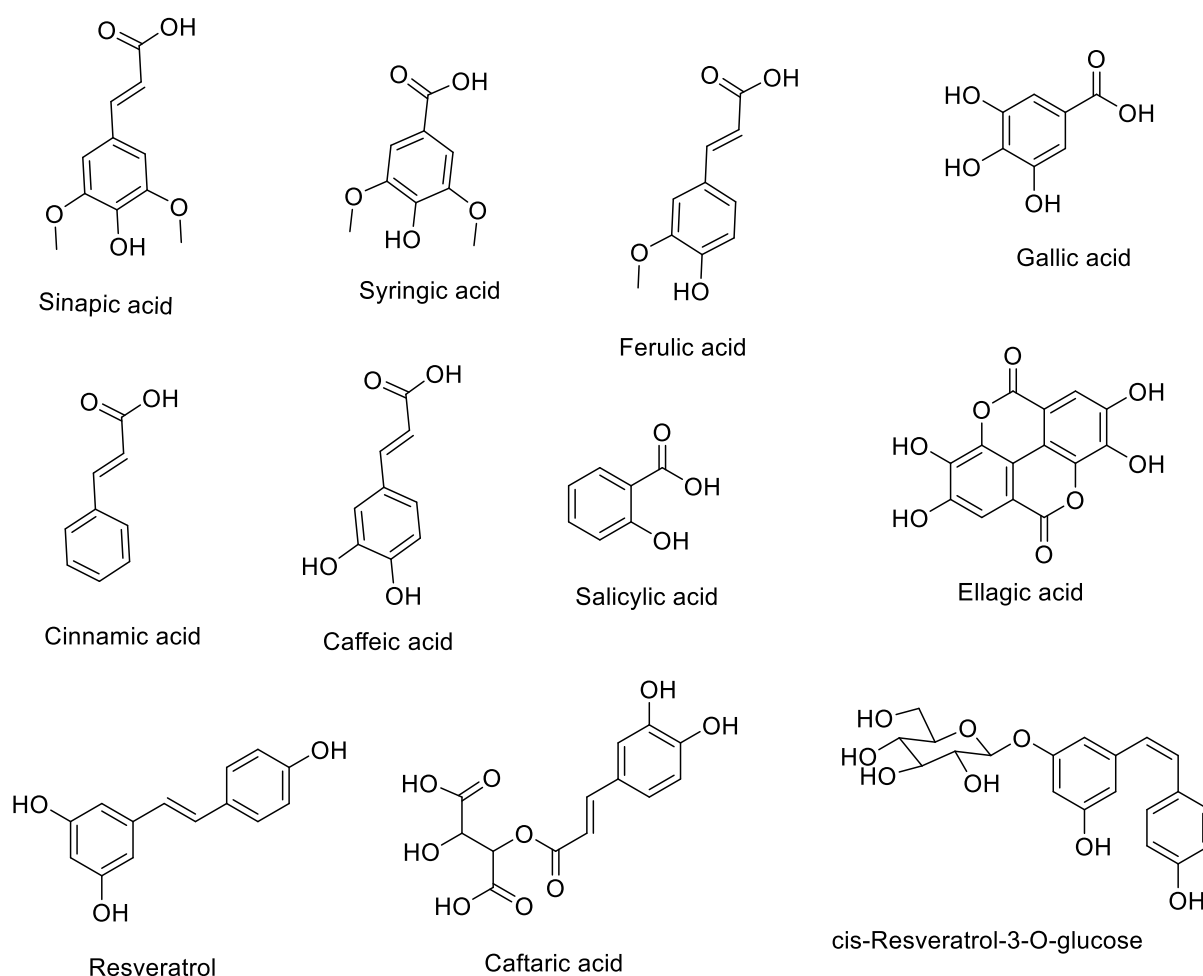


**Figure 2. 4: Chemical structures of some naturally occurring non-flavonoids.**

Plants could be in the form of trees, shrubs, herbs and climbers. Shrubs are medium-sized woody plants that are not as tall as trees but taller than herbs. The woody hard stem is

known as the trunk which gives rise to many branches bearing leaves, fruits and flowers. A good example of a shrub is *Leucosidea sericea* (Aremu et al., 2010).

Different parts of plant have also been employed for many purposes. These include leaves, tubers, bark, rhizome, aerial part and seed. A tuber is more or less the stem and partly the root, usually a swollen structure that is found underground (Nair and Kanfer, 2008). *Hypoxis hemerocallidea* (Hypoxis) is a well-known tuberous plant.

## 2.2 Hypoxis hemerocallidea

### 2.2.1 Occurrence and uses

*Hypoxis hemerocallidea* (HH) is probably the most popular medicinal plant in South Africa (SA) owing to its many traditional uses. It is abundantly found in the Cape region. The core Cape sub-region of the famous Cape Floristic Region (CFR), or simply Cape Flora, is in the South-Western part of Africa. It is a unique and special flora that houses more than 9000 species of plants, most of which are not found in any other part of the world. Although sitting on only about 90,000 km<sup>2</sup>, which is below 5% of the total area of the South African country, it is regarded as one of the six richest floral kingdoms in the world (figure 2.5) (Goldblatt and Manning, 2002).

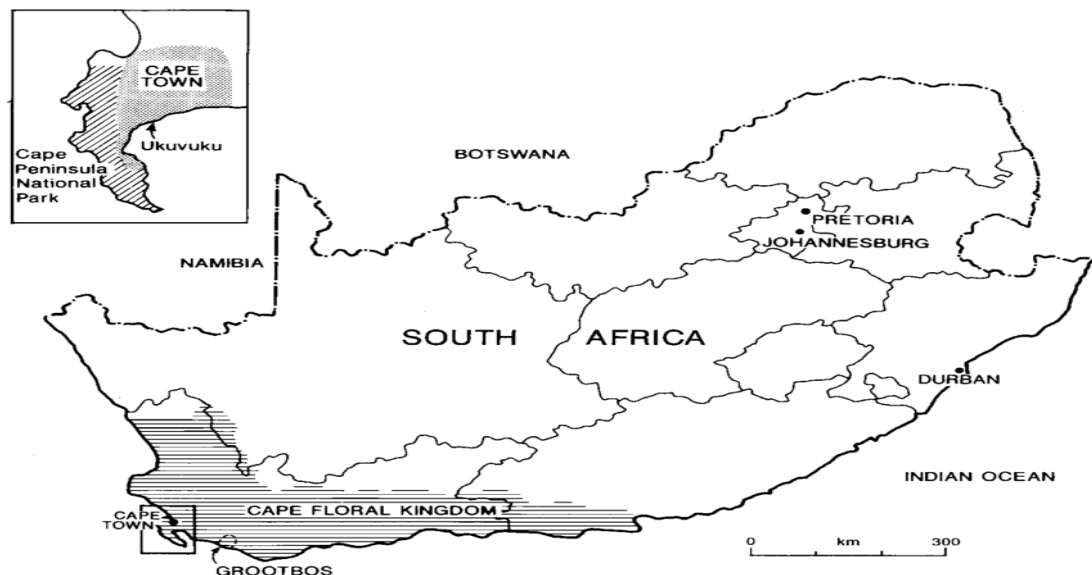


**Figure 2. 5: Map of South Africa showing the Cape Floristic Region. One of the world richest plant kingdoms with certain plant species peculiar to it alone**

*Hypoxis Hemerocallidea*, formerly called *H. rooperi*, belongs to a very big family of *Hypoxidaceae*. The genus is *Hypoxis* with about 90 species, out of which 29 are native to South Africa (Singh, 2007). The plant is widespread in many areas of SA, from the Eastern Cape, through KwaZulu-Natal to Limpopo, Lesotho, and Gauteng and also stretches into Zimbabwe, Mozambique and parts of eastern Africa (Drewes et al., 2008). HH is known to survive different weather conditions, including winter. It can be identified by features such as the "star-like" yellow flowers, as shown in figure 2.6A.



**Figure 2. 6: The aerial part of *Hypoxis Hemerocallidea* with the (A) star-like yellow flowers and the (B) underground tuberous corm with root-like attachments**

In SA, the plant is locally known as "sterblom" by the Afrikaans community, while the isiZulus call it "inkomfe" and the Sesothos call it "lotsane". The English name, which is the most popular, is African potato (Drewes et al., 2008; van Wyk, 2008). This was associated with its underground bulb, "the corm" (figure 2.6B) which can grow to about 10-15 cm in diameter. One of the characteristics of the *Hypoxis* corm is that, if sliced by a knife or a cutlass, a resinous liquid is usually released almost instantaneously to heal the cut (Nair and Kanfer, 2008).

Extracts of HH have been traditionally employed in the management of diseases like cancer, HIV/AIDS, urinary infections (Naidoo et al., 2013), acne, dysentery, dermatitis, wounds, dizziness, testicular tumours, bladder disorders, and high blood pressure (Ncube et al., 2013; Steenkamp and Gouws, 2006). The corm is used to treat gall sickness in cattle, psychiatric problems, to kill small vermin, and as a diuretic (Jäger et al., 1996). The Zulus have been using the infusion from HH to cure impotency for many years (Moyo et al., 2014).

The HH extracts have been topically applied to treat skin-related disorders and sexually transmitted diseases such as pimples, sunburns, body rashes, sores, boils, gonorrhoea and genital warts (Asong et al., 2019; Bassey et al., 2015; De Wet et al., 2012; Mwinga et al., 2019).

### 2.2.2 The chemistry and biology of *Hypoxis hemerocallidea* and its isolated compounds

As a practice, scientists must confirm the validity of these applications necessitating some laboratory activities. The results from different researchers showed good agreement with the claims when extracts of HH was found to possess anticancer, anti-inflammatory, antineoplastic, anti-infective, antibacterial, antioxidant, antidiabetic and antifungal activities (Keneilwe et al., 2018; Laporta et al., 2007; Mwinga et al., 2019; Owira and Ojewole, 2009). Ncube and colleagues added that when the extracts were combined with the extracts of other medicinal plants, the HH extracts demonstrated better antibacterial and anticandidal activities (Ncube et al., 2012).

To date, only few compounds have been isolated from this plant. They include sterols and a major constituent, hypoxoside as shown in figure 2.7 (Boukes et al., 2008; Nair and Kanfer, 2008). These compounds may be responsible for the medicinal properties of the plant.

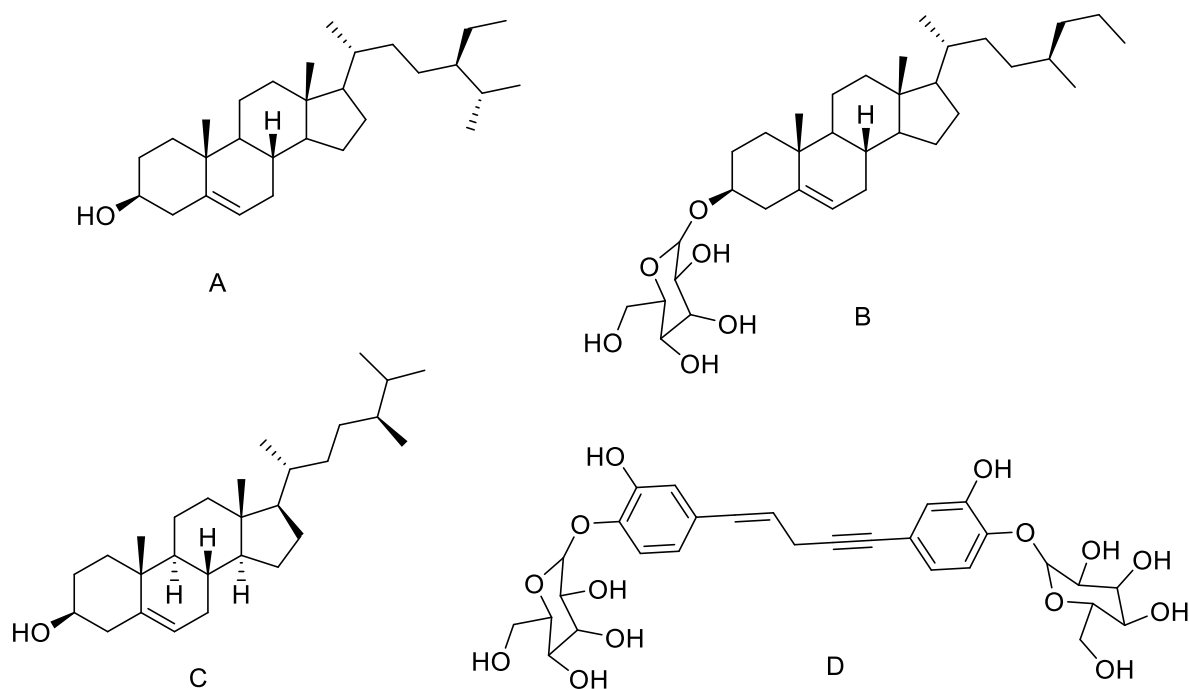
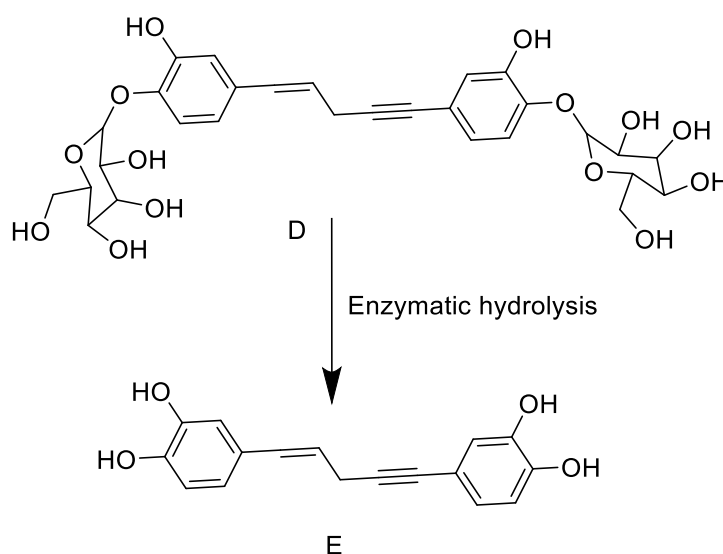




**Figure 2. 7: Structure of (A)  $\beta$ -sitosterol, (B)  $\beta$ -sitosterol glucoside, (C) Campesterol, and (D) Hypoxoside isolated from *Hypoxis Hemerocallidea***

Hypoxoside [(E)-1,5-bis(4'- $\beta$ -D-glucopyranosyloxy-3'-hydroxyphenyl) pent-4-en-1-yne] is a glycosylated norlignan, and it is the major compound found in the corm of HH (Laporta et al., 2007). It has a low toxicity with an uncommon aglycon structure; it is composed of two glucose units at the edges of the two benzene rings in the pentenyne skeleton (figure 2.7D) (Drewes et al., 2008). A lot of research had been conducted on the compound where some associated its presence to many traditional uses of the plant (Drewes & Khan, 2004; Katerere & Eloff, 2008; Ojewole et al., 2006). However, hypoxoside was found to be pharmacologically inactive on its own and is usually converted to its aglycon, rooperol. Conversion of hypoxoside to rooperol is done through hydrolysis of the former by the action of a  $\beta$ -glucosidase enzyme in the human gut (scheme 2.1) (Owira and Ojewole, 2009). Rooperol has fascinating biological activities including anti-inflammatory, anticancer (Boukes and Van De Venter, 2012), antibacterial, immunomodulatory, antioxidant, antitumor, and anti-convulsant activities (Kabanda, 2012).



**Scheme 2.1: Structure of Hypoxoside (D) and the aglycon, Rooperol (E) after conversion using  $\beta$ -glucosidase enzyme.**

## 2.3 *Leucosidea sericea*

### 2.3.1 Occurrence and uses

*Leucosidea sericea* (*L. sericea*) is an evergreen shrub that belongs to the family Rosaceae. This family consists of 3000 species of which only nine are native to southern African

countries like Zimbabwe, Lesotho and South Africa. In South Africa, the shrub is predominantly found in the province of Kwa Zulu-Natal, the Eastern Cape, Free State, Gauteng and Mpumalanga (Sharma et al., 2014).

*L. sericea* is the only species in the genus *Leucosidea*. It occurs mostly near water bodies, at high altitudes, on mountain slopes and grassland. It grows as a dense, small tree (figure 2.8A), a silvery shrub to an approximate height of 7 m (Aremu et al., 2010; Sehlakgwe et al., 2020), with leaves that are star-like and greenish (figure 2.8B). It is commonly called "old wood" in English, from its woody bark (figure 2.8C). In South Africa, it is called "Ouhout" by the Afrikaans and "umTshishi" according to the Zulu people (Sharma et al., 2014). It also has a greenish-yellow floral part as shown in figure 2.8D.



**Figure 2. 8: Images of *Leucosidea sericea* showing (A) whole plant, (B) leaves are alternatively arranged and covered with silver hairs (C) rough dark-brown bark on the surface and reddish inner bark, (D) greenish yellow flowers that brings forth young shoots in spring**

According to the traditional medicinal practitioners, *L. sericea* has been a popular herb among some South Africans for more than one hundred years. Among other uses, the extract of this economic plant has been used as astringent medicine as well as protection against charm. While the Basuto people employed the leaves as a vermifuge, the Zulus used the ground paste from the leaves for ophthalmia (Nair et al., 2012). The leaves are also used by the Sothos to fight intestinal worm infections (Brown et al., 2008). Some of the

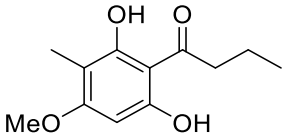
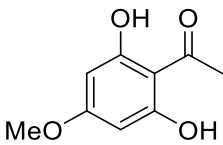
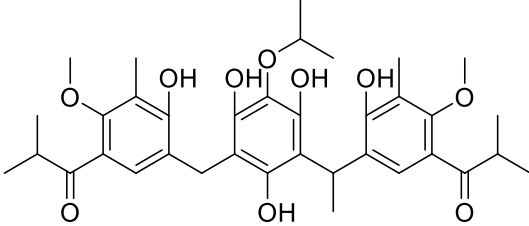
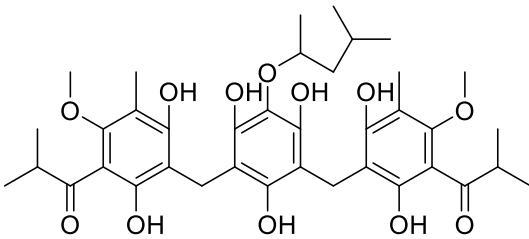
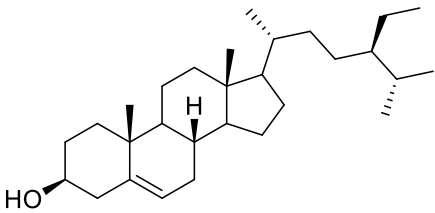
traditional uses were confirmed as the research activities on the different parts of the plant displayed interesting activities.

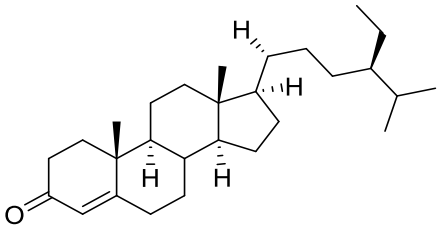
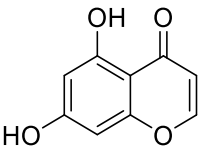
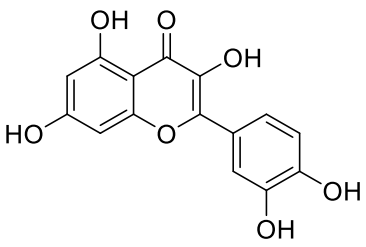
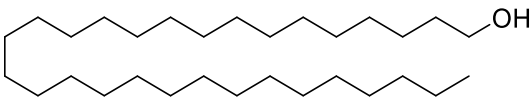
### **2.3.2 The chemistry and biology of *L. sericea* and its isolated compounds**

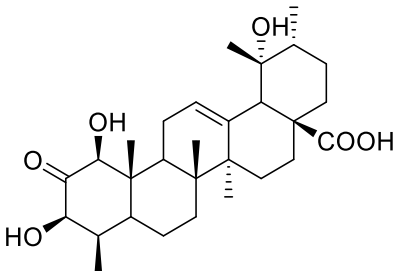
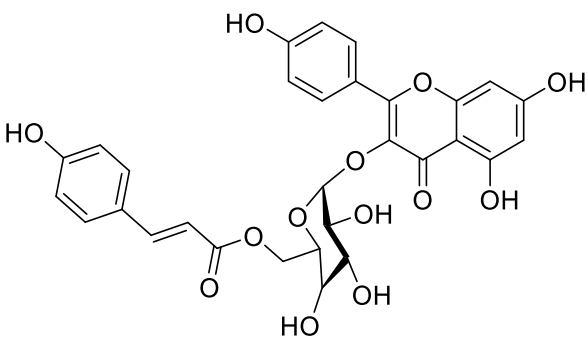
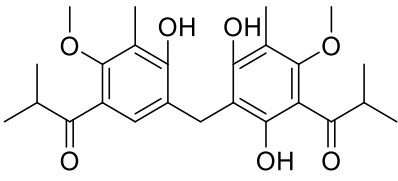
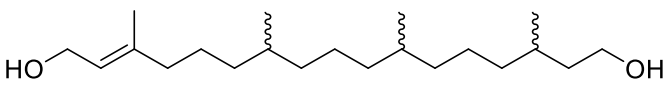
The petroleum ether and dichloromethane (DCM) leaf extracts of this plant showed antibacterial activities against *Bacillus subtilis* and *Staphylococcus aureus* (Aremu et al., 2010). The DCM and ethanolic extract of *L. sericea* also displayed anthelmintic activity (Aremu et al., 2010). Although both leaf and stem showed moderate cyclooxygenase inhibitory activities, the leaf extracts showed better pharmacological activities in general. The leaf also showed a higher quantity of phenolic compounds (Aremu et al., 2010). Other activities such as antioxidant (Adamu et al., 2014; Aremu et al., 2010; Nair et al., 2012), anthelmintic (Adamu et al., 2014; Aremu et al., 2010; Bosman et al., 2004; Nair et al., 2012), and antimicrobial (Aremu et al., 2010; Bosman et al., 2004; Nair et al., 2012) have been reported. The extracts of *L. sericea* have also demonstrated anti-parasitic (Aremu et al., 2012), anti-cancer (Fouche et al., 2008), enzyme inhibitory (Aremu et al., 2010; Sharma et al., 2014), anti-inflammatory (Adamu et al., 2014; Aremu et al., 2010; Bosman et al., 2004; Nair et al., 2012), antiacne (Sharma et al., 2014), antimutagenic, acetylcholinesterase (Aremu et al., 2010; Nair et al., 2012), and skin hyperpigmentation (Lall and Kishore, 2014; Moteetee and Kose, 2017).

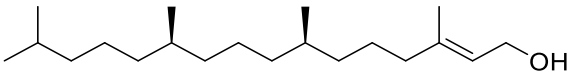
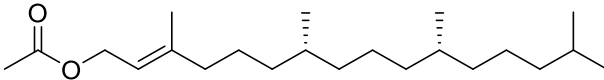
A number of compounds have been isolated and reported from *L. sericea* including triterpenoids (Nair et al., 2012) and a member of the phloroglucinols (Bosman et al., 2004). Other compounds isolated from various parts and extracts of *L. sericea*, together with their biological activities are presented in table 2.1.

**Table 2.1: Compounds isolated from *L. sericea* and their biological activities**

S/N	Isolated compounds	Activity	Reference
1	 <p>Aspidinol</p>	anthelmintic, antiprozoal	(Bosman et al., 2004)
2	 <p>Desaspidinol</p>	N/Av	(Bosman et al., 2004)
3	 <p>Agrimol G</p>	Anthelmintic	(Adamu et al., 2019)
4	 <p>Agrimol A</p>	Anthelmintic	( Adamu et al., 2019)
5	 <p><math>\beta</math>-Sitosterol</p>	Anthelmintic  Anti-inflammatory	(Adamu et al., 2019)  (Nair et al., 2012)

S/N	Isolated compounds	Activity	Reference
6	 <p><math>\beta</math>-Sitosterone</p>	Anti-inflammatory	(Nair et al., 2012)
7	 <p>5,7-dihydroxychromone</p>	N/Av	(Pendota et al., 2018)
8	 <p>3,5,7,3',4'-pentahydroxyflavone</p>	Antioxidant, anti-inflammatory	(Pendota et al., 2018)
9	 <p>Triacontanol</p>	N/Av	(Pendota et al., 2018)

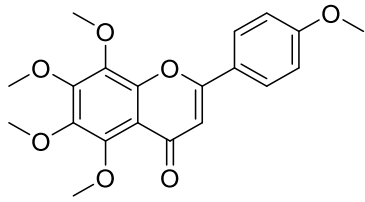
S/N	Isolated compounds	Activity	Reference
10	 <p>1-hydroxy-2-oxopomolic acid</p>	N/Av	(Pendota et al., 2018)
11	 <p>Triliroside</p>	N/Av	(Pendota et al., 2018)
12	 <p>Alpha kosin</p>	Anti-acne	(Sharma et al., 2014)
13	 <p>(E)-3,7,11,15-tetramethylheptadec-2-ene-1,17-diol</p>	N/Av	(Sharma et al., 2014)

S/N	Isolated compounds	Activity	Reference
14	 Phytol	Cytotoxic, antibacterial	(Sharma et al., 2014)
15	 Phytol acetate	N/Av	(Sharma et al., 2014)

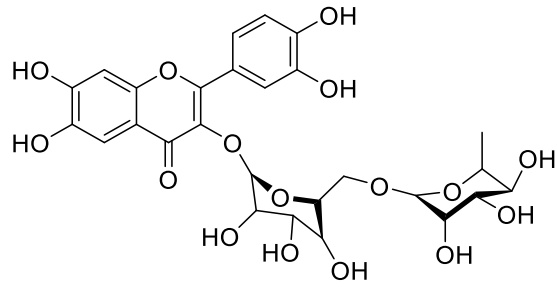
\*N/Av = Information not available in the literature cited

### 2.3.3 Identification of other compounds in *L. sericea* extract based on LC-MS analysis

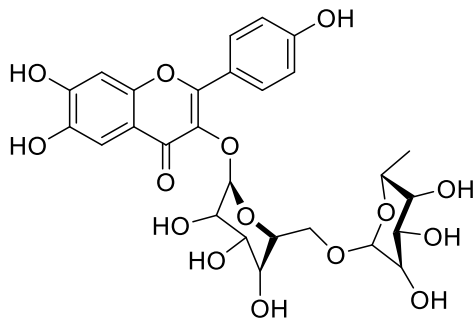
Recently, a group of researchers worked on the aerial parts of this economic plant where they identified additional compounds that were not reported in literature/table 2.1. In their studies, a combination of Nuclear Magnetic Resonance (NMR), Quadrupole Time-of-Flight Mass Spectrometry (q-TOF-MS), and an Ultra-high-performance liquid chromatography that was coupled with mass spectrometry (UHPLC-MS) were employed (Sehlagwe et al., 2020). Some of the newly identified compounds include tangeritin, rutin, Kaempferol-7-O- $\beta$ -D-glucopyranoside, and 2-(4-ethoxyphenyl)-5,6,7,8-tetramethoxy-4*H*-1-benzopyran-4-one, which are presented in figure 2.9.



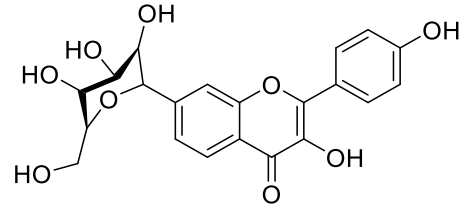
Tangeritin



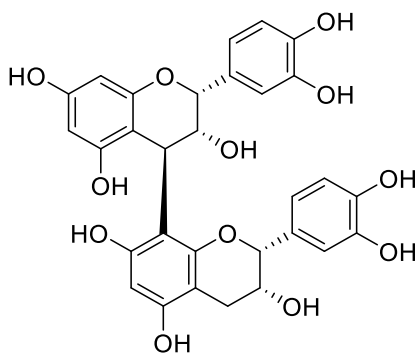
Rutin



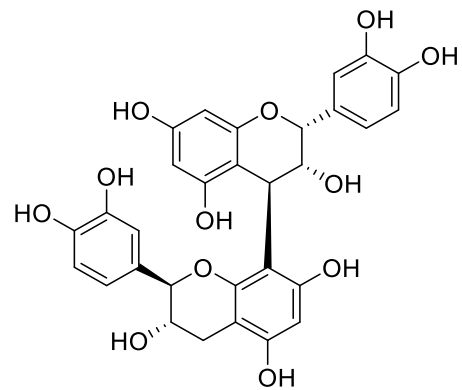
Kaempferol-3-O-rutinoside



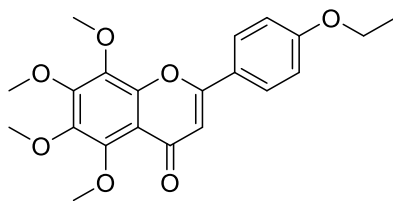
Kaempferol-7-O-beta-D-glucopyranoside



Procyanidin B2



Procyanidin B1



2-(4-ethoxyphenyl)-5,6,7,8-tetramethoxy-4H-1-benzopyran-4-one

Figure 2. 9: Newly identified compounds from the LC-MS analysis of *L. sericea* (Sehlagwe et al., 2020)



### 2.3.2.1 Procyanidins

Procyanidins are a unique group of polyphenols belonging to the anthocyanidins class of flavonoids. They are a representative group of condensed flavan-3-ol. Procyanidins are oligomeric compounds having catechin and epicatechin as the building blocks. They occur in many plants including apples, grape seeds, cranberry, green tea, grape skin and cocoa beans (Souquet et al., 1996; Sun et al., 2013). This class of polyphenols has a special polyphenolic nature which calls for further studies. This characteristic may offer them interesting chemical and pharmacological activities (Berké and De Freitas, 2005; Haslam, 1977).

#### Types and linkages of procyanidins

There are two main types of procyanidins, type A and B. The structural architecture of the procyanidins involves carbon-carbon linkages that are known as the B-type procyanidin linkage. Another type of linkage, referred to as type A, is where procyanidins display a double connection (figure 2.10) (Beecher, 2004).

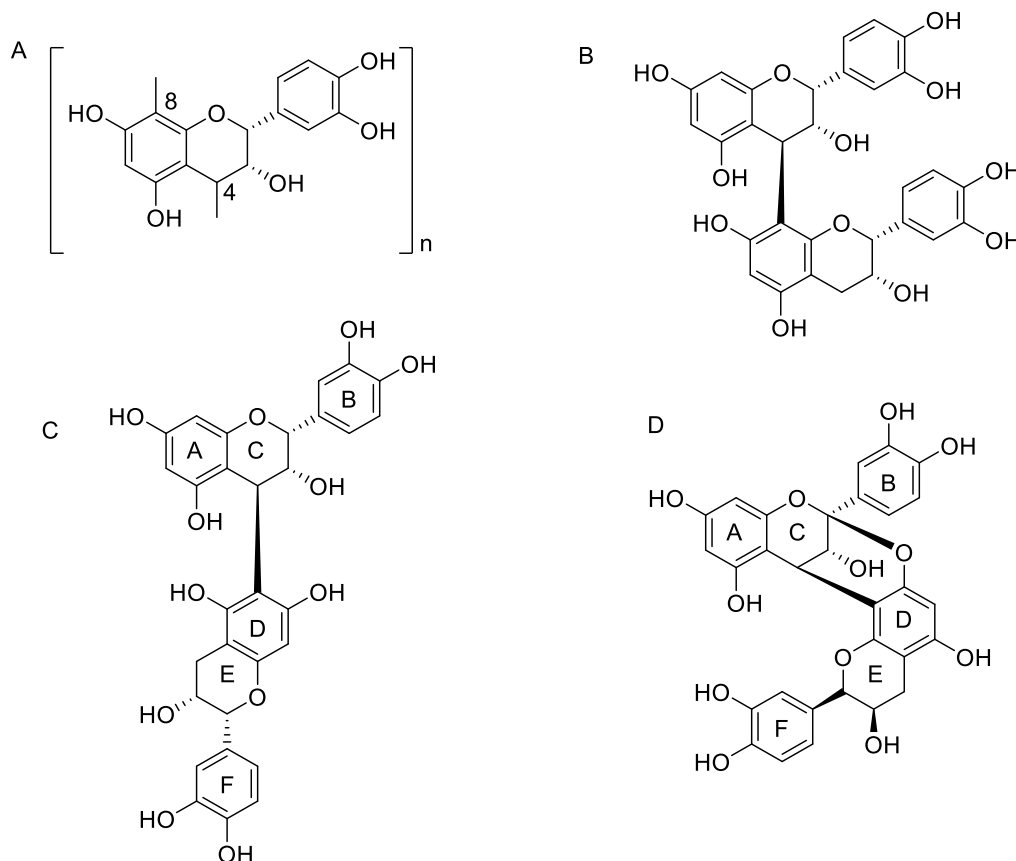


**Figure 2. 10: Demonstration of linkages and types of procyanidin molecules. (A) depicts monomeric (-)-epicatechin with labelled carbon 4 and 8 as the sites for linkage,  $n=1$ ; when  $n=2$ , it's a dimer up to -50. (B) is a procyanidin B2 dimer, showing a B-type (4→8) linkage. (C) shows an example of B-type (4→6) linkage, specifically a procyanidin B5 dimer. (D) represents an A-type dimer, showing (2→7, 4→8) linkages. It is a procyanidin A2 dimer (Beecher, 2004).**

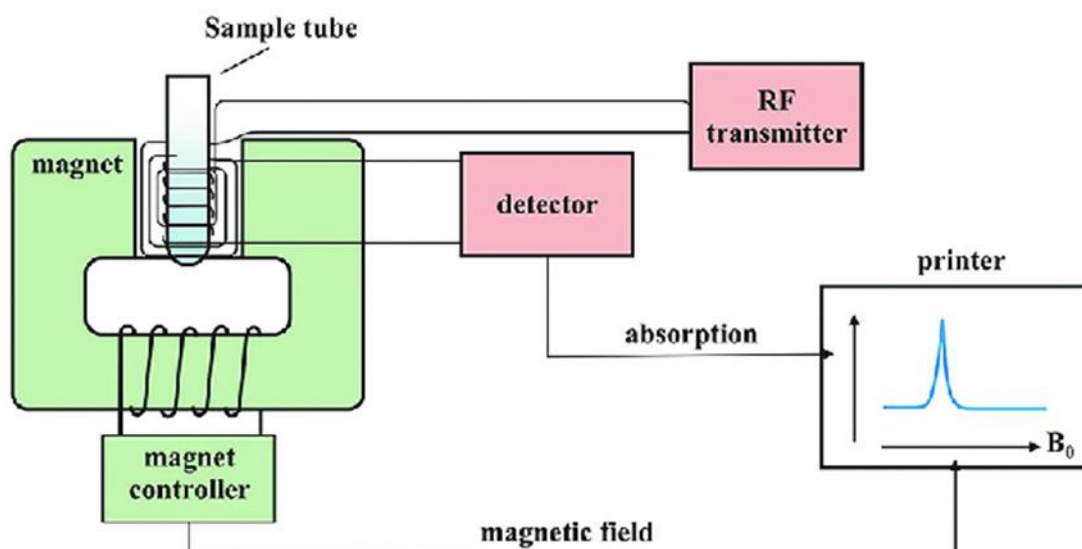
### **Bioactivity of procyanidins**

Although reports have associated these class of polyphenols to many beneficial health effects, the complexity and very similar chemistries of the isomers poses a challenge in their separation and isolation. However, few studies recorded the successful separation of even the A-types from the B-types of these compounds (Dong et al., 2013; Foo & Lu, 1999). In terms of structure-activity relationships, different opinions were reported by various researchers. For instance, while some argue that the A-type dimers exhibited higher activity than the B-types (Maldonado et al., 2005), others believed that the B-types possess more potent activity than the A-types (Beecher, 2004). Yet, some other researchers concluded that there is no difference in the activity between the two types of dimers (Plumb et al., 1998). However, different evaluation protocols were employed in the above studies and as a result, more studies may be required before proper conclusions can be drawn.

## **2.4 Characterization of isolated compounds**

### **2.4.1 Nuclear Magnetic Resonance (NMR) spectroscopy**

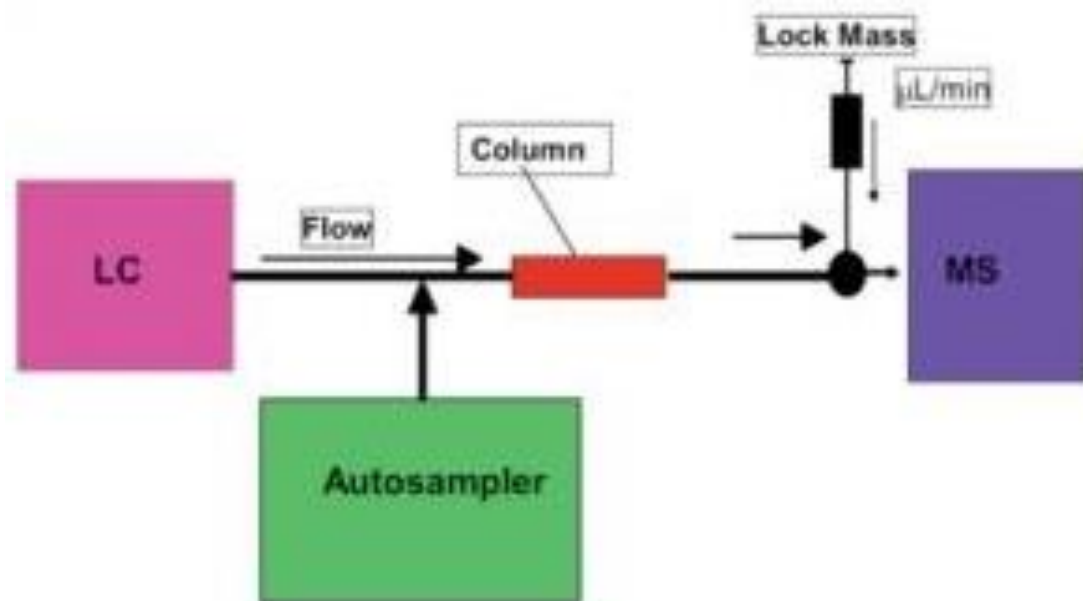
NMR spectroscopy is a commonly used spectroscopic technique often employed to observe the magnetic field around atomic nuclei. From this, the details regarding all the functional groups in a molecule as well as their electronic structure are revealed. Scheme 2.2 shows the major parts of a typical NMR instrument (Zia et al., 2019). The NMR working principle involves placing the sample in a magnetic field. The nuclei of the sample are then excited into nuclear magnetic resonance to produce the NMR signals. This is achieved with the aid of radio waves. Sensitive radio receivers are then used to detect the signals. The resonance frequency of atoms in a molecule is changed by the intramolecular magnetic field surrounding the molecule. While the magnetic coil generates the magnetic field required, the magnetic controller maintains the field homogenously at 60-1000 MHz. The parts work together for a successful operation. Proton and carbon-13 NMR are mostly used, followed by higher 2 D NMR (e.g. COSY, HMBC) depending on the clarity of information from the 1D NMR.



**Scheme 2.2: Schematic diagram showing various components of a typical nuclear magnetic resonance spectrometer (Zia et al., 2019)**

#### **2.4.2 Liquid Chromatography-Mass Spectrometry (LC-MS)**

In the case of complicated fractions, LC-MS may be employed to evaluate the composition before final check on the NMR. The advantage of LC-MS is that it works in synergy, combining physical separation and mass analysis abilities. Because of its sensitivity, as the LC component separates compounds from mixtures, the MS component identifies the individual compounds. The mass-charge ratio, the elution time, and the molecular weight of all the peaks are provided alongside the UV spectra. These are then put together and compared with standard references to identify the compound (Holčapek et al., 2012). A simple schematic diagram is shown in scheme 2.3.



**Scheme 2.3: Schematic representation of a typical Liquid Chromatography-Mass Spectrometry flow chart (Holčapek et al., 2012)**

## 2.5 Nanotechnology

It all started in the run-up to the 1960s, in what was rather termed visionary than science by some quarters when, in his historical lecture in 1959, Richard Feynman, who was a Nobel Prize winner of physics, envisioned the possibility of manipulating matter at the "atomic scale". The title of his lecture "there is plenty of room at the bottom" soon became very popular in the world of science, resulting in several research activities on small metal particles. Although most of the research activities between the 1950s and 1960s were geared towards uncovering Feynman's vision, the term "Nanotechnology" was still not yet used. It was not until 1974 when Dr. Norio Taniguchi from Tokyo Science University first used the terminology when he attempted designing nanosized materials (Pandey et al., 2012). Since then, several advances in the development of NPs were made which served as further confirmation and validation of Feynman's 1959 vision (Bhushan, 2017).

Nanotechnology, therefore, can be defined as "the design, production, characterization, and application of materials, devices and systems by controlling shape and size on the nanoscale" (Bhushan, 2017).

### 2.5.1 Classification of nanostructured materials (NSMs)

When bulky materials are broken down to very tiny pieces, NPs with characteristic features are generated. These unique properties make the hybrid materials very useful in several

industrial applications. Therefore, the overall idea of nanotechnology revolves round the concept of "miniaturization of bulky materials" (Bhatia, 2016).

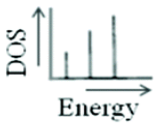
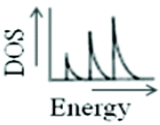
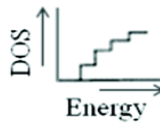
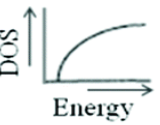


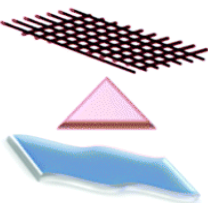

NSMs were first classified by Gleiter in 1995 and further explained by Skorokhod in 2000. However, it was not until Prokropivny and Skorokhod's classification which was an updated version of the previous submissions, that a well-represented classification was achieved (Pokropivny and Skorokhod, 2007). In this all-encompassing categorization, NSMs were broadly classified into four according to their dimensions (figure 2.11) (Gangwar et al., 2015; Tiwari et al., 2012).

**I** - Zero-dimensional (0D) NSMs – All materials have dimensions within the nanoscale (i.e. all dimensions are lower than 100 nm). Examples include metal nanoparticles.

**II** - One-dimensional (1D) NSMs – The materials have two dimensions; one is within the nanoscale and the other outside the nanoscale. Nanowires and nanotubes are examples.

**III** - Two-dimensional (2D) NSMs – The materials here have two of the three dimensions out of the nanoscale. They possess plate-like shapes. Some members are nanolayers and graphene.

**IV** - Three-dimensional (3D) NSMs – These materials have all dimensions in the microscale, not confined to the nanoscale. This group include multi-nanolayers and bundles of nanowires (Tiwari et al., 2012).

Types of nanostructures	0-D	1-D	2-D	3-D
Density of states (DOS)	Quantum dots 	Nano-wires, -tubes, -rods, -fibers, -filaments 	Nano-films, -sheets, -tapes, -layers, -coatings 	Nano-particles, -pores, -flowers, Polycrystals 
Pictorial representation				
Oxides	Al <sub>2</sub> O <sub>3</sub> , TiO <sub>2</sub> , ZnO, CdO	Al <sub>2</sub> O <sub>3</sub> , Y <sub>2</sub> O <sub>3</sub> , Cr <sub>2</sub> O <sub>3</sub> , VO <sub>2</sub> , TiO <sub>2</sub> , MgO	Al <sub>2</sub> O <sub>3</sub> , MoO <sub>3</sub> , NiO, ZnO, TiO <sub>2</sub>	Al <sub>2</sub> O <sub>3</sub> , ZnO, NiO, CuO, MgO
Properties	Optical, Catalysis, Electrical, Electronic, Biological	Thermal fluids, Light detection, Optical, Magnetic, Electrical, Sensors, Biological, Solar cells	Electronics, Mechanical, Photovoltaic, Photocatalytic, Catalytic supports	Optical, Magnetic, Structural, Thermal fluids, Electrochemical

**Figure 2. 11: Classification of nanostructured materials based on dimensionality (Gangwar et al., 2015)**

### Semiconductors nanoparticles (SCNPs)

Semiconductors NPs are important class of NSMs with an array of exciting physical, chemical, optical, mechanical and electronic properties. They have characteristic features of conductors and insulators. SCNPs are formed using different compounds which are in turn obtained when elements of specific groups are combined. Group numbers are used as codes like II-VI and IV-VI (Suresh, 2013). For instance, ZnO and ZnS are SCNPs of the II-VI group, meaning that Zn belongs to the group II whereas O and S belong to the group IV of the periodic table. Because of their unique properties, they have found applications in electronic devices, photo optics, photocatalysis and water splitting (Khan et al., 2019; Suresh, 2013).

### Fullerenes

Fullerenes came to the limelight upon the discovery in 1985 of a molecule of 60-carbon atoms having a hollow sphere that is 1 nm in diameter. The 60-carbon molecule had other names like buckyball or buckminsterfullerene owing to its resemblance with a geodesic dome, which was designed by Buckminster. Subsequent research revealed that fullerenes represent a group of related molecules consisting of 20, 40, 60, 70, or 84 carbon atoms

(figure 2.12). However, the 60-carbon molecule is the most abundant of the group (Bhatia, 2016).

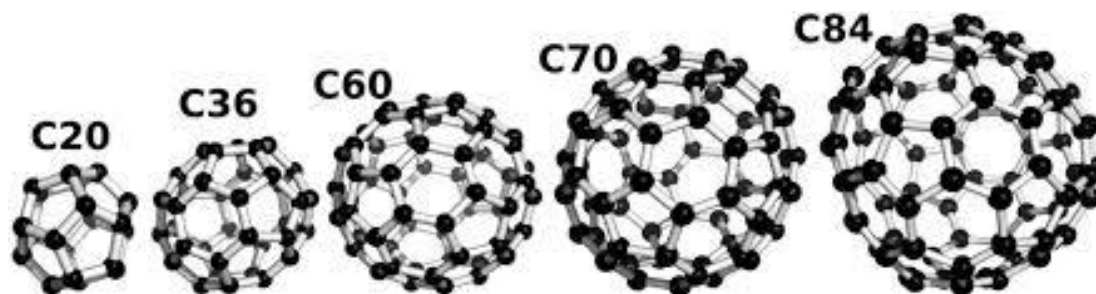


**Figure 2. 12: Structures of C20, C36, C60, C70 and C84 (Huy and Li, 2014)**

Fullerenes are not soluble in water but their derivatives are soluble. The first few studies on the solubility of fullerene derivatives led to the realization of the interactivity of organic fullerene with living cells, DNA and proteins. Fullerene organic derivatives (figure 2.13) soon became very valuable, displaying brilliant biological activities because of their hydrophobicity, photochemistry and radical quenching to form 1-3 dimensional supramolecular complexes. Surprisingly, C60 forms a stable agglomerate under suitable conditions in water. The aggregate of 25-500 nm termed nano-C60 is soluble in water and toxic to bacteria. Fullerenes have been found useful in biomedical applications such as drug delivery, anticancer, antioxidant and are also used in imaging (Mohajeri et al., 2018).

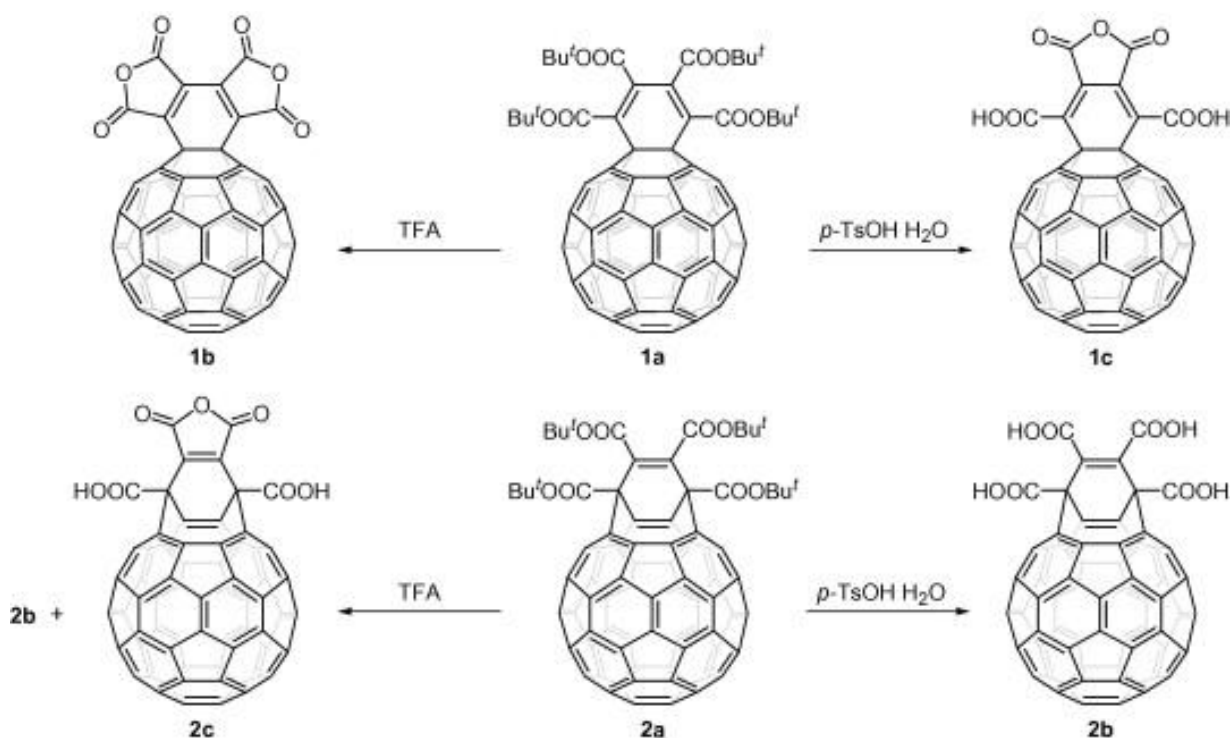


**Figure 2. 13: Scheme showing hydrophilic fullerene organic derivatives (Periya et al., 2004)**

### **Ceramic nanoparticles (CNPs)**

Ceramic NPs are inorganic carbides, oxides, carbonates and phosphates formed by metals and metalloids through heat and successive cooling. CNPs can be fabricated into different forms including hollow, dense and amorphous. (Khan et al., 2019). Because of their unique properties, they have applications in photodegradation of dyes, catalysis, imaging and photocatalysis (Moreno-Vega et al., 2012). Furthermore, the most conspicuous of all the applications of CNPs is in the field of biomedical. CNPs have been reported as excellent carriers of proteins, drugs and genes (Khan et al., 2019).

### **Polymer nanoparticles (PNPs)**

Polymer NPs are synthesized using high molecular weight compounds (macromolecules or polymers). The size, structure and properties of polymers which is as a result of several monomers joined together have especially made them important in nanoparticle fabrication. Their biocompatibility, among other unique qualities, had made them useful in biomedical applications like bioimaging, biosensing but chiefly in drug delivery (Jain et al., 2008). Although these properties are shared irrespective of the nature of the precursor (synthetic or natural), the natural polymers are very popular for drug delivery. Nanopolymers are mostly non-toxic, biocompatible, biodegradable and can be linear or branched. The linear



nanopolymers usually carry the functional groups over the length of the polymer while the branched counterpart have them on the surface (Jain et al., 2008; Vega et al., 2012).

### Carbon nanotubes (CNTs)

From its first discovery in 1991, carbon nanotubes had continued to draw the attention of researchers because of their interesting properties (Iijima, 2002). CNTs are graphene sheets constructed with an allotropic variety of hexagonal carbon atoms that are folded up into beautiful hollow cylinders (figure 2.14) (Bhatia, 2016). The cylindrical shapes can be closed or open at one end or both. They can be made into one graphene layer, single-walled carbon nanotubes (SWCNTs), or more layers, multi-walled carbon nanotubes (MWCNTs). The SWCNTs are about 1-2 nm in diameter whereas the MWCNTs can have a diameter of less than 100 nm (Khan et al., 2019). CNTs have widespread of lengths, from few nanometers to several centimeters, implying that they combine the two scales. They possess high thermal conductivity and surface area and they are mechanically strong. CNTs have been used in antiviral and antibacterial therapies and have demonstrated antibacterial activity against *E. coli*.

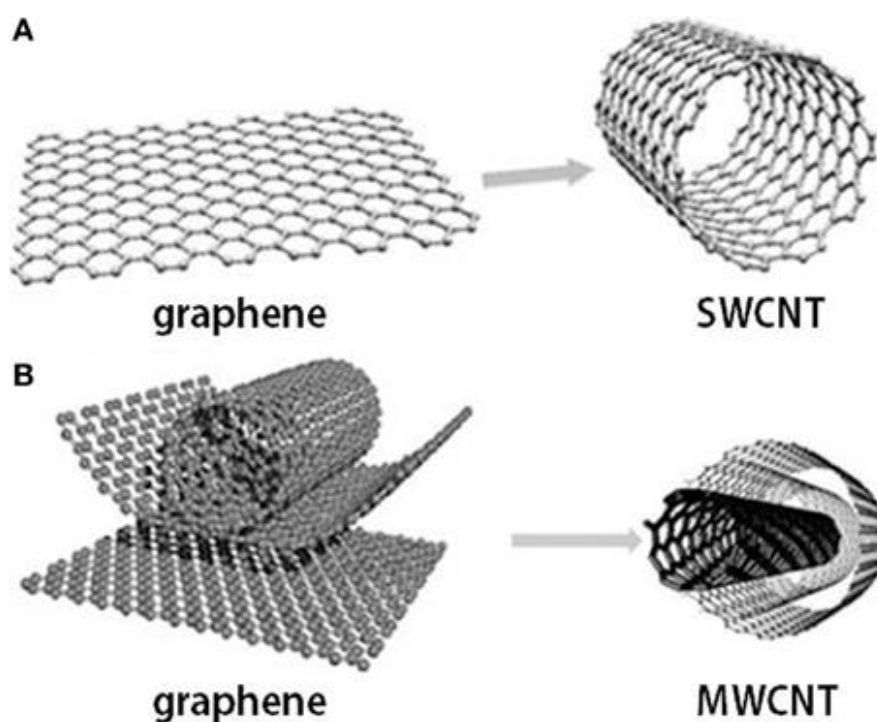


**Figure 2. 14: Structures of graphene (left), (A) single-walled carbon nanotubes and (B) multi-walled carbon nanotubes (Vidu et al., 2014)**

CNTs have very good surface chemistry, thereby making it easy to functionalize with different organic, inorganic and biological molecules to the corresponding derivatives, many

of which have demonstrated interesting biomedical applications like tissue regeneration, bioimaging, biosensing drug targeting and delivery (figure 2.15) (Erol et al., 2018).

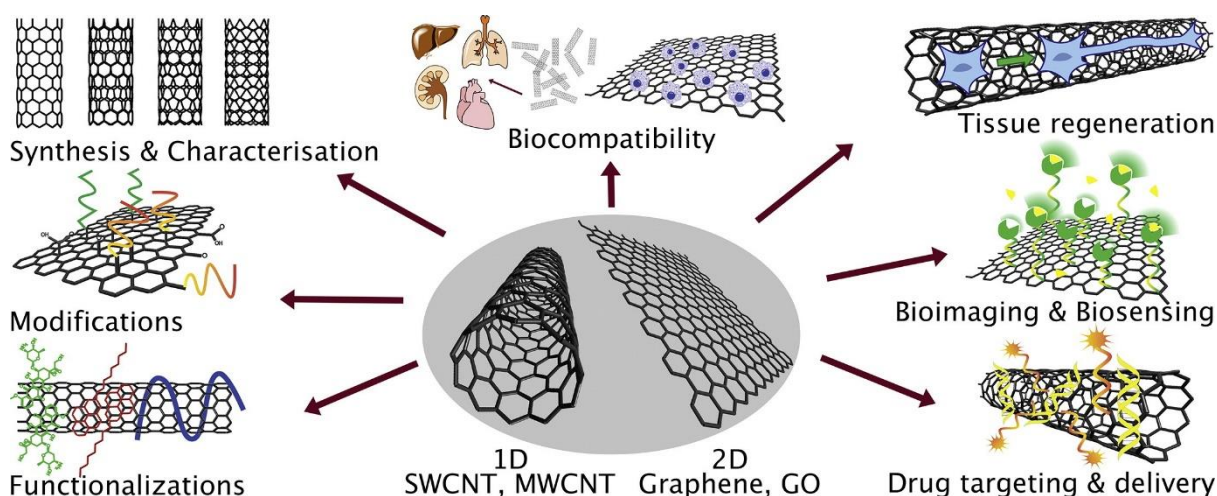


**Figure 2. 15: Functionalization and applications of CNTs (Erol et al., 2018)**

### **Lipid-based nanoparticles (LBNPs)**

Lipid-based NPs are formed using biocompatible, biodegradable and less toxic lipids. There are two types of lipid nanoparticles, the solid lipid nanoparticles with a solid matrix (SLNPs), and the nanostructured lipid carrier (NLC) (Bhatia, 2016). Like liposomes, nanoemulsions and polymer nanoparticles, SLNPs possess excipients that are biocompatible, physiologically accepted and have perfect protection for loaded drugs against degradation in harsh conditions. Thus, SLNPs are nanospheres (50-1000 nm in diameter) with a solid lipid core. Although NLC shares the above qualities with SLNPs, they have advantages such that they compose of a mixture of liquid lipids and solids which offers the mixture more drug incorporation than in SLNPs (figure 2.16) (Sharma, 2019). NLC's matrix is solid at room temperature and remains so when the liquid lipid content is controlled (Kaur and Bhullar, 2016). Both SLNPs and NLC are excellent drug carriers, however, while SLNPs' dispersed drugs are mainly positioned between the fatty acid chains of the glycerides, a blend of solid-liquid lipid is employed for those of NLC (Ganesan and Narayanasamy, 2017).

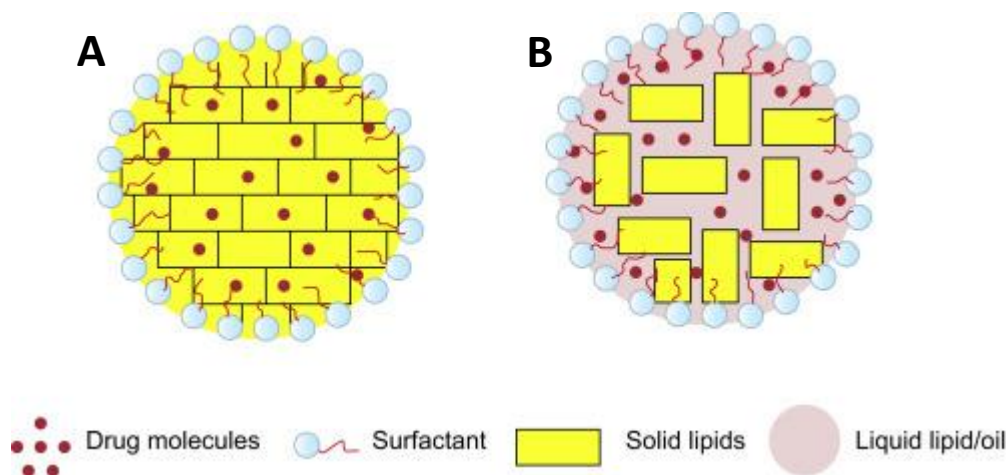


**Figure 2. 16: Scheme representing (A) Solid Lipid Nanoparticle (SLNPs) and (B) Nanostructured lipid carrier (NLC) (Sharma, 2019)**

### **Metal nanoparticles (MNPs)**

Over the past few decades, renewed attention has been given to MNPs by researchers all over the world because of many unique features of these materials. Different metal salt solutions have been employed as a precursor for MNPs synthesis. Therefore, many MNPs like those of silver (Bharathi et al., 2018; Das et al., 2020; Patil et al., 2019; Shah et al., 2020), gold (Ponnanikajamideen and Rajeshkumar, 2019; Shamprasad et al., 2019; Zayed and Eisa, 2014), copper (Bin-Umer et al., 2014), titanium (Prasad et al., 2007) and strontium (Chen and Chen, 2002) have been fabricated. Gold and silver NPs were more extensively explored owing to their superior features over other metal nanoparticles. In the biomedical field, gold and silver NPs have been reported to possess antioxidant (Zayed et al., 2020), antibacterial (Valsalam et al., 2019), antidiabetic (Elobeid, 2016), anticancer (Kasthuri et al., 2009b) and fluorescence quenching (Vasimalai et al., 2012; Zhang et al., 2020) properties. Others include photothermal therapy (Zhang, 2015), photodynamic therapy (Vankayala et al., 2013), drug delivery (Tripathi and Chung, 2019), an x-ray contrast agent (Elahi et al., 2018) and as sensors (Jeon et al., 2016).

### **2.5.2 Synthesis of metallic nanoparticles**

The top-down and bottom-up techniques are the two main techniques employed in the synthesis of metallic nanoparticles (figure 2.17). The top-down route involves the use of physical procedures like thermal decomposition, irradiation, sonochemical, laser ablation, and ball milling for the fabrication of nanoparticles. In this approach, bulky starting materials

would be broken down into smaller pieces of the desired size and shape. To achieve this, the material needs to be cut, etched, milled or ground to such sizes. However, the inability to control the size and shape of the nanoparticles (NPs) fabricated from this method is its major drawback (Zhao et al., 2013).

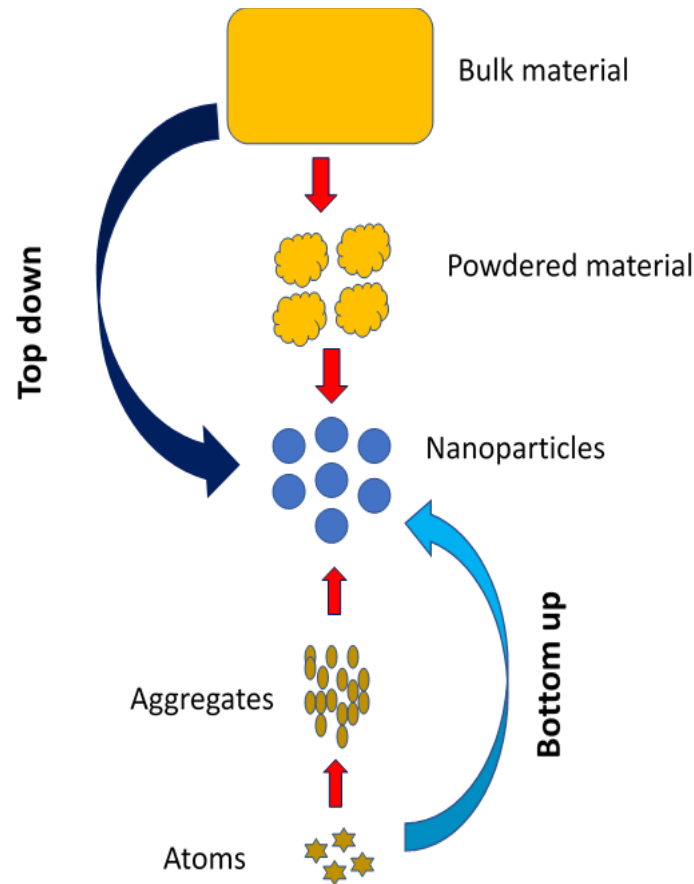


**Figure 2. 17: A scheme showing the top-down and bottom-up procedure for synthesis of nanoparticles**

On the other hand, the bottom-up approach is about building the NPs through the combination of small materials like the atoms and molecules (figure 2.17). Common techniques employed in this process include sol-gel, chemical reduction, electrochemical, and green synthesis (figure 2.18). These methods provide an opportunity for the synthesis of gold and silver NPs. For instance, a pioneering synthesis of gold nanoparticles (AuNPs) by the Turkevich method involves the use of sodium citrate as the reducing agent as well as the stabilizing agent and yields 15 nm spherical NPs (Turkevich et al., 1951). Subsequent modifications to this method resulted in the formation of hundreds of AuNPs with different morphologies and sizes up to 150 nm. These were achieved by changing synthesis conditions like the concentration and ratio of the gold salt solution to sodium citrate or varying the temperature of the reaction (Tran et al., 2016). Sodium borohydride was another

common reducing agent used in the early years of metallic nanoparticle synthesis (MNPs), giving a more rapid synthesis at room temperature when compared to sodium citrate. In order to avoid agglomeration of synthesized NPs, stabilizing agents can be used. External stabilizers have been employed when working with some reducing agents, while in other instances, the reducing agent also served as the stabilizing agent (Zhao et al., 2013).

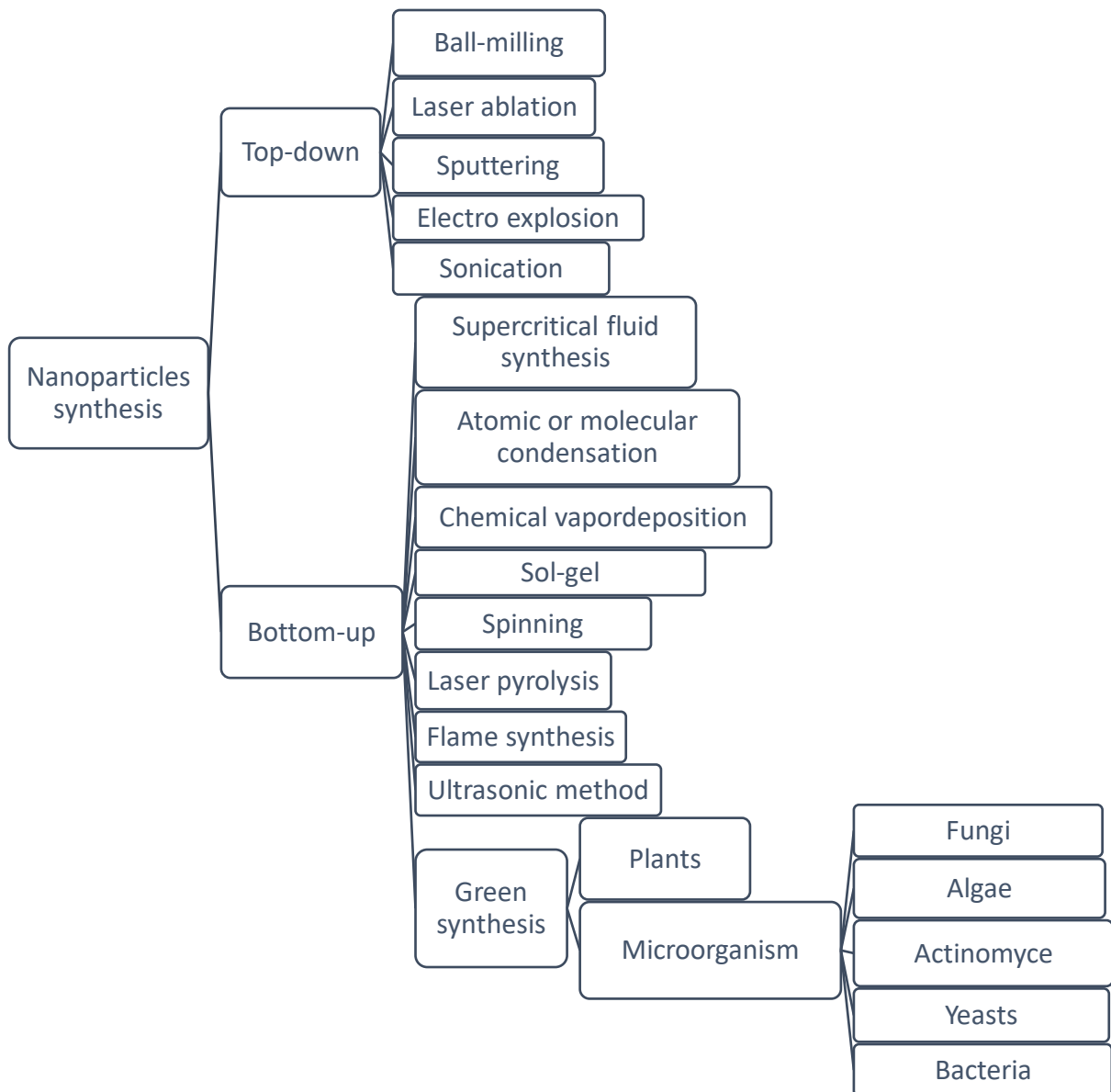


**Figure 2. 18: Different top-down and bottom-up synthesis methods of nanoparticles**

### **2.5.2.1 Green synthesis of nanomaterials using plant resources**

Green nanotechnology has to do with deliberate attempts aimed at the development of reasonable and meaningful procedures to produce materials as well as their related developmental processes in an environmentally friendly manner to reduce the use of harsh and hazardous chemicals (Wong and Karn, 2012). Thus, green nanotechnology is intended to directly or indirectly save living organisms while making sure that reduced or no harm is done to the environment. Although green nanotechnology may involve the use of microorganisms like algae, fungi and bacteria, the use of the plant has a series of advantages such as ease of handling, availability and non-toxicity over other resources.

The physical and chemical protocols of nanomaterials synthesis were popular until subsequent research pointed out some of their demerits. In those methods, the synthesis was conducted at elevated temperatures that consume more energy, requiring specialized instruments and chemicals such as hydrazine, ethylene glycol, dimethylformamide and sodium borohydride were termed hazardous. Unlike the above procedures, green synthesis offers a variety of advantages in line with the principles of green chemistry. For instance, the resources employed are often biological like bacteria, algae, fungi and plants. Plant materials are especially readily available, easily accessible and affordable. The chemicals are usually eco-friendly, making the environment safe from toxic remnants. Other advantages include cost-effectiveness as sophisticated instrumentation is not required. Atom economy is also of significant benefit as small quantities of the plant materials are enough against cutting down kilograms of plant parts. In line with the principles of green chemistry (Table 2.2), the biosynthesis of MNPs is desirable because of its simplicity and the fact that it can be easily scaled up to a larger scale.

**Table 2.2: The 12 principles of green chemistry**

<b>S/N</b>	<b>Postulates</b>	<b>Brief explanations</b>
1	Prevention	It is better to prevent waste than to treat or clean up waste after it is formed
2	Atom economy	Synthetic methods should be designed to maximize incorporation of all materials used in the process into the final product.
3	Less hazardous chemical synthesis	Wherever practicable, synthetic methodologies should be designed to use and generate substances that possess little or no toxicity to human health and the environment
4	Designing safer chemicals	Chemical products should be designed to preserve efficacy of function while reducing toxicity
5	Safer solvents and auxiliaries	The use of auxiliary substances (e.g. solvents, separation agents, etc.) should be made unnecessary wherever possible and innocuous when used
6	Design for energy efficiency	Energy requirements should be recognized for their environmental and economic impacts and should be minimized. Synthetic methods should be conducted at ambient temperature and pressure
7	Use of renewable feedstocks	A raw material of feedstock should be renewable rather than depleting wherever technically and economically practicable
8	Reduce derivatives	Unnecessary derivatization (blocking group, protection/deprotection, temporary modification of physical/chemical processes) should be avoided whenever possible
9	Catalysis	Catalytic reagents (as selective as possible) are superior to stoichiometric reagents
10	Design for degradation	Chemical products should be designed so that at the end of their function they do not persist in the environment and break down into innocuous degradation products
11	Real-time analysis for pollution prevention	Analytical methodologies need to be further developed to allow for real-time, in process monitoring and control prior to the formation of hazardous substances
12	Inherently safer chemistry for accident prevention	Substances and the form of a substance used in a chemical process should be chosen so as to minimize the potential for chemical accidents, including releases, explosions, and fires

As postulated by Anastas and Warner (1998), green synthesis is built on three main guidelines: the selection of eco-friendly and benign (1) solvent (2) reducing agents and (3) safe stabilizing agents. Overall, the synthesis is generally rapid, taking a few minutes to a couple of hours and the hybrid materials have exciting characteristics that had made them the focus of the modern-day research.

Green protocols of synthesizing MNPs (for example, gold, and silver) means the use of plants' phytoconstituents as the reducing agents and at the same time as the stabilizing agents instead of toxic chemicals. Among the disadvantages in the use of harsh chemicals is the toxicity concern which can cause adverse effects in the eventual biomedical applications of such new NPs (Philip, 2010). Thus, attention has been drawn towards the use of phytochemicals from medicinal plants as a source of reduction. Using plant-derived phytoconstituents, several studies have demonstrated complete elimination of such harsh chemicals, thereby resulting in totally green and environmentally friendly procedures to produce NP-based smart materials (Chanda et al., 2011). Thus, through the green chemistry route, hundreds of plant extracts have been used to form nanoparticles of various sizes and shapes that are biodegradable, biocompatible and with improved properties compared to the bulk precursor of metal salts (Dhavan and Jadhav, 2020; Göl et al., 2020; Hemmati et al., 2020).

#### **2.5.2.1.1 Reducing and stabilising ability of plant extracts and its phytoconstituents”**

From time immemorial, plants have played great roles in providing health remedies in most of our rural areas. Thus, hundreds of research reports have demonstrated their antifungal, anti-inflammatory, antibacterial, antioxidant, antiviral and antitumor activities (Ahmad et al., 2017; Valsalam et al., 2019). These biological properties make plant extracts fascinating surface modifiers of nanoparticles which also possess interesting properties. Therefore, plants have multipurpose functionality since the extracts are also able to bring about reduction and serve as capping agents in nanoparticle synthesis (Ranoszek-soliwoda et al., 2019). Teimuri-mofrad et al. (2017) concluded that natural product substances such as plants are endowed with important chemicals possessing both reduction and stabilization capabilities. The list includes extracts of some naturally occurring plants or even parts of plants such as leaves, roots, fruits and stems (Chung et al., 2016). In most of these plants, polyphenols are believed to play important role in the reduction processes. The chemistry of these phenolics offer them diverse metal-chelating ability (Ovais et al., 2018).

To fabricate nanoparticles with plant extracts, different metal salts have been used. Transition metal salts have mostly been employed because of interesting properties of the



metals such as variable oxidation states owing to the availability of empty d or f orbitals. Nanosized gold, silver, iron, copper, platinum as well as oxides of some of these metals have been synthesized using plant materials (Bin-Umer et al., 2014; Shah et al., 2020; Veena et al., 2019).

Green protocols of synthesizing MNPs (for example, gold and silver) mean the use of plants' phytoconstituents as the reducing agents and at the same time as the stabilizing agents instead of toxic chemicals. Among the disadvantages in the use of harsh chemicals is the toxicity concern which can cause adverse effects in the eventual biomedical applications of such new NPs (Philip, 2010). Thus, attention has been drawn towards the use of phytochemicals from medicinal plants as a source of reduction. Using plant-derived phytoconstituents several studies have demonstrated complete elimination of such harsh chemicals resulting in totally green and environmentally friendly procedures to produce NP-based smart materials (Chanda et al., 2011). Thus, through the green chemistry route, hundreds of plant extracts have been used to form nanoparticles of various sizes and shapes that are biodegradable, biocompatible and with improved properties compared to the bulk precursor of metal salts (Dhavan and Jadhav, 2020; Göl et al., 2020; Hemmati et al., 2020). These nanomaterials have found applications in many fields including biomedical (Chokkalingam et al., 2019; Sanjana et al., 2019). The overall benefit is that the biomolecules are in abundance in plant and are not toxic. Examples include flavonoids, tannins, quinines, terpenoids, polyphenols and alkaloids (Islam et al., 2019; Liu et al., 2017).

Interestingly, characteristic features of the nanomaterials can be controlled through manipulation of the parameters like temperature, pH, reaction time, the concentration of both the metal salt solutions and the reducing agent (phytochemicals) to get the desired products (Pandey et al., 2012).

Phytochemicals are bioactive components that are naturally available in plants and have been found to be essential to the plants and also play important roles in the human diet (Nisha and Anbu, 2017). Over the decades, plants have been reported to have interesting properties such as antioxidant (Adamu et al., 2014; Aremu et al., 2010; Nair et al., 2012), anthelmintic (Adamu et al., 2014; Aremu et al., 2010; Bosman et al., 2004; Nair et al., 2012) and antimicrobial (Aremu et al., 2010; Bosman et al., 2004; Nair et al., 2012).

Several plant resources have been shown to contain powerful antioxidants constituents in their parts including leaves, stems, aerial parts, rhizomes, bulbs, tubers, fruits and flowers. As some of these parts also form part of man's food (e.g. vegetables and fruits), the natural antioxidants are ingested as they are consumed. This has been happening for centuries and the antioxidants have been known to be harmless in addition to their health-promoting

potential. Many studies also concluded that natural antioxidants are not toxic to the environment (Chanda et al., 2011). Until the advent of green nanotechnology, the phytoconstituents were mainly popular because of their antioxidant properties. Nowadays, hundreds of studies had been conducted all over the world in the area of green synthesis using several plant materials. It has been found that the phytochemicals play crucial roles in the synthesis of metallic nanoparticles (Ovais et al., 2018; Shah et al., 2020; Subbaiya et al., 2017; Sunderam et al., 2019). In addition, the results indicate that the antioxidants (phytoconstituents) may not only be responsible for the reduction of metal ions but also serving as capping agents (Shukla et al., 2008; Ovais et al., 2018; Hemmati et al., 2019).

#### **2.5.2.1.2 Factors affecting nanoparticle formation and stability using phytochemicals**

According to researchers (Fierascu et al., 2019; Ramzan and Yousaf, 2018), noble metals, including platinum, copper, gold, palladium and silver NPs have been synthesised using the phytoconstituents from plants. The first stage in the process involves the conversion of the metals from their atomic forms to the ionic forms (e.g. silver ion from the silver atom) since they are in solution. Next is the conversion of these ions from their mono-, di- or trivalent states to the zero-valent oxidation states and in the third stage nucleation takes place. This then graduates into the growth stage where nuclei come together to form NPs of different sizes and shapes. The final stage involves growth control which dictates the size and shape of the final product. At this stage, the phytoconstituents play a great role in capping the growing NPs and quenching the growth. This is presumably achieved because of the presence of certain functional groups in the phytoconstituents such as the hydroxy groups (Ovais et al., 2018).

Therefore, the type of phytoconstituents in addition to the pH, the concentration of the precursors, reaction temperature and the reaction time are all factors that can affect the morphology and stability of the given NPs.

#### **Effect of pH**

Several studies have demonstrated how pH can influence the result in the synthesis of NPs. In general, a lower pH has been shown to produce NPs of bigger sizes whereas the smaller ones were fabricated when the pH is neutral or in the basic region (7-14) (Khalil et al., 2014). Singh and Srivastava (2015) observed a decrease in the sizes of NPs when the pH was changed from 3 to 7. They also noticed a gradual increase in size as the pH goes from 7 to 11. Other researchers found that at pH 2.0, the size of NPs was up to 85 nm but became about 20 nm when the pH was increased to about 4.0. The authors associated this to limited

accessibility to more functional groups at very low pH values (Armendariz et al., 2004). Relatively, Khalil and colleagues believed that one of the great influence of pH on the reaction mixture is its ability to alter the electrical charges of the phytochemicals involved, which can affect its capping and subsequently affect the size of the NPs (Khalil et al., 2014). They further observed that a larger size was obtained at pH 3.0 compared to pH 8.0 when they synthesized AgNPs using olive leaf extract. Hence, the alkaline environment enhanced the reducing and capping abilities of the phytoconstituents.

### **Effect of the precursor concentration**

The concentration of precursor starting materials can greatly influence the synthesis of NPs. In this regard, the precursors can be categorized into the metal salt solution and the concentration of the plant extracts or the individual phytochemicals. Taking gold or silver salt solutions into consideration, many reports utilized low concentrations in millimolar (mM). For example, 1 mM (Fatimah, 2016) and 1.75 mM (Sithara et al., 2017) silver nitrate ( $\text{AgNO}_3$ ) solution synthesized interesting AgNPs through various reducing agents. Similarly, 1 mM solutions of various auric acid solutions were used in the formation of AuNPs using banana peel (Bankar et al., 2010), *Chenopodium album* (Dwivedi and Gopal, 2010) and *Sorbus aucuparia* (Dubey et al., 2010) extracts.

Conversely, an increase in the concentration (0.1 – 5 mM) of leaf extract has been reported to affect the colour of the synthesized NPs. A colour change from reddish-yellow to deep red was observed for the AgNPs (Dwivedi and Gopal, 2010). It was also observed that at higher concentrations (5 mM) of leaf extracts, sharper absorbance and smaller sizes of the NPs were obtained (Dwivedi and Gopal, 2010). Chandra and colleagues also shared the same views (Chandran et al., 2006). Recently, Aritonang et al. (2019) reported silver nanoparticles with a broad band distribution when the concentration of *Impatiens balsamina* and *Lantana camara* was 1 mM. As the concentration was increased to 5 mM, particles with a narrow size distribution was obtained.

### **Effect of temperature**

For any reaction to take place, the reactants (atoms, molecules, etc.) must interact and this require some form of energy. The temperature at which every reaction takes place is of great significance to the rate of such reactions. In general, reactions tend to go faster at higher temperatures due to more chances of collision by the reactants. For example, with a temperature increase from 25 to 150 °C, the time taken for the formation of gold NPs decreased and smaller size particles were formed (Dubey et al., 2010). In another study, the

synthesis of gold and silver nanoparticles took up to two hours at 20 °C. However, when the temperature was increased to 100 °C, the nanoparticles were formed within 15 minutes (Dwivedi and Gopal, 2010). Zhan et al. also affirmed that a larger size of 200 nm AuNPs was formed when the temperature was 30 °C but decreased to 115 nm as the temperature was increased to 90 °C (Zhan et al., 2011). They further reported that at elevated temperature, rapid reduction and subsequent stabilization might have prevented aggregation, leading to the NPs with smaller size and narrow particle size distribution.

### **Effect of time**

The time taken by a given reaction to go to completion is another important factor that can affect the synthesis of MNPs. As mentioned earlier, the synthesis of NPs involves different stages including the nucleation and encapsulation stages. It is therefore necessary that a given stage is given its required time of completion for optimum results. In a study conducted by Dubey and colleagues, it was found that it took only 10 mins to achieve the complete synthesis of AgNPs using Tansy fruits (Dubey et al., 2010). Similarly, Das and co-workers reported the initial formation of AuNPs after 10 mins even though the SPR band was broad. Between 10-20 mins, the intensity kept increasing until it became narrower and stable after 20 mins. They, therefore, considered 20 mins as the optimum reaction time for the fabrication of AuNPs using *Calotropis procera* latex leaf extract (Das et al., 2011). Another group of researchers, however, noted that for a reaction at 60 °C, the SPR band for AgNPs appeared after 1h and continued to increase as the reaction time advanced (Darroudi et al., 2011). As the reaction continued, the SPR continued to blue-shift and consequently implied a decrease in the particle size. By the 48th hour, no noticeable changes were observed in the SPR and this was taken as the time when the reaction had reached completion (Darroudi et al., 2011). In summary, it can be inferred that the reaction for the successful synthesis of metallic nanoparticles is subject to factors like the type of plant and its constituents, in addition to the reaction temperature and concentration of the precursors.

### **Effect of phytochemicals as reducing agents**

The quantity and type of reducing agent does not only affect the reaction time but it can also affect the morphology and stability of the NPs. Some researchers (Shervani and Yamamoto, 2011) found that when two different reducing agents were employed, different AuNPs were produced, even though the same method of synthesis was employed. In another study, twenty amino acids were employed as reducing agents in AuNPs synthesis (Maruyama et al., 2015). While some amino acids formed the NPs with red colours, others showed purple

colouration. Yet, some of the acids formed NPs but highly unstable as they easily precipitated. It was further observed that three of the amino acids could not form the NPs (Maruyama et al., 2015). More recently, phloridzin (PLZ), a phytochemical commonly found in fruits and its aglycon, phloretin (PLT) were both used to fabricate AuNPs. Different sizes were obtained for PLZ-AuNPs (15 nm) and PLT-AuNPs (8 nm) (Payne et al., 2018). Furthermore, silver nanoparticles were synthesized using a whole plant extract and a thidiazuron-induced callus extract of *Linum usitatissimum*. Since the phytochemical content of the latter was higher than the former, the synthesis was faster. In addition, smaller and well-distributed particles were observed for the latter (Press, 2016b).

Because of their chemistry, polyphenols are very important phytochemicals with lots of health-related benefits to humans and other animals. They also play significant roles in the protection and repair of damaged tissues to the host plants. However, until the advent of nanotechnology and green chemistry, little was known about their role in nanoparticle formation and capping ability.

Silver nanoparticles were synthesized successfully using the extract of *Gardenia jasminodes* (Lü et al., 2014). The extract did not only reduce but also stabilized the silver nanoparticles. It further was observed that polyphenols, proteins, flavonoids, reducing sugars, genoposide and chlorogenic acid in the extract may have been involved in the synthesis as well as stabilization of the nanoparticles.

Rajawat and Qureshi, (2012) reported theaflavins and thearubigins present in tea as mild reducing and capping agents when introduced to their electrolytic synthesis of silver nanoparticles. They also investigated biosynthesized silver nanoparticles on *Pseudomonas aeruginosa* alongside antibiotics such as ampicillin and gentamicin and concluded that the polyphenols, theaflavins and thearubigins acted as capping agents due to their bulky nature.

Quantitative studies of phytochemicals involved in the synthesis of silver nanoparticles using aqueous leaf extract of *Rhizophora apiculata* were also reported (Karthick et al., 2014). Accordingly, polyphenols were confirmed to be responsible for the biosynthesis. To quantify the bioactive components, spectrophotometric methods were used before and after the reduction process. Closely related to this, Anand and colleagues reported prolonged stability of silver nanoparticles from *Mimusops elengi* seed extract and ascribed it to the capping action of oxidized polyphenols (Anand et al., 2014). It was further showed that gallic acid, ascorbic acid, pyrogallol and resorcinol were present in the extract.

Raja et al. (2015) reported the synthesis of stable silver nanoparticles using the aqueous extract of pods of *Peltrothorum pterocarpum*. They used FTIR to confirm the biomolecules involved as polyphenols. Rabie and Raie, (2015) also exposed seedlings of *Medicago sativa*

to an aqueous solution of silver nitrate and obtained silver nanoparticles of about 30 nm. Spectroscopic techniques were used to confirm that the plant components responsible for the biosynthesis of the silver nanoparticles may be polyphenols.

The leaves and seeds of *Coriandrum sativum* have been evaluated over decades for their interesting antioxidant properties. However, the extracts proved to have more to offer as it showed the ability to synthesize metallic nanoparticles (Luna et al., 2016). Through a green synthetic route for the study of silver nanoparticles, it was observed that carboxylate ions, hydroxyl groups and free amines were responsible for the reduction of silver ions and subsequent stabilization. The hydroxyl groups were believed to be from polyphenols. Ranoszek-soliwoda et al. (2019) successfully synthesized monodispersed silver nanoparticles using *Theobroma cacao* and *Vitis vinifera L. extracts* and attributed it to the abundance of polyphenols e.g. tannic acid, catechin and epicatechin gallate in the plant.

In the continuous search for the phytochemicals responsible for the reduction and/or stabilization of metallic nanoparticles, Liu et al. (2017) gave a detailed and thorough investigation report into what functions the active molecules may be performing in the biosynthesis of gold nanoparticles using *Cacumen platycladi* leaf extract. Taking advantage of the difference in polarity, the phytochemicals were separated into three classes by the aid of chromatography. The research showed that the phytoconstituents can be classified into polyphenols, sugars, and flavonoids. It also revealed that the nanoparticles of polyphenols were highly stable compared to those of sugars (Liu et al., 2017).

Maddinedi et al. (2017) used a biosynthetic approach when they studied the reducing and /or stabilizing ability of the leaf extract of *Cinnamomum tsoi* for silver nanoparticles formation. The success of this was ascribed to the polyphenols in the extract. The surface of the nanoparticles was observed to be covered by oxidized polyphenols serving as capping agents.

Press (2016a) came up with a protocol for the in vitro micropropagation of a very important but endangered plant species known as *phlomis bracteosa*. Antimicrobial silver nanoparticles were synthesized using the aqueous extract of the derived plantlets of the plant and further confirmed that the extract is rich in flavonoids and total phenolic content. FTIR analysis corroborated this with evidence that polyphenols were responsible for the reduction as well as stabilization of the biosynthesized silver nanoparticles. Similarly, several studies have demonstrated the involvement of polyphenols in the AuNPs synthesis. Table 2.3 displays predominantly the involvement of polyphenols in the fabrication of MNPs. The table, however, showed that different phytochemicals may be involved in the reduction of metal salts to MNPs.

Flavonoids in clove pods were believed to be responsible for the formation of AuNPs with anticancer potential (Raghunandan et al., 2011). Many other phytochemicals such as terpenoids, amines, polyols (Dada et al., 2018), phenols, tannins, glycosides (Youssif et al., 2019) and procyanidins (Badeggi et al., 2020) have been demonstrated as reducing agents from various plants.

Evidently, polyphenols, in one form or the other, have participated in MNPs formation using plants, therefore they are the key players in green synthesis involving plants.

**Table 2.3: Recent literature on the green synthesis of silver and gold nanoparticles using plant extracts, depicting the phytochemicals (functional groups) involved**

Plant material	Plant parts	Functional groups	Size of NPs	References
<i>Pelargonium graveolens</i>	Leaf	Polyphenols, amides	122-164 nm	(Arassu and Nambikkairaj, 2018)
<i>Theobroma cacao</i>	Seeds	Polyphenols	11-15 nm	(Ranoszek-soliwoda et al., 2019)
<i>Lycium chinense</i>	Fruits	Polyphenols	20-200 nm	(Chokkalingam et al., 2019)
<i>Tithonia diversifolia</i>	Leaf	Terpenoids, amines, polyols	10-26 nm	(Dada et al., 2018)
<i>Cymbopogon citrates</i>	Stem	Phenolics	10-33 nm	(Ajayi and Afolayan, 2017)
<i>Diospyros Montana</i>	Stem	Phenols, amines	28 nm	(Bharathi et al., 2018)
<i>Ehretia laevis</i>	Leaf	Amino acids, proteins	5-20 nm	(Warghane and Dhankar, 2019)
<i>Lamprathus coccineus &amp; Malephora luteo</i>	Leaf	Flavonoids, phenols, tannins, glycosides	12-28 nm	(Youssif et al., 2019)
<i>Vitis vinifera</i>	Seeds	Polyphenols	42 nm	(González-Ballesteros et al., 2018)
<i>Nigella arvensis L.</i>	Seeds	Flavonoids, alkaloids	2-15 nm	(Chahardoli et al., 2017)
<i>Ducrosia anethifolia</i>	Whole plant	Phenols, carboxylic acids, amines	11.4 nm	(Kouhbanani et al., 2019)
<i>Leucosidea sericea</i>	Aerial part	Procyanidins, Polyphenols	6-24 nm	(Badeggi et al., 2020)
<i>Holoptelea integrifolia</i>	Leaf	Polyphenols and amines	32-38 nm	(Kumar et al., 2019)
<i>Turbinaria conoides</i>	Leaf	Polyphenols	< 1 µm	(Venkatraman et al., 2018)
<i>Combretum erythrophyllum</i>	Leaf	Phenols, aromatic amines	13.62 nm	(Jemilugba et al., 2019)
<i>Punica granatum</i>	Leaf	Flavonoids, aromatic acids	48 nm	(Saratale et al., 2018)
<i>Fritillaria cirrhosa</i>	Whole plant	Polyphenols, alkaloids	40-45 nm	(Guo et al., 2020)



### 2.5.2.1.3 Synthesis of biologically active nanoparticles using isolated phytochemicals

Although several reports on the synthesis of nanoparticles using plant extracts claimed the involvement of polyphenols, additional information was necessary. This is because of the possible synergistic interference of many other components of a given extract. Therefore, it is pertinent to investigate the use of isolated phytochemicals from plant sources in nanoparticle formation. Recently, for specificity, quantification and formulation purposes, nanoparticles (NPs) were fabricated using single isolated phytochemicals endowed with the required site for chelation with the intending metal ion. Plant polyphenols dominated the candidates and was used singly to synthesize NPs (Khan et al., 2018; Ovais et al., 2018). Different phenolic acids including gallic and protocatechuic acid were found to possess reducing abilities for the fabrication of metallic nanoparticles (Ali et al., 2018; Aromal et al., 2012; Kumar et al., 2012)

Stephen and Seethalakshmi reported the synthesis of silver nanoparticles using hesperidin whereas Sahu et al. used hesperidin, diosmin, and naringin to form similar silver nanoparticles (Sahu et al., 2016; Stephen and Seethalakshmi, 2013).

Bisht and co-workers synthesized a polymeric nanoparticle using curcumin that was isolated from *Curcumin longa* (Bisht et al., 2007).

Guavanoic acid, a phytochemical isolated from *Psidium guajava*, was used in the biosynthesis of AuNPs which was found to be stable in various physiological mediums (Khaleel et al., 2010).

Phloridzin, an antidiabetic agent found in fruits and its aglycon served as reducing and stabilizing agents in the biosynthesis of AuNPs (Payne et al., 2018).

A terpenoid glucoside, escin was employed in gold nanoparticles formation that demonstrated antidiabetic properties (Shamprasad et al., 2019).

According to Dong and colleagues, Resveratrol acted as both reducing and stabilizing agents in the green synthesis of AuNPs that displayed similar characteristics with calcium dobesilate in diabetic rats (Dong et al., 2019).

Rajarajeshwari et al. showed that Gymnemic acid was the sole reducing agent in the green synthesis of AuNPs. The biosynthesized Gymnemic acid-AuNPs were found to possess hyperglycemic properties. (Rajarajeshwari et al., 2014).

Safaepour et al. (2009) succeeded in using geraniol, a natural monoterpene found in plants to synthesize stable and uniformly shaped silver nanoparticles.

Kasthuri and colleagues applied a purified apiin compound that was isolated from henna leaf extract in the synthesis of silver and gold nanoparticles and opined that the carbonyl and secondary hydroxyl groups in the compound were responsible for the successful reduction of the metal salts to their zero valency. It was concluded that the nanoparticles were very stable and could have useful biological applications (Kasthuri et al., 2009b).

Using a sonochemical method, Perelshtein et al. synthesized tannic acid silver nanoparticles from an aqueous solution without using any stabilizer. In the one-step process, the tannic acid nanoparticles formed were 40 nm in size. The presence of carbonyl and hydroxyl groups in tannic acid might have offered it the ability to keep the nanoparticles from aggregation, therefore, requiring no other external stabilizer (Perelshtein et al., 2014).

In another study, Aloin A and aloesin isolated from Cape aloe were used as stabilizers in the synthesis of silver and gold nanoparticles. The nanoparticles were water-soluble and different sizes and shapes were obtained by varying the reaction conditions and reducing agents. The study showed that these natural products could be used as stabilizing agents in the synthesis of highly stable water-soluble nanoparticles that were efficiently taken up by macrophages and cancer cells (Krpetic et al., 2009).

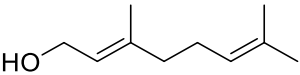
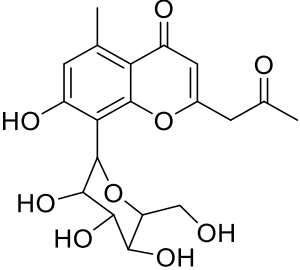
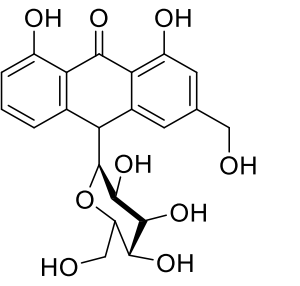
Barnaby et al. (2012) used a polyphenol known as ellagic acid in the synthesis of bimetallic nanoparticles. In the formation of gold and platinum nanoparticles, it was observed that ellagic acid formed micro-fibrillar assemblies which then became compacted under aqueous conditions into micro-bundles. The micro-bundles served as templates for the development of gold nanoparticles as well as bimetallic gold-platinum nanoparticles biomimetically.

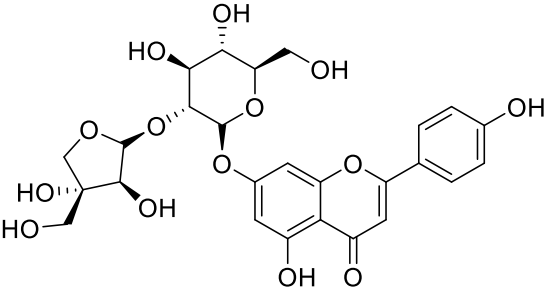
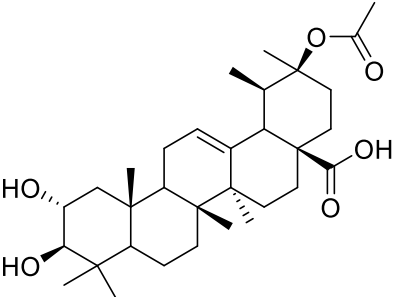
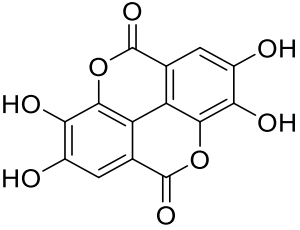
Recently, platinum nanoparticles were synthesized using naturally occurring phytic acid (Zhou et al., 2019). The phytic acid capped-NPs showed a strong affinity to hydroxyapatite *in vitro* and *in vivo*. When compared to the sodium citrate platinum nanoparticles, it was observed that the phytic acid particles displayed four times higher accumulation in the osteolytic lesions. The study also revealed the anti-cancer ability of phytic acid nanoparticles.

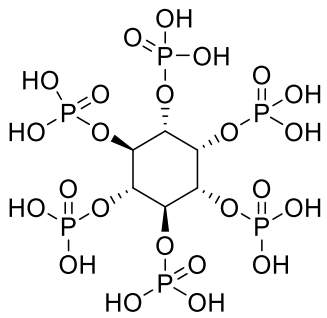
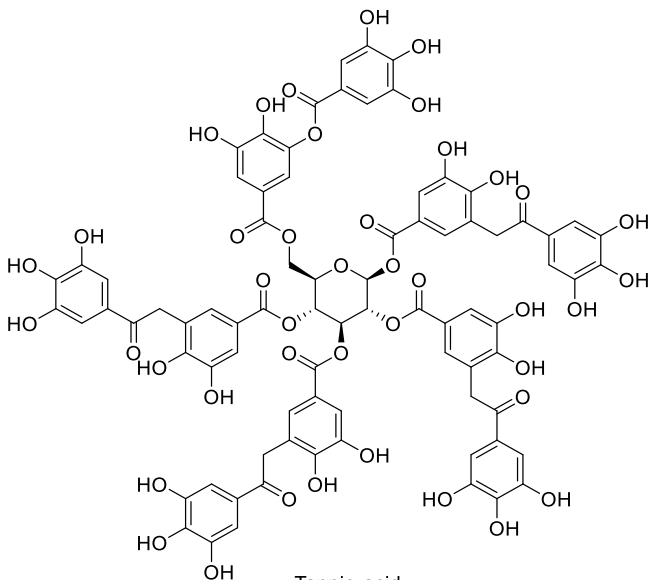
Other compounds that were used in the formation and stabilization of NPs with different biological properties include mangiferin, chlorogenic acid and kaempferol (Table 2.4). The table displayed the chemical structure of the compounds, type of NPs, size and shape and the functional group that is likely involved in the reduction and possible stabilization of the NPs formed. It also gives the time in which the reaction reached completion as well as the stability status of the hybrid NPs. These NPs were found to have different applications as indicated in the table. An important observation in the table is that each compound

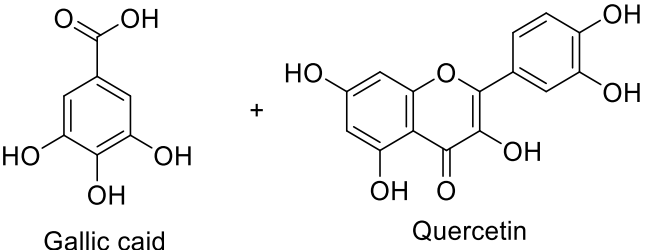
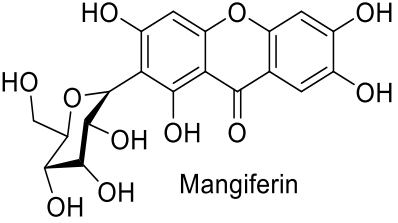
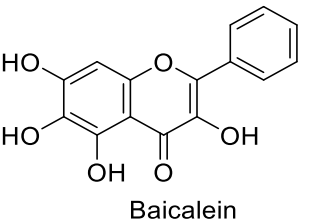
possesses at least one hydroxyl group. This may mean that the presence of hydroxyl groups in compounds is a key requirement for the formation of NPs.

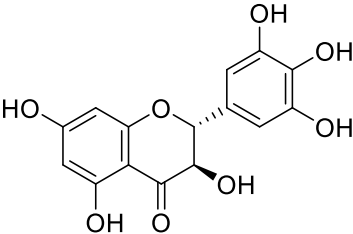
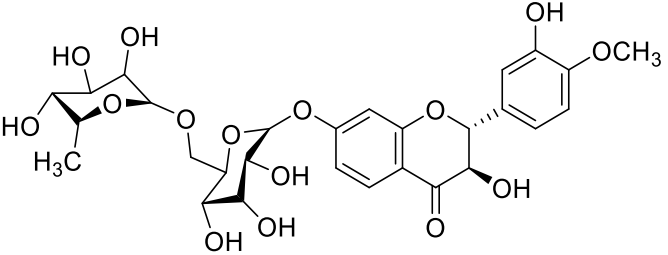
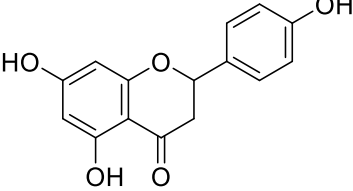
**Table 2.4: The use of single compounds in the green synthesis of MNPs, the size and functional group involved, the reaction time, stability and applications**

Phytochemical	Type of NPs	Size/shape	Functional group	Reaction time	Stability	Application	References
 Geraniol	Ag	1-10 nm	hydroxyl, alkene	40 s	N/Av	anticancer	(Safaepour et al., 2009)
 Aloesin	Au/Ag	5-30 nm, spherical	carbonyl, hydroxyl	1 min	extremely stable	anticancer	(Krpetic et al., 2009)
 Aloin A	Au/Ag	5-30 nm, spherical	carbonyl, hydroxyl	1 min	extremely stable	anticancer	(Krpetic et al., 2009)

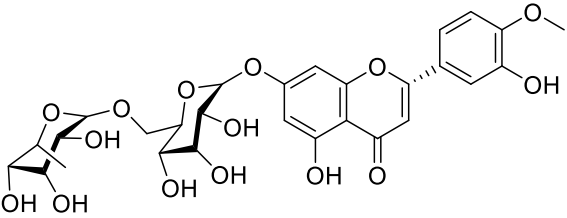
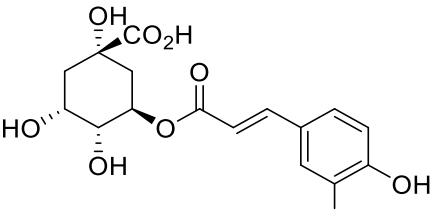
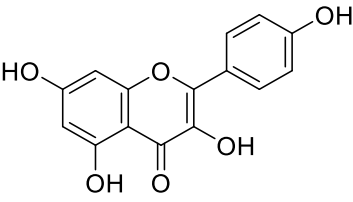
Phytochemical	Type of NPs	Size/shape	Functional group	Reaction time	Stability	Application	References
 <p>Apigin</p>	Au/Ag	21-39 nm, spherical,	hydroxyl, carbonyl	N/Av	3 months	anticancer	(Kasthuri et al., 2009b)
 <p>Guavanoic acid</p>	Au	4-24 nm, spherical	carbonyl, hydroxyl	1 min	6 months	antidiabetic	(Khaleel et al., 2010)
 <p>Ellagic acid</p>	Au/Ag	20-25 nm, spherical	carbonyl, hydroxyl	10 min	N/Av	reduction	(Barnaby et al., 2012)

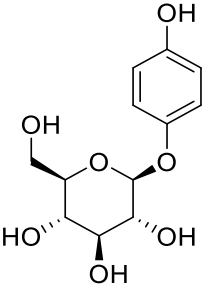
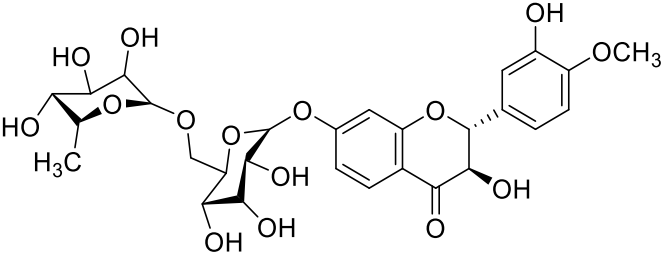
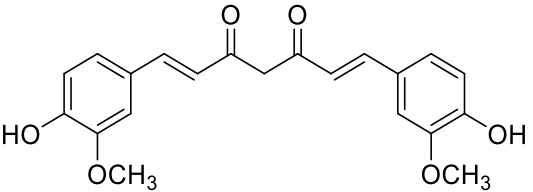
Phytochemical	Type of NPs	Size/shape	Functional group	Reaction time	Stability	Application	References
 <p>Phytic acid</p>	Pt	1-2 nm	hydroxyl, phosphate	5 min	highly stable	anticancer	(Zhou et al., 2019)
 <p>Tannic acid</p>	Ag	40-60 nm	carbonyl, hydroxyl	1 h	N/Av	medical devices	(Perelshtein et al., 2014)

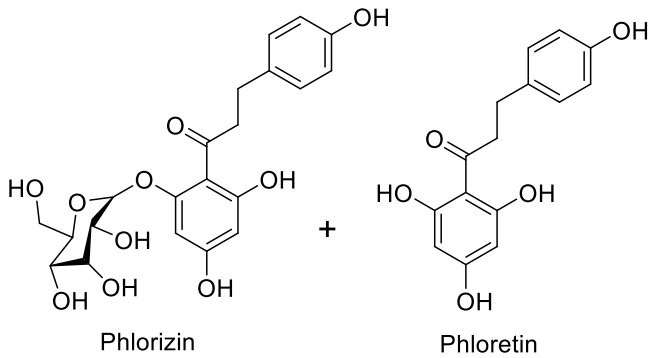
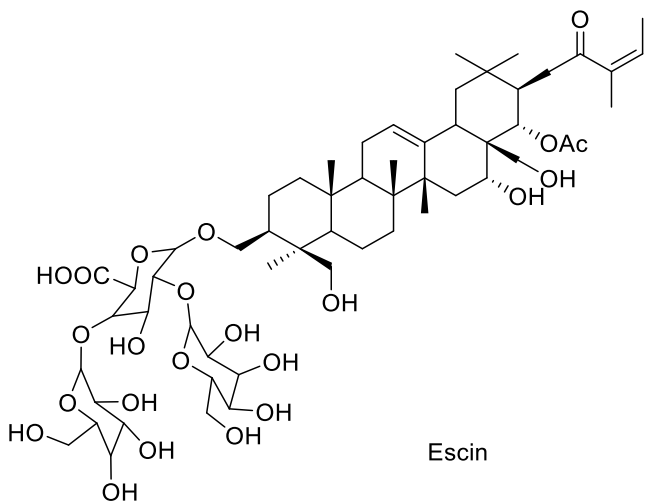
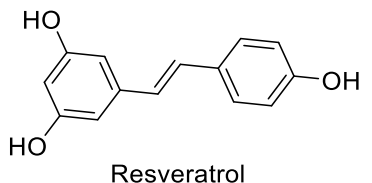
Phytochemical	Type of NPs	Size/shape	Functional group	Reaction time	Stability	Application	References
 <p>Gallic acid + Quercetin</p>	Ag/Se	30-35 nm	Hydroxyl	N/Av	3 months	Antioxidant, antimicrobial, antitumor	(Mittal et al., 2014)
 <p>Mangiferin</p>	Au	35 nm	Hydroxyl	1 h	1 week	Anticancer	(Al-Yasiri et al., 2017)
 <p>Baicalein</p>	Au	26.5 nm, spherical polydisperse	N/Av	15 mins	N/Av	Antibiofilm activity	(Rajkumari et al., 2017)

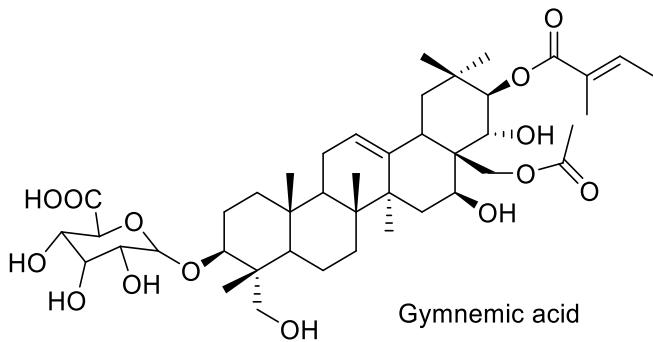
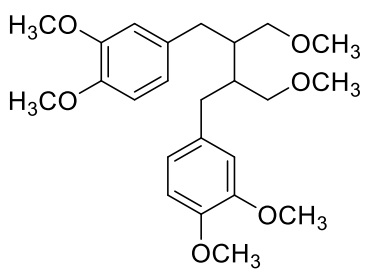
Phytochemical	Type of NPs	Size/shape	Functional group	Reaction time	Stability	Application	References
 <p>Dihydromyricetin</p>	Au	24-43 nm, spherical	Hydroxyl	30 mins	N/Av	N/Av	(Guo et al., 2014)
 <p>Hesperidin</p>	Ag	5-50 nm, Oval shape	Hydroxyl	5 mins	N/Av	Antibacterial, cytotoxicity	(Sahu et al., 2016)
 <p>Naringenin</p>	Ag	5-40 nm, Oval shape	Hydroxyl	5 mins	N/Av	Antibacterial, cytotoxicity	(Sahu et al., 2016)

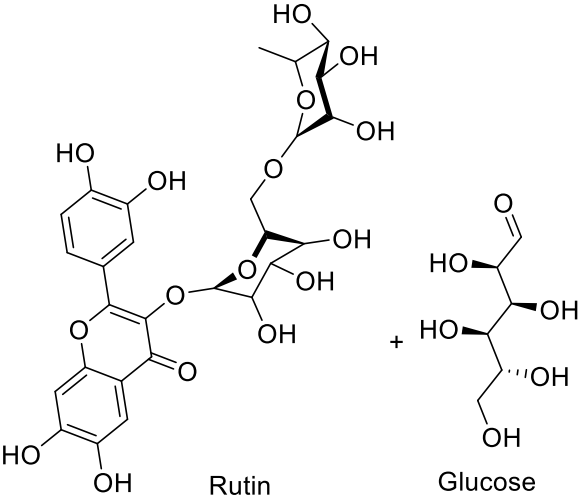
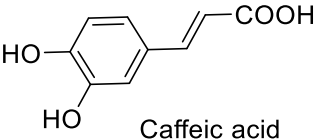
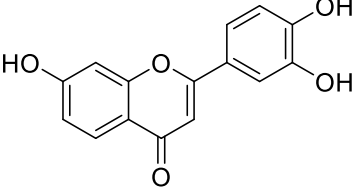


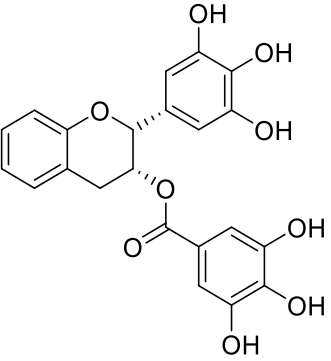
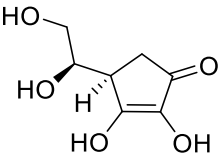
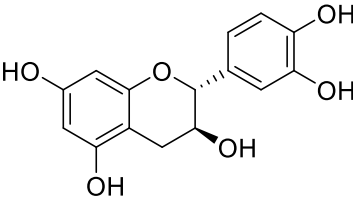
Phytochemical	Type of NPs	Size/shape	Functional group	Reaction time	Stability	Application	References
 <p>Diosmin</p>	Ag	20-80 nm, hexagonal	Hydroxyl	5 mins	N/Av	Antibacterial, cytotoxicity	(Sahu et al., 2016)
 <p>Chlorogenic acid</p>	Au	22 nm, spherical	N/Av	12 h	N/Av	Anti-inflammatory activities	(Hwang et al., 2015)
 <p>Kaempferol</p>	Au	16.5 nm	Phenolic group	1 h	5 months	Anti-cancer	( Raghavan et al., 2015)

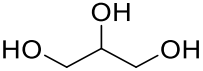
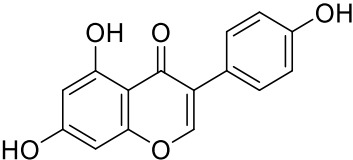
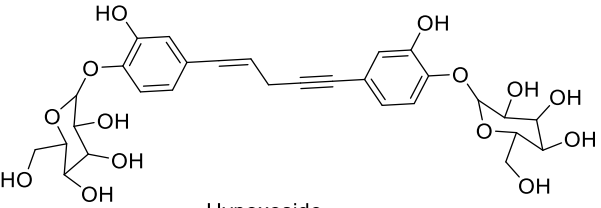
Phytochemical	Type of NPs	Size/shape	Functional group	Reaction time	Stability	Application	References
 <p>Arbutin</p>	Au	10.30–17.13 nm	Hydroxyl	1.5 h	N/Av	Cosmeceutical	(Park et al., 2019)
 <p>Hesperidin</p>	Ag	20-40 nm	Hydroxy	2 mins	N/Av	N/Av	(Stephen and Seethalakshmi, 2013)
 <p>Curcumin</p>	Polymeric	50 nm	N/Av	N/Av	N/Av	Anti-cancer	(Bisht et al., 2007)

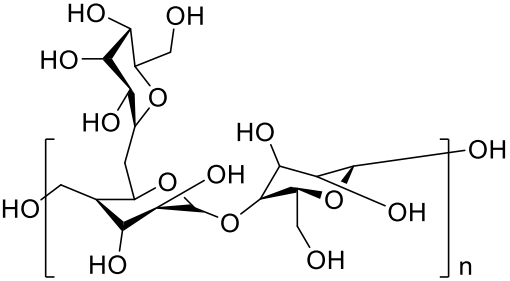
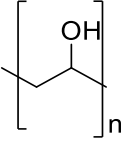
Phytochemical	Type of NPs	Size/shape	Functional group	Reaction time	Stability	Application	References
 <p>Phlorizin + Phloretin</p>	Au	15 and 8 nm	N/Av	10-20 mins	N/Av	Antineoplastic	(Payne et al., 2018)
 <p>Escin</p>	Au	5-10 nm	N/Av	1 h	30 days	Antioxidant, antidiabetic	(Shamprasad et al., 2019)
 <p>Resveratrol</p>	Au	20 nm, spherical	Hydroxyl	30 mins	3 months	Antidiabetic	(Dong et al., 2019)

Phytochemical	Type of NPs	Size/shape	Functional group	Reaction time	Stability	Application	References
	Au	15.5 nm	Hydroxyl	10 mins	4 h	Antioxidant	(Sanna et al., 2014)
 <p>Gymnemic acid</p>	Au	22-55 nm, spherical	N/Av	30 mins	48 h	Glucose uptake	(Rajarajeshwari et al., 2014)
 <p>Phyllanthin</p>	Au & Ag	38 nm, irregular  30 nm, quasi-spherical	Methoxy group  Methoxy group	1 min  1 min	3 months  N/Av	Electrochemical  Electrochemical	(Kasthuri et al., 2009a)  (Kasthuri et al., 2009a)

Phytochemical	Type of NPs	Size/shape	Functional group	Reaction time	Stability	Application	References
 <p>Rutin</p>	Au	N/Av	N/Av	N/Av	N/Av	N/Av	(Zhan et al., 2011)
 <p>Caffeic acid</p>	Au	89.4 nm, Spherical	Hydroxyl	N/Av	N/Av	Growth mechanism	(Kim et al., 2016)
 <p>Fisetin</p>	Au	9.7 nm	Hydroxyl	10 mins	4 h	Antioxidant	(Sanna et al., 2014)

Phytochemical	Type of NPs	Size/shape	Functional group	Reaction time	Stability	Application	References
 <p>Epigallocatechin-3-gallate</p>	Au	25 nm	Hydroxyl	10 mins	4 h	Antioxidant, Antiproliferative	(Sanna et al., 2014)
 <p>Ascorbic acid</p>	Ag	10 nm	Hydroxyl	30 mins	N/Av	N/Av	(Zhang et al., 2015)
 <p>Catechin</p>	Au	16.6 nm	Hydroxyl	1 h	6 days	Catalytic	(Choi et al., 2014)

Phytochemical	Type of NPs	Size/shape	Functional group	Reaction time	Stability	Application	References
 Glycerol	FeO	4.7 nm	carboxyl	2 h	N/Av	Antibacterial	(Iconaru et al., 2013)
 Genistein	Au	14-33 nm	Hydroxyl, carbonyl	20 min	Highly Stable	Anti-cancer	(Stolarczyk et al., 2017)
 Hypoxoside	Au	24-28 nm, spherical	Hydroxyl of sugars	1 h	Stable	Immunomodulation	(Elbagory et al., 2019)

Phytochemical	Type of NPs	Size/shape	Functional group	Reaction time	Stability	Application	References
 <p>Gum acacia</p>	Ag	2-20 nm, spherical	Carboxyl, hydroxyl	N/Av	1 month	Antimicrobial	(Dong et al., 2014)
 <p>PVA</p>	Ag	13-26 nm	Hydroxyl	30 mins	N/Av	Antibacterial	(Ali, 2013)

**Note:** Ag = silver, Au = gold, Au/Ag = gold/silver, Pt =platinum, FeO = Iron oxide, Ag/Se = silver/selenium, N/Av = Information not available in the literature cited



### 2.5.3 Physicochemical properties of metallic nanoparticles

When atoms or molecules bond together to form particles in the size range of 1-100 nm, the hybrid particles are called nanoparticles. Of importance is the characteristic difference in their properties as a result of quantum size effects, large surface to volume ratio and the electro dynamic interactions. Therefore, compared to their bulk precursors, NPs have shown enhanced catalytic properties, better electrical and heat conductivity and enhanced photoemission (Raikar et al., 2011).

#### 2.5.3.1 Optical properties of gold and silver nanoparticles

Gold and silver nanoparticles have optical properties that have allowed them strong scattering and absorption at specific wavelengths due to their size, shape and the dielectric properties of both the particles and the surrounding medium. This phenomenon is known as localised surface plasmon resonance (LSPR) and it occurs when an oscillating electric field of an incident light brings about orderly oscillations of free conducting electrons on the surface of the particles thereby causing a resonant oscillating electric dipole (figure 2.19) (Sevenler et al., 2015).

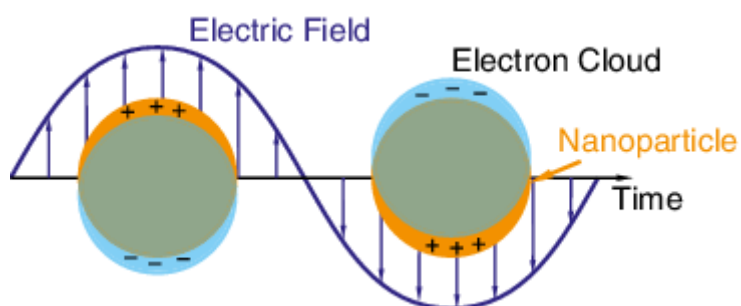


**Figure 2. 19: A scheme representing the oscillation of the free electrons around a nanoparticle (Sevenler et al., 2015)**

The production of absorption bands due to LSPR effect in the visible region is dependent on the MNPs involved. While the AgNPs can be detected between 380 to 450 nm, that of AuNPs is expected to be in the range of 500 to 600 nm (Nakashima, 2009). However, the distinction between the MNPs and their bulk counterpart is that the latter cannot show an absorption band at such regions. The LSPR position can be affected by factors like size, shape, type of reducing agent and surface charge of the particle, solvent used, pH and temperature (Nakashima, 2009).

Gold nanorods have two absorption bands; one at 500-600 nm and the other at the 650-900 nm near the infrared region. This bimodal absorption band is possible because gold nanorods usually resonate along two axes, one along the width, which is the shorter axis and the other along the length of the particle (figure 2.20). Depending on the gold nanorods' aspect ratio, the LSPR can undergo a redshift from the visible to the near-infrared region of the light spectrum thereby conferring a double oscillatory property on it. As the aspect ratio increases (L-R of figure 20), a drastic change in shape and its effect on colour can be observed (Nakashima, 2009).

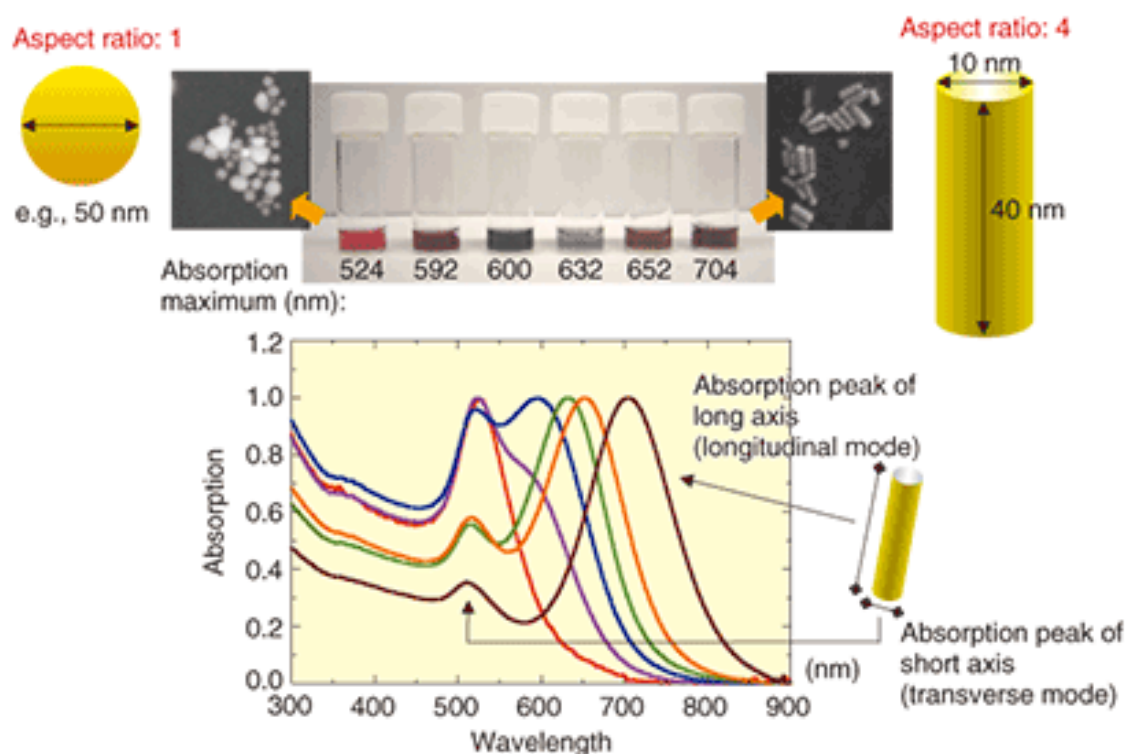


**Figure 2. 20: UV-Visible spectra and colour variation of gold nanorods with different aspect ratios (Nakashima, 2009)**

As shown in figure 2.20, the LSPR position is also associated with the colour and shape of the NPs. When AuNPs with a characteristic ruby red colour were produced, the LSPR was at 524 nm, showing that predominantly spherical NPs were formed. As the colour changed to brownish, a blue shift occurred to 592 nm (blue curve), and subsequent changes in the LSPR were correspondingly depicted in the colour. The trend continued until nanorods were formed at higher LSPR values (704 nm). The position of LSPR has also shown a connection to the colour and size. This fact was supported by Notarianni et al. who observed steady

increments in AuNPs from 10, 20 and up to 40 nm as the colour changed from ruby red to deep blue (Notarianni et al., 2014).

Therefore, for gold and silver NPs, the optical properties change significantly as the shape changes.

### **2.5.3.2 Fluorescence quenching properties of gold and silver nanoparticles**

The fluorescence of fluorochromes that are in the vicinity of MNPs can be quenched by the latter. This occurs when there is an overlap between the emission spectrum of excited fluorochromes and the LSPR absorption band of the MNP. The phenomenon is also referred to as FRET (fluorescence resonance energy transfer). Quenching capability of both gold and silver NPs have been investigated by researchers. A functionalized mercaptothiadiazole capped AgNPs showed strong quenching performance determining Hg (II) in environmental samples (Vasimalai and John, 2013). Similarly, AuNPs have been used to quench the fluorescence of perylene diimide (Zhang et al., 2020). The authors associated the quenching capability to the size and shape of the MNPs.

### **2.5.3.3 Shape and size related activities**

Gold and silver NPs can be synthesized into different shapes and sizes depending on the intended biomedical applications. The concentration of reducing agents among other factors, can influence the shape of NPs which can bring about a change in the LSPR absorption band. Al-Ghamdi and Mahmud fabricated silver NPs of different shapes (nanorods, nanotriangles) and used darkfield microscopy to show their different colours (figure 2.21). They suggested their suitability for biomedical applications (Al-Ghamdi and Mahmoud, 2013). Similarly, gold nanospheres and nanorods have been fabricated with applications in drug delivery and biomedical imaging. Hollow nanospheres and nanocages are other forms of AuNPs with photothermal properties (Zhang et al., 2015). However, spherical AuNPs have been more extensively researched owing to their facile synthesis.

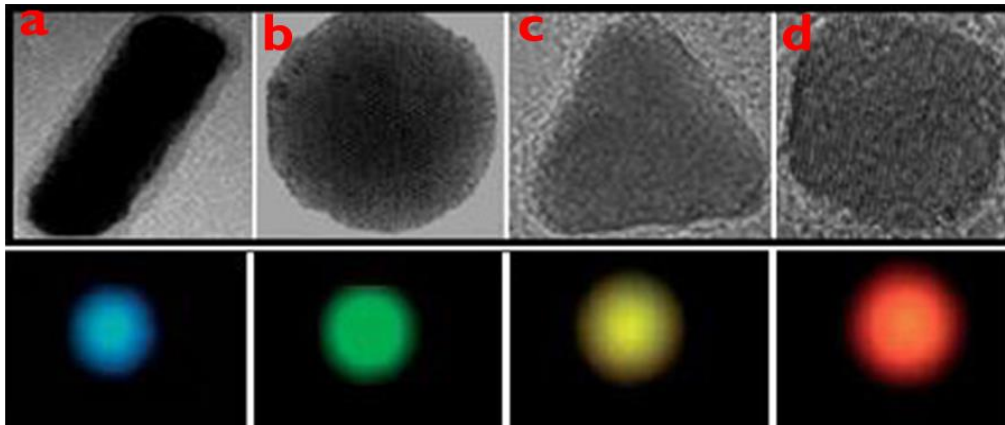


**Figure 2. 21: Different shapes and colours of silver NPs (Al-Ghamdi and Mahmoud, 2013)**

Another key characteristic of MNPs is the size. Since their sizes can be tuned in the desired manner, gold and silver NPs have displayed potential in several applications including in the biomedical sector. When experimental conditions were varied, 7 nm, 29 nm, and 89 nm AgNPs with antibacterial activities were produced (Espinosa-cristóbal et al., 2012). AgNPs have also been employed in wound dressing and catheters because of their antimicrobial activities (Khan et al., 2018).

The uptake of AuNPs by cells, the distribution of the particles in the blood vessels and eventual excretion are equally dependent on the size of the NPs in question (Au et al., 2010). Jiang and colleagues (2008) observed that the interaction of gold nanoparticles with biomolecules is also subject to the size. When they studied AuNPs, they found that 40-50 nm sized particles demonstrated more receptor internalization as well as more cell response induction than the particles of other sizes. In targeting tumorous cells, the size of AuNPs is advantageous in the sense that easy access was gained through the tumour capillaries with larger sizes than the particles. In some instances, they have also gained entrance through damaged surfaces of the blood vessels that linked to tumour cells (Aiello et al., 2019). A study conducted by Niikura and colleagues also concluded that spherical AuNPs of between 20 and 40 nm in diameter induced the west Nile virus better than those of other shapes and sizes (Niikura et al., 2013).

#### **2.5.3.4 Stability studies of gold and silver nanoparticles**

Stability is related to the act of retention of the characteristic properties of NPs. When a particular synthesis passes through various stages until completion, desired shapes, colours

and sizes are formed among other properties. Depending on the nature of the reducing agent, subsequent capping will take place either *in situ* or by using external stabilizers like surfactants. Thereafter, defined morphology, size and the nature of ions surrounding the hybrid particles can be determined using microscopic analysis and the measurement of zeta potential for example. For the NPs to be suitable for certain applications like biomedical, their characteristic properties must be maintained to a large extent for a given period. This can be done by evaluating the properties at intervals and comparing the results with the original values.

Further, the study of the stability can be looked at from two angles; one would be to monitor the interaction of the NPs with the immediate environment, that is, whether the interactions have had any properties altered and to what extent. The second consideration would be the interaction of the NPs when external factors are introduced. Examples include mixing the solutions of certain proteins, saline and buffers with the NPs to observe their behaviours.

#### **2.5.3.4.1 In immediate environment**

The Zeta Potential (ZP) is related to the charges surrounding the surface of NPs and has been used to measure the stability of colloidal suspensions (Elbagory et al., 2017). According to a guideline, ZP values between  $\pm 0-10$  mV is considered highly unstable,  $\pm 10-20$  mV is relatively stable,  $\pm 20-30$  mV is moderately stable while values greater than  $\pm 30$  mV is highly stable (Agrawal and Patel, 2011). In studies involving silver and gold NPs, ZP values of  $-42.5$  mV (Tantra et al., 2010),  $-26.3$  mV (Sadowski, 2010), and  $-2.9$  to  $-90$  mV (Pyell et al., 2015) were recorded. Since ZP is a function of the type of chemicals involved, it is not always negative. Patil et al. obtained both positive ( $+13.89$  mV) and negative ( $-33.34$  mV) ZPs for similar NPs (Patil et al., 2017). NPs with positive ZP values have also been reported by others (Anbu et al., 2019; Li et al., 2019).

It is important to note that the above stabilities are measured on the colloidal solutions alone (without the addition of any other solutions). This way, the stability of the NPs on its own can be evaluated and the extent of stability can also be estimated at intervals. In some instances, a given NP is stable for a few hours and some are stable for months. While gymnemic acid-AuNPs were stable for only 48 hrs (Rajarajeshwari et al., 2014), Khaleel and colleagues reported guavanoic acid-mediated AuNPs that remained intact for six months (Khaleel et al., 2010).

#### **2.5.3.4.2 In different physiological conditions**

##### ***Bovine serum albumin (BSA)***

Bovine serum albumin is a protein that resembles the human serum albumin and the most abundant protein found in human blood plasma. Consequently, studies towards understanding the behaviour and stability of NPs are conducted in BSA, especially when NPs are targeted for biomedical applications. Joseph and colleagues examined the interaction of bare and coated MNPs with BSA and found that BSA-MNPs were more stable in the presence of stabilizers than the bare one (Joseph et al., 2015). According to Joshi et al., when chloroquine alone was added to BSA, there was a disturbance to the structure of BSA (Joshi et al., 2011). However, when chloroquine-AuNPs were added, there was no noticeable perturbation on the structure of the protein. Similarly, Ag, Au and Au-AgNPs were stable in BSA (Singh et al., 2005). On the other hand, Shi and colleagues observed the broadening of the absorption spectrum when AuNPs interacted with BSA and concluded that it was due to different concentrations of BSA that were used (Li et al., 2017).

##### ***Cysteine (CYS)***

Cysteine is one of the sulfur-containing protein amino acids. It is an antioxidant found in human tissues, particularly at higher concentrations in the liver and eyes. The interaction of CYS with AuNPs resulted in a very stable CYS-capped AuNPs. It was further suggested that the thiol moiety of CYS was a very good site that made the interaction possible (Aryal et al., 2006). In their investigation, Mocanu et al. observed a sharp broadening of absorption peak when a 1 mM solution of CYS was added to AuNPs (Mocanu et al., 2009). A change of the reddish gold colour to blue and up to 700 nm maximum wavelength was associated with aggregation of the AuNPs. Recently, the interaction of a few natural organic compounds including CYS with AuNPs was evaluated (Afshinnia et al., 2018). At one point, the UV-Vis absorbance shifted from 394 nm through 560 nm to 500 nm, showing aggregation of the particles. At other points, secondary absorbance peaks appeared that either increased or decreased with varying concentrations of CYS. Different factors such as the concentration of CYS and the type of functional groups in CYS were reported to be responsible for changes in the absorption band of the AuNPs. It is believed that the -COOH and -NH<sub>2</sub> of CYS also participated in the interaction with the NPs in an opposing manner (Ravindran et al., 2013). In addition to this dual functionality, the authors reported that different methods of synthesis also affect the interaction of CYS and the NPs. In general, NPs are stable in low concentrations of CYS.

### **Glycine (GLY)**

Glycine is the simplest amino acid that can fit into hydrophilic or hydrophobic environments due to its limited side chain. In its interaction with AgNPs, different concentrations only resulted in blue or red shifts but the SPR was maintained in the same region indicating the stability of the NPs in GLY solutions (Agasti et al., 2015). In another trial, Hamaguchi and colleagues observed that AuNPs were stable with respect to pH of the solution (Hamaguchi et al., 2010). At pH 9, small and stable NPs were obtained but when the pH was 3 and 6, large and unstable NPs were formed. They further explained that the -COOH and -NH<sub>3</sub> groups of GLY interacts more with the gold surface when GLY is in the anionic state at higher pH. Furthermore, CYS and GLY were employed in a stability study of AuNPs where both exhibited similar size and surface charges (Ning et al., 2017). The hydrodynamic size was increased by 0.4 nm by GLY but it greatly enhanced the AuNPs' stability. Length of GLY, surface charge and size were believed to have played a great role in the physiological stability.

### **Sodium Chloride (NaCl) solution**

Sodium Chloride is one compound that helps in maintaining the right balance of fluids in the human body. Another importance of the salt is that it absorbs and transports nutrients around the body. Therefore, it is important to determine if the NPs retain their properties in NaCl solutions. To confirm this, *in vitro* studies are usually carried out first. The stability of NPs in a mixture of NaCl in water, also known as saline has been reported. Rastogi et al. noted that AuNPs were stable in NaCl solution even at a higher concentration of 0.1 M where no particle agglomeration was observed (Rastogi et al., 2012). Similarly, 0.1 M NaCl was used by Islam and co-workers when they studied the stability of AuNPs and found that at low volumes of the salt, the particles were very stable (Islam et al., 2015). When the volume was between 50-200  $\mu$ L, changes began to appear and at 200  $\mu$ L of 0.1 M NaCl, the peak became broad, the absorbance decreased and the colour faded to colourless. This was an indication of aggregation. Further, Islam et al. studied the interaction of 0.1 M NaCl with *Pistata integerrima*-AuNPs and found that only when the volume of the electrolyte reached 300  $\mu$ L, the changes began to appear, indicating better stability of these NPs compared to their 2015 studies (Islam et al., 2019). AgNPs have also been found stable in 0.1 M NaCl for six months according to other researchers (Venkatpurwar and Pokharkar, 2011). The stability of NPs in NaCl solutions therefore appears to be concentration dependent. MacCuspie (2011) also shared this observation.

### **Water (Dilution)**

Some biomedical applications require different concentrations of MNPs. Tea mediated gold nanoparticles (1 mL) was successively diluted by the addition of 0.1 mL deionized water. The maximum absorption intensity was monitored and found to be intact even at very diluted conditions. It was also found that the absorption was linearly dependent on the concentration of AuNPs in line with Beer Lambert's Law (Nune et al., 2009). Similarly, when 0.2 mL of deionized water was used to successively dilute *acacia gum* mediated gold nanoparticles, the maximum absorption peak remained the same. This shows that the properties of AuNPs were not affected by the dilution. They further observed that even at extreme dilution, the absorption peak remained in the same region (Kattumuri et al., 2007). In this work, a series of dilution studies were performed at different nanoparticle concentrations to confirm the stability of AuNPs. The results, which showed that the SPR wavelength had the same value for all the solutions, meaning that the dilution did not influence the properties of the three AuNPs studied, were published and presented in chapter three of this thesis.

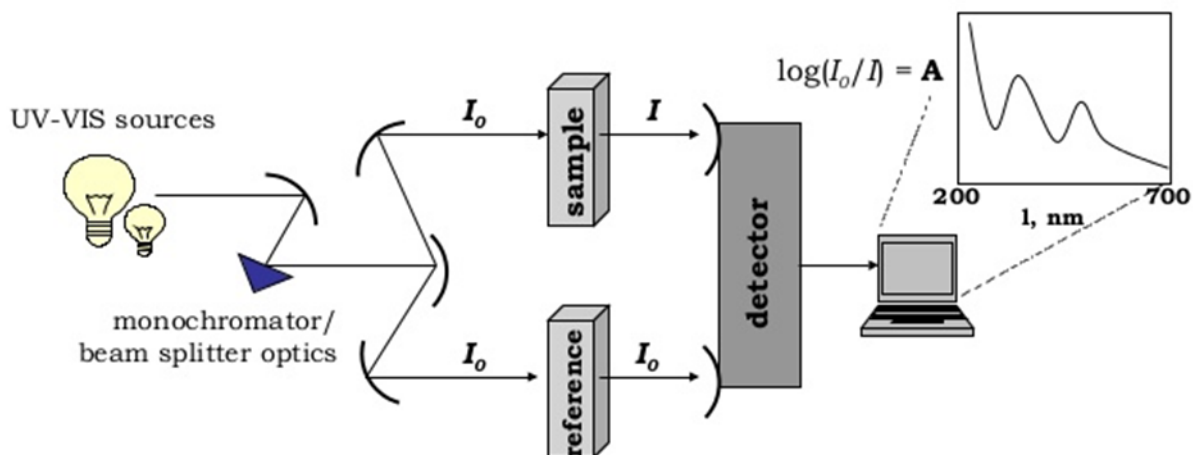
## **2.6 Characterization of gold and silver nanoparticles**

In the field of nanotechnology, characterization of nanomaterials (NMs) is of great significance after synthesis. It involves the use of techniques towards measuring and understanding the nature and type of hybrid NMs through size, morphology and surface chemistry among other features. It is paramount that the characteristics of the newly fabricated NPs are known before any form of application, be it biomedical or others. The techniques commonly employed include Ultra-Violet Visible (UV-Vis) spectroscopy, Dynamic Light Scattering (DLS), High-resolution transmission electron microscopy (HRTEM), Energy dispersive x-ray (EDX) spectroscopy, Selected area electron diffraction (SAED), and X-ray diffraction (XRD) (Mortazavi-Derazkola et al., 2020).

### **2.6.1 Ultra-Violet Visible spectroscopy**

The UV-Vis uses a light beam of different wavelengths to detect the LSPR bands of the MNPs, specifically in the regions of 320-500 nm for silver and between 500-600 nm for gold NPs. Upon exposure to the light beam, the free electrons of the respective MNPs are excited to higher orbital levels which are followed by the absorption of energy by the sample. The wavelength of the highest absorption is therefore calculated and displayed by a computer system attached to the spectrophotometer (Abbasi et al., 2015; Amendola et al 2010). A scheme representing a modern UV-Visible spectrophotometer is illustrated in scheme 2.4.



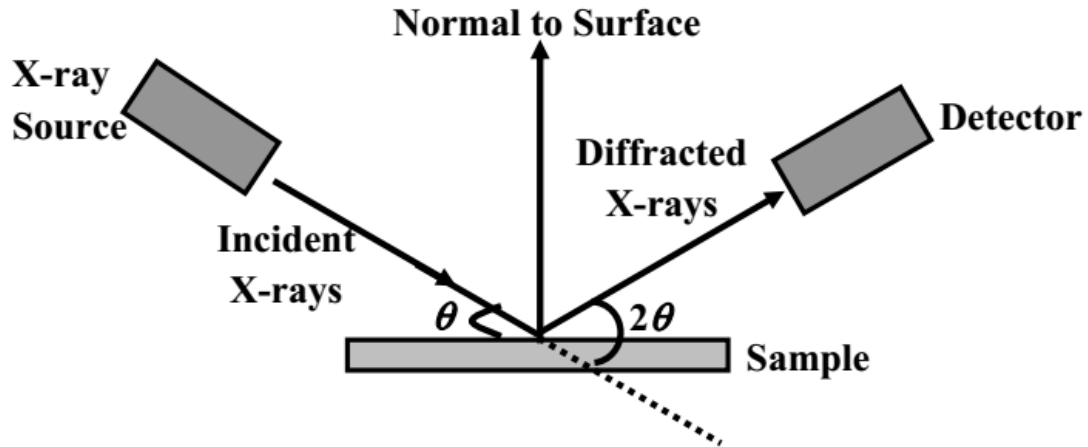


**Scheme 2.4: Schematic representation showing beam of light, sample and reference as well as the detector in a modern UV-Visible spectrophotometer.**

## 2.6.2 X-Ray Diffraction (XRD)

When a sample is bombarded with X-rays of fixed wavelength at certain incident angles, intense reflected X-rays are produced when the wavelength of the scattered X-rays interfere constructively. To achieve this constructive interference of the waves, the differences in the travel path must be equal to the integer multiples of the wavelength. When the interference occurs, the diffracted beam of X-ray will leave the sample at an angle equal to that of the incident beam. (Bunaciu et al., 2015). A schematic representation is given in scheme 2.5.

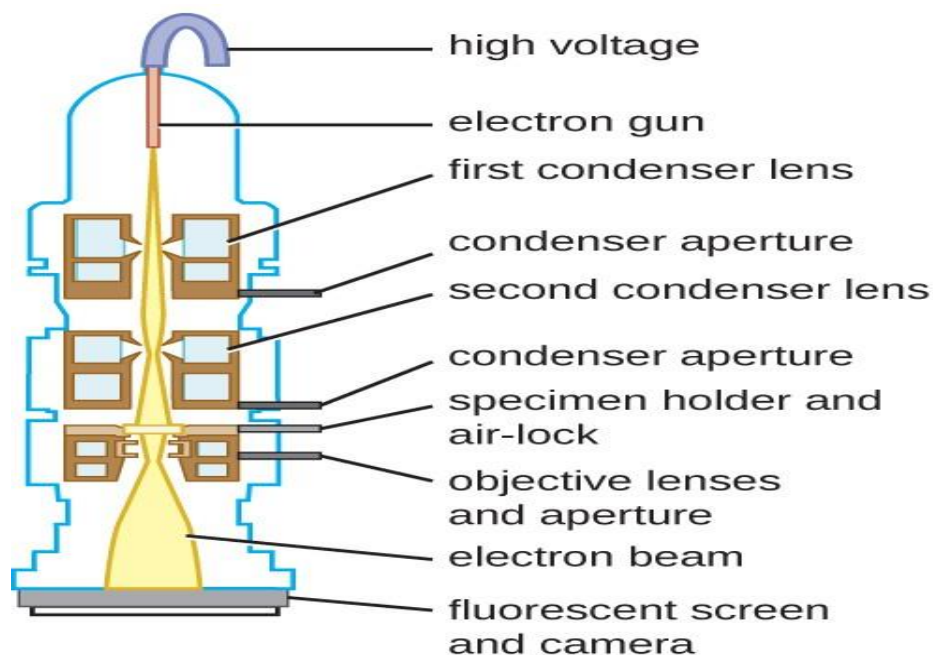
XRD is a powerful analytical tool that is used to identify the crystal structures and phases of NMs. It also gives information about the unit cell dimensions. Most often, the material is in a finely powdered form and the bulk composition is determined. Since each material has unique d-spacings, their identification becomes possible by comparison with the standard reference (Mortazavi-Derazkola et al., 2020).



**Scheme 2.5: Schematic representation of a typical powder X-ray diffractometer**

### **2.6.3 Transmission Electron Microscopy (TEM)**

In the last few decades, TEM has been one of the critical techniques commonly used in material science and nanotechnology in general. It provides information about the shape, size and crystal structure of the nanoscale materials. Its principle involves focusing a beam of electrons on a thin sample (under high vacuum) after which the transmitted electrons is passed through a series of electromagnetic lenses so as to be able to view the enlarged version of the image that appears on layers of photographic film or on a fluorescent screen (Ma et al., 2006). The magnified image of the specimen can be viewed as dark and bright field modes with either the diffracted or transmitted beams respectively. When diffracted and transmitted beams are combined, a high-resolution image, which contains information regarding the atomic structure of the nanomaterial can be obtained (Ma et al., 2006). Scheme 2.6 shows the different parts of a typical TEM instrument.

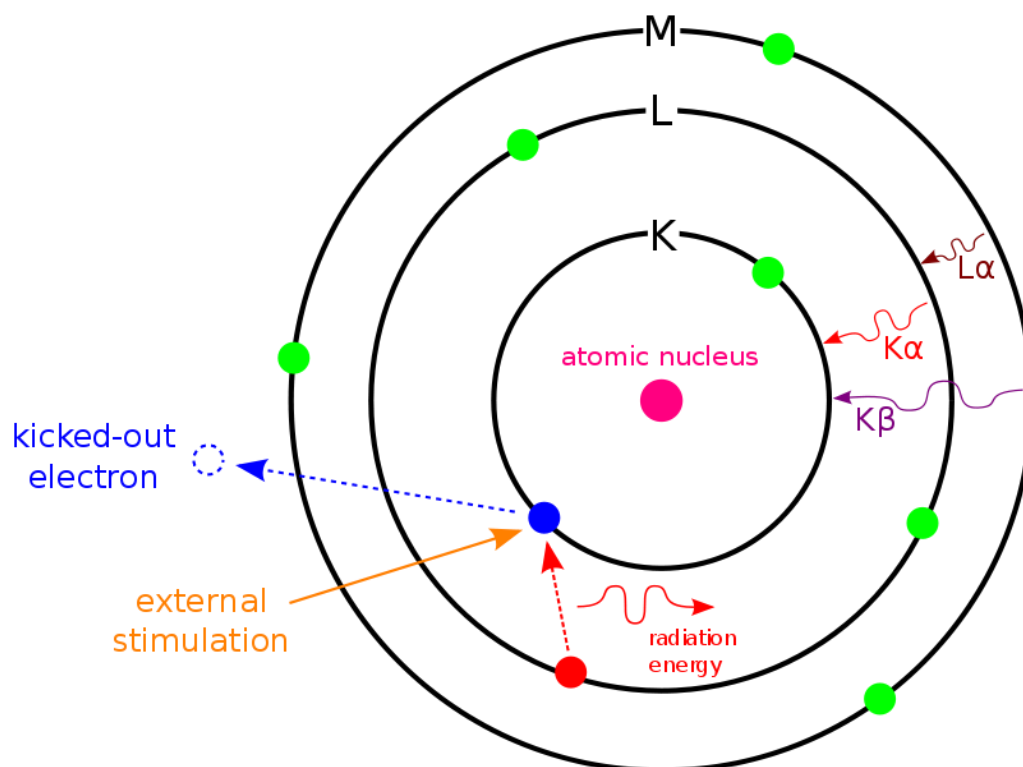


**Scheme 2.6: Different components of a typical transmission electron microscopy**

The information pertaining the symmetry and lattice spacing of the sample under study can be obtained from the diffraction pattern which is also produced during imaging. The diffraction pattern obtained from the TEM is therefore complimentary to XRD analysis and can be used to further support results obtained from the latter technique.

#### **2.6.4 Energy-dispersive X-ray spectroscopy**

Energy-dispersive X-ray (EDX/S) spectroscopy is often employed in elemental identification and quantification of a sample. The principle relies upon the interaction of the electron beam (in the electron microscope) with the sample to be analysed. The incident beam causes an electron from an inner shell (e.g. K shell) to be ejected, creating an electron hole which is filled by an electron from a higher energy shell (e.g. L shell). The difference in energy between the higher and the lower energy shells may then be liberated in the form of an x-ray (scheme 2.7). The x-ray energy is then converted through a detector and then sent to a pulse processor. Here, the signals are measured and passed to an analyser for display and data analysis (Goldstein et al., 2003). The number of x-rays and energy emission from a given sample can then be measured by the EDX spectrometer (Goldstein et al., 2003).



**Scheme 2.7: Showing the incident beam of electrons on an electron in the atom, the subsequent excitation and ejection of inner electron and the replacement of an electron from a higher energy shell in the vacant hole created**

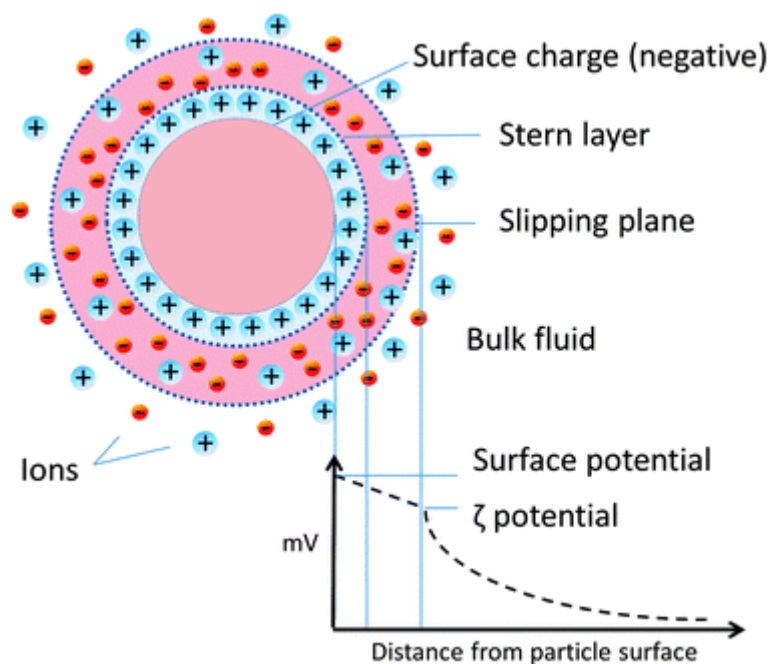
### 2.6.5 Dynamic Light Scattering (DLS)

The hydrodynamic size of gold and silver nanoparticles can be measured using the DLS technique. This is based on the Brownian movement of NPs in solution. Since this technique determines the size of NPs in solution coupled with the sampling volume, the hydrodynamic size by DLS is often not the same as that measured by HRTEM of a given nanoparticle (Patil et al., 2019).

DLS technique also reveals the polydispersity index (PDI) of colloidal solutions. PDI, otherwise referred to as the heterogeneity index, is the degree of non-uniformity of the size distribution of particles (Danaei et al., 2018).

Zeta potential (ZP) is another important measurement that can be obtained by DLS. NPs have surface charges that can attract charges of opposite signs. Therefore, as the NPs diffuse through the solution, a double layer of ions travels with it, thereby creating an electric potential at the boundary that is known as ZP (scheme 2.8). Hence, ZP connotes the charge that can keep two particles away from one another. It typically ranges from -100 mV to +100

mV. Higher ZP values indicate stability and the lower the value, the higher the chances of aggregation which means less stability (Das et al., 2020).



**Scheme 2.8: Showing the zeta potential of colloidal solutions**

## **2.7 Biological applications of gold and silver nanoparticles**

### **2.7.1 Antioxidants**

Antioxidants are substances that can inhibit or delay the oxidation of an oxidizable substance even when present in low concentrations (Kasote et al., 2015). Natural antioxidants are mostly derived from plant materials and are predominantly phenolic compounds such as catechins, rutin, quercetin and curcumin (Lourenço et al., 2019). Antioxidants have been reported to serve as antioxidant enzyme cofactors, radical chain reaction inhibitors, oxidative enzyme inhibitors and metal chelators (Karadag et al., 2009). They have also been reportedly used as supplements, additives and preservatives in food (Esteve et al., 2007). In addition to maintaining the antioxidant status, they help in better physiological functioning of the body (Kaliya et al., 2006). They are useful in the human body by protecting the cells and organs against the effects of free radicals which may be derived from oxygen or nitrogen sources as reactive oxygen and nitrogen species (ROS/RNS) respectively (Ayoub et al., 2018). When this defence mechanism becomes weak or non-existent, other health challenges become enhanced. Oxidative stress has been linked to the cause of many deadly diseases like cancer, diabetics and other cardiovascular

diseases, the management of which is costly (Flora et al., 2007). Hence, materials with both antioxidant and other potential activities will be of great benefit (Laura et al., 2010; Sies, 2015). This necessitates the need to search for antioxidants which may also possess enhanced reducing and capping abilities in NPs formation.

To evaluate the antioxidant potential of a given material, standard methods such as Ferric Reducing Antioxidant Power (FRAP), Folin–Ciocalteu (FC), and 2,2'-azino-bis-3-ethylbenzotiazolin-6- sulfonic acid (ABTS), and 2,2-diphenyl-1-picrylhydrazyl (DPPH) radical scavenging assay are often employed. Different reaction mechanisms are involved. FRAP operates by a mechanism known as single electron transfer (SET), whereby an antioxidant transfers an electron to the corresponding cation which would neutralize it, whereas ABTS is largely operating on hydrogen atom transfer (HAT) (Duletić-Laušević et al., 2018). The oxidizing powers are then compared with that of a control. Often, known antioxidants such as flavonoids and carotenoids.

Like the metal-reducing ability of plant extracts, the antioxidant activity has been associated with the plants' phenolics (Khoshnamvand et al., 2019). Pu and colleagues argued that antioxidants possess free radical scavenging properties, hence, they play a role in promoting health and preventing diseases (Pu et al., 2019). More recently, several antioxidant activities have been carried out on gold and silver nanoparticles of *Cassia angustifolia*, *Alcea rosea*, and *Chamaecostus cuspidatus* (Bharathi and Bhuvaneshwari, 2019; Khoshnamvand et al., 2019; Ponnaniakajamideen and Rajeshkumar, 2019) through the green route. The results demonstrated encouraging scavenging activities. Table 2.5 provides a list of MNPs biosynthesized using different parts of plant including stem, flowers, leaves, fruits and leaves as well as the varying sizes obtained.

**Table 2.5: Recent literature on the application of silver and gold nanoparticles as antioxidant agents**

Plant material	Plant parts	Type of NPs	Size of NPs	Assay type	References
<i>Diospyros Montana</i>	Stem	Ag	28 nm	DPPH, HP	(Bharathi et al., 2018)
<i>Cassia angustifolia</i>	Flowers	Ag	10-80 nm	DPPH, HP, FRAP	(Bharathi and Bhuvaneshwari, 2019)
<i>Agrimonia Pilosa</i>	Aerial part	Au	20-50 nm	DPPH	(Patil et al., 2019)
<i>Alcea rosea</i>	Leaf	Au	4-95 nm	DPPH, FRAP	(Khoshnamvand et al., 2019)
<i>Silybum marianum</i>	Leaf and seed	Ag	13.20-18.12 nm	DPPH, FRAP, TAC, TRP, ABTS	(Shah et al., 2020)
<i>Pisum sativum</i>	Outer peels	Ag	10-25 nm	DPPH	(Patra et al., 2019)
<i>Ipomoea batatas</i>	Outer peels	Ag	8.67-11.52 nm	DPPH, NOx, ABTS, RP	(Das et al., 2019)
<i>Embllica officinalis</i>	Fruit	Au	10 nm	LP	(Mata et al., 2018)
<i>Halymenia dilatate</i>	Leaf	Au	16 nm	DPPH, RP, TA	(Vinosha et al., 2019)
<i>Pimpinella anisum</i>	Seeds	Ag and Au	16-48 nm	DPPH	(Zayed et al., 2020)
<i>Vitex negundo</i>	Leaf	Au	20-70 nm	DPPH	(Veena et al., 2019)
<i>Tropaeolum majus L.</i>	Flower	Ag	10.1-15.7 nm	DPPH, ABTS	(Valsalam et al., 2019)
<i>Lamprathus coccineus &amp; Malephora luteo</i>	Leaf	Ag	12-28 nm	MDA, GSH	(Youssif et al., 2019)
<i>Thymus vulgaris</i>	Leaf	Au	35 nm	DPPH	(Hamelian et al., 2018)
<i>Chamaecostus cuspidatus</i>	Leaf	Au	50 nm	DPPH, HR, RP, LP, SA, NOx	(Ponnanikajamideen and Rajeshkumar, 2019)

**NOTE:** DPPH = 2,2-diphenyl- 1-picrylhydrazyl, HP = hydrogen peroxide, FRAP = ferric reducing antioxidant power, TAC = total antioxidant capacity, TRP= total reducing power, ABTS = 2,2-azinobis-3-ethylbenzthiazoline-6-sulphonic acid, RP = reducing power, NOx = nitric oxide, LP= lipid peroxidation, TA = total antioxidant, MDA = brain malondialdehyde, GSH = brain glutathione, SA = superoxide anion, HR = hydroxyl radical

### 2.7.2 Antidiabetic activities

Diabetes mellitus has undoubtedly become a serious health challenge. More worrisome is type II diabetes mellitus (T2DM), which accounts for 90% of diabetes mellitus. It occurs as a result of the inefficient processing of insulin (Lysy et al., 2016). According to a recent report, the population of adults between the ages of 20 and 79 that suffered from diabetes was 425 million. This is equivalent to 9.9% of the world's population (Renner et al., 2020). By estimation, this disease would have drastically increased by 48% in 28 years if not properly managed (Cho et al., 2018). Although antidiabetic drugs such as miglitol, viglibose as well as acarbose are available in the market, they are costly and their continuous use is associated with side effects like weight gain, hyperglycemia and flatulence. Therefore, the need for more potent and newer remedies has emerged (Ahmad et al., 2018; Lorenzati et al., 2010; Santos et al., 2016).

Bioactive compounds in various plants have shown significant activity in the delay and management of T2DM. Extracts from different plants have been reported as alpha-glucosidase and alpha-amylase inhibitors (Furman et al., 2020; Nammi et al., 2003; Tariq et al., 2020; Yilmazer-Musa et al., 2012).

More importantly, biosynthesized metallic nanomaterials prepared from plant extracts have been employed in ameliorating this menace recently. *Chamalcostus cuspidatus*-AuNPs improved glycogen, glucose and insulin levels when administered to diabetic rats for 21 days (Ponnanikajamdeen and Rajeshkumar, 2019). In related studies, the green synthesized gold and silver NPs of *Gymnema sylvestre* (Agarwal et al., 2018) and *Cassia fistula* (Lysy et al., 2016) have shown antidiabetic properties. Furthermore, the *Cinnamomum tsoi*-nanoparticles showed inhibition of alpha-amylase and alpha-glucosidase enzymes. The authors observed that the antidiabetic activity may be because of the presence of oxidized polyphenols on the surface of the biosynthesized silver nanomaterial (Maddinedi et al., 2017). Recently, the use of single molecules as reducing/stabilizing agents for NP formation with antidiabetic activity has been reported (Dong et al., 2019; Payne et al., 2018; Shamprasad et al., 2019).

Table 2.6 details recent studies on the antidiabetic activities of other gold and silver NPs from different parts of plant. The size of the nanoparticles vary from less than 1  $\mu\text{m}$  to 117.59 nm depending on the phytochemical composition of the plant used. Most of the studies were done *in vitro*, employing two popular enzymes, the alpha-glucosidase and alpha-amylase for the antidiabetic potential evaluation. The nanoparticles were generated in an eco-friendly manner, making them suitable for the test.



**Table 2.6: Recent literature on the application of silver and gold nanoparticles as antidiabetic agents**

Plant material	Plant parts	Type of NPs	Size of NPs	Assay type	References
<i>Holoptelea integrifolia</i>	Leaf	Ag	32-38 nm	Amy	(Kumar et al., 2019)
<i>Pisum sativum</i>	Outer peels	Ag	10-25 nm	Glu	(Patra et al., 2019)
<i>Fritillaria cirrhosa</i>	Whole plant	Au	40-45 nm	RTM	(Guo et al., 2020)
<i>Sambucus nigra</i>	Leaf	Au	4-26 nm	RTM	(Opris et al., 2017)
<i>Allium cepa</i>	Bulb	Ag	49-73 nm	Glu and Amy	(Jini and Sharmila, 2020)
<i>Tephrosia tinctoria</i>	Leaf	Ag	73 nm	Glu and Amy	(Rajaram et al., 2015)i
<i>Cassia fistula</i>	Stem	Au	55.2-98.4 nm	RTM	(Daisy and Saipriya, 2012)
<i>Justicia diffusa</i>	Leaf	Ag	40-78 nm	Antidiabetic	(Ahmad et al., 2018)
<i>Sargassum swartzii</i>	Whole plant	Au	37 nm	RTM	(Dhas et al., 2016)
<i>Chamaecostus cuspidatus</i>	Leaf	Au	50 nm	RTM	(Ponnanikajamdeen and Rajeshkumar, 2019)
<i>Punica granatum</i>	Leaf	Ag	48 nm	Glu and Amy	(Saratale et al., 2018)
<i>Vitis vinifera</i>	Leaf and seed	Au	18-25 nm	Glu and Amy	(Khalil, 2016)
<i>Ipomoea batatas</i>	Outer peels	Ag	8.67-11.52 nm	Glu	(Das et al., 2019)
<i>Turbinaria conoides</i>	Leaf	Au	< 1 $\mu$ m	Amy	(Venkatraman et al., 2018)
<i>Gelidiella acerosa</i>	Leaf	Au	5.81-117.59 nm	Glu and Amy	(Senthilkumar et al., 2019)
<i>Ocimum basilicum</i>	Leaf and flower	Au and Ag	3-25 nm	Glu and Amy	(Malapermal et al., 2015)
<i>Leucosidea sericea</i>	Aerial part	Au	6-24 nm	Glu and Amy	(Badeggi et al., 2020)

**NOTE:** Amy= alpha-amylase enzyme, Glu = alpha-glucosidase enzyme, RTM= rat model, Glu and Amy = alpha-glucosidase and alpha-amylase enzyme evaluated

### 2.7.3 Antibacterial activities

Bacteria are single-celled tiny organisms that can be found in different environments. Although some bacteria are helpful such as those in the human digestive system, pathogenic bacteria are harmful and cause bacterial infections and diseases. Common pathogenic bacteria include *Escherichia coli* and *Salmonella*, known to cause food poisoning whereas *Staphylococcus aureus* causes a series of infections like pneumonia, boils, wound infections and cellulitis. Bacterial infections are contagious and can be complicated in some instances, especially with individuals having a compromised immune system due to diabetes, cancer and immunodeficiency disorders. Antibiotics such as quinolones, penicillin, tetracycline and aminoglycosides have been employed to manage infections. However, shortly after the discovery of penicillin, drug resistance occurred. This was due to misuse or overuse of the antibiotics (Mahady et al., 2008). Resistance is when certain antibiotics no longer kill or retard the activity of bacteria. Bacterial infections that are resistant to antibiotics are dangerous and can be lethal. Apart from the global economic challenges, the burden of drug-resistant infections is alarming, as it is estimated to cause 10 million deaths each year by 2050. It is also predicted to result in low productivity of goods and services by the industries as it will affect manpower. The cost of treating antimicrobial resistant microbes globally, may also be up to 100 trillion US dollars by the year 2050 (Phodha et al., 2019). In search for alternatives, scientists have focused on natural sources. Interesting activities have been reported from thousands of plants species on different bacterial species.

Two types of bacteria exist, the Gram-positive and Gram-negative. They can be differentiated in many ways. For instance, while the Gram-negative possess a thin cell wall (8-10 nm), the Gram-positive has a thick cell wall (20-80 nm). The Gram-positive does not have outer membrane which is present in the Gram-negative. This have in turn led to high lipid and lipoprotein content in the Gram-negative type compared the Gram-positive. Several amino acids have also been found to be present in the cell wall of the Gram-negative bacteria with only few ones in the cell wall of the Gram-positive. These differences often lead to different resistance and inhibition of the bacterial species. *Escherichia coli*, *Salmonella enterica*, *Serratia marcescens* and *Pseudomonas aeruginosa* are examples of Gram-negative bacterial species while those of Gram-positive include *Staphylococcus aureus*, *Bacillus cereus*.

The extracts from *Plumeria obtusa* displayed significant antimicrobial activities against four bacterial species. The Gram-negative species used in these studies were *Escherichia coli* and *Proteus vulgaris* while the Gram-positive ones were *Staphylococcus aureus* and *Staphylococcus epidermidis*. The phytochemical studies revealed the presence of alkaloids,

tannins, saponins, terpenoids, coumarins and flavonoids in the plant (Chudasama et al., 2018). Other phytochemicals with antibacterial activities such as Curcumin, Resveratrol, tryptanthrin and kaempferol have been isolated and tested against *Helicobacter pylori* species (Mahady et al., 2008; Kataoka et al., 2001).

Green nanotechnology has drawn further attention as MNPs have equally displayed fascinating inhibitory activities against several pathogenic bacterial species. Both gold and silver NPs have been used as antibacterial agents with AgNPs taking the lead because of their unique characteristics as demonstrated in table 2.7 (Jemilugba et al., 2019; Shah et al., 2020). The inhibitory concentrations as well as the different bacterial strains evaluated were also provided in the table. It is evident from the table that plants of different families possess bioreductants capable of forming MNPs. The reducing and capping agents were also distributed in various parts of plant such as leaves and flowers. The NPs reported were of sizes ranging between 10-55 nm and demonstrated bactericidal effects against different bacterial species as indicated. The minimum inhibitory concentrations also vary across the NPs. Since different evaluation methods were used, the MICs were expressed in millimetre for the disc diffusion and microlitre for the microplate method. The table showed that both gold and silver NPs have been used as potential antibacterial agents in recent studies.

**Table 2.7: Recent literature on the application of silver and gold nanoparticles with antibacterial activities. The size of the nanoparticles, the inhibitory concentration and the bacterial species studied are included.**

Plant material	Plant parts	Size of NPs	MIC	Bacteria evaluated	References
<i>Silybum marianum</i>	Leaf/seed	* 13-18nm	6 mm	KP	(Shah et al., 2020)
<i>Pisum sativum</i>	Outer peels	* 10-25 nm	8.70– 11.10 mm	EC, EF, ST, SE	(Patra et al., 2019)
<i>Eulophia herbacea</i>	Tuber	* 11.70 nm	10-12.5 µg/mL	BS, SA, EC, PA	(Pawar and Patil, 2020)
<i>Convolvulus arvensis</i>	Leaf	* 28 nm	20 and 50 µg/mL	SA and PA	(Hamedi et al., 2017)
<i>Crataegus microphylla fruit</i>	Fruit	* 30-50 nm	1.75-14 µg/mL	SA, EF, PA, AB, EC, KP, PM	(Mortazavi-Derazkola et al., 2020)
<i>Daucus carota</i>	Tuber	* 20 nm	50 µg/mL	BC, SA, KP, PA	(Shanmuganathan et al., 2018)
<i>Combretum erythrophyllum</i>	Leaf	* 13.62 nm	11-15 mm	SA, SEP, EC, PV	(Jemilugba et al., 2019)
<i>Bauhinia purpurea</i>	Leaf	*** N/Av	4.2-11.9 mm	SA, BS, EC, PA	(Vijayan et al., 2019)
<i>Anacardium occidentale</i>	Leaf	** 40 nm	8-24 mm	EC and BS	(Veena et al., 2019)
<i>Tropaeolum majus</i>	Flower	* 35-55 nm	6.25 µg/mL	SA, EF, EC, ST, PA	(Valsalam et al., 2019)
<i>Halymenia dilatate</i>	Leaf	** 16 nm	13-21 mm	AH	(Vinosha et al., 2019)
<i>Thymus vulgaris</i>	Leaf	** 35 nm	22-25 mm	EC, PA, SA, BS	(Hamelian et al., 2018)
<i>Diospyros Montana</i>	Stem	* 28 nm	5-22 mm	BS, SA, EC, KA	(Bharathi et al., 2018)

**NOTE:** \* = silver nanoparticles, \*\* = gold nanoparticles, \*\*\* = gold and silver nanoparticles, N/Av = information on the size not available in the literature cited, MIC = minimum inhibitory concentration, AB = *Acinetobacter baumannii*, AH = *Aeromonas hydrophila*, BC = *Bacillus cereus*, BS = *Bacillus subtilis*, EC= *Escherichia coli*, EF= *Enterococcus faecium*, KA= *K. aerogenes*, KP= *Klebsiella pneumonia*, PA = *Pseudomonas aeruginosa*, PM = *Proteus mirabilis*, PV = *Proteus vulgaris*, SA = *Staphylococcus aureus*, SE = *Salmonella enterica*, SEP = *Staphylococcus epidermidis*, ST = *Salmonella typhimurium*.

## **2.8 Other potential biomedical applications of gold and silver nanoparticles**

Gold and silver nanoparticles possess unique characteristics such as tunable surface chemistry, biocompatibility, controllable morphology and size. These special attributes qualify them for many other biomedical applications including photodynamic therapy (PDT), photothermal therapy (PTT) and drug delivery carriers.

### **2.8.1 Photodynamic therapy (PDT)**

Because of the potential side effects in the use of both the chemo- and the radiotherapy means of cancer treatment, PDT presents a better alternative. It uses photosensitizers (PST) that can be activated by a laser of a given wavelength at the targeted tumour site (Lucky et al., 2015). This activation then leads to the generation of reactive oxygen species (ROS) when energy is transferred to molecular oxygen. ROS causes the oxidation of cellular molecules which will result in tumour cell death (Lucky et al., 2015; Elahi et al., 2018). According to a study by Vankayala et al., silver triangles and decahedron NPs, which generated singlet  $O_2$  through photo-irradiation were found to be useful photodynamic therapeutic reagents (Vankayala et al., 2013). The authors also reported that singlet  $O_2$  can be formed on Au surfaces like Au (100) and (111) in atomic form. They concluded that the photodynamic property was dependent on the morphology of the MNPs. Hence, NPs like silver decahedrons and gold tetrahedrons possess dual functions as photodynamic and photothermal therapeutic agents (Vankayala et al., 2013).

### **2.8.2 Photothermal therapy (PTT)**

Photothermal therapy, also referred to as optical hyperthermia has been used severally in the treatment of cancer. Boca and colleagues found that as photothermal transducers, the chitosan-AgNPs recorded high cell mortality than a known hyperthermia agent used as a reference (Boca et al., 2011). The triangular AgNPs were biocompatible and highly effective in cancer therapy. Similarly, AgNPs tuned to near 800 nm, generated heat upon

exposure to light thereby inducing breast cancer cell death through heat (Thompson et al., 2014). AuNPs also generated heat upon exposure to light at specific tumour cells thereby causing cell death (Riley and Day, 2017). Depending on the size and shape of MNPs (e.g. gold and silver), a different amount of heat can be generated for hyperthermia (Thompson et al., 2014).

### **2.8.3 Drug delivery carriers**

Any substrate employed in the process of getting a biologically active molecule (drug) to the required site is termed a drug carrier. Among the benefits of the drug carriers are improved selectivity, effectiveness, bioavailability and safety of drug administration (Ghosh et al., 2008). Interestingly, the drug release can be controlled slowly through a given period or triggered at the targeted site when application conditions are manipulated such that the non-tumorous cells are not affected. The unique properties of AuNPs made them very useful as drug delivery agents. For instance, their large surface to volume ratio accommodates large drugs such that multiples of drugs can be loaded on the surface for onward delivery to the right site (Kong et al., 2017; Elahi et al., 2018). AgNPs have also been employed as drug delivery systems. Nadeem and Ijaz showed an efficient reduction of the hemodynamics of stenosis (Nadeem and Ijaz, 2016). Further, organically synthesized AgNPs doped with an anticancer drug [2-devinyl-2-(1-hexyloxyethyl) pyropheophorbide] was efficiently taken up by tumour cells and upon irradiation, displayed significant cell death (Roy et al., 2003).

## References

- Abbasi, T., Anuradha, J., Ganaie, S.U. & Abbasi, S.A. 2015. Gainful utilization of the highly intransigent weed ipomoea in the synthesis of gold nanoparticles. *Journal of King Saud University - Science*, 27(1): 15–22.
- Adamu, M., Mukandiwa, L., Awouafack, M.D., Ahmed, A.S., Eloff, J.N. & Naidoo, V. 2019. Ultrastructure changes induced by the phloroglucinol derivative agrimol G isolated from *Leucosidea sericea* in *Haemonchus contortus*. *Experimental Parasitology*, 207: 107780.
- Adamu, M., Naidoo, V. & Eloff, J.N. 2013. Efficacy and toxicity of thirteen plant leaf acetone extracts used in ethnoveterinary medicine in South Africa on egg hatching and larval development of *Haemonchus contortus*. *BMC Veterinary Research*, 9(1): 38-45.
- Adamu, M., Naidoo, V. & Eloff, J.N. 2014. The antibacterial activity, antioxidant activity and selectivity index of leaf extracts of thirteen South African tree species used in ethnoveterinary medicine to treat helminth infections. *BMC Veterinary Research*, 10:52-58.
- Afshinnia, F., Rajendiran, T.M., Soni, T., Byun, J., Wernisch, S., Sas, K.M., Hawkins, J., Bellovich, K., Gipson, D., Michailidis, G., Pennathur, S., Kretzler, M., Gipson, D., Bellovich, K., Bhat, Z., Gadegbeku, C., Massengill, S. & Perumal, K. 2018. Impaired B-oxidation and altered complex lipid fatty acid partitioning with advancing CKD. *Journal of the American Society of Nephrology*, 29(1): 295–306.
- Agarwal, H., Venkat Kumar, S. & Rajeshkumar, S. 2018. Antidiabetic effect of silver nanoparticles synthesized using lemongrass (*Cymbopogon citratus*) through conventional heating and microwave irradiation approach. *Journal of Microbiology, Biotechnology and Food Sciences*, 7(4): 371–376.
- Agasti, N., Singh, V.K. & Kaushik, N.K. 2015. Synthesis of water soluble glycine capped silver nanoparticles and their surface selective interaction. *Materials Research Bulletin*, 64: 17–21.
- Agrawal, Y. & Patel, V. 2011. Nanosuspension: An approach to enhance solubility of drugs. *Journal of Advanced Pharmaceutical Technology and Research*, 2(2): 81.
- Ahmad, B., Hafeez, N., Bashir, S., Rauf, A. & Mujeeb-ur-Rehman. 2017. Phytofabricated gold nanoparticles and their biomedical applications. *Biomedicine and Pharmacotherapy*, 89: 414–425.
- Ahmad, T., Azmi, M., Irfan, M., Moniruzzaman, M., Asghar, A. & Bhattacharjee, S. 2018. Green synthesis of stabilized spherical shaped gold nanoparticles using novel aqueous *Elaeis guineensis* (oil palm) leaves extract. , 1159: 167–173.
- Aiello, P., Consalvi, S., Poce, G., Raguzzini, A., Toti, E., Palmery, M., Biava, M., Bernardi,

- M., Kamal, M.A., Perry, G. & Peluso, I. 2019. Dietary flavonoids: Nano delivery and nanoparticles for cancer therapy. *Seminars in Cancer Biology*, 1–16.
- Ajayi, E. & Afolayan, A. 2017. Green synthesis, characterization and biological activities of silver nanoparticles from alkalized *Cymbopogon citratus* Stapf. *Advances in Natural Sciences: Nanoscience and Nanotechnology*, 8: 015017.
- Al-Ghamdi, H.S. & Mahmoud, W.E. 2013. One pot synthesis of multi-plasmonic shapes of silver nanoparticles. *Materials Letters*, 105: 62–64.
- Al-Yasiri, A.Y., Khoobchandani, M., Cutler, C.S., Watkinson, L., Carmack, T., Smith, C.J., Kuchuk, M., Loyalka, S.K., Lugão, A.B. & Katti, K. V. 2017. Mangiferin functionalized radioactive gold nanoparticles (MGF-198AuNPs) in prostate tumor therapy: Green nanotechnology for production: *In vivo* tumor retention and evaluation of therapeutic efficacy. *Dalton Transactions*, 46(42): 14561–14571.
- Ali, I.O. 2013. Synthesis and characterization of Ag<sup>0</sup>/PVA nanoparticles via photo- and chemical reduction methods for antibacterial study. *Colloids and Surfaces A: Physicochemical and Engineering Aspects*, 436: 922–929.
- Ali, M., Khan, T., Fatima, K., Ali, Q. ul A., Ovais, M., Khalil, A.T., Ullah, I., Raza, A., Shinwari, Z.K. & Idrees, M. 2018. Selected hepatoprotective herbal medicines: Evidence from ethnomedicinal applications, animal models, and possible mechanism of actions. *Phytotherapy Research*, 32(2): 199–215.
- Amendola, V., Bakr, O.M. & Stellacci, F. 2010. A study of the surface plasmon resonance of silver nanoparticles by the discrete dipole approximation method: Effect of shape, size, structure, and assembly. *Plasmonics*, 5(1): 85–97.
- Anand, H., Kumar, K., Kumar, B., Mohan, K., Sai, T., Madhiyazhagan, P. & Ranjan, A. 2014. Molecular and biomolecular spectroscopy antimicrobial and antioxidant activities of *Mimusops elengi* seed extract mediated isotropic silver nanoparticles. *Spectrochimica Acta Part A: Molecular And Biomolecular Spectroscopy*, 130: 13–18.
- Anastas, P.T. 1999. Green Chemistry and the role of analytical methodology development. *Critical Reviews in Analytical Chemistry*, 29(3): 167–175.
- Anastas, P.T., Warner, J.C., 1998. Green chemistry: Theory and practice. Oxford University Press.
- Anbu, P., Gopinath, S.C.B., Yun, H.S. & Lee, C.G. 2019. Temperature-dependent green biosynthesis and characterization of silver nanoparticles using balloon flower plants and their antibacterial potential. *Journal of Molecular Structure*, 1177: 302–309.
- Arassu, R.R.T. & Nambikkairaj, B. 2018. *Pelargonium graveolens* plant leaf essential oil mediated green synthesis of silver nanoparticles and its antifungal activity against human pathogenic fungi. *Journal of Pharmacognosy and Phytochemistry*, 7(6): 1778–1784.



- Aremu, A.O., Finnie, J.F. & Van Staden, J. 2012. Potential of South African medicinal plants used as anthelmintics- Their efficacy, safety concerns and reappraisal of current screening methods. *South African Journal of Botany*, 82: 134–150.
- Aremu, A.O., Ndhllala, A.R., Fawole, O.A., Light, M.E., Finnie, J.F. & Van Staden, J. 2010. *In vitro* pharmacological evaluation and phenolic content of ten South African medicinal plants used as anthelmintics. *South African Journal of Botany*, 76(3): 558–566.
- Aritonang, H.F., Koleangan, H. & Wuntu, A.D. 2019. Synthesis of silver nanoparticles using aqueous extract of medicinal plants' (*Impatiens balsamina* and *lantana camara*) fresh leaves and analysis of antimicrobial activity. *International Journal of Microbiology*, 2019: 8642303.
- Armendariz, V., Herrera, I., Peralta-Videa, J.R., Jose-Yacaman, M., Troiani, H., Santiago, P. & Gardea-Torresdey, J.L. 2004. Size controlled gold nanoparticle formation by *Avena sativa* biomass: Use of plants in nanobiotechnology. *Journal of Nanoparticle Research*, 6(4): 377–382.
- Aromal, S.A., Vidhu, V.K. & Philip, D. 2012. Green synthesis of well-dispersed gold nanoparticles using *Macrotyloma uniflorum*. *Spectrochimica Acta - Part A: Molecular and Biomolecular Spectroscopy*, 85: 99– 104
- Nisha, J. & Anbu, N. 2017. Pharmacological properties of turmeric– A review. *World Journal of Pharmaceutical Research*, 6(8): 2489–2503.
- Aryal, S., Remant, B.K.C., Dharmaraj, N., Bhattarai, N., Kim, C.H. & Kim, H.Y. 2006. Spectroscopic identification of SAu interaction in cysteine capped gold nanoparticles. *Spectrochimica Acta - Part A: Molecular and Biomolecular Spectroscopy*, 63(1): 160–163.
- Asong, J.A., Ndhlovu, P.T., Khosana, N.S., Aremu, A.O. & Otang-Mbeng, W. 2019. Medicinal plants used for skin-related diseases among the Batswanas in Ngaka Modiri Molema District Municipality, South Africa. *South African Journal of Botany*, 126: 11–20.
- Au, L., Zhang, Q., Cobley, C.M., Gidding, M., Schwartz, A.G., Chen, J. & Xia, Y. 2010. Quantifying the cellular uptake of antibody-conjugated Au nanocages by two-photon microscopy and inductively coupled plasma mass spectrometry. *American Chemical Society Nano*, 4(1): 35–42.
- Ayoub, Z., Mehta A. & Mishra, S. 2018. Medicinal plants as natural antioxidants: A review medicinal plants as natural antioxidants. *Asian Journal of Pharmaceutica and Clinical Research*, 11(6): 32-44.
- Badeggi, U.M., Ismail, E., Adeloye, A.O., Botha, S., Badmus, J.A., Marnewick, J.L., Cupido, C.N. & Hussein, A.A. 2020. Green synthesis of gold nanoparticles capped with procyanidins from *Leucosidea sericea* as potential antidiabetic and antioxidant

- agents. *Biomolecules*, 10(3): 452-475.
- Bankar, A., Joshi, B., Ravi Kumar, A. & Zinjarde, S. 2010. Banana peel extract mediated synthesis of gold nanoparticles. *Colloids and Surfaces B: Biointerfaces*, 80(1): 45–50.
- Barnaby, S.N., Sarker, N.H. & Banerjee, I.A. 2012. Ellagic acid directed growth of Au–Pt bimetallic nanoparticles and their catalytic applications . *International Journal of Nanoscience*, 12(1): 1250037.
- Basse, K., Viljoen, A., Combrinck, S. & Choi, Y.H. 2015. New phytochemicals from the coroms of medicinally important South African *Hypoxis* species. *Phytochemistry Letters*, 10: lxxix–lxxv.
- Beecher, G.R. 2004. Proanthocyanidins: Biological activities associated with human health. *Pharmaceutical Biology*, 42: 2–20.
- Berké, B. & De Freitas, V.A.P. 2005. Influence of procyanidin structures on their ability to complex with oenin. *Food Chemistry*, 90(3): 453–460.
- Bharathi, D. & Bhuvaneshwari, V. 2019. Evaluation of the cytotoxic and antioxidant activity of phyto-synthesized silver nanoparticles using *Cassia angustifolia* flowers. *BioNanoScience*, 9(1): 155–163.
- Bharathi, D., Diviya Josebin, M., Vasantharaj, S. & Bhuvaneshwari, V. 2018. Biosynthesis of silver nanoparticles using stem bark extracts of *Diospyros montana* and their antioxidant and antibacterial activities. *Journal of Nanostructure in Chemistry*, 8(1): 83–92.
- Bhatia S. (2016) Nanoparticles Types, Classification, Characterization, Fabrication Methods and Drug Delivery Applications. In: Natural Polymer Drug Delivery Systems. Springer, Cham. pp. 33-93. [https://doi.org/10.1007/978-3-319-41129-3\\_2](https://doi.org/10.1007/978-3-319-41129-3_2).
- Bhushan B. (2017) Introduction to Nanotechnology. In: Bhushan B. (eds) Springer Handbook of Nanotechnology. Springer Handbooks. Springer, Berlin, Heidelberg. [https://doi.org/10.1007/978-3-662-54357-3\\_1](https://doi.org/10.1007/978-3-662-54357-3_1).
- Bin-Umer, M.A., McLaughlin, J.E., Butterly, M.S., McCormick, S. & Tumer, N.E. 2014. Elimination of damaged mitochondria through mitophagy reduces mitochondrial oxidative stress and increases tolerance to trichothecenes. *Proceedings of the National Academy of Sciences of the United States of America*, 111(32): 11798–11803.
- Bisht, S., Feldmann, G., Soni, S., Ravi, R., Karikar, C., Maitra, Amarnath & Maitra, Anirban. 2007. Polymeric nanoparticle-encapsulated curcumin ('nanocurcumin'): A novel strategy for human cancer therapy. *Journal of Nanobiotechnology*, 5: 1–18.
- Boca, S.C., Potara, M., Gabudean, A.M., Juhem, A., Baldeck, P.L. & Astilean, S. 2011. Chitosan-coated triangular silver nanoparticles as a novel class of biocompatible, highly effective photothermal transducers for in vitro cancer cell therapy. *Cancer*

*Letters*, 311(2): 131–140.

- Bosman, A.A., Combrinck, S., Roux-Van Der Merwe, R., Botha, B.M. & McCrindle, R.I. 2004. Isolation of an anthelmintic compound from *Leucosidea sericea*. *South African Journal of Botany*, 70(4): 509–511.
- Boukes, G.J. & Van De Venter, M. 2012. Rooperol as an antioxidant and its role in the innate immune system: An in vitro study. *Journal of Ethnopharmacology*, 144(3): 692–699.
- Boukes, G.J., Venter, M. Van De & Oosthuizen, V. 2008. Quantitative and qualitative analysis of sterols/sterolins and hypoxoside contents of three *Hypoxis* (African potato) spp . *African Journal of Biotechnology*, 7(11): 1624–1629.
- Brandon, G. 1991. The uses of plants in healing in an Afro–Cuban religion, Santeria. *Journal of Black Studies*, 22(1): 55–76.
- Brown, L., Heyneke, O., Brown, D., van Wyk, J.P.H. & Hamman, J.H. 2008. Impact of traditional medicinal plant extracts on antiretroviral drug absorption. *Journal of Ethnopharmacology*, 119(3): 588–592.
- Bunaciu, A.A., Udriștioiu, E., Aboul-enein, H.Y., Bunaciu, A.A., Udriștioiu, E., Aboul-enein, H.Y., Bunaciu, A.A. & S, E.G.U. 2015. X-Ray Diffraction: Instrumentation and applications. *Critical reviews in analytical chemistry*, 45(4): 289-299.
- Chahardoli, A., Karimi, N. & Fattahi, A. 2017. Biosynthesis, characterization, antimicrobial and cytotoxic effects of silver nanoparticles using *Nigella arvensis* seed extract. *Iranian Journal of Pharmaceutical Research*, 16(3): 1167-1175.
- Chanda, N., Shukla, R., Zambre, A., Mekapothula, S., Kulkarni, R.R., Katti, Kavita, Bhattacharyya, K., Fent, G.M., Casteel, S.W., Boote, E.J., Viator, J.A., Upendran, A., Kannan, R. & Katti, Kattesh V. 2011. An effective strategy for the synthesis of biocompatible gold nanoparticles using cinnamon phytochemicals for phantom CT imaging and photoacoustic detection of cancerous cells. *Pharmaceutical Research*, 28(2): 279–291.
- Chandran, S.P., Chaudhary, M., Pasricha, R., Ahmad, A. & Sastry, M. 2006. Synthesis of gold nanotriangles and silver nanoparticles using *Aloe vera* plant extract. *Biotechnology Progress*, 22(2): 577–583.
- Chen, D.H. & Chen, Y.Y. 2002. Synthesis of strontium ferrite nanoparticles by coprecipitation in the presence of polyacrylic acid. *Materials Research Bulletin*, 37(4): 801–810.
- Cho, N.H., Shaw, J.E., Karuranga, S., Huang, Y., da Rocha Fernandes, J.D., Ohlrogge, A.W. & Malanda, B. 2018. IDF Diabetes Atlas: Global estimates of diabetes prevalence for 2017 and projections for 2045. *Diabetes Research and Clinical Practice*, 138: 271–281.

- Choi, Y., Choi, M.J., Cha, S.H., Kim, Y.S., Cho, S. & Park, Y. 2014. Catechin-capped gold nanoparticles: Green synthesis, characterization, and catalytic activity toward 4-nitrophenol reduction. *Nanoscale Research Letters*, 9(1): 1–8.
- Chokkalingam, M., Singh, P., Huo, Y., Soshnikova, V., Ahn, S., Kang, J., Mathiyalagan, R., Kim, Y.J. & Yang, D.C. 2019. Facile synthesis of Au and Ag nanoparticles using fruit extract of *Lycium chinense* and their anticancer activity. *Journal of Drug Delivery Science and Technology*, 49: 308–315.
- Chung, I.M., Park, I., Seung-Hyun, K., Thiruvengadam, M. & Rajakumar, G. 2016. Plant-mediated synthesis of silver nanoparticles: Their characteristic properties and therapeutic applications. *Nanoscale Research Letters*, 11: 40-53.
- Dada, A.O., Inyinbor, A.A., Idu, E.I., Bello, O.M., Oluyori, A.P., Adelani-Akande, T.A., Okunola, A.A. & Dada, O. 2018. Effect of operational parameters, characterization and antibacterial studies of green synthesis of silver nanoparticles using *Tithonia diversifolia*. *PeerJ*, 6: 1–17.
- Daisy, P. & Saipriya, K. 2012. Biochemical analysis of *Cassia fistula* aqueous extract and phytochemically synthesized gold nanoparticles as hypoglycemic treatment for diabetes mellitus. *International Journal of Nanomedicine*, 7: 1189–1202.
- Danaei, M., Dehghankhold, M., Ataei, S., Hasanzadeh Davarani, F., Javanmard, R., Dokhani, A., Khorasani, S. & Mozafari, M.R. 2018. Impact of particle size and polydispersity index on the clinical applications of lipidic nanocarrier systems. *Pharmaceutics*, 10(2): 1–17.
- Darroudi, M., Ahmad, M. Bin, Zamiri, R., Zak, A.K., Abdullah, A.H. & Ibrahim, N.A. 2011. Time-dependent effect in green synthesis of silver nanoparticles. *International Journal of Nanomedicine*, 6(1): 677–681.
- Das, A., Dutta, A., Razzaque, S., Saha, B., Gope, P.S. & Choudhury, N. 2011. Analgesic and antidiarrheal properties of the latex of *Calotropis procera*. *International Journal of Pharmaceutical and Biological Archives*, 2(1): 521–525.
- Das, G., Patra, J.K., Basavegowda, N., Vishnuprasad, C.N. & Shin, H.S. 2019. Comparative study on antidiabetic, cytotoxicity, antioxidant and antibacterial properties of biosynthesized silver nanoparticles using outer peels of two varieties of *Ipomoea batatas* (L.). *International Journal of Nanomedicine*, 14: 4741–4754.
- Das, G., Patra, J.K. & Shin, H.S. 2020. Biosynthesis, and potential effect of fern mediated biocompatible silver nanoparticles by cytotoxicity, antidiabetic, antioxidant and antibacterial, studies. *Materials Science and Engineering C*, 114: 111011.
- Dhas, T.S., Kumar, V.G., Karthick, V., Vasanth, K., Singaravelu, G. & Govindaraju, K. 2016. Enzyme and microbial technology effect of biosynthesized gold nanoparticles by *Sargassum swartzii* in alloxan induced diabetic rats. *Enzyme and Microbial Technology*, 95: 100–106.

- Dhavan, P.P. & Jadhav, B.L. 2020. Eco-friendly approach to control dengue vector *Aedes aegypti* larvae with their enzyme modulation by *Lumnitzera racemosa* fabricated zinc oxide nanorods. *SN Applied Sciences*, 2(5).
- Dong, C., Zhang, X., Cai, H. & Cao, C. 2014. Facile and one-step synthesis of monodisperse silver nanoparticles using *gum acacia* in aqueous solution. *Journal of Molecular Liquids*, 196: 135–141.
- Dong, X.Q., Zou, B., Zhang, Y., Ge, Z.Z., Du, J. & Li, C.M. 2013. Preparation of A-type proanthocyanidin dimers from peanut skins and persimmon pulp and comparison of the antioxidant activity of A-type and B-type dimers. *Fitoterapia*, 91: 128–139.
- Dong, Y., Wan, G., Yan, P., Qian, C., Li, F. & Peng, G. 2019. Fabrication of resveratrol coated gold nanoparticles and investigation of their effect on diabetic retinopathy in streptozotocin induced diabetic rats. *Journal of Photochemistry and Photobiology, B: Biology*, 195(1): 51–57.
- Drewes, S.E., Elliot, E., Khan, F., Dhlamini, J.T.B. & Gcumisa, M.S.S. 2008. *Hypoxis hemerocallidea*- Not merely a cure for benign prostate hyperplasia. *Journal of Ethnopharmacology*, 119(3): 593–598.
- Drewes, S.E. & Khan, F. 2004. The African potato (*Hypoxis hemerocallidea*): A chemical-historical perspective. *South African Journal of Science*, 100(9–10): 425–430.
- Dubey, S.P., Lahtinen, M. & Sillanpää, M. 2010. Tansy fruit mediated greener synthesis of silver and gold nanoparticles. *Process Biochemistry*, 45(7): 1065–1071.
- Duletić-Laušević, S., Aradski, A.A., Kolarević, S., Vuković-Gačić, B., Oalde, M., Živković, J., Šavikin, K. & Marin, P.D. 2018. Antineurodegenerative, antioxidant and antibacterial activities and phenolic components of *Origanum majorana* L. (*Lamiaceae*) extracts. *Journal of Applied Botany and Food Quality*, 91: 126–134.
- Dwivedi, A.D. & Gopal, K. 2010. Biosynthesis of silver and gold nanoparticles using *Chenopodium album* leaf extract. *Colloids and Surfaces A: Physicochemical and Engineering Aspects*, 369(1–3): 27–33.
- Elahi, N., Kamali, M. & Baghersad, M.H. 2018. Recent biomedical applications of gold nanoparticles: A review. *Talanta*, 184: 537-556.
- Elbagory, A.M., Hussein, A.A. & Meyer, M. 2019. The *in vitro* immunomodulatory effects of gold nanoparticles synthesized from *Hypoxis hemerocallidea* aqueous extract and hypoxoside on macrophage and natural killer cells. *International Journal of Nanomedicine*, 14: 9007–9018.
- Elbagory, A.M., Meyer, M., Cupido, C.N. & Hussein, A.A. 2017. Inhibition of bacteria associated with wound infection by biocompatible green synthesized gold nanoparticles from south african plant extracts. *Nanomaterials*, 7(12): 417-438.
- Elobeid, M.A. 2016. Amelioration of streptozotocin induced diabetes in rats by eco-friendly

- composite nano-cinnamon extract. *Pakistan Journal Zoology*, 48(3): 645–650.
- Erol, O., Uyan, I., Hatip, M., Yilmaz, C., Tekinay, A.B. & Guler, M.O. 2018. Recent advances in bioactive 1D and 2D carbon nanomaterials for biomedical applications. *Nanomedicine: Nanotechnology, Biology, and Medicine*, 14(7): 2433–2454.
- Espinosa-cristóbal, L.F., Martínez-castañón, G.A., Martínez-martínez, R.E. & Loyola-rodríguez, J.P. 2012. Antimicrobial sensibility of *Streptococcus mutans* serotypes to silver nanoparticles. *Materials Science and Engineering C*, 32(4): 896–901.
- Esteve, J., Frascuet, I., Fri, A. & Zulueta, A. 2007. Vitamin C, vitamin A, phenolic compounds and total antioxidant capacity of new fruit juice and skim milk mixture beverages marketed in Spain. *Food Chemistry*, 103: 1365–1374.
- Fatimah, I. 2016. Green synthesis of silver nanoparticles using extract of *Parkia speciosa* Hassk pods assisted by microwave irradiation. *Journal of Advanced Research*, 7(6): 961–969.
- Fierascu, R.C., Ortan, A., Avramescu, S.M. & Fierascu, I. 2019. Phyto-nanocatalysts: Green synthesis characterization, and applications. *Molecules*, 24(19): 1–35.
- Flora, S.J.S., Flora, G., Saxena, G. & Mishra, M. 2007. Arsenic and lead induced free radical generation and their reversibility following chelation. *Cellular and Molecular Biology*, 53(1): 26–47.
- Fouche, G., Cragg, G.M., Pillay, P., Kolesnikova, N., Maharaj, V.J. & Senabe, J. 2008. *In vitro* anticancer screening of South African plants. *Journal of Ethnopharmacology*, 119(3): 455–461.
- Furman, B.L., Candasamy, M., Bhattamisra, S.K. & Veettil, S.K. 2020. Reduction of blood glucose by plant extracts and their use in the treatment of diabetes mellitus; discrepancies in effectiveness between animal and human studies. *Journal of Ethnopharmacology*, 24: 112264.
- Ganesan, P. & Narayanasamy, D. 2017. Lipid nanoparticles: Different preparation techniques, characterization, hurdles, and strategies for the production of solid lipid nanoparticles and nanostructured lipid carriers for oral drug delivery. *Sustainable Chemistry and Pharmacy*, 6: 37–56.
- Ganesh Kumar, V., Dinesh Gokavarapu, S., Rajeswari, A., Stalin Dhas, T., Karthick, V., Kapadia, Z., Shrestha, T., Barathy, I.A., Roy, A. & Sinha, S. 2011. Facile green synthesis of gold nanoparticles using leaf extract of antidiabetic potent *Cassia auriculata*. *Colloids and Surfaces B: Biointerfaces*, 87(1): 159–163.
- Gangwar, J., Gupta, B.K., Tripathi, S.K. & Srivastava, A.K. 2015. Phase dependent thermal and spectroscopic responses of Al<sub>2</sub>O<sub>3</sub> nanostructures with different morphogenesis. *Nanoscale*, 7(32): 13313–13344.
- Ghosh, P., Han, G., De, M., Kim, C.K. & Rotello, V.M. 2008. Gold nanoparticles in delivery

- applications. *Advanced Drug Delivery Reviews*, 60(11): 1307–1315.
- Goldblatt, P. and Manning, J.C., 2002. Plant diversity of the Cape region of southern Africa. *Annals of the Missouri Botanical Garden*, pp.281-302.
- Göl, F., Aygün, A., Seyrankaya, A., Gür, T., Yenikaya, C. & Şen, F. 2020. Green synthesis and characterization of *Camellia sinensis* mediated silver nanoparticles for antibacterial ceramic applications. *Materials Chemistry and Physics*, 250: 123037.
- Goldstein, J., Newbury, D.E., Joy, D.C., Lyman, E., Echlin, P., Lifshin, E., Sawyer, L.C., Eds, J.R.M., Academic, K. & Publishers, P. 2003. Scanning Electron Microscopy and X-Ray Microanalysis. *Micron*, 34: 453.
- González-Ballesteros, N., Rodríguez-González, J.B. & Rodríguez-Argüelles, M.C. 2018. Harnessing the wine dregs: An approach towards a more sustainable synthesis of gold and silver nanoparticles. *Journal of Photochemistry and Photobiology B: Biology*, 178: 302–309.
- Guo, Qingquan, Guo, Qiulan, Yuan, J. & Zeng, J. 2014. Biosynthesis of gold nanoparticles using a kind of flavonol: Dihydromyricetin. *Colloids and Surfaces A: Physicochemical and Engineering Aspects*, 441: 127–132.
- Guo, Y., Jiang, N., Zhang, L. & Yin, M. 2020. Green synthesis of gold nanoparticles from *Fritillaria cirrhosa* and its anti-diabetic activity on Streptozotocin induced rats. *Arabian Journal of Chemistry*, 13(4): 5096–5106.
- Halberstein, R.A. 2005. Medicinal plants: Historical and cross-cultural usage patterns. *Annals of Epidemiology*, 15(9): 686–699.
- Hamaguchi, K., Kawasaki, H. & Arakawa, R. 2010. Photochemical synthesis of glycine-stabilized gold nanoparticles and its heavy-metal-induced aggregation behavior. *Colloids and Surfaces A: Physicochemical and Engineering Aspects*, 367(1–3): 167–173.
- Hamed, S., Shojaosadati, S.A. & Mohammadi, A. 2017. Evaluation of the catalytic, antibacterial and anti-biofilm activities of the *Convolvulus arvensis* extract functionalized silver nanoparticles. *Journal of Photochemistry and Photobiology B: Biology*, 167: 36–44.
- Hamelian, M., Varmira, K. & Veisi, H. 2018. Green synthesis and characterizations of gold nanoparticles using *Thyme* and survey cytotoxic effect, antibacterial and antioxidant potential. *Journal of Photochemistry and Photobiology B: Biology*, 184: 71–79.
- Haslam, E. 1977. Symmetry and promiscuity in procyanidin biochemistry. *Phytochemistry*, 16(11): 1625–1640.
- Hemmati, S., Joshani, Z., Zangeneh, A. & Zangeneh, M.M. 2020. Green synthesis and chemical characterization of *Thymus vulgaris* leaf aqueous extract conjugated gold nanoparticles for the treatment of acute myeloid leukemia in comparison to

- doxorubicin in a leukemic mouse model. *Applied Organometallic Chemistry*, 34(2): 1–14.
- Hemmati, S., Rashtiani, A., Zangeneh, M.M., Mohammadi, P., Zangeneh, A. & Veisi, H. 2019. Green synthesis and characterization of silver nanoparticles using *Fritillaria* flower extract and their antibacterial activity against some human pathogens. *Polyhedron*, 158: 8–14.
- Holčapek, M., Jirásko, R. & Lísa, M. 2012. Recent developments in liquid chromatography-mass spectrometry and related techniques. *Journal of Chromatography A*, 1259: 3–15.
- Huy, P.D.Q. & Li, M.S. 2014. Binding of fullerenes to amyloid beta fibrils: Size matters. *Physical Chemistry Chemical Physics*, 16(37): 20030–20040.
- Hwang, S.J., Jun, S.H., Park, Yohan, Cha, S.H., Yoon, M., Cho, S., Lee, H.J. & Park, Youmie. 2015. Green synthesis of gold nanoparticles using chlorogenic acid and their enhanced performance for inflammation. *Nanomedicine: Nanotechnology, Biology, and Medicine*, 11(7): 1677–1688.
- Iconaru, S.L., Prodan, A.M., Le Coustumer, P. & Predoi, D. 2013. Synthesis and antibacterial and antibiofilm activity of iron oxide glycerol nanoparticles obtained by coprecipitation method. *Journal of Chemistry*, 2013: 412079.
- Iijima, S. 2002. Carbon nanotubes: Past, present, and future. *Physica B: Condensed Matter*, 323(1–4): 1–5.
- Islam, N.U., Jalil, K., Shahid, M., Muhammad, N. & Rauf, A. 2019. *Pistacia integerrima* gall extract mediated green synthesis of gold nanoparticles and their biological activities. *Arabian Journal of Chemistry*, 12(8): 2310–2319.
- Islam, N.U., Khan, I., Rauf, A., Muhammad, N., Shahid, M. & Shah, M.R. 2015. Antinociceptive, muscle relaxant and sedative activities of gold nanoparticles generated by methanolic extract of *Euphorbia milii*. *BMC Complementary and Alternative Medicine*, 15(1): 1–11.
- Jäger, A.K., Hutchings, A. & Van Staden, J. 1996. Screening of Zulu medicinal plants for prostaglandin-synthesis inhibitors. *Journal of Ethnopharmacology*, 52(2): 95–100.
- Jain, P.K., Huang, X., El-Sayed, I.H. & El-Sayed, M.A. 2008. Noble metals on the nanoscale: Optical and photothermal properties and some applications in imaging, sensing, biology, and medicine. *Accounts of Chemical Research*, 41(12): 1578–1586.
- Jemilugba, O.T., Sakho, E.H.M., Parani, S., Mavumengwana, V. & Oluwafemi, O.S. 2019. Green synthesis of silver nanoparticles using *Combretum erythrophyllum* leaves and its antibacterial activities. *Colloids and Interface Science Communications*, 31: 100191.
- Jeon, T.Y., Kim, D.J., Park, S.-G., Kim, S.-H. & Kim, D.-H. 2016. Nanostructured



- plasmonic substrates for use as SERS sensors. *Nano Convergence*, 3: 18-37.
- Jiang, W.E.N., Kim, B.Y.S., Rutka, J.T. & Chan, W.C.W. 2008. Nanoparticle-mediated cellular response is size-dependent. *Letters*, 3: 145–150.
- Jini, D. & Sharmila, S. 2020. Green synthesis of silver nanoparticles from *Allium cepa* and its in vitro antidiabetic activity. *Materials Today: Proceedings*, 22: 432–438.
- Joseph, D., Sachar, S., Kishore, N. & Chandra, S. 2015. Mechanistic insights into the interactions of magnetic nanoparticles with bovine serum albumin in presence of surfactants. *Colloids and Surfaces B: Biointerfaces*, 135: 596–603.
- Joshi, P., Chakraborty, S., Dey, S., Shanker, V., Ansari, Z.A., Singh, S.P. & Chakrabarti, P. 2011. Binding of chloroquine-conjugated gold nanoparticles with bovine serum albumin. *Journal of Colloid and Interface Science*, 355(2): 402–409.
- Kabanda, M.M. 2012. Antioxidant activity of rooperol investigated through Cu (I and II) chelation ability and the hydrogen transfer mechanism: A DFT study. *Chemical Research in Toxicology*, 25(10): 2153–2166.
- Kaliora, A.C., Dedoussis, G.V.Z. & Schmidt, H. 2006. Dietary antioxidants in preventing atherogenesis. *Atherosclerosis*, 187: 1–17.
- Karadag, A., Ozcelik, B. & Saner, S. 2009. Review of methods to determine antioxidant capacities. *Food Analytical Methods*, 2: 41–60.
- Karthick, V., Kumar, V.G., Dhas, T.S., Singaravelu, G., Sadiq, A.M. & Govindaraju, K. 2014. Effect of biologically synthesized gold nanoparticles on alloxan-induced diabetic rats-An *in vivo* approach. *Colloids and Surfaces B: Biointerfaces*, 122: 505–511.
- Kasote, D.M., Katyare, S.S., Hegde, M. V & Bae, H. 2015. Significance of antioxidant potential of plants and its relevance to therapeutic applications. *International Journal of Biological Sciences*, 11(8): 982-991.
- Kasthuri, J., Kathiravan, K. & Rajendiran, N. 2009a. Phyllanthin-assisted biosynthesis of silver and gold nanoparticles: A novel biological approach. *Journal of Nanoparticle Research*, 11(5): 1075–1085.
- Kasthuri, J., Veerapandian, S. & Rajendiran, N. 2009b. Biological synthesis of silver and gold nanoparticles using apiin as reducing agent. *Colloids and Surfaces B: Biointerfaces*, 68(1): 55–60.
- Kataoka, M., Hirata, K., Kunikata, T., Ushio, S., Iwaki, K., Ohashi, K., Ikeda, M. & Kurimoto, M. 2001. Antibacterial action of tryptanthrin and kaempferol, isolated from the indigo plant (*Polygonum tinctorium Lour.*), against *Helicobacter pylori*-infected Mongolian gerbils. *Journal of Gastroenterology*, 36(1): 5–9.
- Katerere, D.R. & Eloff, J.N. 2008. Anti-bacterial and anti-oxidant activity of *Hypoxis hemerocallidea* (Hypoxidaceae): Can leaves be substituted for corms as a

- conservation strategy? *South African Journal of Botany*, 74(4): 613–616.
- Kattumuri, V., Katti, Kavita, Bhaskaran, S., Boote, E.J., Casteel, S.W., Fent, G.M., Robertson, D.J., Chandrasekhar, M., Kannan, R. & Katti, Kattesh V. 2007. Gum arabic as a phytochemical construct for the stabilization of gold nanoparticles: *In vivo* pharmacokinetics and X-ray-contrast-imaging studies. *Small*, 3(2): 333–341.
- Kaur, M. & Bhullar, G.K. 2016. Partial characterization of tamarind (*Tamarindus indica* L.) Kernel starch oxidized at different levels of sodium hypochlorite. *International Journal of Food Properties*, 19(3): 605–617.
- Keneilwe, M., Saramma, G. & Kelvin, C. 2018. An *in-vitro* antioxidant and antidiabetic evaluation of traditional medicinal plants of Botswana. *Journal of Pharmaceutical Research International*, 22(6): 1–12.
- Khaleel, S., Govindaraju, K., Manikandan, R., Seog, J., Young, E. & Singaravelu, G. 2010. Phytochemical mediated gold nanoparticles and their PTP 1B inhibitory activity. *Colloids and Surfaces B: Biointerfaces*, 75: 405–409.
- Khalil, M. 2016. Biosynthesis of gold nanoparticles using extract of grape (*Vitis vinifera*) leaves and seeds. *Arabian Journal of Chemistry*, 7: 1131–1139.
- Khalil, M.M.H., Ismail, E.H., El-Baghdady, K.Z. & Mohamed, D. 2014. Green synthesis of silver nanoparticles using olive leaf extract and its antibacterial activity. *Arabian Journal of Chemistry*, 7(6): 1131–1139.
- Khan, H.A., Sakharkar, M.K., Nayak, A., Kishore, U. & Khan, A. 2018. *Nanoparticles for biomedical applications: An overview*. In: Narayan, R. (Ed.), *Nanobiomaterials*. Woodhead Publishing, pp. 357-384.
- Khan, Ibrahim, Saeed, K. & Khan, Idrees. 2019. Nanoparticles: Properties, applications and toxicities. *Arabian Journal of Chemistry*, 12(7): 908–931.
- Khan, M.A., Raza, A., Ovais, M., Sohail, M.F. & Ali, S. 2018. Current state and prospects of nano-delivery systems for sorafenib. *International Journal of Polymeric Materials and Polymeric Biomaterials*, 67(18): 1105–1115.
- Khoshnamvand, M., Huo, C. & Liu, J. 2019. Silver nanoparticles synthesized using *Allium ampeloprasum* L. leaf extract: Characterization and performance in catalytic reduction of 4-nitrophenol and antioxidant activity. *Journal of Molecular Structure*, 1175: 90–96.
- Kim, H. seok, Seo, Y.S., Kim, K., Han, J.W., Park, Y. & Cho, S. 2016. Concentration effect of reducing agents on green synthesis of gold nanoparticles: Size, morphology, and growth mechanism. *Nanoscale Research Letters*, 11: 230-238.
- Kong, F.Y., Zhang, J.W., Li, R.F., Wang, Z.X., Wang, W.J. & Wang, W. 2017. Unique roles of gold nanoparticles in drug delivery, targeting and imaging applications. *Molecules*, 22:1445-1457.

- Kouhbanani, M.A.J., Beheshtkhoo, N., Nasirmoghadas, P., Yazdanpanah, S., Zomorodian, K., Taghizadeh, S. & Amani, A.M. 2019. Green synthesis of spherical silver nanoparticles using *Ducrosia anethifolia* aqueous extract and its antibacterial activity. *Journal of Environmental Treatment Techniques*, 7(3): 461–466.
- Krpetić, Ž., Scari, G., Caneva, E., Speranza, G. & Porta, F. 2009. Gold nanoparticles prepared using cape aloe active components. *Langmuir*, 25(13): 7217–7221.
- Kumar, V., Singh, S., Srivastava, B., Bhadouria, R. & Singh, R. 2019. Green synthesis of silver nanoparticles using leaf extract of *Holoptelea integrifolia* and preliminary investigation of its antioxidant, anti-inflammatory, antidiabetic and antibacterial activities. *Journal of Environmental Chemical Engineering*, 7(3): 103094.
- Lall, N. & Kishore, N. 2014. Are plants used for skin care in South Africa fully explored? *Journal of Ethnopharmacology*, 153(1): 61–84.
- Laporta, O., Funes, L., Garzón, M.T., Villalaín, J. & Micol, V. 2007. Role of membranes on the antibacterial and anti-inflammatory activities of the bioactive compounds from *Hypoxis rooperi* corm extract. *Archives of Biochemistry and Biophysics*, 467(1): 119–131.
- Laporta, O., Pérez-Fons, L., Mallavia, R., Caturla, N. & Micol, V. 2007. Isolation, characterization and antioxidant capacity assessment of the bioactive compounds derived from *Hypoxis rooperi* corm extract (African potato). *Food Chemistry*, 101(4): 1425–1437.
- Laura, P.F., Garzón, M.T. & Vicente, M. 2010. Relationship between the antioxidant capacity and effect of rosemary (*Rosmarinus officinalis* L.) polyphenols on membrane phospholipid order. *Journal of Agricultural and Food Chemistry*, 58(1): 161–171.
- Li, D., Fang, W., Feng, Y., Geng, Q. & Song, M. 2019. Stability properties of water-based gold and silver nanofluids stabilized by cationic gemini surfactants. *Journal of the Taiwan Institute of Chemical Engineers*, 97: 458–465.
- Li, Y., Zhang, J., Gu, J., Chen, S., Wang, C. & Jia, W. 2017. Biosynthesis of polyphenol-stabilised nanoparticles and assessment of anti-diabetic activity. *Journal of Photochemistry and Photobiology B: Biology*, 169: 96–100.
- Liu, H., Lian, T., Liu, Y., Hong, Y., Sun, D. & Li, Q. 2017. Plant-mediated synthesis of Au nanoparticles: Separation and identification of active biomolecule in the water extract of *Cacumen platycladi*. *Industrial and Engineering Chemistry Research*, 56(18): 5262–5270.
- Lorenzati, B., Zucco, C., Miglietta, S., Lamberti, F. & Bruno, G. 2010. Oral hypoglycemic drugs: Pathophysiological basis of their mechanism of action. *Pharmaceuticals*, 3(9): 3005–3020.
- Lourenço, S.C., Mold, M. & Alves, V.D. 2019. Antioxidants of natural plant origins: From

- sources to food industry applications. *Molecules*, 24: 4132-4156.
- Lü, F., Gao, Y., Huang, J., Sun, D. & Li, Q. 2014. Roles of biomolecules in the biosynthesis of silver nanoparticles: Case of *Gardenia jasminoides* extract. *Chinese Journal of Chemical Engineering*, 22(6): 706–712.
- Lucky, S.S., Soo, K.C. & Zhang, Y. 2015. Nanoparticles in photodynamic therapy. *Chemical Reviews*, 115(4): 1990–2042.
- Luna, C., Barriga-castro, E.D. & Gómez-treviño, A. 2016. Properties of silver-based hybrid nanostructures biosynthesized using extracts of coriander leaves and seeds. *International Journal of Nanomedicine*, 11: 4787–4798.
- Lysy, P.A., Corritore, E. & Sokal, E.M. 2016. New insights into diabetes cell therapy. *Current Diabetes Reports*, 16: 38-48.
- Ma H., Shieh, K. & Tracy X. Qiao, T. X. 2006. Study of transmission electron microscopy (TEM) and scanning electron microscopy (SEM), *Nature and Science*, 4(3): 14-22.
- MacCuspie, R.I. 2011. Colloidal stability of silver nanoparticles in biologically relevant conditions. *Journal of Nanoparticle Research*, 13(7): 2893–2908.
- Maddinedi, S. babu, Mandal, B.K. & Maddili, S.K. 2017. Biofabrication of size controllable silver nanoparticles– A green approach. *Journal of Photochemistry and Photobiology B: Biology*, 167: 236–241.
- Mahady, G.B., Huang, Y., Doyle, B.J. & Locklear, T. 2008. Natural products as antibacterial agents. *Studies in Natural Products Chemistry*, 35(C): 423–444.
- Malapermal, V., Mbatha, N., Gengan, R. & Anand, K. 2015. Biosynthesis of bimetallic Au-Ag nanoparticles using *Ocimum basilicum* (L.) with antidiabetic and antimicrobial properties. *Advanced Materials Letters*, 6(12): 1050-1057.
- Maldonado, P.D., Rivero-Cruz, I., Mata, R. & Pedraza-Chaverrí, J. 2005. Antioxidant activity of A-type proanthocyanidins from *Geranium niveum* (Geraniaceae). *Journal of Agricultural and Food Chemistry*, 53(6): 1996–2001.
- Martins, S., Mussatto, S.I., Martínez-Avila, G., Montañez-Saenz, J., Aguilar, C.N. & Teixeira, J.A. 2011. Bioactive phenolic compounds: Production and extraction by solid-state fermentation. A review. *Biotechnology Advances*, 29(3): 365–373.
- Maruyama, T., Fujimoto, Y. & Maekawa, T. 2015. Synthesis of gold nanoparticles using various amino acids. *Journal of Colloid And Interface Science*, 447: 254–257.
- Mata, R., Nakkala, J.R., Chandra, V.K., Raja, K. & Sadras, S.R. 2018. *In vivo* bio-distribution, clearance and toxicity assessment of biogenic silver and gold nanoparticles synthesized from *Abutilon indicum* in Wistar rats. *Journal of Trace Elements in Medicine and Biology*, 48: 157–165.
- Mittal, A.K., Kumar, S. & Banerjee, U.C. 2014. Quercetin and gallic acid mediated

- synthesis of bimetallic (silver and selenium) nanoparticles and their antitumor and antimicrobial potential. *Journal of Colloid and Interface Science*, 431: 194–199.
- Mocanu, A., Cernica, I., Tomoaia, G., Bobos, L.D., Horovitz, O. & Tomoaia-Cotisel, M. 2009. Self-assembly characteristics of gold nanoparticles in the presence of cysteine. *Colloids and Surfaces A: Physicochemical and Engineering Aspects*, 338(1–3): 93–101.
- Mohajeri, M., Behnam, B. & Sahebkar, A. 2018. Biomedical applications of carbon nanomaterials: Drug and gene delivery potentials. *Journal of Cellular Physiology*, 234(1): 298–319.
- Mohan Kumar, K., Mandal, B.K., Sinha, M. & Krishnakumar, V. 2012. *Terminalia chebula* mediated green and rapid synthesis of gold nanoparticles. *Spectrochimica Acta - Part A: Molecular and Biomolecular Spectroscopy*, 86: 490–494.
- Moreno-Vega, A.I., Gómez-Quintero, T., Nuñez-Anita, R.E., Acosta-Torres, L.S. & Castaño, V. 2012. Polymeric and ceramic nanoparticles in biomedical applications. *Journal of Nanotechnology*, 2012: 936041.
- Mortazavi-Derazkola, S., Ebrahimzadeh, M.A., Amiri, O., Goli, H.R., Rafiei, A., Kardan, M. & Salavati-Niasari, M. 2020. Facile green synthesis and characterization of *Crataegus microphylla* extract-capped silver nanoparticles (CME@Ag-NPs) and its potential antibacterial and anticancer activities against AGS and MCF-7 human cancer cells. *Journal of Alloys and Compounds*, 820: 153186.
- Moyo, M., Amoo, S.O., Aremu, A.O., Gruz, J., Šubrtová, M., Doležal, K. & Van Staden, J. 2014. Plant regeneration and biochemical accumulation of hydroxybenzoic and hydroxycinnamic acid derivatives in *Hypoxis hemerocallidea* organ and callus cultures. *Plant Science*, 227: 157–164.
- Mwinga, J.L., Asong, J.A., Amoo, S.O., Nkadameng, S.M., McGaw, L.J., Aremu, A.O. & Otang-Mbeng, W. 2019. *In vitro* antimicrobial effects of *Hypoxis hemerocallidea* against six pathogens with dermatological relevance and its phytochemical characterization and cytotoxicity evaluation. *Journal of Ethnopharmacology*, 242: 112048.
- Nadeem, S. & Ijaz, S. 2016. Impulsion of nanoparticles as a drug carrier for the theoretical investigation of stenosed arteries with induced magnetic effects. *Journal of Magnetism and Magnetic Materials*, 410: 230–241.
- Naidoo, D., Van Vuuren, S.F., Van Zyl, R.L. & De Wet, H. 2013. Plants traditionally used individually and in combination to treat sexually transmitted infections in northern Maputaland, South Africa: Antimicrobial activity and cytotoxicity. *Journal of Ethnopharmacology*, 149(3): 656–667.
- Nair, J.J., Aremu, A.O. & Van Staden, J. 2012. Anti-inflammatory effects of *Leucosidea sericea* (Rosaceae) and identification of the active constituents. *South African Journal*

of *Botany*, 80: 75–76.

- Nair, Vipin Devi Prasad & Kanfer, I. 2008. Development of dissolution tests for the quality control of complementary/alternate and traditional medicines: Application to African Potato products. *Journal of Pharmacy and Pharmaceutical Sciences*, 11(3): 35–44.
- Nair, Vipin D.P. & Kanfer, I. 2008. Sterols and sterolins in *Hypoxis hemerocallidea* (African potato). *South African Journal of Science*, 104(7–8): 323–324.
- Nakashima, H. 2009. Control of gold nanorod arrays through self-assembly of biomolecules. *NTT Technical Review*, 7(8):1-5.
- Nammi, S., Boini, M.K., Lodagala, S.D. & Behara, R.B.S. 2003. The juice of fresh leaves of *Catharanthus roseus* Linn. reduces blood glucose in normal and alloxan diabetic rabbits. *BMC Complementary and Alternative Medicine*, 3: 2–5.
- Ncube, B., Finnie, J.F. & Van Staden, J. 2012. *In vitro* antimicrobial synergism within plant extract combinations from three South African medicinal bulbs. *Journal of Ethnopharmacology*, 139(1): 81–89.
- Ncube, B., Ndhlala, A.R., Okem, A. & Van Staden, J. 2013. *Hypoxis* (*Hypoxidaceae*) in African traditional medicine. *Journal of Ethnopharmacology*, 150(3): 818–827.
- Niikura, K., Matsunaga, T., Suzuki, T., Kobayashi, S., Yamaguchi, H., Orba, Y., Kawaguchi, A., Hasegawa, H., Kajino, K., Ninomiya, T., Ijiro, K. & Sawa, H. 2013. Gold nanoparticles as a vaccine platform: Influence of size and shape on immunological responses *in vitro* and *in vivo*. *American Chemical Society Nano*, 7(5): 3926–3938.
- Ning, X., Peng, C., Li, E.S., Xu, J., Vinluan, R.D., Yu, M. & Zheng, J. 2017. Physiological stability and renal clearance of ultrasmall zwitterionic gold nanoparticles: Ligand length matters. *APL Materials*, 5: 053406.
- Notarianni, M., Vernon, K., Chou, A., Aljada, M., Liu, J. & Motta, N. 2014. Plasmonic effect of gold nanoparticles in organic solar cells. *Solar Energy*, 106: 23–37.
- Nune, S.K., Chanda, N., Shukla, R., Katti, Kavita, Kulkarni, R.R., Thilakavathy, S., Mekapothula, S., Kannan, R. & Katti, Kattesh V. 2009. Green nanotechnology from tea: Phytochemicals in tea as building blocks for production of biocompatible gold nanoparticles. *Journal of Materials Chemistry*, 19(19): 2912–2920.
- Ojewole, J., Kamadyaapa, D.R. & Musabayane, C.T. 2006. Some *in vitro* and *in vivo* cardiovascular effects of *Hypoxis hemerocallidea* Fisch & CA Mey (*Hypoxidaceae*) corm (African potato) aqueous extract in experimental animal models. *Cardiovascular Journal of South Africa*, 17(4): 166–171.
- Opris, R., Tatomir, C., Olteanu, D., Moldovan, R., Moldovan, B., David, L., Nagy, A., Decea, N., Ludovic, M. & Adriana, G. 2017. The effect of *Sambucus nigra* L. extract and phytosynthesized gold nanoparticles on diabetic rats. *Colloids and Surfaces B*:

*Biointerfaces*, 150: 192–200.

- Ovais, M., Khalil, A.T., Islam, N.U., Ahmad, I., Ayaz, M., Saravanan, M., Shinwari, Z.K. & Mukherjee, S. 2018. Role of plant phytochemicals and microbial enzymes in biosynthesis of metallic nanoparticles. *Applied Microbiology and Biotechnology*, 102(16): 6799–6814.
- Owira, P.M.O. & Ojewole, J.A.O. 2009. 'African Potato' (*Hypoxis hemerocallidea* corm): A plant-medicine for modern and 21st century diseases of mankind? – A review. *Phytotherapy Research*, 152: 147–152.
- Park, J.J., Hwang, S.J., Kang, Y.S., Jung, J., Park, S., Hong, J.E., Park, Y. & Lee, H.J. 2019. Synthesis of arbutin–gold nanoparticle complexes and their enhanced performance for whitening. *Archives of Pharmacal Research*, 42(11): 977–989.
- Patil, A.H., Jadhav, S.A., Gurav, K.D., Waghmare, S.R., Patil, G.D., Jadhav, V.D., Vhanbatte, S.H., Kadole, P. V., Sonawane, K.D. & Patil, P.S. 2019. Single step green process for the preparation of antimicrobial nanotextiles by wet chemical and sonochemical methods. *Journal of the Textile Institute*, 111(9): 1380-1388.
- Patil, M.P., Seo, Y.B., Lim, H.K. & Kim, G. Do. 2019. Biofabrication of gold nanoparticles using *Agrimonia pilosa* extract and their antioxidant and cytotoxic activity. *Green Chemistry Letters and Reviews*, 12(3): 208–216.
- Patil, P.O., Bhandari, P. V., Deshmukh, P.K., Mahale, S.S., Patil, A.G., Bafna, H.R., Patel, K. V. & Bari, S.B. 2017. Green fabrication of graphene-based silver nanocomposites using agro-waste for sensing of heavy metals. *Research on Chemical Intermediates*, 43(7): 3757–3773.
- Patra, J.K., Das, G. & Shin, H. 2019. Facile green biosynthesis of silver nanoparticles using *Pisum sativum* L . outer peel aqueous extract and its antidiabetic, cytotoxicity, antioxidant, and antibacterial activity. *International Journal of Nanomedicine*, 14: 6679–6690.
- Pawar, J.S. & Patil, R.H. 2020. Green synthesis of silver nanoparticles using *Eulophia herbacea* (Lindl.) tuber extract and evaluation of its biological and catalytic activity. *SN Applied Sciences*, 2(1): 1–12.
- Payne, J.N., Badwaik, V.D., Waghvani, H.K., Moolani, H. V., Tockstein, S., Thompson, D.H. & Dakshinamurthy, R. 2018. Development of dihydrochalcone-functionalized gold nanoparticles for augmented antineoplastic activity. *International Journal of Nanomedicine*, 13: 1917–1926.
- Pendota, S.C., Aremu, A.O., Slavětínská, L.P., Rárová, L., Grúz, J., Doležal, K. & Van Staden, J. 2018. Identification and characterization of potential bioactive compounds from the leaves of *Leucosidea sericea*. *Journal of Ethnopharmacology*, 220: 169–176.
- Perelshtein, I., Ruderman, E., Francesko, A., Fernandes, M.M., Tzanov, T. & Gedanken,

- A. 2014. Tannic acid NPs - Synthesis and immobilization onto a solid surface in a one-step process and their antibacterial and anti-inflammatory properties. *Ultrasonics Sonochemistry*, 21(6): 1916–1920.
- Periya, V.K., Koike, I., Kitamura, Y., Iwamatsu, S.I. & Murata, S. 2004. Hydrophilic [60]fullerene carboxylic acid derivatives retaining the original 60 $\pi$  electronic system. *Tetrahedron Letters*, 45(45): 8311–8313.
- Philip, D. 2010. Rapid green synthesis of spherical gold nanoparticles using *Mangifera indica* leaf. *Spectrochimica Acta - Part A: Molecular and Biomolecular Spectroscopy*, 77(4): 807–810.
- Phillipson, J.D. 1995. A matter of some sensitivity. *Phytochemistry*, 38(6): 1319–1343.
- Phillipson, J.D. 1999. New drugs from nature— It could be yew. *Phytotherapy Research*, 13(1): 2–8.
- Phodha, T., Riewpaiboon, A., Malathum, K. & Coyte, P.C. 2019. Excess annual economic burdens from nosocomial infections caused by multi-drug resistant bacteria in Thailand. *Expert Review of Pharmacoeconomics and Outcomes Research*, 19(3): 305–312.
- Moteetee, A. & Kose, L.S. 2017. Moteetee and Seleteng Kose. A review of medicinal plants used by the Basotho for treatment of skin disorders. *African Journal of Traditional Complementary Alternative Medicinal*, 14: 121–137.
- Plumb, Geoffrey w.; Pascuala-Teresa, Sonia; Santos-Buelga, Celestino; Cheynier, Veronique; Williamson, G. 1998. Antioxidant properties of catechins and proanthocyanidins: Effect of polymerisation, galloylation and glycosylation, Free Radical Research, Informa Healthcare. *Free Radical Research*, 29(4): 351–358.
- Pokropivny, V. V. & Skorokhod, V. V. 2007. Classification of nanostructures by dimensionality and concept of surface forms engineering in nanomaterial science. *Materials Science and Engineering C*, 27(5-8): 990–993.
- Ponnanikajamideen, M. & Rajeshkumar, S. 2019. *In vivo* type 2 diabetes and wound-healing effects of antioxidant gold nanoparticles synthesized using the insulin plant *Chamaecostus cuspidatus* in albino rats. *Canadian Journal of Diabetes*, 43(2): 82-89.
- Prasad, K., Jha, A.K. & Kulkarni, A.R. 2007. *Lactobacillus* assisted synthesis of titanium nanoparticles. *Nanoscale Research Letters*, 2(5): 248–250.
- Press, D. 2016a. Biomimetic synthesis of antimicrobial silver nanoparticles using *in vitro*-propagated plantlets of a medicinally important endangered species: *Phlomis bracteosa*. *International Journal of Nanomedicine*, 11: 1663–1675.
- Press, D. 2016b. Thidiazuron-enhanced biosynthesis and antimicrobial efficacy of silver nanoparticles via improving phytochemical reducing potential in callus culture of *Linum usitatissimum* L. *International Journal of Nanomedicine*, 11: 715–728.



- Pu, S., Li, J., Sun, L., Zhong, L. & Ma, Q. 2019. An *in vitro* comparison of the antioxidant activities of chitosan and green synthesized gold nanoparticles. *Carbohydrate Polymers*, 211: 161–172.
- Pyell, U., Jalil, A.H., Pfeiffer, C., Pelaz, B. & Parak, W.J. 2015. Characterization of gold nanoparticles with different hydrophilic coatings via capillary electrophoresis and Taylor dispersion analysis. Part I: Determination of the zeta potential employing a modified analytic approximation. *Journal of Colloid and Interface Science*, 450: 288–300.
- Rabie, G. & Raie, D. 2015. Extracellular bio-synthesis of bio-active nano-silver using alfalfa seedling. *Research Journal of Pharmaceutical, Biological and Chemical Sciences*, 6(1): 0975-8585.
- Raghunandan, D., Ravishankar, B., Sharanbasava, G., Mahesh, D.B., Harsoor, V., Yalagatti, M.S., Bhagawanraju, M. & Venkataraman, A. 2011. Anti-cancer studies of noble metal nanoparticles synthesized using different plant extracts. *Cancer Nanotechnology*, 2(1–6): 57–65.
- Raikar, U.S., Tangod, V.B., Mastiholi, B.M. & Fulari, V.J. 2011. Fluorescence quenching using plasmonic gold nanoparticles. *Optics Communications*, 284(19): 4761–4765.
- Raja, S., Ramesh, V. & Thivaharan, V. 2015. Antibacterial and anticoagulant activity of silver nanoparticles synthesised from a novel source – pods of *Peltophorum pterocarpum*. *Journal of Industrial and Engineering Chemistry*, 29: 257–264.
- Rajarajeshwari, T., Shivashri, C. & Rajasekar, P. 2014. Synthesis and characterization of biocompatible gymnemic acid – gold nanoparticles: A study on glucose uptake stimulatory effect in 3T3-L1 adipocytes. *Royal Society of Chemistry Advances*: 63285–63295.
- Rajaram, K., Aiswarya, D.C. & Sureshkumar, P. 2015. Green synthesis of silver nanoparticle using *Tephrosia tinctoria* and its antidiabetic activity. *Materials Letters*, 138: 251–254.
- Rajawat, S. & Qureshi, M.S. 2012. Comparative study on bactericidal effect of silver nanoparticles, synthesized using green technology, in combination with antibiotics on *Salmonella typhi*. *Journal of Biomaterials and Nanobiotechnology*, 3(4): 480–485.
- Rajkumari, J., Busi, S., Vasu, A.C. & Reddy, P. 2017. Facile green synthesis of baicalein fabricated gold nanoparticles and their antibiofilm activity against *Pseudomonas aeruginosa* PAO1. *Microbial Pathogenesis*, 107: 261–269.
- Ramzan, H. & Yousaf, Z. 2018. Green fabrication of metallic nanoparticles, In: Grumezescu, A.M. (Ed.), *Inorganic Frameworks as Smart Nanomedicines*, William Andrew Publishing, pp. 137-183.
- Ranoszek-soliwoda, K., Tomaszewska, E., Ma, K. & Celichowski, G. 2019. The synthesis

- of monodisperse silver nanoparticles with plant extracts. *Colloids and Surfaces B: Biointerfaces*, 177: 19–24.
- Rastogi, L., Kora, A.J. & Arunachalam, J. 2012. Highly stable, protein capped gold nanoparticles as effective drug delivery vehicles for amino-glycosidic antibiotics. *Materials Science and Engineering C*, 32(6): 1571–1577.
- Ravindran, A., Dhas, S.P., Chandrasekaran, N. & Mukherjee, A. 2013. Differential interaction of silver nanoparticles with cysteine. *Journal of Experimental Nanoscience*, 8(4): 589–595.
- Renner, S., Blutke, A., Clauss, S., Deeg, C.A., Kemter, E., Merkus, D., Wanke, R. & Wolf, E. 2020. Porcine models for studying complications and organ crosstalk in diabetes mellitus. *Cell and Tissue Research*, 380(2): 341–378.
- Rg, C., Dhanani, N.J., Amrutiya, R.M., Chandni, R. & Jayanthi, G. 2018. Screening of selected plants from semi-arid region for its phytochemical constituents and antimicrobial activity. *Journal of Pharmacognosy and Phytochemistry*, 7(2): 2983–2988.
- Riley, R.S. & Day, E.S. 2017. Gold nanoparticle-mediated photothermal therapy: applications and opportunities for multimodal cancer treatment. *Wiley Interdisciplinary Reviews: Nanomedicine and Nanobiotechnology*, 9: e1449.
- Roy, I., Ohulchanskyy, T.Y., Pudavar, H.E., Bergey, E.J., Oseroff, A.R., Morgan, J., Dougherty, T.J. & Prasad, P.N. 2003. Ceramic-based nanoparticles entrapping water-insoluble photosensitizing anticancer drugs: A novel drug-carrier system for photodynamic therapy. *Journal of the American Chemical Society*, 125(26): 7860–7865.
- S Pandey, G Oza, A Mewada & M Sharon. 2012. Green synthesis of highly stable gold nanoparticles using *Momordica charantia* as nano fabricator. *Archives of Applied Science Research*, 4(2): 1135–1141.
- Sadowski, Z. 2010. Biosynthesis and application of silver and gold nanoparticles, In: Perez D. P. (Ed), *Silver Nanoparticles*, InTech Publishing, pp. 257–277.
- Safaepour, M., Shahverdi, A.R., Shahverdi, H.R., Khorramizadeh, M.R. & Gohari, A.R. 2009. Green synthesis of small silver nanoparticles using geraniol and its cytotoxicity against *fibrosarcoma-wehi* 164. *Avicenna Journal of Medical Biotechnology*, 1(2): 111–5.
- Sahu, N., Soni, D., Chandrashekhar, B., Satpute, D.B., Saravanadevi, S., Sarangi, B.K. & Pandey, R.A. 2016. Synthesis of silver nanoparticles using flavonoids: Hesperidin, naringin and diosmin, and their antibacterial effects and cytotoxicity. *International Nano Letters*, 6(3): 173–181.
- Sanjana, S., Medha, M.U., Meghna, M.R., Shruthi, T.S., Srinivas, S.P., Madhyastha, H.,

- Navya, P.N. & Daima, H.K. 2019. Enzyme immobilization on quercetin capped gold and silver nanoparticles for improved performance. *Materials Today: Proceedings*, 10: 92–99.
- Sanna, V., Pala, N., Dessì, G., Manconi, P., Mariani, A., Dedola, S., Rassu, M., Crosio, C., Iaccarino, C. & Sechi, M. 2014. Single-step green synthesis and characterization of gold-conjugated polyphenol nanoparticles with antioxidant and biological activities. *International Journal of Nanomedicine*, 9(1): 4935–4951.
- Santos, M.S.C., Azevedo, R.B., Teixeira, P.R., Sales, M.J.A., Bão, S.N., Paterno, L.G. & Silva, A.L.G. 2016. Photochemically-assisted synthesis of non-toxic and biocompatible gold nanoparticles. *Colloids and Surfaces B: Biointerfaces*, 148: 317–323.
- Saratale, R.G., Shin, H.S., Kumar, G., Benelli, G., Kim, D. & Saratale, G.D. 2018. Exploiting antidiabetic activity of silver nanoparticles synthesized using *Punica granatum* leaves and anticancer potential against human liver cancer cells (HepG2). *Artificial Cells, Nanomedicine, and Biotechnology*, 46(1): 211–222.
- Sehlagwe, P.F., Lall, N. & Prinsloo, G. 2020. <sup>1</sup>H-NMR metabolomics and LC-MS analysis to determine seasonal variation in a cosmeceutical plant *Leucosidea sericea*. *Frontiers in Pharmacology*, 11: 1–11.
- Senthilkumar, P., Surendran, L., Sudhagar, B. & Ranjith Santhosh Kumar, D.S. 2019. Facile green synthesis of gold nanoparticles from marine algae *Gelidium acerosa* and evaluation of its biological Potential. *SN Applied Sciences*, 1(4): 1–12.
- Sevenler, D., Ünlü, N. L. & Ünlü, M. S. 2015. Nanoparticle biosensing with interferometric reflectance imaging, In: Vestergaard, M.C. (Eds), *Nanobiosensors and Nanobioanalyses*, Springer Tokyo Heidelberg New York Dordrecht London: pp. 1–379.
- Shah, M., Nawaz, S., Jan, H., Uddin, N., Ali, A., Anjum, S., Giglioli-Guivarc'h, N., Hano, C. & Abbasi, B.H. 2020. Synthesis of bio-mediated silver nanoparticles from *Silybum marianum* and their biological and clinical activities. *Materials Science and Engineering C*, 112: 110889.
- Shaik, S., Govender, K. & Leanya M. 2014. Ga<sub>3</sub>-mediated dormancy alleviation in the reputed African potato, *Hypoxis hemerocallidea*. *African Journal of Traditional Complementary and Alternative Medicine*, 11(2):330-333.
- Shamprasad, B.R., Keerthana, S., Megarajan, S., Lotha, R., Aravind, S. & Veerappan, A. 2019. Photosynthesized escin stabilized gold nanoparticles exhibit antidiabetic activity in L6 rat skeletal muscle cells. *Materials Letters*, 241: 198–201.
- Shanmuganathan, R., MubarakAli, D., Prabakar, D., Muthukumar, H., Thajuddin, N., Kumar, S.S. & Pugazhendhi, A. 2018. An enhancement of antimicrobial efficacy of biogenic and ceftriaxone-conjugated silver nanoparticles: Green approach.

*Environmental Science and Pollution Research*, 25(11): 10362–10370.

- Sharma, M. 2019. Transdermal and intravenous nano drug delivery systems. *Applications of Targeted Nano Drugs and Delivery Systems*: 499-550.
- Sharma, R., Kishore, N., Hussein, A. & Lall, N. 2014. The potential of *Leucosidea sericea* against *Propionibacterium acnes*. *Phytochemistry Letters*, 7(1): 124–129.
- Shervani, Z. & Yamamoto, Y. 2011. Size and morphology controlled synthesis of gold nanoparticles in green solvent: Effect of reducing agents. *Materials Letters*, 65(1): 92–95.
- Shukla, R., Nune, S.K., Chanda, N., Katti, Kavita, Mekapothula, S., Kulkarni, R.R., Welshons, W. V., Kannan, R. & Katti, Kattesh V. 2008. Soybeans as a phytochemical reservoir for the production and stabilization of biocompatible gold nanoparticles. *Small*, 4(9): 1425–1436.
- Sies, H. 2015. Oxidative stress: A concept in redox biology and medicine. *Redox Biology*, 4: 180–183.
- Singh, A. V., Bandgar, B.M., Kasture, M., Prasad, B.L.V. & Sastry, M. 2005. Synthesis of gold, silver and their alloy nanoparticles using bovine serum albumin as foaming and stabilizing agent. *Journal of Materials Chemistry*, 15(48): 5115–5121.
- Singh, A.K. & Srivastava, O.N. 2015. One-step green synthesis of gold nanoparticles using black cardamom and effect of pH on its synthesis. *Nanoscale Research Letters*, 10: 353-364.
- Singh, Y. 2007. *Hypoxis (Hypoxidaceae)* in Southern Africa: Taxonomic notes. *South African Journal of Botany*, 73(3): 360–365.
- Sithara, R., Selvakumar, P., Arun, C., Anandan, S. & Sivashanmugam, P. 2017. Economical synthesis of silver nanoparticles using leaf extract of *Acalypha hispida* and its application in the detection of Mn(II) ions. *Journal of Advanced Research*, 8(6): 561–568.
- Souquet, J.M., Cheynier, V., Brossaud, F. & Moutounet, M. 1996. Polymeric proanthocyanidins from grape skins. *Phytochemistry*, 43(2): 509–512.
- Srinivas Raghavan, B., Kondath, S., Anantanarayanan, R. & Rajaram, R. 2015. Kaempferol mediated synthesis of gold nanoparticles and their cytotoxic effects on MCF-7 cancer cell line. *Process Biochemistry*, 50(11): 1966–1976.
- Steenkamp, V. & Gouws, M.C. 2006. Cytotoxicity of six South African medicinal plant extracts used in the treatment of cancer. *South African Journal of Botany*, 72(4): 630–633.
- Stephen, A. & Seethalakshmi, S. 2013. Phytochemical synthesis and preliminary characterization of silver nanoparticles using hesperidin. *Journal of Nanoscience*,

2013: 1–6.

- Stolarczyk, E.U., Stolarczyk, K., Łaszcz, M., Kubiszewski, M., Maruszak, W., Olejarz, W. & Bryk, D. 2017. Synthesis and characterization of genistein conjugated with gold nanoparticles and the study of their cytotoxic properties. *European Journal of Pharmaceutical Sciences*, 96: 176–185.
- Subbaiya, R., Saravanan, M., Priya, A.R., Shankar, K.R., Selvam, M., Ovais, M., Balajee, R. & Barabadi, H. 2017. Biomimetic synthesis of silver nanoparticles from *Streptomyces atrovirens* and their potential anticancer activity against human breast cancer cells. *IET Nanobiotechnology*, 11(8): 965–972.
- Sun, X., Jin, Z., Yang, L., Hao, J., Zu, Y., Wang, W. & Liu, W. 2013. Ultrasonic-assisted extraction of procyanidins using ionic liquid solution from *larix gmelinii* Bark. *Journal of Chemistry*, 2013.
- Sunderam, V., Thiyagarajan, D., Lawrence, A.V., Mohammed, S.S.S. & Selvaraj, A. 2019. *In-vitro* antimicrobial and anticancer properties of green synthesized gold nanoparticles using *Anacardium occidentale* leaves extract. *Saudi Journal of Biological Sciences*, 26(3): 455–459.
- Suresh, S. 2013. Semiconductor Nanomaterials, Methods and Applications: A Review. *Nanoscience and Nanotechnology*, 3(3): 62–74.
- Tantra, R., Schulze, P. & Quincey, P. 2010. Effect of nanoparticle concentration on zeta-potential measurement results and reproducibility. *Particuology*, 8(3): 279–285.
- Tariq, A., Sadia, S., Fan, Y., Ali, S., Amber, R., Mussarat, S., Ahmad, M., Murad, W., Zafar, M. & Adnan, M. 2020. Herbal medicines used to treat diabetes in Southern Regions of Pakistan and their pharmacological evidence. *Journal of Herbal Medicine*, 21: 100323.
- Teimuri-mofrad, R., Hadi, R., Tahmasebi, B., Farhoudian, S., Mehravar, M. & Nasiri, R. 2017. Green synthesis of gold nanoparticles using plant extract: Mini-review. *Nanochemistry Research*, 2(1): 8–19.
- Thompson, E.A., Graham, E., Macneill, C.M., Young, M., Donati, G., Wailes, E.M., Jones, B.T. & Levi-Polyachenko, N.H. 2014. Differential response of MCF7, MDA-MB-231, and MCF 10A cells to hyperthermia, silver nanoparticles and silver nanoparticle-induced photothermal therapy. *International Journal of Hyperthermia*, 30(5): 312–323.
- Tiwari, J.N., Tiwari, R.N. & Kim, K.S. 2012. Zero-dimensional, one-dimensional, two-dimensional and three-dimensional nanostructured materials for advanced electrochemical energy devices. *Progress in Materials Science*, 57(4): 724–803.
- Tran, M., DePenning, R., Turner, M. & Padalkar, S. 2016. Effect of citrate ratio and temperature on gold nanoparticle size and morphology. *Materials Research Express*, 3(10): 1–10.

- Tripathi, R.M. & Chung, S.J. 2019. Biogenic nanomaterials: Synthesis, characterization, growth mechanism, and biomedical applications. *Journal of Microbiological Methods*, 157: 65–80.
- Tsao, R. 2010. Chemistry and biochemistry of dietary polyphenols. *Nutrients*, 2: 1231-1246.
- Turkevich, J., Stevenson, P.C. & Hillier, J. 1951. A study of the nucleation and growth processes in the synthesis of colloidal gold. *Discussions of the Faraday Society*, 11(c): 55–75.
- Valsalam, S., Agastian, P., Valan, M., Al-dhabi, N.A., Ghilan, A.M., Kaviyarasu, K. & Ravindran, B. 2019. Rapid biosynthesis and characterization of silver nanoparticles from the leaf extract of *Tropaeolum majus* L. and its enhanced *in-vitro* antibacterial, antifungal, antioxidant and anticancer properties. *Journal of Photochemistry and Photobiology, B: Biology*, 191: 65–74.
- Vankayala, R., Kuo, C.L., Sagadevan, A., Chen, P.H., Chiang, C.S. & Hwang, K.C. 2013. Morphology dependent photosensitization and formation of singlet oxygen ( $^1\Delta_g$ ) by gold and silver nanoparticles and its application in cancer treatment. *Journal of Materials Chemistry B*, 1(35): 4379–4387.
- Vasimalai, N. & John, S.A. 2013. Micromolar Hg(II) induced the morphology of gold nanoparticles: A novel luminescent sensor for femtomolar Hg(II) using triazole capped gold nanoparticles as a fluorophore. *Journal of Materials Chemistry A*, 1(14): 4475–4482.
- Vasimalai, N., Sheeba, G. & John, S.A. 2012. Ultrasensitive fluorescence-quenched chemosensor for Hg(II) in aqueous solution based on mercaptothiadiazole capped silver nanoparticles. *Journal of Hazardous Materials*, 213–214: 193–199.
- Veena, S., Devasena, T., Sathak, S.S.M., Ysasve, M. & Vishal, L.A. 2019. Green synthesis of gold nanoparticles from *Vitex negundo* leaf extract: Characterization and *in vitro* evaluation of antioxidant–antibacterial activity. *Journal of Cluster Science*, 30(6): 1591–1597.
- Vega, A., Bose, P., Buyuktosunoglu, A., Derby, J., Franceschini, M., Johnson, C. & Montoye, R. 2012. Architectural perspectives of future wireless base stations based on the IBM PowerEN™ processor. *Proceedings - International Symposium on High-Performance Computer Architecture*: 423–432.
- Venkatpurwar, V. & Pokharkar, V. 2011. Green synthesis of silver nanoparticles using marine polysaccharide: Study of *in-vitro* antibacterial activity. *Materials Letters*, 65(6): 999–1002.
- Venkatraman, A., Yahoob, S.A.M., Nagarajan, Y., Harikrishnan, S., Vasudevan, S. & Murugasamy, T. 2018. Pharmacological activity of biosynthesized gold nanoparticles from brown algae- seaweed *Turbinaria conoides*. *NanoWorld Journal*, 4(1): 17–22.

- Vidu, R., Rahman, M., Mahmoudi, M., Enachescu, M., Poteca, T.D. & Opris, I. 2014. Nanostructures: A platform for brain repair and augmentation. *Frontiers in Systems Neuroscience*, 8(91): 1-24.
- Vijayan, R., Joseph, S. & Mathew, B. 2019. Anticancer, antimicrobial, antioxidant, and catalytic activities of green-synthesized silver and gold nanoparticles using *Bauhinia purpurea* leaf extract. *Bioprocess and Biosystems Engineering*, 42(2): 305–319.
- Vinoshia, M., Palanisamy, S., Muthukrishnan, R., Selvam, S., Kannapiran, E., You, S.G. & Prabhu, N.M. 2019. Biogenic synthesis of gold nanoparticles from *Halymenia dilatata* for pharmaceutical applications: Antioxidant, anti-cancer and antibacterial activities. *Process Biochemistry*, 85: 219–229.
- Warghane, U.K. & Dhankar, R.P. 2019. Novel biosynthesis of silver nanoparticles for catalytic oxidation of alcohols containing aromatic ring. *Materials Today: Proceedings*, 15: 526–535.
- De Wet, H., Nzama, V.N. & Van Vuuren, S.F. 2012. Medicinal plants used for the treatment of sexually transmitted infections by lay people in northern Maputaland, KwaZulu-Natal Province, South Africa. *South African Journal of Botany*, 78: 12–20.
- Wong, S. & Karn, B. 2012. Ensuring sustainability with green nanotechnology. *Nanotechnology*, 23(29): 22–24.
- van Wyk, B.E. 2008. A broad review of commercially important southern African medicinal plants. *Journal of Ethnopharmacology*, 119(3): 342–355.
- Yeap Foo, L. & Lu, Y. 1999. Isolation and identification of procyanidins in apple pomace. *Food Chemistry*, 64(4): 511–518.
- Yilmazer-Musa, M., Griffith, A.M., Michels, A.J., Schneider, E. & Frei, B. 2012. Grape seed and tea extracts and catechin 3-gallates are potent inhibitors of  $\alpha$ -amylase and  $\alpha$ -glucosidase activity. *Journal of Agricultural and Food Chemistry*, 60(36): 8924–8929.
- Yoon, H., Eom, S., Hyun, J., Jo, G., Hwang, D., Lee, S., Yong, Y., Park, J.C., Lee, Y.H. & Lim, Y. 2011.  $^1\text{H}$  and  $^{13}\text{C}$  NMR data on hydroxy/methoxy flavonoids and the effects of substituents on chemical shifts. *Bulletin of the Korean Chemical Society*, 32(6): 2101–2104.
- Youssif, K.A., Haggag, E.G., Elshamy, A.M., Rabeh, M.A., Gabr, N.M., Seleem, A., Alaraby Salem, M., Hussein, A.S., Krischke, M., Mueller, M.J. & Abdelmohsen, U.R. 2019. Anti-Alzheimer potential, metabolomic profiling and molecular docking of green synthesized silver nanoparticles of *Lampranthus coccineus* and *Malephora lutea* aqueous extracts. *PLoS ONE*, 14(11): 1–19.
- Zayed, M.F. & Eisa, W.H. 2014. *Phoenix dactylifera* L. leaf extract phytosynthesized gold nanoparticles: Controlled synthesis and catalytic activity. *Spectrochimica Acta - Part A: Molecular and Biomolecular Spectroscopy*, 121: 238–244.

- Zayed, M.F., Mahfoze, R.A., El-kousy, S.M. & Al-Ashkar, E.A. 2020. *In-vitro* antioxidant and antimicrobial activities of metal nanoparticles biosynthesized using optimized *Pimpinella anisum* extract. *Colloids and Surfaces A: Physicochemical and Engineering Aspects*, 585: 124167.
- Zhan, G., Huang, J., Lin, L., Lin, W., Emmanuel, K. & Li, Q. 2011. Synthesis of gold nanoparticles by *Cacumen platycladi* leaf extract and its simulated solution: Toward the plant-mediated biosynthetic mechanism. *Journal of Nanoparticle Research*, 13(10): 4957–4968.
- Zhang, A., Tian, Y., Xiao, Y., Sun, Y. & Li, F. 2015. Large scale synthesis and formation mechanism of silver nanoparticles in solid-state reactions at ambient temperature. *Materials Science and Engineering B: Solid-State Materials for Advanced Technology*, 197: 5–9.
- Zhang, T., Dang, M., Zhang, W. & Lin, X. 2020. Gold nanoparticles synthesized from *Euphorbia fischeriana* root by green route method alleviates the isoprenaline hydrochloride induced myocardial infarction in rats. *Journal of photochemistry and photobiology. B, Biology*, 202: 111705.
- Zhang, X. 2015. Gold Nanoparticles: Recent advances in the biomedical applications. *Cell Biochemistry and Biophysics*, 72(3): 771–775.
- Zhao, P., Li, N. & Astruc, D. 2013. State of the art in gold nanoparticle synthesis. *Coordination Chemistry Reviews*, 257(3–4): 638–665.
- Zhou, Z., Fan, T., Yan, Y., Zhang, S., Zhou, Y., Deng, H., Cai, X., Xiao, J., Song, D., Zhang, Q. & Cheng, Y. 2019. One stone with two birds: Phytic acid-capped platinum nanoparticles for targeted combination therapy of bone tumors. *Biomaterials*, 194: 130–138.
- Zia, K., Siddiqui, T., Ali, S., Farooq, I., Zafar, M.S. & Khurshid, Z. 2019. Nuclear magnetic resonance spectroscopy for medical and dental applications: A comprehensive review. *European Journal of Dentistry*, 13(1): 124–128.



## CHAPTER THREE

### **Green Synthesis of Gold Nanoparticles Capped with Procyanidins from *Leucosidea sericea* as Potential Antidiabetic and Antioxidant Agents**

Umar M. Badeggi <sup>1</sup>, Enas Ismail <sup>1</sup>, Adewale O. Adeloye <sup>1</sup>, Subelia Botha <sup>2</sup>, Jelili A. Badmus <sup>3</sup>, Jeanine L. Marnewick <sup>3</sup>, Christopher N. Cupido <sup>4</sup> and Ahmed A. Hussein <sup>1,\*</sup>

<sup>1</sup> Chemistry Department, Cape Peninsula University of Technology, Symphony Rd. Bellville 7535, South Africa; 217064221@mycput.ac.za (U.M.B); enas.ismail4@yahoo.com (E.I.); aowale@gmail.com (A.O.A.)

<sup>2</sup> Electron Microscope Unit, University of the Western Cape, Bellville, 7535, South Africa; subotha@uwc.ac.za (S.B.)

<sup>3</sup> Oxidative Stress Research Centre, Institute of Biomedical and Microbial Biotechnology, Cape Peninsula University of Technology, Symphony Rd. Bellville 7535, South Africa; jabadmus@lautech.edu.ng (J.A.B.); Marnewickj@cput.ac.za (J.L.M.)

<sup>4</sup> Department of Botany, University of Fort Hare, Private Bag X1314, Alice 5700, South Africa; ccupido@ufh.ac.za (C.N.C)

\* Correspondence: mohammedam@cput.ac.za; Tel.: +27-21-959-6193; Fax: +27-21-959-3055

Received: 05 January 2020; Accepted: 02 March 2020; Published: 13 March 2020

## Abstract

In this study, procyanidin fractions, containing dimers and trimers (F1–F2) from the *Leucosidea sericea* total extract (LSTE) were investigated for their chemical constituents. The total extract and the procyanidins were employed in the synthesis of gold nanoparticles (AuNPs) and fully characterized. AuNPs of  $15.4 \pm 2$ ,  $24.8 \pm 9$  and  $13.1 \pm 2$  nm were obtained using LSTE, F1 and F2 respectively. Zeta potential and in vitro stability studies confirmed the stability of the particles. The enzymatic activity of LSTE, F1, F2 and their corresponding AuNPs showed strong inhibitory alpha-amylase activity where F1 AuNPs demonstrated the highest with  $IC_{50}$  of  $1.88 \mu\text{g/mL}$ . On the other hand, F2 AuNPs displayed the strongest alpha-glucosidase activity at  $4.5 \mu\text{g/mL}$ . F2 and F2 AuNPs also demonstrated the highest antioxidant activity,  $1834.0 \pm 4.7 \mu\text{M AAE/g}$  and  $1521.9 \pm 3.0 \mu\text{M TE/g}$  respectively. The study revealed not only the ability of procyanidins dimers (F1 and F2) in forming biostable and bioactive AuNPs but also a significant enhancement of the natural products activities which could improve the smart delivery in future biomedical applications.

**Keywords:** *Leucosidea sericea*; alpha-amylase; alpha-glucosidase; diabetics; gold nanoparticles

## 3.1 Introduction

Unlike typical physical and chemical protocols, methods that utilise green synthesis techniques offer a variety of positive advantages that are in line with the principles of green chemistry [1]. For instance, the resources employed are often plant materials that are readily available, accessible and affordable [2]. Plants contain complex structures that can be used in the reduction and stabilization of the nanoparticles requiring no external stabilizers [3]. The solvents employed are usually eco-friendly, making the environment safe from remnants of toxic chemicals and the products are comparatively less toxic [4]. Other advantages include cost-effectiveness as sophisticated instrumentation is not required [5]. Small quantities (in grams) from part of plant such as leaves are usually enough for synthesis [5,6]. Furthermore, the synthesis is generally fast [6]. It takes a few minutes to a couple of hours and the new materials have exciting characteristics that had made them the focus of modern-day research [7]. It has been reported that their increased surface area, size and shape contributed to their properties [8,9]. Among other great benefits of synthesizing and applying nanoparticles through the green route is their biocompatibility [5]. Many green synthesized nanoparticles have demonstrated interesting biological activities [5,10] including antimicrobial and antidiabetic properties.

Diabetes mellitus has undoubtedly become a serious health challenge. More worrisome is type II diabetes mellitus (T2DM), which accounts for 90% of diabetes mellitus. It occurs as a result of the inefficient processing of insulin [11]. The international Diabetes Foundation (IDF) reported that more than 70% of the African population have undiagnosed diabetes mellitus. Among these, 50% were documented to be residing in South Africa, Nigeria, Ethiopia and the Democratic Republic of Congo [12]. As of 2017, the population of adults between the ages of 20 and 79 that suffered from diabetes was 425 million [13]. This is equivalent to 9.9% of the world's population [13]. By estimation, this disease would have drastically increased by 48% in 28 years if not properly managed [14]. Also, drugs like miglitol, viglibose as well as acarbose are available in the market. However, they are costly and their continuous use is associated with side effects like diarrhea, dropsy, heart failure, damage to the liver, weight gain, abdominal pain, hyperglycemia and flatulence. These challenges necessitate the need for more potent and newer remedies [15–17].

It is well established that bioactive compounds in various plants possess significant effects in delaying and management of T2DM [18]. Extracts from different plants have been reported as alpha-glucosidase and alpha-amylase inhibitors [19–28]. Additionally, biologically synthesized AuNPs using plant extracts showed interesting antidiabetic activity. The extracts of *Chamalcostus cuspidatus* [29], *Gymnema sylvestre* [30], *Cassia fistula* stem bark [31], *Hericium erinaceus* [32], *Turbinaria conoides* [33], *Sambucus nigra* [34] and *Sargassum swartzii* [35] displayed antidiabetic activities in various investigations. Silver/gold NPs of *Ocimum basilicum* [36] and cinnamon extract [37] also lowers glucose levels. The use of single molecules as reducing/stabilizing agents for nanoparticle formation with certain bioactivity has been reported. Plant polyphenols are among the preferred candidates [38,39]. It has been shown that gallic and protocatechuic acids possess reducing abilities in forming nanoparticles [40–43]. Hesperidin [44,45], diosmin, and naringin [45], curcumin [46], guavanoic acid [47], phloridzin, an antidiabetic agent found in fruits and its aglycon [48], escin [49], resveratrol [50] and gymnemic acid [51] were found to be responsible for the biosynthesis of AuNPs. Other compounds that have been used in the formation of AuNPs with antidiabetic properties include chitosan, chondroitin sulfate, tyrosine and tryptophan [52–54].

Like the metal-reducing ability of plant extracts, the antioxidants activity has been associated with the plants' phenolics [55]. Pu and colleagues [56] argued that antioxidants possess free radical scavenging properties, hence, they play a role in promoting health and preventing diseases. In 2019 alone, several antioxidant activities [57–64] have been

carried out on gold nanoparticles through the green route. The results demonstrated encouraging scavenging activities.

*Leucosidea sericea* (Rosaceae family) is the only species belonging to the genus *Leucosidea* in the Southern part of Africa [65]. Family Rosaceae consists of approximately 300 species out of which only nine are native to Southern African countries like Zimbabwe, Lesotho and South Africa. It is a very popular plant among the South Africans with names like 'Ouhout' by the Afrikaans and 'umTshitshi' according to the Zulu people [66]. Traditionally, it is used as protection against charm, vermifuge, astringent, for expelling parasitic worms and as a treatment for ophthalmia [67,68]. Extracts from this economic plant have been prepared from different solvents and have shown anti-inflammatory, antioxidant, antiparasitic, antimicrobial, anthelmintic, antibacterial, antiacne and acetylcholinesterase inhibitory activities [65,68–71]. A handful of active compounds have been identified and isolated from *L. sericea* including triterpenes [67] and phloroglucinols [71]. As far as we know, procyanidins have not been identified from the plant previously and no nanoparticle synthesis reported.

Gold nanoparticles is one of the most widely used nanomaterials because of an array of interesting properties including the ease of its surface chemistry [41]. Among the importance of AuNPs is the ease of synthesis, characterization, surface modification, low toxicity, tunable surface plasmon resonance, biostability and biocompatibility [5,34,41,48,57,59]. The advantage that comes with these is the applications in biomedical. Due to its small size, AuNPs can penetrate cells to interact with different molecules without causing damage making it the preferred candidate in drug delivery, cancer therapy among other applications [48,57].

Therefore, the aim of the present work was to identify procyanidins, a class of phytochemicals with unique structure from *Leucosidea sericea* and use same for the fabrication and characterization of gold nanoparticles in order to understand the involvement of the functional groups in the gold nanoparticle formation. Biological activities of the intact fractions and nanoparticles were also evaluated through enzymatic and antioxidant studies.

## **3.2 Materials and Methods**

### **3.2.1 Chemicals and materials**

Organic solvents, methanol (HPLC grade), ethanol, ethyl acetate and hexane, were supplied by Merck (Cape Town, WC, South Africa). All solvents used for extraction and column chromatography were general-purpose reagents. Silica gel 60 H (0.040–0.063 mm

particle size supplied by Merck (Gauteng, Modderfontein, South Africa) and Sephadex LH-20 supplied by Sigma-Aldrich (Cape Town, WC, South Africa) were used as stationary phases, supported with a glass column of different diameters. Polystyrene 96-well microtitre plates were obtained from Greiner bio-one GmbH (Frickenhausen, BY, Germany). Sodium tetrachloroaurate (III) dihydrate, iron (III) chloride hexahydrate, 2,4,6-Tris(2-pyridyl)-s-triazine, hydrochloric acid (HCl) and sodium chloride were procured from Sigma-Aldrich (Cape Town, WC, South Africa). N-Acetyl-L-cysteine and Folin–Ciocalteu's phenol reagent were purchased from Boehringer Mannheim GmbH (Mannheim, BW, Germany). Glycine and phosphate buffered saline (PBS) were purchased from Lonza (Cape Town, WC, South Africa). Bovine serum albumin was procured from Miles Laboratories (Pittsburgh, PA, United States of America). Alpha-glucosidase (*Saccharomyces cerevisiae*), alpha-amylase (procaine pancreas), 3,5-dinitro salicylic acid (DNS), *p*-nitrophenyl- $\alpha$ -D-glucopyranoside (*p*-NPG), sodium carbonate ( $\text{Na}_2\text{CO}_3$ ), sodium dihydrogen phosphate, and disodium hydrogen phosphate, Trolox (6-hydroxyl-2, 5, 7, 8-tetramethylchroman-2-carboxylic acid), 2,2-azino-bis (3-ethylbenzothiazoline-6-sulfonic acid) (ABTS) diammonium salt, potassium peroxodisulphate, gallic acid and ascorbic acid were purchased from Sigma-Aldrich (Cape Town, WC, South Africa).

### 3.2.2 Characterisation

The  $^1\text{H}$ ,  $^{13}\text{C}$  and DEPT-135 Nuclear Magnetic Resonance spectra were run on a Bruker spectrometer operating at 400 (for H)/100 (for C) MHz. A polar star Omega microtitre plate reader (BMG Labtech, Ortenberg, BW, Germany) was used to monitor the characteristic peaks of the AuNPs. High-Resolution Transmission Electron Microscopy (FEI Tecnai G2 F20 S-Twin HRTEM, operated at 200 kV) was used to study the morphology of the AuNPs. A few drops of the gold suspension were dropped on a carbon-coated copper grid and allowed to dry completely at room temperature. An Oxford EDS system inside a Zeiss Auriga Field Emission Scanning Electron Microscope was used for elemental analysis. A few drops of the gold suspension were dropped on a Mica glass substrate and allowed to dry. The crystal structures of the samples were determined by X-ray diffraction (XRD; X-ray diffraction Model Bruker AXS D8 advance) with radiation at  $\text{CuK}\alpha 1 = 1.5406 \text{ \AA}$ . Dynamic Light Scattering (DLS) analysis was done using a Malvern Zetasizer Instrument (Malvern Ltd., United Kingdom) at 25 °C and a 90° angle. Zetasizer software version 7.11 was used to analyze the data. The absorbance readings of biological activities were measured at 540 nm using Multiplate Reader (Multiska Thermo scientific, version 1.00.40).

### 3.2.2 Extraction and Purification of F1 and F2 from LSTE

The leaves and stem twigs of *Leucosidea sericea* was obtained from Afriplex Ltd, South Africa and air-dried in the laboratory at ambient conditions. The dry aerial parts were carefully weighed to afford 107.40 g and ground to powdered form before extraction. The powdered material was then extracted using 1.5 L of 50% aqueous-methanol mixture. The extraction was allowed to stand for 72 hours under ambient conditions with occasional manual agitation of the round-bottomed extraction flasks (2.0 L). The filtrate after concentration in vacuo afforded 36.20 g (33.71%). About 35.30 g was dissolved in 0.5 L of water and successively partitioned with 0.6 L hexane, dichloromethane (1.0 L), and 1.0 L of ethyl acetate. Ethyl acetate fraction (2.00 g) was applied to a silica gel column (24x3 cm) and eluted with a mixture of hexane-DCM/DCM-EtOAc/EtOAc-MeOH of increasing polarity. Collected fractions were pooled together according to their profiles (on the TLC) to afford 6 major fractions coded as LST1–6. Fraction LST 4 (79.2 mg) was further subjected to the Sephadex column (LH-20) using 80% toluene-ethanol and resulted in the isolation of one single spot (62.3 mg) and named F1. The more polar fraction LST 6 was subjected to Sephadex column using 20% aqueous ethanol and resulted in one single spot (18.0 mg), more polar than the previous one and coded as F2. The analysis was achieved by <sup>1</sup>H, <sup>13</sup>C, DEPT-135 NMR (Supplementary data, Appendix A-F) and LC–MS.

### 3.2.3. Liquid Chromatography–Mass Spectrometry (LC–MS) Analysis.

The method and conditions described in reference [71] was adopted. Briefly, the analysis was carried out using a Waters Synapt G2 quadrupole time-of-flight (QTOF) mass spectrometer (MS) connected to a Waters Acquity ultra-performance liquid chromatography (UPLC) (Waters, Milford, MA, USA). Electrospray ionization (in negative mode) was used with a cone voltage of 15 V. The desolvation temperature was set at 275 °C, desolvation gas at 650 L/h, and the rest of the MS settings optimized for best resolution and sensitivity. Data acquisition was done by scanning from *m/z* 150 to 1500 *m/z* in resolution mode as well as in MSE mode. In MSE mode, two channels of MS data were acquired, one at low collision energy (4 V) and the second using a collision energy ramp (40–100 V) to obtain fragmentation data as well. Leucine enkephalin was used as lock mass (reference mass) for accurate mass determination and the instrument was calibrated with sodium formate and the separation was achieved on a Waters HSS T3, 2.1 × 100 mm, 1.7 μm column. An injection volume of 2 μL was used and the mobile phase consisted of 0.1% formic acid (solvent A) and acetonitrile containing 0.1% formic acid as solvent B. The gradient started at 100% solvent A for 1 min and changed to 28% B

over 22 min in a linear way. It then went to 40% B over 50 s and a wash step of 1.5 min at 100% B. This was followed by re-equilibration to initial conditions for 4 min. The flow rate was 0.3 mL/min and the column temperature were maintained at 55 °C.

#### **3.2.4. Green Synthesis of Gold Nanoparticles**

The AuNPs was synthesized by dissolving 0.01 g of the total extract, F1 or F2 in 1 mL of deionized Milli-Q water and vortexed for 10 min giving a clear yellowish solution. This solution was emptied into a pre-heated 1.0 mM sodium chloroaurate solution at about 90–100 °C. An instantaneous change of colour from light yellow to reddish indicated successful synthesis of AuNPs. Source of heat was turned off while reaction mixture continued to stir for additional 60 s. UV-Vis, particle size and zeta potential measurements were done upon cooling to room temperature.

#### **3.2.5. Stability Study**

The method description of [72] was adopted. Slight changes were only in the monitoring period, which was 0, 12 and 24 h. The stability was evaluated as soon as the solutions were mixed with the nanoparticles and after incubation at 37 °C.

#### **3.2.6. Dilution Study**

To get the AuNPs in the powdered form, 100 µL of the sample was freeze-dried after several washing and centrifuge steps. Of the synthesized AuNPs, 200 µL at different concentrations (60, 40, 20 and 10 µg/mL) were prepared using deionized water in a 96-well microtitre plate and the absorbance was taken by using a polar star Omega microtitre plate reader.

#### **3.2.7 In-Vitro Methods Employed in Antidiabetic Studies**

##### **3.2.7.1 Alpha-Amylase Inhibitory Activity**

The alpha-amylase inhibitory activity of the *Leucosidea sericea* total extract (LSTE), F1, F2 and their corresponding gold nanoparticles were carried out according to the standard method with slight modifications [73]. In a 96-well plate, 50 µL phosphate buffer (100 mM, pH = 6.9) was added followed by 20 µL alpha-amylase (2 U/mL) and 20 µL of varying concentrations of above solutions (200, 100, 50, 25 and 12.5 µg/mL) were pre-

incubated at 37 °C for 20 min. Thereafter, 20 µL of 1% soluble starch (100 mM phosphate buffer pH 6.9) was added as a substrate and incubated again at 37 °C for 30 min. Then, 100 µL of the DNS colour reagent was added and boiled for 10 min. The absorbance of the resulting mixture was measured at 540 nm using a plate reader (Multiskan Thermo scientific, version 1.00.40). Acarbose at various concentrations (0.1–0.5 mg/mL) was used as a standard. Without test (solutions of extract, F1, F2 and nanoparticles) were set up in parallel as control and each experiment was performed in triplicate. The results were expressed as percentage inhibition, which was calculated using the formula below;

$$\text{Inhibitory activity (\%)} = (1 - A/B) \times 100$$

where A is the absorbance in the presence of test substance and B is the absorbance of control.

### **3.2.7.2 Alpha-Glucosidase Inhibitory Activity**

A standard procedure of the alpha-glucosidase assay was followed with slight modification [74]. Briefly, 20 µg/mL of the three AuNP samples was serially diluted in a 96-well plate using a 100 mM phosphate buffer (PBS) at pH 6.8. The mixture was gently agitated and allowed to stand for 15 min at 25 °C. Thereafter, 20 µL of a 5 mM *p*-nitrophenyl- $\alpha$ -D-glucopyranoside (*p*-NPG) was added as the substrate and the plate was incubated at 37 °C for 20 min. Hereafter, 50 µL of a 0.1 M sodium carbonate (Na<sub>2</sub>CO<sub>3</sub>) solution was added to each well to stop the reaction. With the aid of a plate reader, the absorbance measurement was then taken at 540 nm. The wells with enzyme, buffer, and substrate but without samples served as positive controls and each experiment was conducted in triplicate. The percentage inhibition of the enzymatic property of alpha-glucosidase was determined using Equation (1) in Section 3.2.7.1.

### **3.2.8. Antioxidant Activity**

#### **3.2.8.1. Ferric Reducing Antioxidant Power (FRAP) Assay**

FRAP assay was done on LSTE, F1 and F2 and their corresponding AuNPs. The method of [75] was followed with a slight adjustment. Absorbance was measured at 593 nm and the results were expressed as µM ascorbic acid equivalents per milligram of dry weight (µM AAE/g DW) of the samples.



### 3.2.8.2. Total Phenolic Content

This evaluation of amount of phenolics in LSTE, F1 and F2, as well as their corresponding AuNPs, was done by the method of Salar and colleagues [76] with slight modification. The plate was read at 593 nm and the results expressed as gallic acid equivalent.

### 2.8.3. 2'-Azino-Bis-3-Ethylbenzotiazolin-6- Sulfonic Acid (ABTS) Assay

The ABTS assay was conducted adopting a combined procedure reported in [77, 78]. Briefly, 25  $\mu$ L of the standard (Trolox) and samples were added to a 96-well plate followed by the ABTS reagent. The reaction mixture was allowed to stand for 30 min before the absorbance was read at 734 nm. The ABTS reagent was prepared 30 min before the experiment at 70 °C. The assay was repeated two more times. The results were expressed as mM Trolox equivalents per Gram sample (mM TE/g).

## 3.3 Results and Discussion

### 3.3.1 The *L. sericea* Constituents and Gold Nanoparticle Formation

Chromatographic manipulation of the LSTE using different chromatographic techniques resulted in the purification of two fractions (F1 and F2) with potential to form AuNPs. The total extract and purified fractions were investigated for their chemical constituents using different techniques. Although the NMR spectroscopy is the most important technique for structural elucidation in natural products, the LC–MS techniques are the best and fastest method in case of the complicated mixture and to unveil the nature of the chemical constituents.

The LC–MS analysis of the LSTE (Figure 3.1) showed a wide range of  $m/z$  (M-H) ions, which indicated the presence of different phenolic compounds including phenolic acids (ferulic ( $m/z$  195/ $R_t$  1.52 min)/quinic (191/2.72)/hydroxyferulic (209/24.26) and caffeic (177/17.18) acids); flavonones ((luteolin (285/9.76), quercetin (301/23.09), hyperoside (463/17.34), kaempferol galactoside (447/18.95) and kaempferol rutinoside (593/23.95)) and procyanidin dimers (577/10.89, 11.98; B type). These types of compounds have a strong ability to donate electrons and are playing a key role in the oxidation–reduction process; the removal of the electrons results in a stable quinonoidal structure (Scheme 3.1).

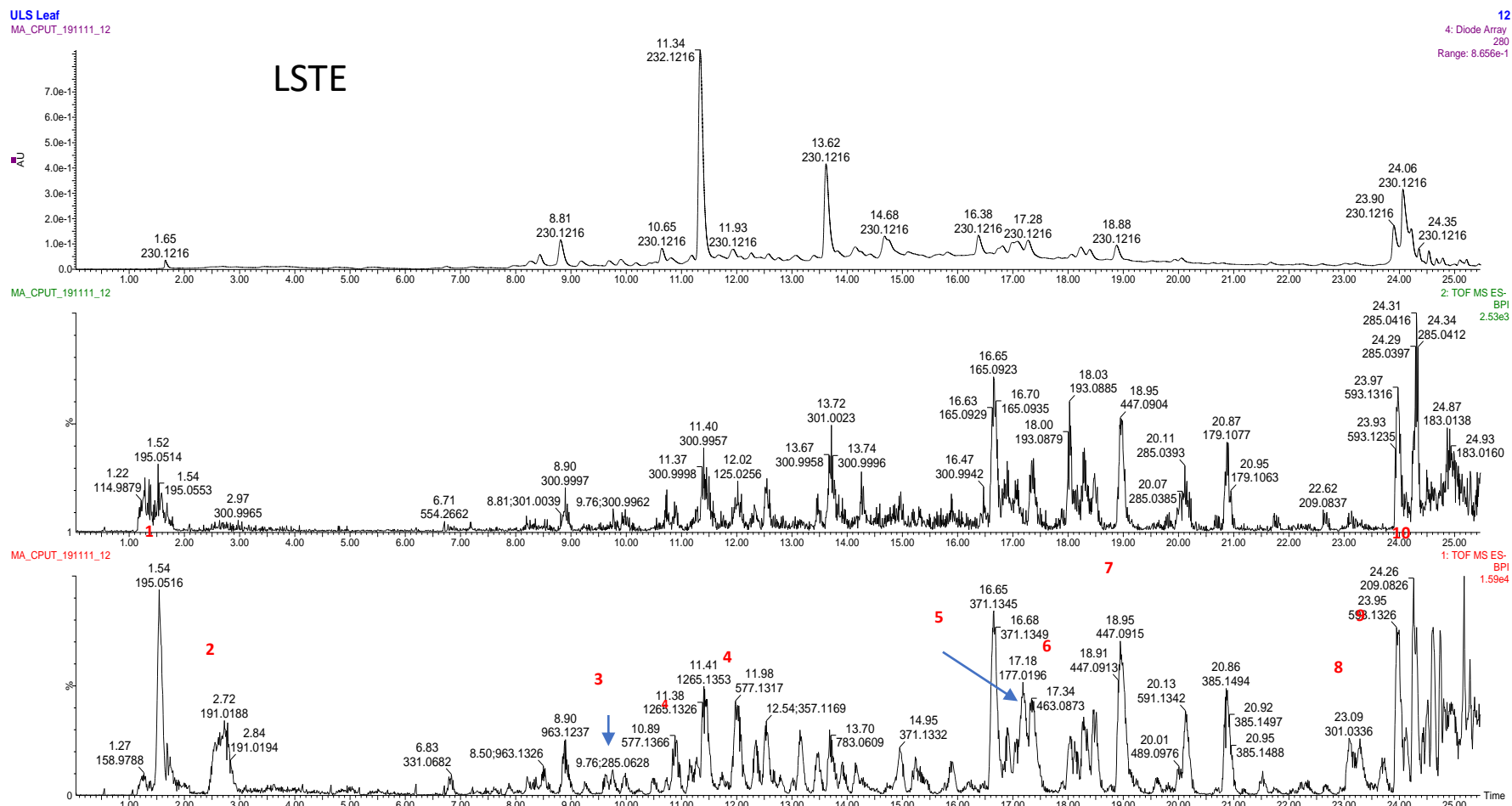


Figure 3. 1: LC-MS profile of the *L. sericea* aerial part extract. 1: ferulic acid; 2: quinic acid; 3: luteolin 4: procyanidin dimer; 5: caffeic acid; 6: hyperoside, 7: kaempferol galactoside; 8: quercetin; 9: kaempferol rutinoside; 10: hydroxyferulic acid

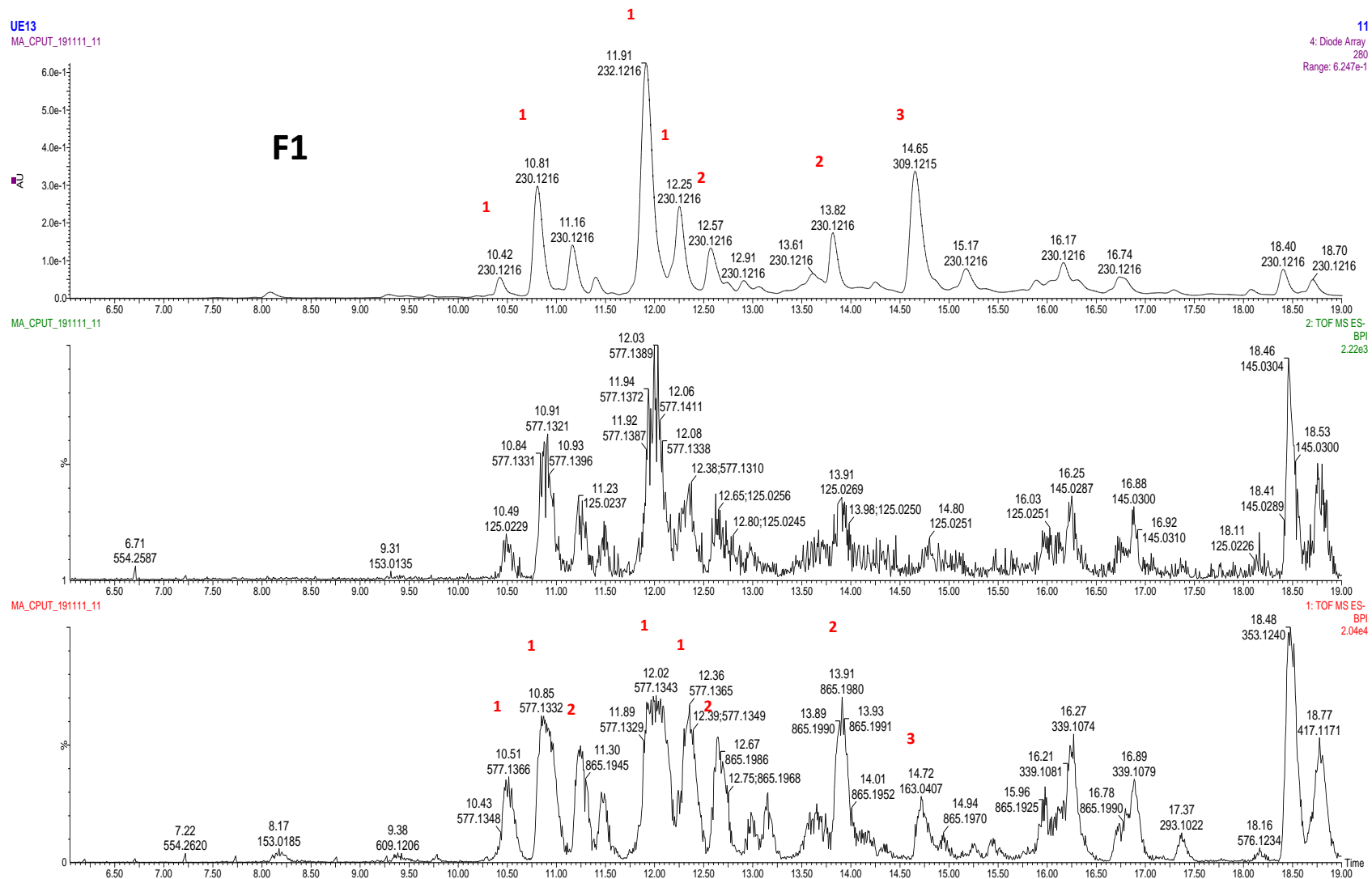


Figure 3. 2: LC-MS profile of F1. 1: procyanidin dimer (type B); 2: procyanidin trimer (type B); 3: coumaric acid

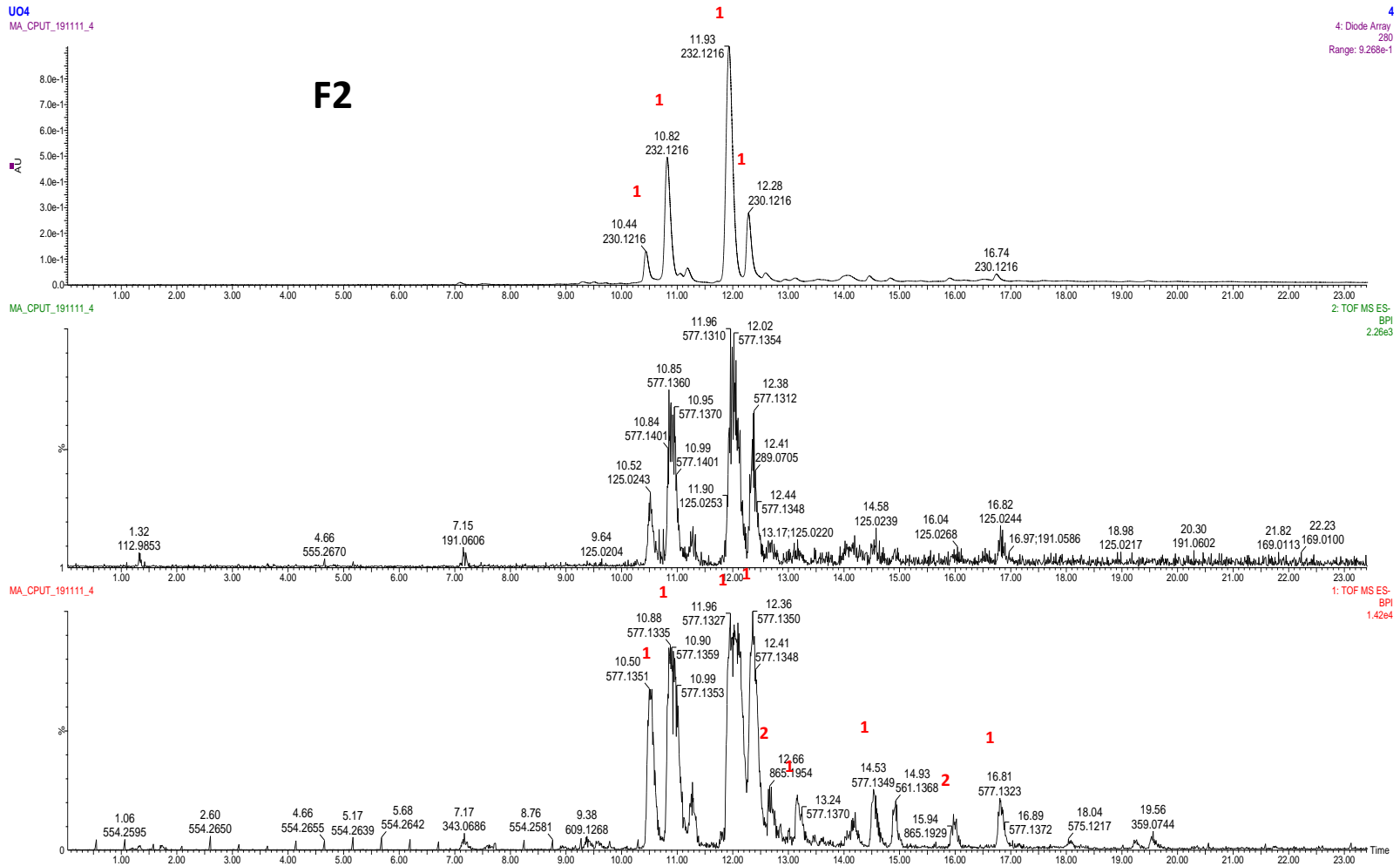
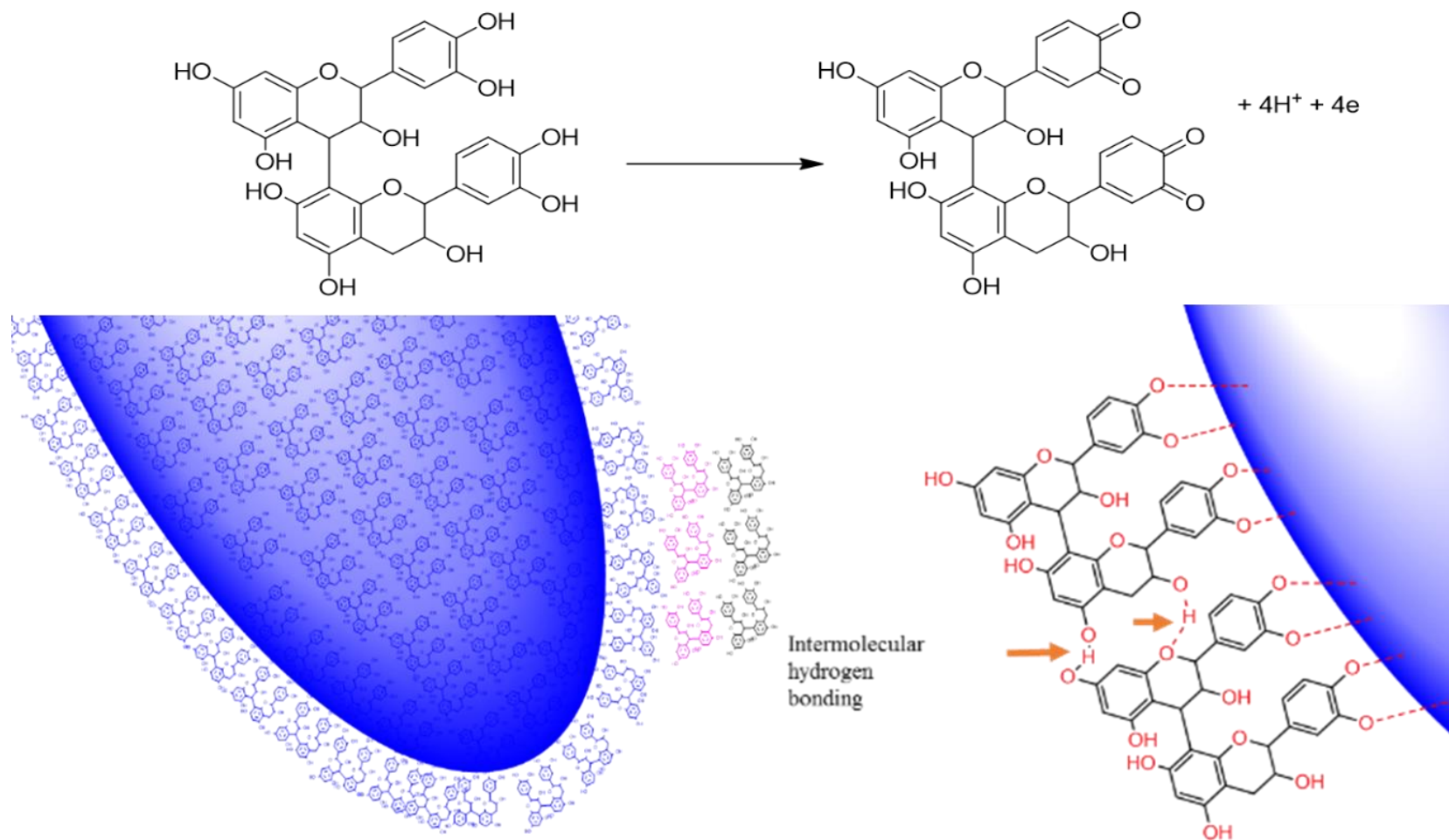


Figure 3. 3: LC-MS profile of F2. 1: procyanidin dimer (type B), 2: procyanidin trimer (type B)

Attempted purification of fraction (F1) showed both dimers ( $R_t$  10.51; 10.85; 12.02; 12.36) and trimers ( $R_t$ : 11.30; 12.67; 13.91; 14.94; 15.96; 16.78), however, the relative quantity of dimers was higher than trimers (Figure 3.2).

Further purification of fraction LSTE4 produces a single spot, which initially was believed to be a pure compound. However, the NMR ( $^1\text{H}$  and  $^{13}\text{C}$  NMR), and LC–MS analysis showed an isomeric mixture. The LC–MS of F2 (Figure 3) showed procyanidin dimer peaks B-type ( $m/z$  577) at  $R_t$  of 10.50; 10.88; 11.96; 12.36; 13.24; 14.53 and 16.81; the first four peaks were major while the others were minor. The trimers (B-type;  $m/z$  865) were also detected in minute quantities at 12.66 and 15.94 (Figure 3.3).

LSTE, F1 and F2 were then used to successfully form AuNPs. The polyphenolic nature of these fractions makes them hydrophilic, a requirement for green synthesis. The reducing and capping ability of polyphenolics has been associated with the presence of electronegative atoms [79]. The lone pairs of electrons on oxygen further provide a suitable chelation site for binding with gold. The arrangement of certain functional groups in the structure of polyphenolics is also of great significance in their reactivity. Hydroxyl groups at adjacent positions may offer two or more binding sites which may enhance the easy reduction of gold and subsequent capping of the particles that are formed [80]. Oxidation reactions are common to phenolic compounds where the hydroxyl groups at ortho and para positions convert to carbonyl groups (*ortho* and/or *para* quinones) [81]. In the case of the procyanidins, the oxidation will occur at ortho positions (Scheme 3.1) when 4 and 6 electrons are lost for the dimer and trimer respectively [82]. Subsequent interaction of the particles with the molecule probably brought about weak forces of attraction and encapsulation in the F1 and F2 matrix (Scheme 3.1). As would be discussed later, the particles are covered with negative charges providing stability and confirming the negative zeta potential values as measured by zetasizer.



**Scheme 3.1:** The proposed reduction of gold salt and encapsulation of the hybrid gold NPs in the F1 and F2 matrix. In addition to the chelating power of the oxygen atom to the metal surface, the intermolecular hydrogen bonding between procyanidins can also make double and triple capping shells and contributing to the stability of the NPs. The reduction power of the phenolic structures with *ortho*-OH, can be facilitated by the formation of stable *ortho*-quinone structure [80-82]

### 3.3.2. UV-Visible Spectroscopic Analysis

Gold nanoparticles are known to have surface plasmon resonance (SPR) at around 530 nm [71]. Here, the prepared AuNPs from LSTE, F1 and F2 revealed SPR of 528–534 nm, confirming successful AuNPs fabrication. Before the reduction process, no absorption peaks were observed in such a region. The colour of (a) gold salt solution, (b) LSTE, (c) F1 and (d) F2 ranges from deep yellow to pale yellow (inset in Figure 3.4). These colours changed to ruby red when the gold salt was introduced, which served as a visual confirmation of the gold nanoparticle fabrication. The phytochemicals in LSTE, F1 and F2 therefore, acted as reducing and subsequently as capping agents in the respective newly formed AuNPs. It was observed from figure 4 that LSTE- and F1 -AuNPs displayed a very close absorption band, almost the same peak area and the maximum absorption approximately the same. This is probably because of the similar constituents as F1 possess more procyanidin trimers than F2. Hence, dimers and trimers of procyanidins were clearly involved in the successful fabrication of F1 and F2 AuNPs. Furthermore, since no external stabilizers were employed, it could also be concluded that the same constituents were responsible for the stabilization of the nanoparticles (see Scheme 3.1). Many investigations concluded that polyphenols which are abundant in plants, are associated with the reduction of metal salts when combined with plant extracts [47,48]. This may also explain why F1 and F2 (which contain similar functionality) were able to reduce gold to its zero-valence.

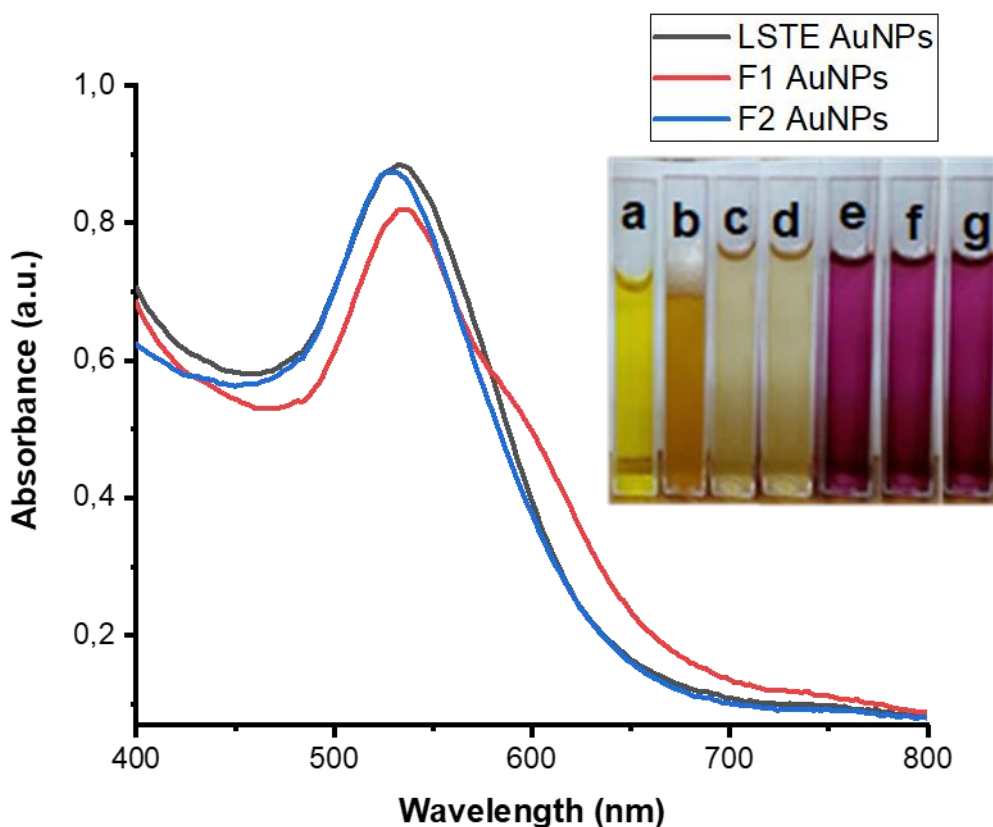


**Figure 3. 4: Absorption spectra of gold nanoparticles. It also carries (a) gold salt solution, (b) aqueous solution of the *Leucosidea sericea* total extract (LSTE), aqueous solution of (c) F1 and (d) F2 and the corresponding gold nanoparticles of (e) LSTE, (f) F1 and (g) F2**

### 3.3.3 High-Resolution Transmission Electron Microscopy (HR-TEM)

HRTEM provides information regarding morphology, crystallinity and size of nanoparticles. Figure 3.5 (A–G) displayed the HRTEM results and the evaluation of particle size of LSTE, F1 and F2 AuNPs. The mean diameters of the particles were  $15.4 \pm 2$ ,  $24.8 \pm 9$  and  $13.1 \pm 2$  nm respectively. The figure shows AuNPs with a mixture of shapes. A combination of triangles, rod-like, cone and cubic shapes were all observed. The spherical shapes were, however, dominant in all the three nanoparticles. Coatings were also observed having a width between 2 and 3 nm around LSTE and F2 AuNPs [83]. This combination of shapes is characteristic of AuNPs and it has been associated with the different chemical constituents forming the AuNPs [84-85]. The approximate size recorded by LSTE and F2 gold nanoparticles was not surprising. This is because of the similarity of their absorption bands and peak areas as earlier suggested from the UV-Vis spectra. Similarly, the difference of size of the F1 AuNPs with those of others is equally obvious.

Another evidence of the similarity of both the LSTE and F2 AuNPs is the percentage composition of particles with rod-like and triangular shapes. Figure 3.5 G indicated about



1.9 % of rod-like particles and approximately 2.26 % of triangles were recorded for both LSTE and F1 gold nanoparticles. The rod-like particles in the case of LSTE AuNPs possess a length ranging between 3.71 – 10.06 nm and a diameter of 2.08 – 5.42 nm. The corresponding size for F1 AuNPs was found to be 1.11 – 38.65 nm and 0.91 – 26.55 nm. F2 AuNPs had a length in the range of 1.87 to 6.61 nm with a diameter of 0.82 to 3.07 nm. Again, green synthesis using plant phytochemicals often result in variety of shapes according previous studies [85]. The inset in Figure 3.5 (A-C) shows the selected area electron diffraction (SAED) pattern of LSTE, F1 and F2 AuNPs respectively. The bright circular rings indicate that the particles are polycrystalline, and can be linked to the (111), (200), (220) and (311) planes of a face-centered (FCC) structure of gold [86].

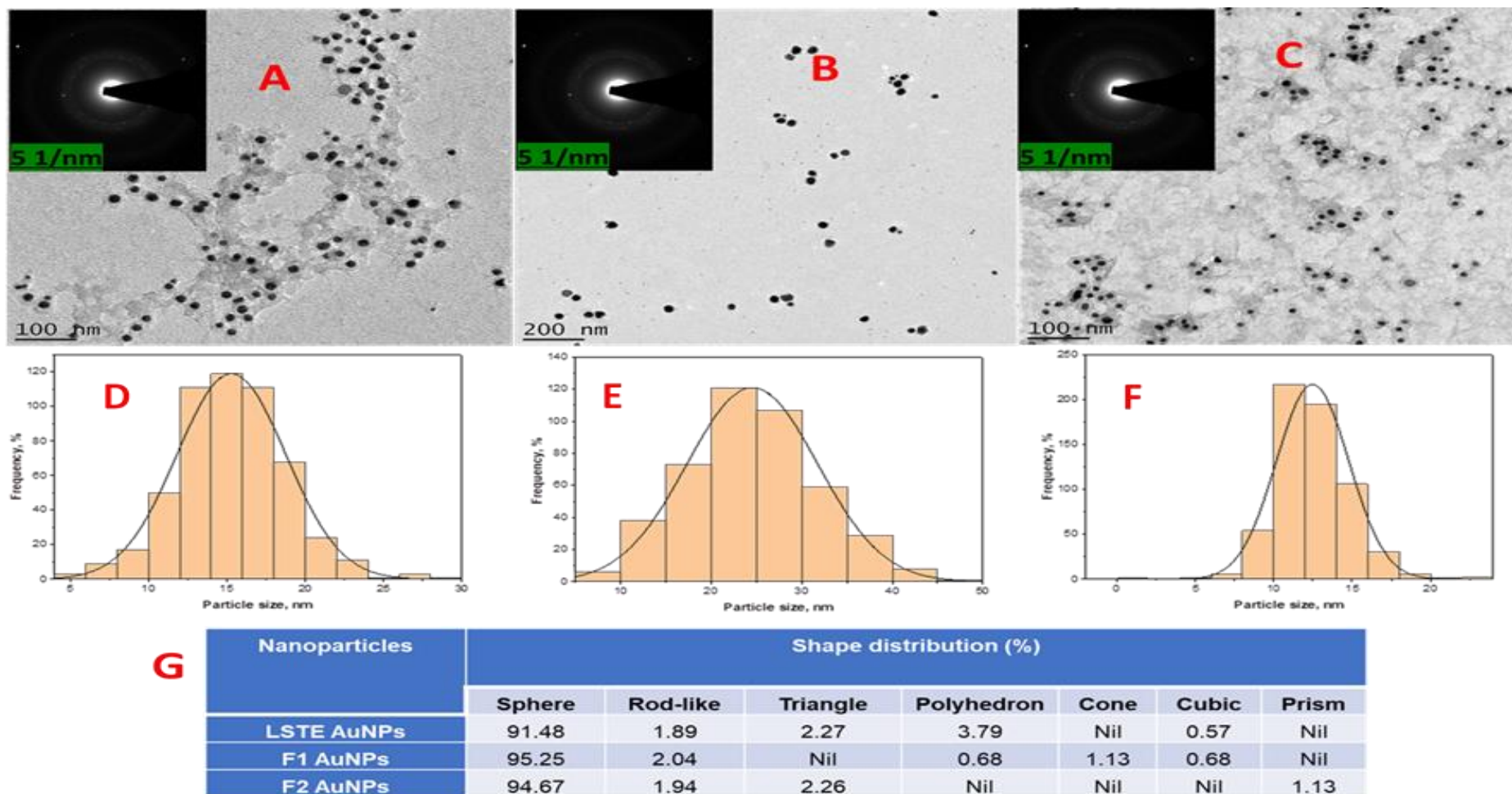


Figure 3. 5: HRTEM images for LSTE, F1 and F2 AuNPs are represented as (A, B, C) and the corresponding particle size distributions as (D, E, F) respectively. The inset in A, B and C showing the bright rings are the SAED of the respective TEM images. Other TEM images used in evaluation of the particle size, shape and distribution has been included in appendix (G, H and I)

The EDS spectra of the blank/glass substrate (Figure 3.6a) and the AuNPs (Figure 6b–d) confirmed the presence of Au in the solution. Other elemental peaks such as C, O and Na (Figure 3.6a–d) were likely from the sample preparation/glass substrate used to prepare the samples for the analysis. The small sulfur peak (Figure 3.6b) could be a contaminant while Cl and perhaps some of the Na were possibly from the sodium chloroaurate solution used as a precursor.

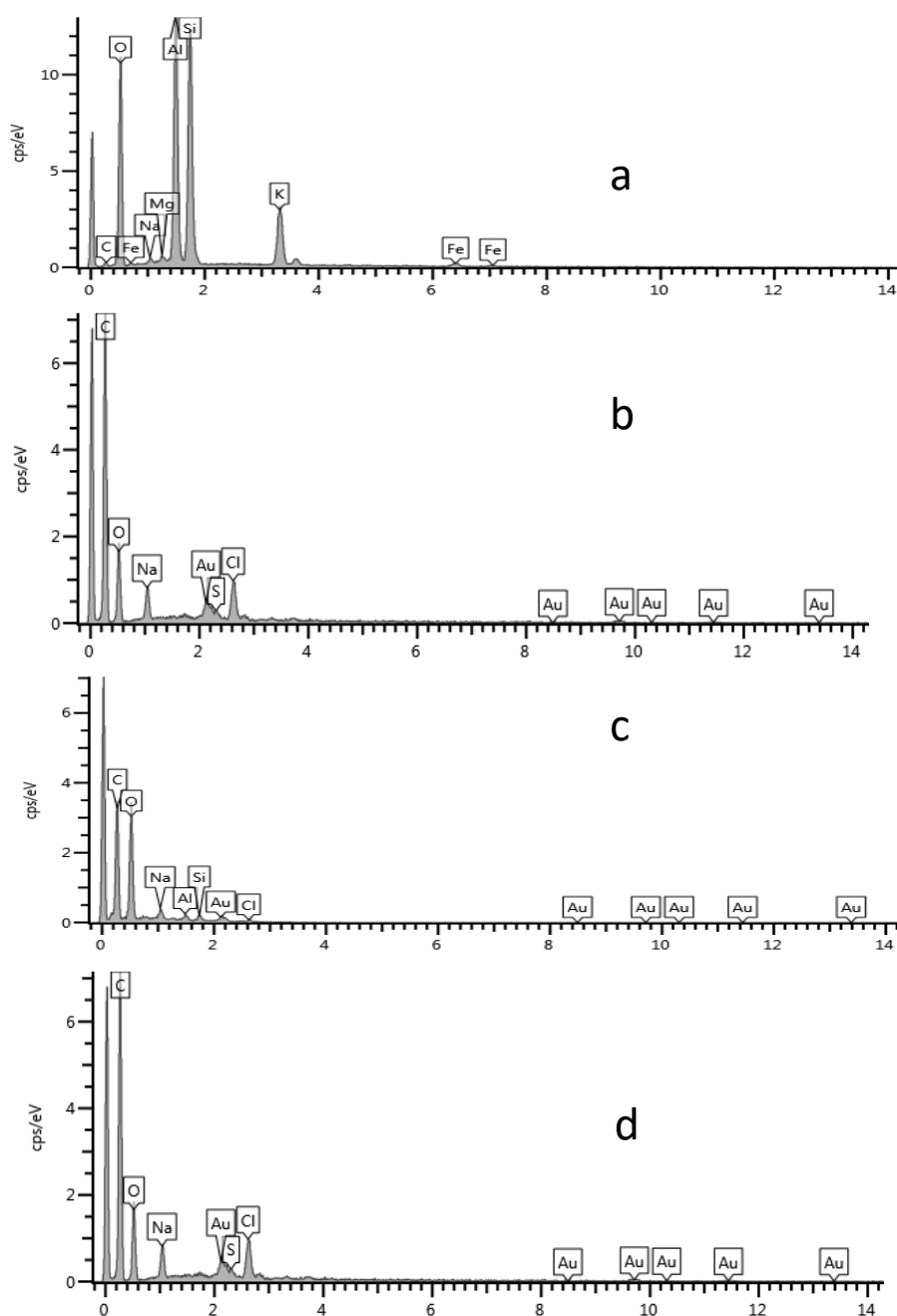


Figure 3. 6: EDS spectra of (a) blank, (b) LSTE AuNPs, (c) F1 AuNPs and (d) F2 AuNPs

### 3.3.4 X-Ray Diffraction (XRD) Analysis

Figure 7 depicts XRD patterns of AuNPs of LSTE, F1 and F2. Four distinct peaks (Figure 3.7(a–c)) were observed at 2 theta degree values equal to 38.2, 44.4, 64.6 and 77.5. These corresponds to the (111), (200), (220) and (311) planes respectively of the FCC gold lattice [74], in agreement with that of the pure crystalline gold structure published by XRD Joint Committee on Powder Diffraction Standards (file nos. 04-0784). XRD data were further corroborated by the bright circular rings observed in the SAED patterns, as shown earlier (Figure 3.5).

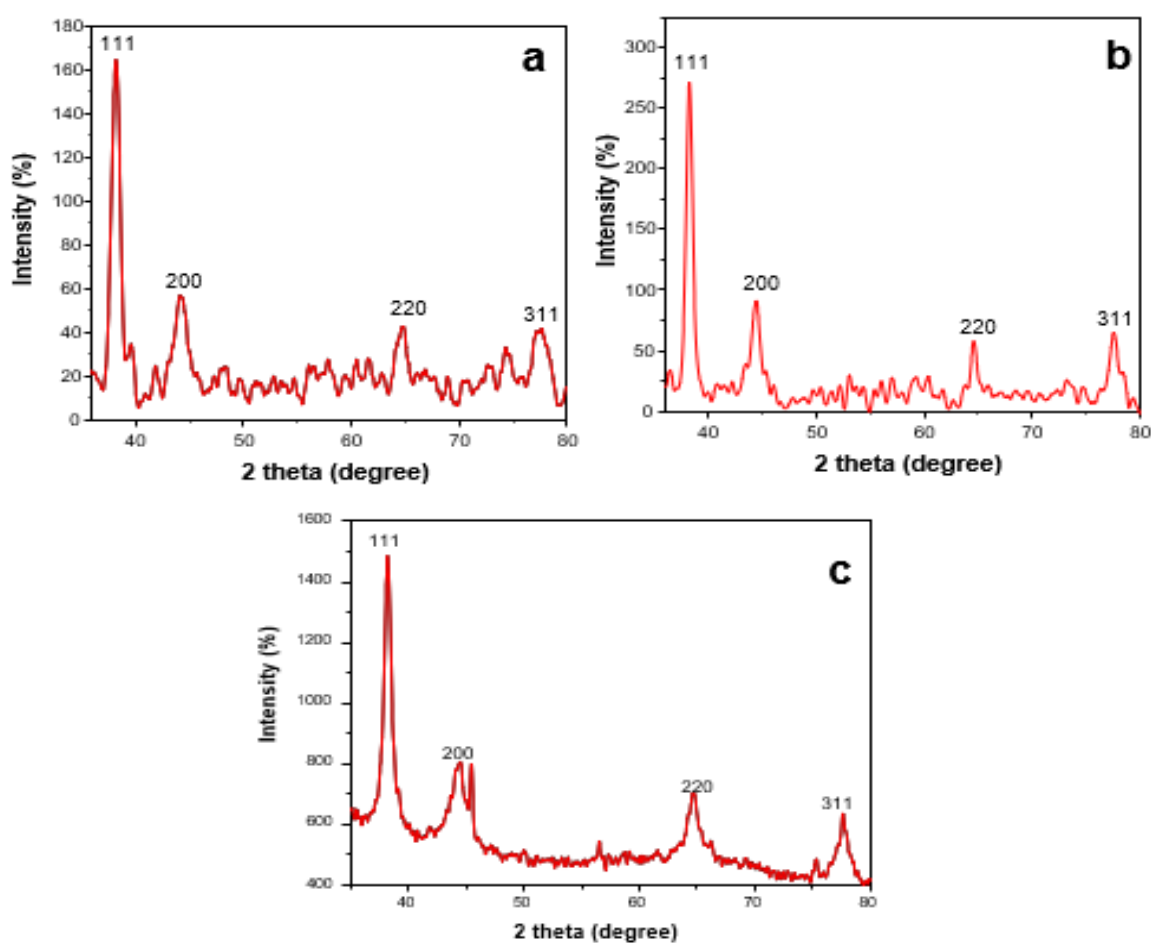
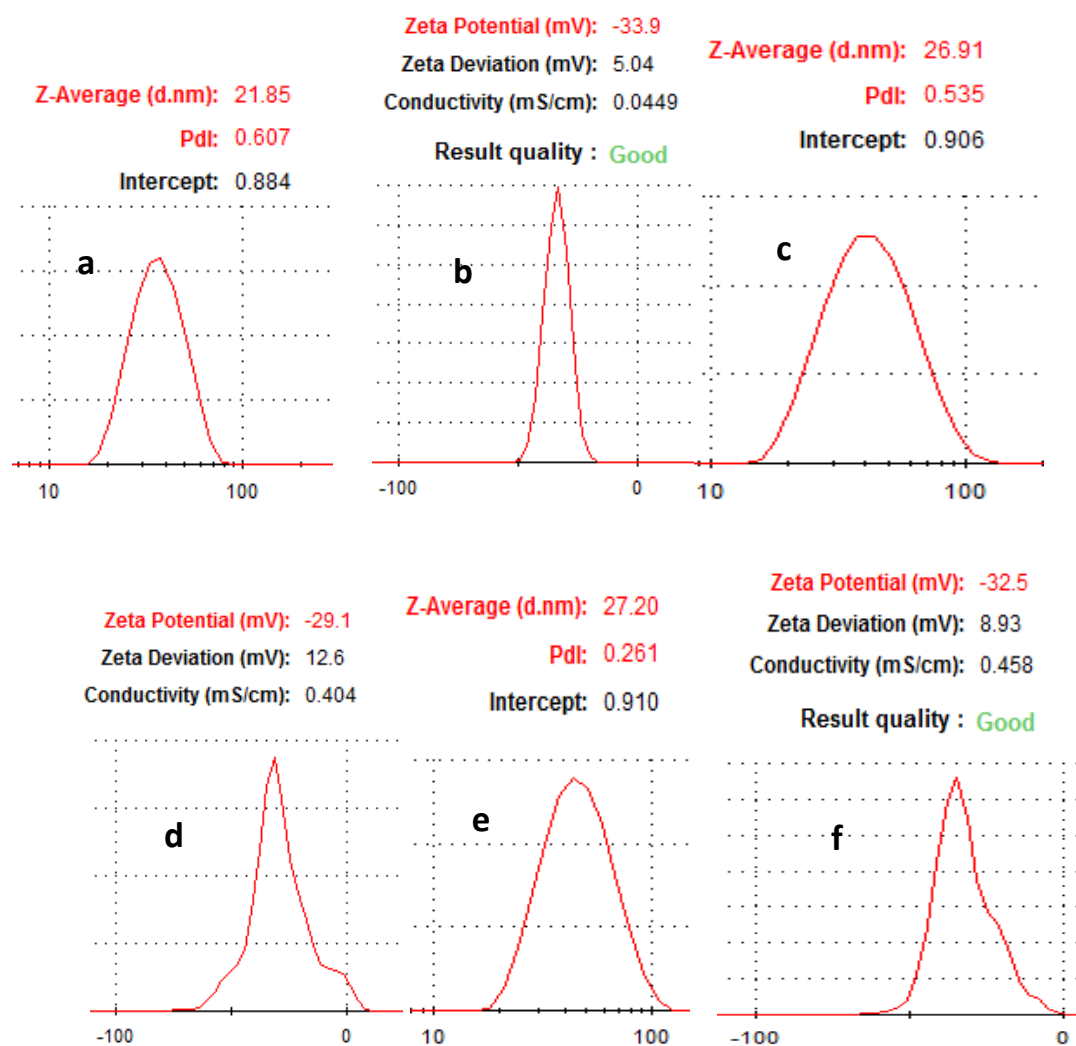


Figure 3. 7: XRD patterns of the (a) LSTE AuNPs, (b) F1 AuNPs and (c) F2 AuNPs

### 3.3.5 Dynamic Light Scattering (DLS) Measurement of AuNPs

Among other important factors to be considered before the application of nanoparticles is the phase behavior. Light scattering is one of the techniques to understand this phenomenon. DLS, a non-intrusive technique, was employed to measure

the size and zeta potential of the AuNPs. The average size of LSTE, F1 and F2 AuNPs was found to be 21.85, 26.91 and 27.20 nm respectively (Figure 3.8). Size characterization of nanoparticles is of immense importance in nanomedicine. However, it is noteworthy that the size measured by DLS technique is often different from that of TEM for some reasons. One, the size relates to the metallic core of the nanoparticles. The size is also influenced by all the substances surrounding the surface of the nanoparticles such as the capping agents and thirdly, the thickness of solvation shell, moving along with the particles. The thickness of the solvation shell as well as its influence on the size of measured nanoparticles is, in turn, dependent on the nature of the substances in the colloidal suspension and on the surface of the nanoparticles [87]. Hence, the size measured by the DLS technique was bigger than that measured by TEM [88]. Additionally, the difference in size is also due to the instrument used since different instrument uses specific operation techniques. For instance, while TEM the geometric size of the nanoparticle deposited on a surface, the DLS measures the hydrodynamic size. Again, large particles scatter more lights than the smaller ones and even a small number of such large particles can obscure the contribution of the smaller particles [89].



**Figure 3. 8: Hydrodynamic size of (a) LSTE, (c) F1, (e) F2 and zeta potential of (b) LSTE, (d) F1 and (f) F2 AuNPs measured using Dynamic Light Scattering (DLS)**

The zeta potentials (ZP) taken immediately after particle formation are displayed in Table 1. Values of  $-33.59$ ,  $-32.5$  and  $-29.1$  mV (Table 3.8) were obtained for the LSTE-, F1- and F2 AuNPs respectively. ZP is related to the surface charge of nanoparticles, and particles with ZP values  $-30$  mV and below are taken to be mostly covered with negatively charged ions. The opposite is true for positive ZP values. The extent of ZP is therefore, a subject of repulsion and attraction that has been used to estimate how long the nanoparticle dispersions would remain stable. The negative zeta-potential values obtained for the AuNPs fall in the range that is typical of stable colloidal dispersions [72]. The ZP measurement for the nanomaterials was repeated on the seventh day through to the fourteenth day showing only slight changes. From the DLS measurement, a slightly higher value of ZP for LSTE AuNPs could be due to the synergistic effect of other compounds present, probably providing enhanced capping ability. Both the hydrodynamic sizes and ZP

values for F1 and F2 can be observed to be approximately the same and therefore can be explained by the similarity of phytochemicals involved. This was also supported by their HRTEM results, where the average particle sizes were 24.4 and 22.4 nm for F1- and F2 AuNPs respectively. Interestingly, their ZP values equally indicated that the particles are stable to a similar extent, further confirming the presence of capping agents with similar functional groups. This is because procyanidins, share the same basic structures and may only differ in the molecular weights. Significant changes were not noticed in the ZP values of the gold nanoparticles (as provided in Table 3.1) for the given days. This suggests no agglomeration as they repelled each other. Therefore, the particles were quite stable. This stability was also supported by UV-Vis analysis. It was observed that there was no change in the SPR of the gold nanoparticles as the measurement was repeated over time. No new peaks were also noticed, therefore, the nanoparticles did not aggregate.

**Table 3.1: Particle size and zeta potential for AuNPs obtained from DLS.**

Sample	Hydrodynamic Size (nm)	Zeta Potential (mV)
LSTE AuNPs	21.85	-33.9
F1 AuNPs	27.20	-32.5
F2 AuNPs	26.91	-29.1

### 3.3.6 In Vitro Stability Study

The effectiveness of nanoparticles in medical applications depends on its stability in biological solutions for a reasonable period. Figure 9 displayed the evaluation of stability when 0.5% bovine serum albumin (BSA), glycine (GLY), sodium chloride (NaCl), cysteine (CYS) and phosphate buffers at pH 7 and 9 were mixed with LSTE, F1 and F2 particles [90]. These were carried out before and after incubation at 37 °C. Even though the pH 9 solution is higher than the pH of human body fluids, it was considered to get additional information about whether nanoparticles are still stable at such a high pH. The results showed that the SPR remained the same in all the formulations. However, a noticeable shift by BSA especially from the 12th h is a behavior of certain proteins. BSA has been reported to have preference of binding to negatively charged surfaces [91]. This has been ascribed to the presence of over 50 surface lysine groups, which enable easy electrostatic interactions with negative surfaces. Consequently, the negative ZP values of our particles implies that the surfaces were largely covered by negative ions, hence more interaction with BSA. Overall, the shifts of less than 1.0 nm in all solutions was minimal, the  $\lambda_{\max}$

remained intact thereby affirming the stability of LSTE and F2 particles in the solutions at the tested period.

Conversely, addition of these reagents to the F1 AuNPs brought about increase in the absorption bands which is due to interaction of the molecules with the ions surrounding the surface of the nanoparticle. Zeta potential showed that negative ions surrounds the particles whereas the proteins such as BSA is covered with several lysine that are positively charged. Glycine and cysteine also possess positive ions in solution. The introduction of these proteins, therefore, might have caused the aggregation of the F1 AuNPs due to electrostatic interaction [92-93]. Additionally, the presence of amine groups may also influence aggregation of the particles. Proteins contain good binding site (-COOH and -NH<sub>2</sub>) which may allow such coordination with gold nanoparticles. Easy hydrogen bond can be formed especially with high number of dimers and trimers serving as the capping agents in the solution and at the surface of the nanoparticles [94]. Hence, the intensity of absorption band continued to expand, indicating growth which is due to aggregation of particles. As the time passes (0-24 h), changes continued to appear at the absorption band and the peaks also widens, all suggesting growth of the nanoparticles. Similarly, other researchers reported aggregation of gold nanoparticles upon introduction of sodium chloride to it [95-96].

This slow aggregation was not observed in LSTE and F2- AuNPs probably for the following reasons; LC-MS showed higher number of trimers in F1 than F2. The molecular weight is higher, and it contains more hydroxyl groups than the dimers. Therefore, there may be more interaction with the proteins. As for the LSTE, many phytochemicals are involved in the formation of the nanoparticle as well as serving as capping agents. Thus, their interaction with one another may affect that with the proteins and the surrounding medium. Therefore, F1 AuNPs aggregates slowly and will lose stability faster than the F2 and LSTE-AuNPs.



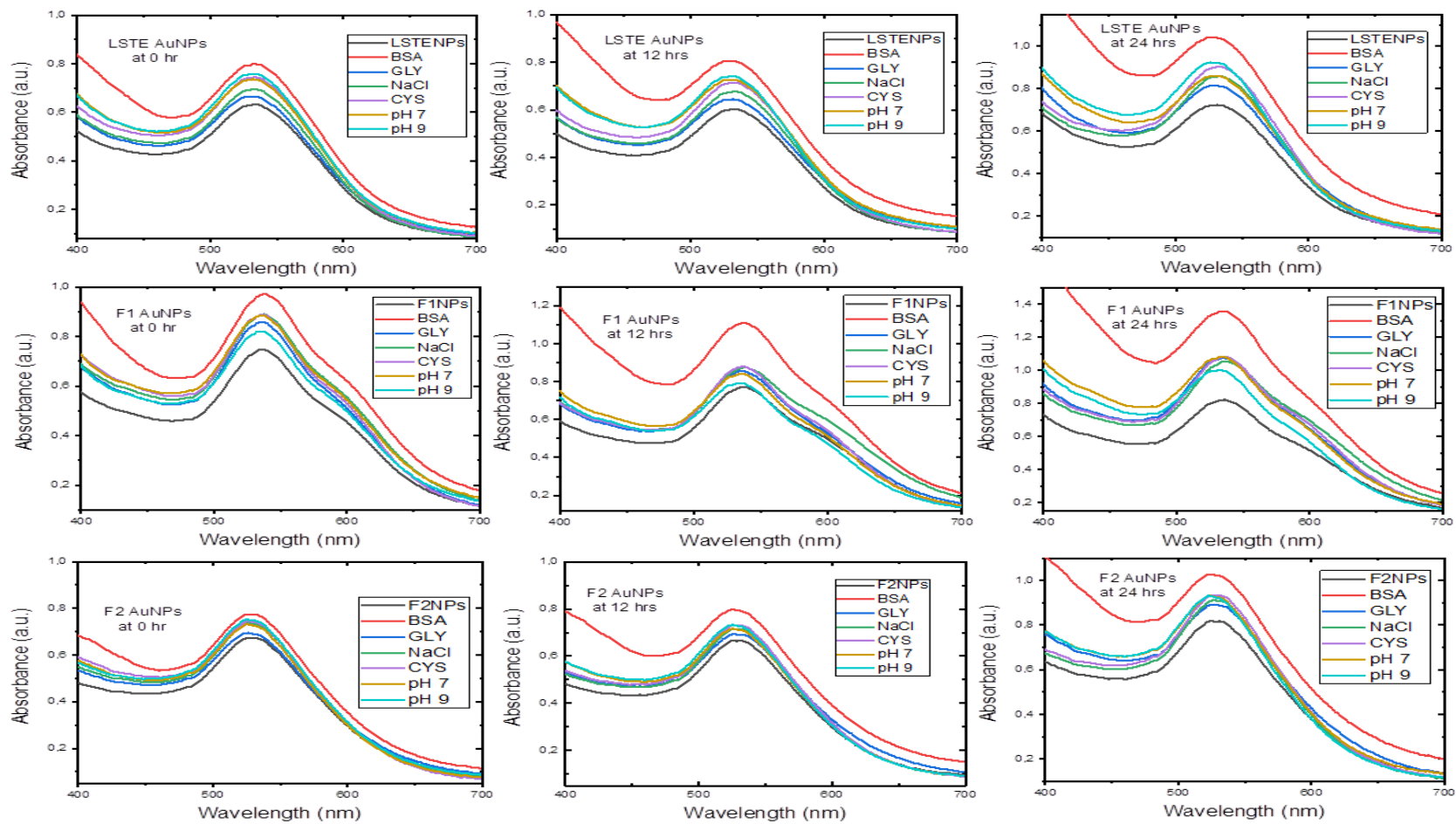
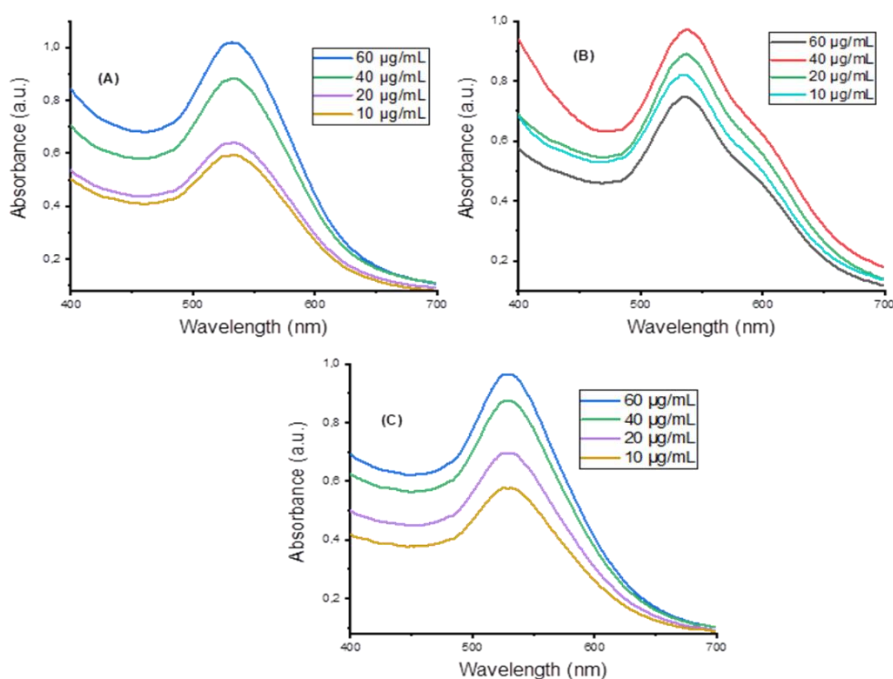


Figure 3.9: Stability of the particles at given time intervals

### 3.3.7 Dilution Study

Some biomedical applications require different concentrations of gold nanoparticles. Figure 3.10 shows the absorbance of the hybrid (a) LSTE-, (b) F1- and (c) F2 AuNPs at different concentrations. To confirm that dilution of nanoparticles into different concentrations does not affect their stability and does not alter their physical and chemical properties in vivo, a dilution study was carried out at different concentrations of the nanoparticles (100, 80, 60, 40, 20 and 10  $\mu\text{g}/\text{mL}$ ), and UV-Vis spectroscopy (350–850 nm) was recorded for each concentration. From the UV-Vis spectra, the SPR wavelength had the same value for all the solutions of a given particle. This means that the dilution did not have effect on the properties of LSTE-, F1- and F2-AuNPs, and the nanoparticles remained stable. The maximum absorption intensity of all the nanoparticles was found to be in the same region. Similarly, Tea mediated gold nanoparticles was successively diluted by the addition of 0.1 mL deionized water in a previous study. The maximum absorption intensity was monitored and found to be intact even at very diluted conditions [97]. Also, when *acacia gum* mediated gold nanoparticles were diluted, the maximum absorption peak remained the same. This shows that the properties of the AuNPs were not affected by the dilution. They authors further observed that at all the tested concentrations, the absorption peak remained in the same region [98]. These studies further confirm the findings being reported here.



**Figure 3. 9. Surface plasmon resonance wavelength ( $\lambda_{\max}$ ) of diluted concentrations of (A) LSTE-, (B) F1- and (C) F2- AuNPs. The  $\lambda_{\max}$  of each nanoparticle remained in the same region at different concentrations indicating retention of properties**

### 3.3.8 In-Vitro Antidiabetic Studies

Since T2DM is associated with neurological and cardiovascular complications as a result of metabolic disorders emanating from hyperglycemia, the most critical remedy is to keep the blood sugar within the normal range. Two special enzymes, alpha-glucosidase and -amylase have good records of breaking down the long-chains of carbohydrates thereby enhancing the breakup of the glucose unit from the disaccharide. Therefore, the inhibition of these enzymes has been among the popular therapies for T2DM [99]. Although the antidiabetic properties of many plant extracts have been reported [100], scarce literature exist on the antidiabetic activity of the constituents of *Leucosidea sericea*. In this study, *Leucosidea sericea* leaves extract, the fractions (F1 and F2) and gold nanoparticles biosynthesized from them were studied and their potential as antidiabetic and antioxidant agents evaluated.

For the enzymatic studies, strong inhibitory activities were displayed by the constituents of *Leucosidea sericea* as well as the fabricated AuNPs (Table 3.2). F1 and F2 are fractions from the extract and demonstrated high alpha-glucosidase activity. IC<sub>50</sub> values of 8.1, 7.3 and 7.1  $\mu\text{g/mL}$  were obtained for LSTE, F1 and F2 respectively. The alpha-amylase inhibition resulted in 3.5  $\mu\text{g/mL}$  for LSTE and 18.9  $\mu\text{g/mL}$  for F2. F1 did not show any activity at the tested concentrations. In general, the results showed that LSTE, F1, F2 and their AuNPs had the potential to be used as antidiabetic agents. Pure isolated phytochemicals have demonstrated activities against alpha-glucosidase in previous studies [47,48]. Recently, Etsassala et al. [101] reported a strong antidiabetic activity of ten abietane diterpenes. In their study, the antidiabetic activity was due to the type and position of different functional groups in the compounds. Additionally, some compounds displayed either alpha-glucosidase or alpha-amylase activity and not both. For instance, 11,12-dehydrousolic acid lactone displayed moderate alpha-glucosidase activity but showed no activity for amylase [101]. Although, both fractions (F1 and F2) have similar structures, F1 did not show activity against alpha-amylase compared to F2, this may be due to the antagonistic effect of one of the trimers, and this effect disappeared when this compound(s) conjugated with AuNPs and showed enhanced activities. Furthermore, among the three popular antidiabetic standard drugs currently in the market, only acarbose inhibits both alpha glucosidase and alpha amylase. Vigliobose showed little effect on amylase whereas miglitol does not have any effects on amylase [102]. Therefore, the high

activity displayed by F1 on alpha-glucosidase and not for amylase agrees with the above studies. Furthermore, a close examination of the IC<sub>50</sub> of LSTE, F1 and F2 for alpha-glucosidase indicates a similar functionality as mentioned above. Almost the same values were obtained for F1 and F2, which further supports the occurrence of the dimers and trimers of procyanidins, as rightly suggested by the NMR and LC–MS analysis. Procyanidins possessed similar arrangements of the hydroxyl groups as well as the aromatic ring systems and therefore, might have similar behaviors. However, the mechanism of action of alpha-glucosidase and alpha-amylase might not necessarily be the same. This has been demonstrated by the reports of many assays where different values were recorded for the two enzymes, even though the aim of inhibition is the same [103].

**Table 3.2: Inhibitory activities of LSTE, F1, F2 and AuNPs on alpha-glucosidase and alpha-amylase.**

<b>Items</b>	<b>Alpha-Glucosidase IC<sub>50</sub> (µg/mL)</b>	<b>Alpha-Amylase IC<sub>50</sub> (µg/mL)</b>
LSTE	8.1 ± 0.6	3.5 ± 0.7
LSTE AuNPs	14.5 ± 0.8	3.0 ± 0.3
F1	7.3 ± 0.5	NA
F1 AuNPs	7.3 ± 0.3	1.8 ± 0.3
F2	7.1 ± 0.4	18.9 ± 0.2
F2 AuNPs	4.5 ± 0.6	10.5 ± 0.1
Acarbose	610 ± 2.6	10.2 ± 0.6

NA: not active at the tested concentrations, Acarbose: positive control.

AuNPs of LSTE, F1 and F2 demonstrated activities that compete well with the intact extract/fractions. Although the activity of F1 AuNPs was identical to that of F1 for alpha-glucosidase, an enhanced alpha-amylase inhibition was recorded for F1 AuNPs. This behavior is similar to that reported by Shamprasad et al. [58], where Escin-AuNPs showed better activity compared to Escin in their study, thereby confirming our submission on the activity of F1 and F2 AuNPs. The activities in each case were almost two-fold of the corresponding precursor. This continuous resemblance of activity may stem from the starting materials of the nanoparticles. As earlier stated, F1 and F2 fractions are composed of dimer and trimer procyanidins as the major constituents. Therefore, closely related behaviors in the same experimental conditions are obvious. Accordingly, the improved antidiabetic performance of bimetallic Ag-AuNPs over their precursor extracts and acarbose has been reported [45,46]. The IC<sub>50</sub> values of alpha-amylase on LSTE and its gold form also showed improved activity in agreement with previous studies [45]. The inhibiting powers of the nanomaterials may be a function of size and shape. As noted

earlier, our AuNPs had a size range of 6–24 nm. These values are similar to the sizes in previous investigations [58]. Similarly, Niikura et al. [104] affirmed that spherical AuNPs of sizes 20 and 40 nm in diameter induced the west Nile virus better than those of other sizes and shapes. This may be the reason for an improved enzymatic activity of F1 and F2 AuNPs.

### 3.3.9 Antioxidant Activity/Total Phenolic Content

Oxidative stress has been linked to the cause of many deadly diseases like diabetes, the management of which is costly. Thus, plant extracts and nanoparticles with both antidiabetic and antioxidant properties will be greatly beneficial [105]. Therefore, the need to search for antioxidants with enhanced reducing abilities is crucial. Antioxidants are substances that can inhibit or delay the oxidation of a substrate when present in low concentrations. Due to the relationship of oxidative stress to other diseases, we, therefore, investigated the antioxidant capacities of LSTE, F1, F2 and the corresponding AuNPs. Three assays; Ferric reducing antioxidant power (FRAP), Folin–Ciocalteu (FC), and 2,2'-azino-bis-3-ethylbenzotiazolin-6- sulfonic acid (ABTS) were carried out and the results are presented in Table 3.3.

**Table 3.3: Antioxidant activities of LSTE, F1, F2 and the corresponding AuNPs**

Items	FRAP ( $\mu\text{M AAE/g}$ )	ABTS ( $\mu\text{M TE/g}$ )	FC ( $\mu\text{M GAE/g}$ )	FC% (AuNPs)
LSTE	1113.2 $\pm$ 6.7	814.9 $\pm$ 6.1	602.6 $\pm$ 6.1	
LSTE AuNPs	113.8 $\pm$ 9.5	1059.4 $\pm$ 7.4	179.8 $\pm$ 6.2	29.3
F1	1834.0 $\pm$ 4.7	818.2 $\pm$ 7.7	889.6 $\pm$ 6	
F1 AuNPs	748.6 $\pm$ 1.4	1521.9 $\pm$ 3.0	356.7 $\pm$ 6.6	40.1
F2	1166.0 $\pm$ 2.1	816.9 $\pm$ 8.6	685.7 $\pm$ 6.7	
F2 AuNPs	1083.8 $\pm$ 1.2	861.9 $\pm$ 5.3	523.1 $\pm$ 4.4	76.3
Standard	3976.8 $\pm$ 3.8 *	7525.0 $\pm$ 4.9 **		

\* = vitamin C, \*\* = trolox. The results are expressed as mean  $\pm$  SD for  $n = 3$ .

The mechanism with which FRAP operates is known as single electron transfer (SET), whereby an antioxidant transfers an electron to the corresponding cation, which would neutralize it [106]. In Table 3.3, strong activities were exhibited on FRAP with F1 displaying the highest activity (1834.0  $\pm$  4.7  $\mu\text{M AAE/g}$ ). From the NMR and LC–MS analysis, F1 was found to contain a dimer and trimer of procyanidins that might have acted together in synergy to bring about this high activity. They possess hydroxyl groups attached to aromatic rings, which will perfectly participate in oxidation during the process. Similar activities were recorded for LSTE and F2 because they contained phenolic compounds of similar functionality. It is well known that phenolics have strong antioxidant activities [107].

The huge presence of many phenolics in LSTE has been demonstrated previously by LC–MS analysis, therefore its high activity is reasonable, while similar compounds, although different proportions were found in F2, accounted for its activity as well. However, since the FRAP's mechanism is by electron transfer, the hydroxyl groups of the compound might be interacting with the nanoparticles, thereby limiting the site for the oxidation process.

This may contribute to slightly reduced activity. In contrast, high activities in close ranges were demonstrated for all samples in FC assay except for LSTE AuNPs. Size, shape and the surrounding environment/medium is critical to the activity of nanoparticles. Owing to the type and number of phytochemicals taking part in the fabrication of LSTE AuNPs, there is a large size difference from those of F1 and F2 and the stability was also slightly higher. Therefore, it is expected to behave somewhat differently since the smaller sized particles have a higher surface area. In addition, more phytochemicals are present in LSTE, which creates a different surrounding environment for the NPs. Previously, nanoparticles with smaller sizes were reported to show enhanced activity in comparison to relatively larger ones [108]. On the other hand, a clear trend can be observed for the ABTS assay. This is probably because of the difference in the mechanism of operation between the assays. ABTS is largely operating on hydrogen atom transfer (HAT). The trend in the ABTS results is such that individual AuNPs demonstrated better antioxidant capacity relative to their respective precursors. Recent research reports [54,57–58,107] supported the above submission. AuNPs biosynthesized from *Halymenia dilatata* also demonstrated higher antioxidant activity than the starting plant extract [109].

However, results of antioxidant activities often vary from one assay to the other, probably because of the difference in mechanism of operation where some operate by SET or HAT or both. The nature of the sample, the medium of operation and the functionality might account for the variations in our results from one assay to the other (Table 3.3).

### **3.3.10 Quantification of the Total Phenolic Content in the AuNPs from the FC Assay**

Results from Table 3.3 revealed the phenolic content of the intact fractions (F1 and F2) and the total extracts, as well as the phenolic content (FC) of the corresponding AuNPs. According to the HRTEM and DLS analysis, the average diameter was smaller in case of the LSTE AuNPs relative to the others. Hence, the higher surface area available for interaction with the compounds may explain the smaller phenolic content (29.3%) observed. However, an increase in the percentage FC was observed in the case of F1 and F2, with maximum concentration of F2 (76.3%). The high payload of F2 may be explained

in terms of the homogeneity of the compound in that fraction as well as its high packing power.

### 3.3.11 Conclusions

The preliminary screening of the *L. sericea* total extract showed the potential of generating stable AuNPs. An intent made to purify the pure compound(s) responsible for such activity resulted in the purification of two inseparable procyanidins fractions namely F1 and F2. The first fraction, F1, contained a mixture of procyanidins dimer (B series) and trimers, while the second fraction, F2, contained four major procyanidin dimers belonging to B series. These fractions successfully formed stable AuNPs confirming the ability of these class of phytochemicals to act as reducing agents. DLS measurements and in vitro stability examinations further affirmed their stability in physiological conditions without the introduction of any external stabilizers. This means that the compounds also doubled as capping agents that prevented agglomeration for the given period. Thereafter, biological activities were carried out. LSTE constituents and hybrid nanoparticles showed interesting inhibitory activities on both alpha-glucosidase and alpha-amylase at low concentrations. F1 and its AuNPs demonstrated enhanced alpha-glucosidase activities compared to LSTE and LSTE AuNPs. For alpha-amylase, F2 AuNPs showed the highest inhibitory activities, which were another interesting behavior that calls for further attention. The particles also exhibited interesting antioxidant activity thereby buttressing their potential biological applications since this activity has been linked to some diseases. As far as we know, this work is the first scientific report on the identification of procyanidins from the aerial parts of *Leucosidea sericea*, and the use thereof in nanoparticle synthesis. The results suggest that procyanidins had the ability to reduce gold to form biostable and bioactive gold nanoparticles with potential antidiabetic and antioxidant applications.

### Author Contributions

A.A.H. conceived the research idea. U.M.B. carried out the synthesis of AuNPs, dilution studies, UV-Vis and DLS measurements under the guidance of A.A.H. and S.B. A.O.A. carried out extraction, purification of F1 and F2. J.A.B. carried out enzymatic studies under the guidance of J.L.M. while S.B. carried out TEM, SAED and EDS analysis. C.N.C identified, collected and prepared the plant material. E.I. was responsible for stability studies and coordinated the writing of the manuscript. All authors read, edited and contributed to the manuscript. A.A.H. and S.B. are U.M.B.'s supervisors.

### **Supplementary Materials**

The supplementary documents for this research article has been attached here as appendix (A-F)

### **Funding**

The Tertiary Education Trust Fund (IBB University, Lapai 2016 intervention), Nigeria was used for this research. Cost of chemicals was covered by NRF with a call number (106055) under Professor Ahmed A. Hussein.

### **Acknowledgments**

We would like to appreciate Hamza Elsayed Mohammed of iThemba labs for XRD analysis, Electron microscope unit, UWC for TEM, EDS and SAED analysis.

### **Conflicts of Interest**

The authors declare no conflict of interest in this work.



## References

1. Duan, H.; Wang, D.; Li, Y. Green chemistry for nanoparticle synthesis. *Chem. Soc. Rev.* **2015**, *44*, 5778–5792.
2. Saravanakumar, A.; Peng, M.M.; Ganesh, M.; Jayaprakash, J.; Mohankumar, M.; Jang, H.T. Low-cost and eco-friendly green synthesis of silver nanoparticles using *Prunus japonica* (Rosaceae) leaf extract and their antibacterial, antioxidant properties. *Artif. Cells Nanomed. Biotechnol.* **2017**, *45*, 1165–1171.
3. Jha, A.K.; Prasad, K. Green synthesis of silver nanoparticles using *Cycas* leaf. *Int. J. Green Nanotechnol. Phys. Chem.* **2010**, *1*, 110–117.
4. Liu, J.; Qin, G.; Raveendran, P.; Ikushima, Y. Facile “green” synthesis, characterization, and catalytic function of  $\beta$ -D-glucose-stabilized Au nanocrystals. *Chem. Eur. J.* **2006**, *12*, 2131–2138.
5. Kumar, V.; Mohan, S.; Singh, D.K.; Verma, D.K.; Singh, V.K.; Hasan, S.H. Photo-mediated optimized synthesis of silver nanoparticles for the selective detection of iron (III), antibacterial and antioxidant activity. *Mater. Sci. Eng. C* **2017**, *71*, 1004–1019.
6. Tekale, S.U.; Kauthale, S.S.; Pagore, V.P.; Jadhav, V.B.; Pawar, R.P. ZnO nanoparticle-catalyzed efficient one-pot three-component synthesis of 3, 4, 5-trisubstituted furan-2 (5*H*)-ones. *J. Iran. Chem. Soc.* **2013**, *10*, 1271–1277.
7. Ergin, A. D.; Bayindir, Z. S.; Yüksel, N. Characterization and optimization of colon targeted S-adenosyl-L-methionine loaded chitosan nanoparticles. *Marmara Pharm. J.* **2019**, *23*(5).
8. Liu, Y.; Welch, M.J. Nanoparticles labelled with positron emitting nuclides: Advantages, methods and applications. *Bioconj. Chem.* **2012**, *23*, 671–682.
9. Xie, Y.; Kocaefer, D.; Chen, C.; Kocaefer, Y. Review of research on template methods in preparation of nanomaterials. *J. Nanomater.* **2016**, *2016*, 2302595.
10. Singh, P.; Kim, Y.J.; Zhang, D.; Yang, D.C. Biological synthesis of nanoparticles from plants and microorganisms. *Trends Biotechnol.* **2016**, *34*, 588–599.
11. Lysy, P.A.; Corritore, E.; Sokal, E.M. New insights into diabetes cell therapy. *Curr. Diabetes Rep.* **2016**, *16*, 38-48.
12. Renner, S.; Blutke, A.; Clauss, S.; Deeg, C.A.; Kemter, E.; Merkus, D.; Wanke, R.; Wolf, E. Porcine models for studying complications and organ crosstalk in diabetes mellitus. *Cell Tissue Res.* **2020**, 1–38.
13. Cho, N.; Shaw, J.E.; Karuranga, S.; Huang, Y.; da Rocha Fernandes, J.D.; Ohlrogge, A.W.; Malanda, B. IDF diabetes atlas: Global estimates of diabetes prevalence for 2017 and projections for 2045. *Diabetes Res. Clin. Pract.* **2018**, *138*, 271–281.

14. Lorenzati, B.; Zucco, C.; Miglietta, S.; Lamberti, F.; Bruno, G. Oral hypoglycemic drugs: Pathophysiological basis of their mechanism of action. *Pharmaceuticals* **2010**, *3*, 3005–3020.
15. Santos, M.S.C.; Azevedo, R.B.; Teixeira, P.R.; Sales, M.J.A.; Bao, S.N.; Paterno, L.G.; Silva, A.L.G. Photochemically-assisted synthesis of non-toxic and biocompatible gold nanoparticles. *Colloids Surf. B Biointerfaces* **2016**, *148*, 317–323.
16. Ahmad, T.; Azmi, M.; Irfan, M.; Moniruzzaman, M.; Asghar, A.; Bhattacharjee, S. Green synthesis of stabilized spherical shaped gold nanoparticles using novel aqueous *Elaeis guineensis* (Oil palm) leaves extract. *J. Mol. Struct.* **2018**, *1159*, 167–173.
17. Zhang, G.; Li, Y.; Gao, X. An asynchronous-alternating merging-zone flow-injection gold nanoparticles probe method for determination of antidiabetic pioglitazone hydrochloride medicine. *New J. Chem.* **2018**, *42*, 4337–4343.
18. Yilmazer-Musa, M.; Griffith, A.M.; Michels, A.J.; Schneider, E.; Frei, B. Grape seed and tea extracts and catechin 3-gallates are potent inhibitors of  $\alpha$ -amylase and  $\alpha$ -glucosidase activity. *J. Agric. Food Chem.* **2012**, *60*, 8924–8929.
19. Tanko, Y.; Yerima, M.; Mahdi, M.A.; Yaro, A.H.; Musa, K.Y.; Mohammed, A. Hypoglycemic activity of methanolic stem bark of *Adansonia digitata* extract on blood glucose levels of streptozocin-induced diabetic wistar rats. *Int. J. Appl. Res. Nat. Prod.* **2008**, *1*, 32–36.
20. van de Venter, M.; Roux, S.; Bungu, L.C.; Louw, J.; Crouch, N.R.; Grace, O.M.; Folb, P. Anti-diabetic screening and scoring of 11 plants traditionally used in South Africa. *J. Ethnopharmacol.* **2008**, *119*, 81–86.
21. Eidi, A.; Eidi, M.; Esmaeili, E. Anti-diabetic effect of garlic (*Allium sativum* L.) in normal and streptozotocin-induced diabetic rats. *Phytomedicine* **2006**, *13*, 624–629.
22. Rizvi, M.M.A.; El Hassadi, I.M.G.; Younis, S.B. Bioefficacies of *Cassia fistula*: An Indian labrum. *Afr. J. Pharm. Pharmacol.* **2009**, *3*, 287–292.
23. Sethi, J.; Sood, S.; Seth, S.; Talwar, A. Evaluation of hypoglycemic and antioxidant effect of *Ocimum sanctum*. *Indian J. Clin. Biochem.* **2004**, *19*, 152–155.
24. Nammi, S.; Boini, M.; Lodagala, S.; Behara, R. The juice of fresh leaves of *Catharanthus roseus* Linn. reduces blood glucose in normal and alloxan diabetic rabbits. *BMC Complement. Altern. Med.* **2003**, *3*, 1–4.
25. Yagi, A.; Hegazy, S.; Kabbash, A.; Abd-El Wahab, E. Possible hypoglycemic effect of *Aloe vera* L. high molecular weight fractions on type 2 diabetic patients. *Saudi Pharm. J.* **2009**, *17*, 209–215.
26. Yalçın, S.; Erkan, M.; Ünsoy, G.; Parsian, M.; Kleeff, J.; Gündüz, U. Effect of gemcitabine and retinoic acid loaded PAMAM dendrimer-coated magnetic

- nanoparticles on pancreatic cancer and stellate cell lines. *BioMed Pharm.* **2014**, *68*, 737–743.
27. Kaleem, M.; Sheema, S.H.; Bano, B. Protective effects of *Piper nigrum* and *Vinca rosea* in alloxan induced diabetic rats. *Indian J. Physiol. Pharmacol.* **2005**, *49*, 65–71.
  28. Ponnaiyandurai, M.; Rajeshkumar, S. *In vivo* type 2 diabetes and wound-healing effects of antioxidant gold nanoparticles synthesized using the insulin plant *Chamaecostus cuspidatus* in albino rats. *Can. J. Diabetes* **2019**, *43*, 82–89.
  29. Khalil, M. Biosynthesis of gold nanoparticles using extract of grape (*Vitis vinifera*) leaves and seeds. *Prog. Nanotechnol. Nanomater.* **2016**, *3*, 1–12.
  30. Daisy, P.; Saipriya, K. Biochemical analysis of *Cassia fistula* aqueous extract and phytochemically synthesized gold nanoparticles as hypoglycemic treatment for diabetes mellitus. *Int. J. Nanomed.* **2012**, *7*, 1189–1202.
  31. John, P.A.; Zhijian, C.; Naidu, M. Neurite outgrowth stimulatory effects of myco-synthesized AuNPs from *Hericium erinaceus* (Bull.: Fr.) Pers. on pheochromocytoma (PC-12) cells. *Int. J. Nanomed.* **2015**, *10*, 5853–5863.
  32. Venkatraman, A.; Yahoob, S.A.M.; Nagarajan, Y.; Harikrishnan, S.; Vasudevan, S.; Murugasamy, T. Pharmacological activity of biosynthesized gold nanoparticles from brown algae-*Seaweed Turbinaria conoides*. *Nanoworld J.* **2018**, *4*, 17–22.
  33. Opris, R.; Tatomir, C.; Olteanu, D.; Moldovan, R.; Moldovan, B.; David, L.; Adriana, G. The effect of *Sambucus nigra* L. extract and phyto-synthesized gold nanoparticles on diabetic rats. *Colloids Surf. B Biointerfaces* **2017**, *150*, 192–200.
  34. Dhas, T.S.; Kumar, V.G.; Karthick, V.; Vasanth, K.; Singaravelu, G.; Govindaraju, K. Enzyme and microbial technology effect of biosynthesized gold nanoparticles by *Sargassum swartzii* in alloxan induced diabetic rats. *Enzyme Microb. Technol.* **2016**, *95*, 100–106.
  35. Malapermal, V.; Mbatha, N.; Gengan, R.; Anand, K. Biosynthesis of bimetallic Au-Ag nanoparticles using *Ocimum basilicum* (L.) with anti-diabetic and antimicrobial properties. *Adv. Mater. Lett.* **2015**, *6*, 1050–1057.
  36. Elobeid, M.A. Amelioration of streptozotocin induced diabetes in rats by eco-friendly composite nano-cinnamon extract. *Pak. J. Zool.* **2016**, *48*, 645–650.
  37. Ovais, M.; Khalil, A.T.; Islam, N.U.; Ahmad, I.; Ayaz, M.; Saravanan, M.; Mukherjee, S. Role of plant phytochemicals and microbial enzymes in biosynthesis of metallic nanoparticles. *Appl. Microbiol. Biotechnol.* **2018**, *102*, 6799–6814.
  38. Khan, M.A.; Raza, A.; Ovais, M.; Sohail, M.F.; Ali, S. Current state and prospects of nano-delivery systems for sorafenib. *Int. J. Polym. Mater. Polym. Biomater.* **2018**, *67*, 1105–1115.

39. Ali, M.; Khan, T.; Fatima, K.; Aliqul, A.; Ovais, M.; Khalil, A.T.; Idrees, M. Selected hepatoprotective herbal medicines: Evidence from ethnomedicinal applications, animal models and possible mechanism of actions. *Phytother. Res.* **2018**, *32*, 199–215.
40. Aromal, S.A.; Vidhu, V.K.; Philip, D. Green synthesis of well-dispersed gold nanoparticles using *Macrotyloma uniflorum*. *Spectrochim. Acta Part A* **2012**, *85*, 99–104.
41. Edison, T.J.I.; Sethuraman, M.G. Instant green synthesis of silver nanoparticles using *Terminalia chebula* fruit extract and evaluation of their catalytic activity on reduction of methylene blue. *Process Biochem.* **2012**, *47*, 1351–1357.
42. Mohan Kumar, K.; Mandal, B.K.; Sinha, M.; Krishnakumar, V. *Terminalia chebula* mediated green and rapid synthesis of gold nanoparticles. *Spectrochim. Acta Part A* **2012**, *86*, 490–494.
43. Stephen, A.; Seethalakshmi, S. Phytochemical synthesis and preliminary characterization of silver nanoparticles using hesperidin. *J. Nanosci.* **2013**, doi:10.1155/2013/126564.
44. Sahu, N.; Soni, D.; Chandrashekhar, B.; Satpute, D.B.; Saravanadevi, S.; Sarangi, B.K.; Pandey, R.A. Synthesis of silver nanoparticles using flavonoids: Hesperidin, naringin and diosmin, and their antibacterial effects and cytotoxicity. *Int. Nano Lett.* **2016**, *6*, 173–181.
45. Bisht, S.; Feldmann, G.; Soni, S.; Ravi, R.; Karikar, C.; Maitra, A.; Maitra, A. Polymeric nanoparticle-encapsulated curcumin ('nanocurcumin'): A novel strategy for human cancer therapy. *J. Nanobiotechnol.* **2007**, *5*, 1–18.
46. Khaleel, S.; Govindaraju, K.; Manikandan, R.; Seog, J.; Young, E.; Singaravelu, G. Phytochemical mediated gold nanoparticles and their PTP 1B inhibitory activity. *Colloids Surf. B Biointerfaces* **2010**, *75*, 405–409.
47. Castellano, J.M.; Guinda, A.; Delgado, T.; Rada, M.; Cayuela, J.A. Biochemical Basis of the Antidiabetic Activity of Oleanolic Acid and Related Pentacyclic Triterpenes. *Diabetes* **2013**, *62*, 1791–1799.
48. Shamprasad, B.R.; Keerthana, S.; Megarajan, S.; Lotha, R.; Aravind, S.; Veerappan, A. Photosynthesized escin stabilized gold nanoparticles exhibit anti-diabetic activity in L6 rat skeletal muscle cells. *Mater. Lett.* **2019**, *241*, 198–201.
49. Dong, Y.; Wan, G.; Yan, P.; Qian, C.; Li, F.; Peng, G. Biology fabrication of resveratrol coated gold nanoparticles and investigation of their effect on diabetic retinopathy in streptozotocin induced diabetic rats. *J. Photochem. Photobiol. B Biol.* **2019**, *195*, 51–57.

50. Rajarajeshwari, T.; Shivashri, C.; Rajasekar, P. Synthesis and characterization of biocompatible gymnemic acid—Gold nanoparticles: A study on glucose uptake stimulatory effect in 3T3-L1 adipocytes. *RSC Adv.* **2014**, *4*, 63285.
51. Bhumkar, D.R.; Joshi, H.M.; Sastry, M.; Pokharkar, V.B. Chitosan reduced gold nanoparticles as novel carriers for transmucosal delivery of insulin. *Pharm. Res.* **2007**, *24*, 1415–1426.
52. Cho, H.J.; Oh, J.; Choo, M.K.; Ha, J.I.; Park, Y.; Maeng, H.J. Chondroitin sulfate-capped gold nanoparticles for the oral delivery of insulin. *Int. J. Biol. Macromol.* **2014**, *63*, 15–20.
53. Dubey, K.; Anand, B.G.; Badhwar, R.; Bagler, G. Tyrosine and tryptophan coated gold nanoparticles inhibit amyloid aggregation of insulin. *Amino Acids* **2015**, *47*, 2551–2560.
54. Khoshnamvand, M.; Ashtiani, S.; Huo, C.; Saeb, S.P.; Liu, J. Use of *Alcea rosea* leaf extract for biomimetic synthesis of gold nanoparticles with innate free radical scavenging and catalytic activities. *J. Mol. Struct.* **2019**, *1179*, 749–755.
55. Pu, S.; Li, J.; Sun, L.; Zhong, L.; Ma, Q. An *in vitro* comparison of the antioxidant activities of chitosan and green synthesized gold nanoparticles. *Carbohydr. Polym.* **2019**, *211*, 161–172.
56. Torabi, N.; Nowrouzi, A.; Ahadi, A.; Vardasbi, S.; Etesami, B. Green synthesis of gold nanoclusters using seed aqueous extract of *Cichorium intybus L.* and their characterization. *SN Appl. Sci.* **2019**, *1*, 981.
57. Nakkala, J.R.; Bhagat, E.; Suchiang, K.; Sadras, S.R. Comparative study of antioxidant and catalytic activity of silver and gold nanoparticles synthesized from *Costus pictus* leaf extract. *J. Mater. Sci. Technol.* **2015**, *31*, 986–994.
58. Benedec, D.; Oniga, I.; Cuibus, F.; Sevastre, B.; Stiufiuc, G.; Duma, M.; Lucaciu, C.M. *Origanum vulgare* mediated green synthesis of biocompatible gold nanoparticles simultaneously possessing plasmonic, antioxidant and antimicrobial properties. *Int. J. Nanomed.* **2018**, *13*, 1041-1058.
59. Zhaleh, M.; Zangeneh, A.; Goorani, S.; Seydi, N.; Zangeneh, M.M.; Tahvilian, R.; Pirabbasi, E. *In vitro* and *in vivo* evaluation of cytotoxicity, antioxidant, antibacterial, antifungal, and cutaneous wound healing properties of gold nanoparticles produced via a green chemistry synthesis using *Gundelia tournefortii L.* as a capping and reducing agent. *Appl. Organomet. Chem.* **2019**, *33*, e5015.
60. Patil, M.P.; Seo, Y.B.; Lim, H.K.; Kim, G.D. Biofabrication of gold nanoparticles using *Agrimonia pilosa* extract and their antioxidant and cytotoxic activity. *Green Chem. Lett. Rev.* **2019**, *12*, 208–216.

61. Veena, S.; Devasena, T.; Sathak, S.S.M.; Ysasve, M.; Vishal, L.A. Green Synthesis of gold nanoparticles from *Vitex negundo* leaf extract: Characterization and *in vitro* evaluation of antioxidant-antibacterial activity. *J. Clust. Sci.* **2019**, *30*, 1591–1597.
62. Bharathi, D.; Bhuvaneshwari, V. Evaluation of the cytotoxic and antioxidant activity of phyto-synthesized silver nanoparticles using *Cassia angustifolia* flowers. *J. Bionanosci.* **2019**, *9*, 155–163.
63. Zayed, M.F.; Mahfoze, R.A.; El-kousy, S.M.; Al-Ashkar, E.A. *In-vitro* antioxidant and antimicrobial activities of metal nanoparticles biosynthesized using optimized *Pimpinella anisum* extract. *Colloid Surf. A Phys. Eng.* **2020**, *585*, 124167.
64. Aremu, A.O.; Amoo, S.O.; Ndhlala, A.R.; Finnie, J.F.; Van Staden, J. Antioxidant activity, acetylcholinesterase inhibition, iridoid content and mutagenic evaluation of *Leucosidea sericea*. *Food Chem. Toxicol.* **2011**, *49*, 1122–1128.
65. Pendota, S.C.; Aremu, A.O.; Slavětínská, L.P.; Rárová, L.; Grúz, J.; Doležal, K.; Van Staden, J. Identification and characterization of potential bioactive compounds from the leaves of *Leucosidea sericea*. *J. Ethnopharmacol.* **2018**, *220*, 169–176.
66. Nair, J.J.; Aremu, A.O.; Van Staden, J. Anti-inflammatory effects of *Leucosidea sericea* (Rosaceae) and identification of the active constituents. *S. Afr. J. Bot.* **2012**, *80*, 75–76.
67. Mafole, T.C.; Aremu, A.O.; Mthethwa, T.; Moyo, M. An overview on *Leucosidea sericea* Eckl. & Zeyh.: A multi-purpose tree with potential as a phytomedicine. *J. Ethnopharmacol.* **2017**, *203*, 288–303.
68. Adamu, M.; Mukandiwa, L.; Awouafack, M.D.; Ahmed, A.S.; Eloff, J.N.; Naidoo, V. Ultrastructure changes induced by the phloroglucinol derivative agrimol G isolated from *Leucosidea sericea* in *Haemonchus contortus*. *Exp. Parasitol.* **2019**, *207*, 107780.
69. Sharma, R.; Kishore, N.; Hussein, A.; Lall, N. The potential of *Leucosidea sericea* against *Propionibacterium acnes*. *Phytochem. Lett.* **2014**, *7*, 124–129.
70. Bosman, A.A.; Combrinck, S.; Roux-Van der Merwe, R.; Botha, B.M.; McCrindle, R.I.; Houghton, P.J. Isolation of an anthelmintic compound from *Leucosidea sericea*. *S. Afr. J. Bot.* **2004**, *70*, 509–511.
71. Stander, M.A.; Van Wyk, B.E.; Taylor, M.J.; Long, H.S. Analysis of phenolic compounds in rooibos tea (*Aspalathus linearis*) with a comparison of flavonoid-based compounds in natural populations of plants from different regions. *J. Agric. Food Chem.* **2017**, *65*, 10270–10281.
72. Elbagory, A.M.; Meyer, M.; Cupido, C.N.; Hussein, A.A. Inhibition of bacteria associated with wound infection by biocompatible green synthesized gold nanoparticles from South African plant extracts. *Nanomaterials* **2017**, *7*, 417–438.

73. Ademiluyi, A.O.; Oboh, G. Experimental and toxicologic pathology soybean phenolic-rich extracts inhibit key-enzymes linked to type 2 diabetes ( $\alpha$ -amylase and  $\alpha$ -glucosidase) and hypertension (angiotensin I converting enzyme) *in vitro*. *Exp. Toxicol. Pathol.* **2013**, *65*, 305–309.
74. Jeremia, L. Inhibitory effects of five medicinal plants on rat alpha-glucosidase: Comparison with their effects on yeast alpha-glucosidase. *J. Med. Plant Res.* **2014**, *5*, 2863–2867.
75. Ranjan Sarker, S.; Polash, S.A.; Boath, J.; Kandjani, A.E.; Poddar, A.; Dekiwadia, C.; Bhargava, S.K. Functionalization of elongated tetrahedral Au nanoparticles and their antimicrobial activity assay. *ACS Appl. Mater. Interfaces* **2019**, *11*, 13450–13459.
76. Salar, R.K.; Certik, M.; Brezova, V. Modulation of phenolic content and antioxidant activity of maize by solid state fermentation with *Thamnidium elegans* CCF 1456. *Biotechnol. Bioprocess Eng.* **2012**, *17*, 109–116.
77. Arts, M.J.; Haenen, G.R.; Voss, H.P.; Bast, A. Antioxidant capacity of reaction products limits the applicability of the trolox equivalent antioxidant capacity (TEAC) assay. *Food Chem. Toxicol.* **2004**, *42*, 45–49.
78. Re, R.; Pellegrini, N.; Proteggente, A.; Pannala, A.; Yang, M.; Rice-Evans, C. Antioxidant activity applying an improved ABTS radical cation decolourization assay. *Free Radic. Biol. Med.* **1999**, *26*, 1231–1237.
79. Raveendran, P.; Fu, J.; Wallen, S.L. Completely 'Green' synthesis and stabilization of metal nanoparticles. *J. Am. Chem. Soc.* **2003**, *125*, 13940–13941.
80. Hwang, S.J.; Jun, S.H.; Park, Y.; Cha, S.H.; Yoon, M.; Cho, S.; Lee, H.J.; Park, Y. Green synthesis of gold nanoparticles using chlorogenic acid and their enhanced performance for inflammation. *Nanomedicine: Nanotechnology, Biology and Medicine*, **2015**, *11*(7), 1677-1688.
81. Gomes, J.F.; Garcia, A.C.; Ferreira, E.B.; Pires, C.; Oliveira, V.L.; Tremiliosi-Filho, G.; Gasparotto, L.H. New insights into the formation mechanism of Ag, Au and Ag/Au nanoparticles in aqueous alkaline media: Alkoxides from alcohols, aldehydes and ketones as universal reducing agents. *Phys. Chem. Chem. Phys.* **2015**, *17*, 21683–21693, doi:10.1039/C5CP02155C.
82. Podstawczyk, D.; Pawłowska, A.; Bastrzyk, A.; Czeryba, M.; Oszmianski, J. Reactivity of (+)-Catechin with Copper (II) Ions: The Green Synthesis of Size-Controlled Sub-10 nm Copper Nanoparticles. *ACS Sustainable Chemistry & Engineering*, **2019**, *7*(20), 17535-17543.
83. Elbagory, A.M.; Cupido, C.N.; Meyer, M.; Hussein, A.A. Large scale screening of southern African plant extracts for the green synthesis of gold nanoparticles using microtitre-plate method. *Molecules* **2016**, *21*, 1498-1517.

84. Elia, P.; Zach, R.; Hazan, S.; Kolusheva, S.; Porat, Z.; Zeiri, Y. Green synthesis of gold nanoparticles using plant extracts as reducing agents. *Int. J. Nanomed.* **2014**, *9*, 4007–4021.
85. Chen, R.; Wu, J.; Li, H.; Cheng, G.; Lu, Z.; Che, C.M. Fabrication of gold nanoparticles with different morphologies in HEPES buffer. *Rare Metals* **2010**, *29*, 180–186.
86. Foss, C.A.; Hornyak, G.L.; Stockert, J.A.; Martin, C.R. Template-synthesized nanoscopic gold particles: Optical spectra and the effects of particle size and shape. *J. Phys. Chem.* **1994**, *98*, 2963–2971.
87. Fang, C.; Ma, Z.; Chen, L.; Li, H.; Jiang, C.; Zhang, W. Biosynthesis of gold nanoparticles, characterization and their loading with zonisamide as a novel drug delivery system for the treatment of acute spinal cord injury. *J. Photochem. Photobiol. B Biol.* **2019**, *190*, 72–75.
88. Tomaszewska, E.; Soliwoda, K.; Kadziola, K.; Tkacz-Szczesna, B.; Celichowski, G.; Cichomski, M.; Szmaja, W.; Grobelny, J. Detection limits of DLS and UV-Vis spectroscopy in characterization of polydisperse nanoparticles colloids. *Journal of Nanomaterials*, **2013**.
89. Mourdikoudis, S.; Pallares, R. M.; Thanh, N. T. Characterization techniques for nanoparticles: comparison and complementarity upon studying nanoparticle properties. *Nanoscale*, **2018**, *10*(27), 12871-12934.
90. Krishnamurthy, S.; Esterle, A.; Sharma, N.C.; Sahi, S.V. Yucca-derived synthesis of gold nanomaterial and their catalytic potential. *Nanoscale Res. Lett.* **2014**, *9*, 627-635.
91. Brewer, S.H.; Glomm, W.R.; Johnson, M.C.; Knag, M.K.; Franzen, S. Probing BSA binding to citrate-coated gold nanoparticles and surfaces. *Langmuir* **2005**, *21*, 9303–9307.
92. Xue, W.; Zhang, G.; Zhang, D. A sensitive colorimetric label-free assay for trypsin and inhibitor screening with gold nanoparticles. *Analyst*, **2011**, *136*(15), 3136-3141.
93. Vilela, D.; González, M. C.; Escarpa, A. Sensing colorimetric approaches based on gold and silver nanoparticles aggregation: chemical creativity behind the assay. A review. *Analytica chimica acta*, **2012**, *751*, 24-43.
94. Li, L.; Li, B.; Cheng, D.; Mao, L. Visual detection of melamine in raw milk using gold nanoparticles as colorimetric probe. *Food Chemistry*, **2010**, *122*(3), 895-900.
95. Wang, X.; Xu, Y.; Chen, Y.; Li, L.; Liu, F.; Li, N. The gold-nanoparticle-based surface plasmon resonance light scattering and visual DNA aptasensor for lysozyme. *Analytical and bioanalytical chemistry*, **2011**, *400*(7), 2085-2091.
96. Kim, J. H.; Chung, B. H. Naked eye detection of mutagenic DNA photodimers using gold nanoparticles. *Biosensors and Bioelectronics*, **2011**, *26*(5), 2805-2809.



97. Nune, S.K.; Chanda, N.; Shukla, R.; Katti, K.; Kulkarni, R.R.; Thilakavathy, S.; Mekapothula, S.; Kannan, R.; Katti, K.V. Green nanotechnology from tea: phytochemicals in tea as building blocks for production of biocompatible gold nanoparticles. *Journal of materials chemistry*, **2009**, *19*(19), 2912-2920.
98. Kattumuri, V.; Katti, K.; Bhaskaran, S.; Boote, E.J.; Casteel, S.W.; Fent, G.M.; Robertson, D.J.; Chandrasekhar, M.; Kannan, R.; Katti, K.V. Gum arabic as a phytochemical construct for the stabilization of gold nanoparticles: in vivo pharmacokinetics and X-ray-contrast-imaging studies. *Small*, **2007**, *3*(2), 333-341.
99. Thilagam, E.; Parimaladevi, B.; Kumarappan, C.; Mandal, S.C.  $\alpha$ -Glucosidase and  $\alpha$ -Amylase inhibitory activity of *Senna surattensis*. *J. Acupunct. Meridian Stud.* **2013**, *6*, 24–30.
100. Sofowora, A.; Ogunbodede, E.; Onayade, A.; Dentistry, C. The role and place of medicinal plants in the strategies for disease. *J. Afr. Tradit. Complement.* **2013**, *10*, 210–229.
101. Etsassala, N.G.; Badmus, J.A.; Waryo, T.T.; Marnewick, J.L.; Cupido, C.N.; Hussein, A.A.; Iwuoha, E.I. Alpha-glucosidase and alpha-amylase inhibitory activities of novel abietane diterpenes from *Salvia africana-lutea*. *Antioxidants* **2019**, *8*, 421-432.
102. Coman, C.; Rugină, O.D.; Socaciu, C. Plants and natural compounds with antidiabetic action. *Not. Bot. Horti Agrobo* **2012**, *40*, 314–325.
103. Niikura, K.; Matsunaga, T.; Suzuki, T.; Kobayashi, S.; Yamaguchi, H.; Orba, Y.; Sawa, H. Gold nanoparticles as a vaccine platform: Influence of size and shape on immunological responses *in vitro* and *in vivo*. *ACS Nano* **2013**, *7*, 3926–3938.
104. Virk, P. Anti-diabetic activity of green gold-silver nanocomposite with *Trigonella foenum graecum* L. seeds extract on streptozotocin-induced diabetic rats. *Pak. J. Zool.* **2018**, *50*, 711-718.
105. Perez-Fons, L.; Garzón, M.T.; Micol, V. Relationship between the antioxidant capacity and effect of rosemary (*Rosmarinus officinalis* L.) polyphenols on membrane phospholipid order. *J. Agric. Food Chem.* **2009**, *58*, 161–171.
106. Duletić-Laušević, S.; Aradski, A.A.; Kolarević, S.; Vuković-Gačić, B.; Oalde, M.; Živković, J.; Šavikin, K.; Marin, P.D. Antineurodegenerative, antioxidant and antibacterial activities and phenolic components of *Origanum majorana* L. (*Lamiaceae*) extracts. *J. Appl. Bot. Food Qual.* **2018**, *91*, 126–134.
107. BarathManiKanth, S.; Kalishwaralal, K.; Sriram, M.; Pandian, S.R.K.; Youn, H.S.; Eom, S.; Gurunathan, S. Anti-oxidant effect of gold nanoparticles restrains hyperglycemic conditions in diabetic mice. *J. Nanobiotechnol.* **2010**, *8*, 16-30.

108. Ajitha, B.; Reddy, Y.A.K.; Reddy, P.S. Enhanced antimicrobial activity of silver nanoparticles with controlled particle size by pH variation. *Powder Technol.* **2015**, *269*, 110–117.
109. Vinosha, M.; Palanisamy, S.; Muthukrishnan, R.; Selvam, S.; Kannapiran, E.; You, S.; Prabhu, N.M. Biogenic synthesis of gold nanoparticles from *Halymenia dilatata* for pharmaceutical applications: Antioxidant, anti-cancer and antibacterial activities. *Process Biochem.* **2019**, *85*, 219–229.

## CHAPTER FOUR

### **Biosynthesis, Characterization, and Biological Activities of Procyanidin Capped Silver Nanoparticles**

Umar M. Badeggi <sup>1,†</sup>, Jelili A. Badmus <sup>2,#</sup>, Subelia S. Botha <sup>3</sup>, Enas Ismail <sup>1,‡</sup>, Jeanine L. Marnewick <sup>2</sup>, Charlene W. J. Africa <sup>4</sup> and Ahmed A. Hussein <sup>1,\*</sup>

<sup>1</sup> Department of Chemistry, Cape Peninsula University of Technology, Symphony Rd. Bellville 7535, South Africa; 217064221@mycput.ac.za (U.M.B.); enas.ismail4@yahoo.com (E.I.)

<sup>2</sup> Applied Microbial and Health Biotechnology Institute, Cape Peninsula University of Technology, Symphony Rd. Bellville 7535, South Africa; jabadmus@lautech.edu.ng (J.A.B.); marnewickj@cput.ac.za (J.L.M.)

<sup>3</sup> Electron Microscope Unit, University of the Western Cape, Bellville 7535, South Africa; subotha@uwc.ac.za (S.S.B.)

<sup>4</sup> Department of Medical Biosciences, University of the Western Cape, Bellville, 7535, South Africa; cafrica@uwc.ac.za (C.W.J.A)

\* Correspondence: mohammedam@cput.ac.za (A.A.H); Tel.: +27-21-959-6193; Fax: +27-21-959-3055

† Permanent address: Department of Chemistry, Ibrahim Badamasi Babangida University Lapai, PMB 11, Minna, 4947, Niger State, Nigeria.

‡ Permanent address: Physics Department, Faculty of Science (Girls branch), Al Azhar University, Nasr city, Cairo, Egypt, 11884.

# Permanent address: Department of Biochemistry, Ladoke Akintola University of Technology, Ogbomoso, 210214, Nigeria.

## Abstract

In this study, procyanidin dimers and *Leucosidea sericea* total extract (LSTE) were employed in the synthesis of silver nanoparticles (AgNPs) and characterized by ultraviolet-visible (UV-Visible) spectroscopy, high-resolution transmission electron microscopy (HRTEM), selected area electron diffraction (SAED), x-ray diffraction (XRD), and dynamic light scattering (DLS) techniques. AgNPs of about 2–7 nm were obtained. DLS and stability evaluations confirmed that the AgNPs/procyanidins conjugates were relatively stable. The nanoparticles exhibited good inhibitory activities against the two enzymes studied. The IC<sub>50</sub> values against the amylase enzyme were 14.92 ± 1.0, 13.24 ± 0.2, and 19.13 ± 0.8 µg/mL for AgNPs coordinated with LSTE, F1 and F2, respectively. The corresponding values for the glucosidase enzyme were 21.48 ± 0.9, 18.76 ± 1.0, and 8.75 ± 0.7 µg/mL. The antioxidant activities were comparable to those of the intact fractions. The AgNPs also demonstrated bacterial inhibitory activities against six bacterial species. While the minimum inhibitory concentrations (MIC) of F1-AgNPs against *Pseudomonas aeruginosa* and *Staphylococcus aureus* were 31.25 and 15.63 µg/mL respectively, those of LSTE-AgNPs and F2-AgNPs against these organisms were both 62.50 µg/mL. The F1-AgNPs demonstrated a better bactericidal effect and may be useful in food packaging. This research also showed the involvement of the procyanidins as reducing and capping agents in the formation of AgNPs with potential biological applications.

**Keywords:** biosynthesis; procyanidins dimers; *Leucosidea sericea*; silver nanoparticles; phytoconstituents; antimicrobial; antidiabetic; antioxidant

## 4.1 Introduction

Metallic nanoparticles are of great interest owing to their unique physicochemical characteristics as well as their potential biomedical applications [1]. The characteristic properties of metallic nanoparticles (MNPs) such as silver nanoparticles (AgNPs) depend on the methods of preparation and the nature of precursors [1]. Physical methods [2-3] have been used to prepare AgNPs. They are, however, not cost-effective, consume high amount of energy and involve the use of sophisticated instruments [4]. Through the chemical procedures, reducing agents such as hydrazine have been employed in the formation of MNPs [1]. Although the nanoparticles possess interesting characteristic features, they have limited biological applications due to toxicity concerns [5]. Their stability is usually enhanced with the use of external stabilizers, some of which are also toxic [6]. Using biological resources to synthesize AgNPs, among which plants are more

popular [7-9], could eliminate the toxicity problem. Plants are readily accessible, non-toxic, and can be easily handled [10]. Plants also possess phytochemicals, serving not only as reducing but also as capping agents making the synthesis a facile process [11].

Several AgNPs have been successfully biosynthesized using various plant extracts such as *Nigella arvensis* L [12], *Pelargonium graveolens* [13], *Theobroma cacao* and *Vitis vinifera* seed [14], *Putranjiva roxburghii* [15], *Combretum erythrophyllum* [16], and *Ducrosia anethifolia* [17]. An array of spectroscopic and microscopic techniques have been employed to characterize the AgNPs [11, 13, 15-16, 18]. In these extracts, phytoconstituents such as polyphenols are believed to be responsible for the reduction and stabilization of the AgNPs. To identify them, Fourier-transform infrared (FTIR) spectroscopy was employed [19] in addition to nuclear magnetic resonance (NMR) spectroscopy [20] and high-performance liquid chromatography coupled with mass detector (LC-MS) [21]. Fractions or pure natural compounds have also been used in the green synthesis of nanoparticles [22] and examples include tannic acid [23], quercetin, gallic acid [24] and other compounds [25-26]. Green synthesis is the preferred procedure for the formation of biocompatible nanoparticles [27]. However, better knowledge of the chemical composition of the extracts or fractions is necessary to further understand the role of phytochemicals either as the reducing or capping agent or both. Moreover, little is known about procyanidins in higher plants and their reducing/capping abilities in green synthesis. This was one of the aims of the present study.

Furthermore, biosynthesized AgNPs prepared from the chemical constituents of various plant extracts and compounds have shown potent antioxidant [28-29], antidiabetic [30-33] and antibacterial [34] activities. However, further studies are necessary on these greener alternatives.

*Leucosidea sericea* Eckl and Zeyh is an evergreen shrub that belongs to the family *Rosaceae*. Nine out of its 3000 species are found in South Africa and its neighboring countries. Commonly called "old wood," the plant grows on both dry and wetlands. It has a silvery, woody bark and can be up to 7 m in height [35]. The extract from this plant has been used to cure many ailments and has proven biological properties [36-37]. A number of compounds have been isolated from the extract of *L. sericea* and showed various bio-activities [35, 38-39]. The mentioned traits awaken the curiosity to further investigate this wonder plant. Recently, our group identified procyanidins in the extract for the first time [40]. Procyanidins are a higher class of polyphenols with unique chemical structure and mostly occur in fruits and vegetables. Because of the abundant presence in fruits, legumes, cereals and a variety of beverages, procyanidins represent up to 50% of dietary polyphenols we consume daily [42]. In fact, the quality of raw materials used as food

depends largely on phenolic compounds such as procyanidins [41]. These procyanidins have displayed diverse biological activities and their polyphenolic nature may offer them enhanced biochemical activities [43-44]. Recent studies reported an increase of bioavailability for the flavonoid epigallocatechin gallate when capped with metal NPs [45] and this may be applicable to procyanidins as well. The unique chemical structure of procyanidins have also rendered them excellent reducing and capping agents [40], that have the capability to synthesize stable, safe and bio-active metal nanoparticles with possible future medical applications. In the same context and to avoid using toxic ingredients, the present study employed highly purified procyanidin dimers and fractions for the formation of stable and bioactive AgNPs. Their potential antioxidant, antidiabetic, and antimicrobial properties were evaluated and a detailed mechanism on the involvement of procyanidins in the formation of AgNPs was proposed.

## **4.2 Materials and Methods**

### **4.2.1 Materials and chemicals**

Polystyrene 96-well microtitre plates were supplied by Greiner bio-one GmbH (Frickhausen, Baden-Württemberg, Germany). Silver nitrate, iron (III) chloride hexahydrate, 2,4,6-tris(2-pyridyl)-s-triazine, hydrochloric acid (HCl), alpha-glucosidase (*Saccharomyces cerevisiae*), alpha-amylase (procaine pancreas), 3,5-dinitro salicylic acid (DNS), *p*-nitrophenyl- $\alpha$ -D-glucopyranoside (*p*-NPG), sodium carbonate (Na<sub>2</sub>CO<sub>3</sub>), sodium dihydrogen phosphate, Ampicillin, disodium hydrogen phosphate, trolox (6-hydroxyl-2, 5, 7, 8- tetramethylchroman-2-carboxylic acid), 2,2-azino-bis (3-ethylbenzothiazoline-6-sulfonic acid) (ABTS) diammonium salt, iodinitrotetrazolium chloride (INT), potassium peroxodisulphate, gallic acid, ascorbic acid, and sodium chloride (NaCl) were bought from Sigma-Aldrich (Cape Town, Western Cape, South Africa). N-Acetyl-L-cysteine (CYS), glycine (GLY), and Folin-Ciocalteu's phenol reagent (FC) were procured from Boehringer Mannheim GmbH (Mannheim, Baden-Württemberg, Germany). Phosphate buffered saline (PBS) was purchased from Lonza (Cape Town, Western Cape, South Africa). Bovine serum albumin (BSA) was procured from Miles Laboratories (Pittsburgh, PA, USA). Brain-heart infusion broth (BHI) and Mueller-Hinton Agar were purchased from Biolab (Merck, Modderfontein, South Africa).

#### **4.2.2 Characterisation**

A microtitre plate reader (BMG Labtech, Ortenberg, Germany) was employed in reading the absorbance of the AgNPs and in biological studies. A high-resolution transmission electron microscope (FEI Tecnai G2 F20 S-Twin HRTEM, operated at 200 kV) was used to study the morphology of the AgNPs. X-ray diffraction (XRD; Bruker AXS D8 advance diffractometer with CuK $\alpha$ 1 radiation ( $\lambda = 1.5406 \text{ \AA}$ ) was employed to study the crystallinity of the particles. A Malvern Zetasizer Instrument (Malvern Ltd., Worcestershire, United Kingdom) was used for DLS examinations.

#### **4.2.3 Extraction of phytochemicals and formation of Silver nanoparticles**

##### **4.2.3.1 Extraction and purification of chemical constituents**

The aerial parts of *Leucosidea sericea* were extracted with 50% aqueous-ethanol to render the total extract (referred to as LSTE). A portion of the total extract was partitioned in ethyl acetate and subsequently purified using different chromatographic techniques [40]. Briefly, silica gel column chromatography was employed using a gradient of hexane and ethyl acetate of increasing polarity. The fractions containing procyanidins were further chromatographed on silica gel using isocratic ethyl acetate. The combined fractions from the above were then subjected to smaller column (3  $\times$  30 cm) chromatography using sephadex using methanol/water (90:10 and/or 80-20). The fraction(s) which demonstrated a single spot on the TLC were submitted for NMR analysis to further confirm the purity. These fractions were labelled F1 and F2 and submitted for both NMR and LC-MS analyses. The spectra revealed the presence of procyanidins in F1 and F2.

##### **4.2.3.2 Biosynthesis of silver nanoparticles**

The synthesis of AgNPs was done by dissolving 20 mg of the aerial part extract (LSTE), F1, or F2 in 2 mL of deionized Milli-Q water and vortexing for 5 min. The resulting yellowish solution was then added to a 70 mL of 1.0 mM silver nitrate solution at 70 °C. After 10 min, a colour change was observed from yellowish to brown, which confirmed the successful synthesis of AgNPs. The reaction was monitored with absorbance reading (300–650 nm) until no further changes were noticed. The heat was removed, and the reaction mixture stirred for another 1 h in the dark. The colloidal solutions were allowed to cool to room temperature before several washing centrifuge steps. This was done to remove any unreacted substances that may still be in the solution.

### 4.3 Stability Evaluation of AgNPs

The procedure of Elbagory et al. [46] was adopted with minor adjustments. Briefly, 0.5% (NaCl, CYS, GLY, and BSA), deionized water, and PBS (pH 7 and 9) were used. The evaluation was carried out in a 96-well plate where the colloidal solution and the freshly prepared media and buffers were added. For every 160  $\mu\text{L}$  of the colloidal solution, a volume of 80  $\mu\text{L}$  of the above solutions was added in a different well. This was manually agitated for proper mixing and the absorbance immediately measured. This was termed as the zero-hour reading. The plate was then covered, wrapped in aluminum foil, and incubated at 37 °C for 24 h. After 24 h, another measurement was then taken and the plate was returned to the oven for an additional 24 h. At the end of this time, the 48 h reading was taken. This process was followed for each of the three (LSTE, F1, and F2) AgNPs.

### 4.4 Dilution study

The sample of AgNPs in the powdered form was obtained as reported by Badeggi and colleagues [40]. Briefly, 15 mL of the sample was freeze-dried in a falcon tube after several washing and centrifugation steps. 300  $\mu\text{L}$  of the synthesized AgNPs were measured at different concentrations. The concentrations were also plotted alongside the intensity to understand the linearity of the readings.

### 4.5 In-vitro Enzymatic assay

#### 4.5.1 Alpha-amylase inhibitory activity

A standard protocol was employed where 50  $\mu\text{L}$  of phosphate buffer (0.01 M, pH 6.9), 20  $\mu\text{L}$  of procaine pancreatic alpha-amylase (2U/mL) solution, and 20  $\mu\text{L}$  of the samples were all added in a 96-well plate and incubated for 20 min at room temperature [47]. After this pre-incubation, 20  $\mu\text{L}$  of 1% soluble starch was added to the mixture and incubated for an additional 30 min. This was immediately followed by the addition of 100  $\mu\text{L}$  of 3,5-dinitro salicylic acid (DNS) which stopped the reaction. The reaction mixture was then incubated in a boiling water bath for 10 min before the absorbance was read at 540 nm. Acarbose was used as the standard and each experiment was done in triplicate. Equation (1) was used to calculate the percentage inhibition of the alpha-amylase activity.

$$\text{Percentage inhibition (\%)} = \left( C - \frac{T}{C} \right) * 100 \quad (1)$$



where C and T are absorbance readings of the control and the treated sample, respectively.

#### **4.5.2 Alpha-glucosidase inhibitory activity**

A standard procedure of the alpha-glucosidase assay was followed with slight modification [30]. Briefly, 20 µg/mL of the three AgNP samples was serially diluted in a 96-well plate using a 100 mM phosphate buffer (PBS) at pH 6.8. The mixture was gently agitated and allowed to stand for 15 min at 25 °C. Thereafter, 20 µL of a 5 mM *p*-nitrophenyl- $\alpha$ -D-glucopyranoside (*p*-NPG) was added as the substrate and the plate was incubated at 37 °C for 20 min. Hereafter, 50 µL of a 0.1 M sodium carbonate (Na<sub>2</sub>CO<sub>3</sub>) solution was added to each well to stop the reaction. With the aid of a plate reader, the absorbance measurement was then taken at 540 nm. The wells with enzyme, buffer, and substrate but without samples served as positive controls and each experiment was conducted in triplicate. The percentage inhibition of the enzymatic property of alpha-glucosidase was determined using Equation (1) in Section 4.5.1.

#### **4.6 Antibacterial activity**

The protocol description of Elbagory et al. [46] was adopted with slight changes. Briefly, BHI was used for the serial dilution of the three AgNPs to include six concentrations, i.e., 125.00, 62.50, 31.25, 15.63, 7.81, and 3.90 µg/mL. The six bacterial test species *Pseudomonas aeruginosa*, *Staphylococcus aureus*, *Bacillus cereus*, *Salmonella enterica*, *Escherichia coli* and *Serratia marcescens* (in PBS) were standardized to 0.5 McFarland equivalents and further diluted in BHI. Three negative controls were included and consisted of (i) 200 µL BHI, (ii) 200 µL of sterilized deionized water, and (iii) a mixture of 100 µL of bacterial cells and 100 µL of sterilized deionized water. After 24 h incubation at 37 °C, 40 µL of INT was added and further incubated for 2 h before visualization for turbidity. All tests were done in triplicate. Ampicillin was employed as a positive control and the selected bacteria were wild types.

#### **4.7 Antioxidant activity**

##### **4.7.1 Ferric Reducing Antioxidant Power (FRAP) assay**

The FRAP assay was conducted by adding 10 µL of the sample as well as the standard (ascorbic acid) to a 96-well plate [48]. Thereafter, 300 µL of the FRAP reagent (3

mL of iron (III) chloride hexahydrate + 3 mL of 2,4,6-tris(2-pyridyl)-s-triazine + 30 mL of acetate buffer + 6 mL of water) was added to all the wells. The reaction mixture was allowed to stand for 30 min at room temperature before the absorbance reading was taken at 593 nm. This assay was done in triplicate and the results were expressed as mM ascorbic acid equivalents per Gram (mM AAE/g).

#### **4.7.2 Folin–Ciocalteu (FC) assay**

The procedure of Salari et al. [49] was adopted with slight changes. Briefly, 25  $\mu$ L of both the standard and the samples were added to a 96-well plate. The Folin–Ciocalteu's phenol reagent (125  $\mu$ L) was added followed by 100  $\mu$ L of Na<sub>2</sub>CO<sub>3</sub> solution. The plate was allowed to stand on the bench for 2 h at room temperature before the absorbance reading was taken at 765 nm. The experiment was conducted in triplicate and the results expressed in mM gallic acid equivalents per Gram (mM GAE/g).

#### **4.7.3 2,2'-azino-bis-3-ethylbenzotiazolin-6- sulfonic acid (ABTS) assay**

The method of Pu and co-workers [48] was adopted and slightly modified. In this experiment, 25  $\mu$ L of the standard (Trolox) and samples were added to a 96-well plate followed by the ABTS reagent. The reaction mixture was allowed to stand for 30 min before the absorbance was read at 734 nm. The ABTS reagent was prepared 30 min before the experiment at 70 °C. The assay was repeated two more times. The results were expressed as mM Trolox equivalents per Gram sample (mM TE/g).

### **4.8 Statistical analysis**

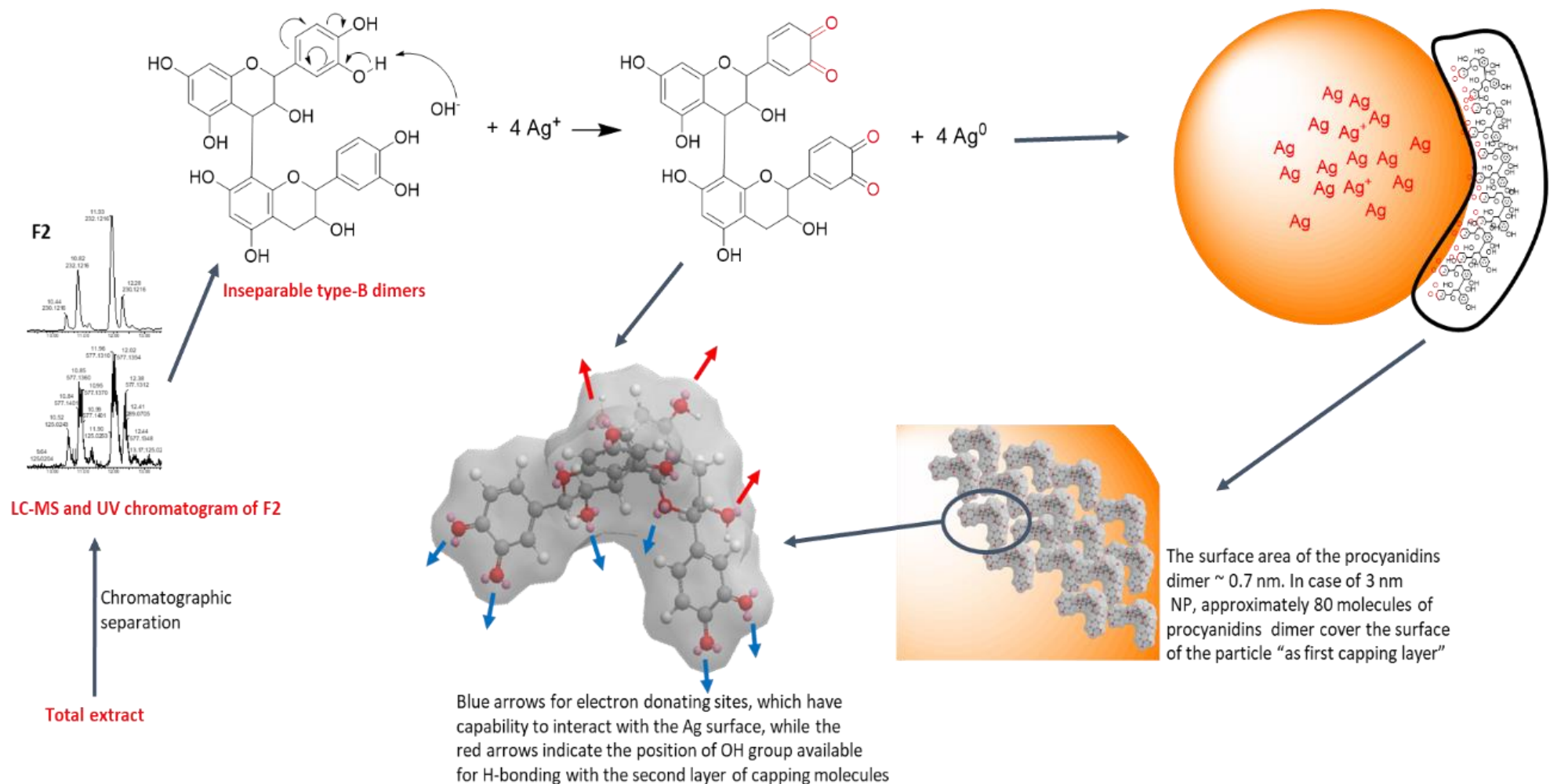
The results of the bioactivities were analysed using two-way ANOVA followed by post hoc Tukey's multiple comparisons test using GraphPad Prism software version 6.05 for Windows (GraphPad Software, La Jolla, CA, USA ([www.graphpad.com](http://www.graphpad.com))). The image analysis software ImageJ 1.50b version 1.8.0\_60 (<http://imagej.nih.gov/ij>) and Origin pro 2019 64 bits were used to analyse the TEM and XRD images.

## **4.9. Results and discussion**

### **4.9.1 Identification and mechanism of procyanidin-AgNPs formation**

In our previous work, nuclear magnetic resonance (NMR) spectroscopy and liquid chromatography-mass spectrometry (LC-MS) aided the identification of F2, F1 and LSTE

[40] contents. F1 showed a mixture of procyanidin dimers and trimers, while F2 showed a very pure isomeric structure of procyanidin dimers (type-B). On the other hand, the total extract (LSTE) showed, in addition to procyanidins dimers and trimers, small flavonoids, and phenolic acids. Taking the B-type procyanidin dimers as an example (fraction F2), the mechanism of formation of AgNPs is demonstrated (Scheme 1). Following the green synthesis protocols, the starting materials were dissolved in ultrapure water. As water ionizes into protons and hydroxyl ions, the  $\text{OH}^-$  abstracts a proton from one of the hydroxyl groups on the compound (e.g. procyanidin B3) and an alkoxide ion is generated. The alkoxide species then reduces the silver ion ( $\text{Ag}^+$ ) to  $\text{Ag}^0$ , thereby generating the NPs, and since the oxidation products depend on the alkoxide precursor, quinones are formed (Scheme 1) [50].



**Scheme 4.1: Proposed mechanism of procyanidin-mediated silver nanoparticles formation**

The proposed mechanisms were based on the following: Firstly, several polyphenols have been employed in Au- and AgNPs formation, the success of which has been ascribed to the presence of one or more hydroxyl groups [11, 20, 51-52]. Interestingly, procyanidins are poly-hydroxy compounds, confirming their suitability. In addition, to date, there has not been any report, as far as we know, on the successful fabrication of Au- or AgNPs using pure compounds without at least one hydroxyl functional group. Secondly, we hypothesized that alkoxide ions generated from the compounds are the chief reducing agents in the biosynthesis of AgNPs. This conclusion was made based upon potassium *tert*-butoxide being used as a reducing agent for the formation of Au and AgNPs through the green method. Upon the addition of *tert*-butoxide solution to gold and silver solutions, red and yellow colours appeared respectively [50]. Since the solution contained only K<sup>+</sup> and *tert*-butoxide ion, it is evident that the latter was responsible for the reduction. Similarly, phenolate (a phenoxide) has also been used in the synthesis of AgNPs [53]. One of the advantages of this proposal is that all -OH carrying compounds can generate alkoxide ions before transforming to ketones. This can be more generalized, as all 'reducing agents' must possess at least one -OH group.

Further, most of the molecules employed as capping agents possess high molecular weights in addition to at least one electro-negative element or group such as -NH<sub>2</sub>, -COOH, -SH, -OH, and -CO. It is, therefore, hypothesized that groups such as -CO and -OH, being part of the precursors, must have provided such stability. This is because the NPs were stable without the use of any external stabilizers. The procyanidins dimers (and trimers) have great potential as antioxidant agents because of the phenolic hydroxyls and ease of transferring an electron and H<sup>+</sup> to enzymes and/or metals. Because of the presence of stereogenic centres at C-2, C-3, and C-4, there are possible combinations for B-type dimers (different possibilities of interflavane bonds between C<sub>α/β</sub>-4 to C6/ C<sub>α/β</sub>-4 to C-8). In addition, there are different conformers for each of the B-type dimers, however the extended (where B-rings are facing each other) and compact (where B-rings are opposite each other) are the most dominant. In the case of O-dioxy derivatives, the compact conformer has the minimum energy since the intra-hydrogen bonding doesn't play an important role in the stabilization of the extended conformer [54]. Not all the procyanidin constituents were used in the formation of NPs. Therefore, the molecules in direct contact with the metal NPs, are most probably the dioxy derivatives. The second and even third capping layers can then be formed due to the inter-hydrogen bonding.

#### 4.9.2 UV-Visible Analysis

The result of UV-Visible analysis of (A) LSTE-, (B) F1-, and (C) F2-AgNPs are shown in Figure 1. The AgNPs exhibited surface plasmon resonance (SPR) bands between 424–432 nm, which confirmed the successful formation of the nanoparticles. A colour change was also observed within 10 min from yellowish to brownish (inset in Figure 1) when 1 mM silver nitrate ( $\text{AgNO}_3$ ) solution (D) was added, which indicated the successful synthesis of AgNPs. Hence, phytoconstituents in LSTE, F1, and F2, acted as reducing agents and thereafter as capping agents during the synthesis of the AgNPs. The similarity in the composition might have caused close SPR of the nanoparticles. No external capping agents were used, implying that the respective constituents served as both the reducing and capping agent. It is believed that polyphenols, abundantly available in plants, are responsible for the reduction of metal salts in NP synthesis [55]. In this case, procyanidins are undoubtedly responsible for the reduction and stabilization in both F1- and F2-AgNPs. The plasmonic resonance of AgNPs spans the range of 320–500 nm according to previous studies [56-57]. In this study, the SPR of the three AgNPs was observed to fall in the same range, which implies that the procyanidins with similar functional groups are the major contributing reducing and capping agents, even in the extract.

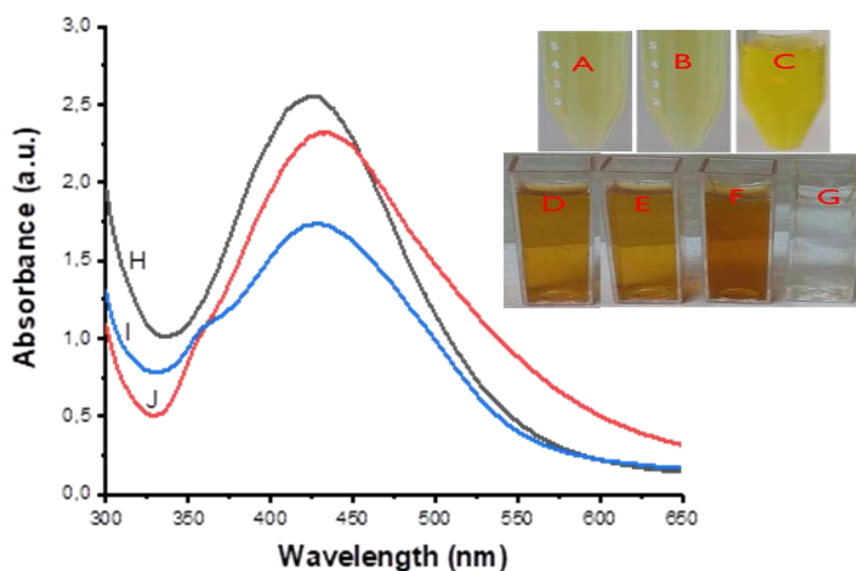


**Figure 4. 1: Letters (A-C) represents the colour of the fractions/extract before mixing with silver nitrate solution (G). Silver nanoparticles represented as (D), (E) and (F) corresponds to absorption spectra of (D) *Leucosidea sericea* total extract-, (E) F1-, and (F) F2-mediated silver nanoparticles.**

### 4.9.3 HRTEM Analysis

Figure 2A–F shows the HRTEM images, the corresponding particle size distributions, and SAED patterns of LSTE-, F1-, and F2-AgNPs. The average particle sizes were found to be  $7.8 \pm 2.9$ ,  $2.9 \pm 0.8$ , and  $3.3 \pm 1.2$  nm respectively. From the TEM micrograph, the LSTE-AgNPs (Figure 2A) presents agglomerates of silver nanoparticles. Other HRTEM images for the agglomerates was included in (Appendix J). The total extract used for the synthesis of the silver nanoparticles consist of phytochemicals of different chemical structure. The individual bioactive compound may interact with silver ions leading to the formation of nanoparticles of different shapes. Moreover, shape control for biological synthesis is still in its infancy [58]. Again, because of the interaction of other biomolecules such as capping agents with the surface of the synthesized nanoparticles, there is a high chance of particle aggregation. Although, quasi-spherical shapes were predominant for F1- and F2-AgNPs, there appeared the tendency for the silver nanoparticles to also agglomerates. The green synthesis of MNPs often results in nanoparticles of different shapes. The presence of a mixture of shapes is because of phytochemicals of different functional groups serving as reducing as well as stabilizing agents [59]. On the other hand, previous studies have shown that polyphenols in their pure forms often account for nanoparticles with spherical shapes, which were also observed in this study with F1- and F2-AgNPs [51, 60]. Similar shapes and sizes have also been reported by other researchers, in agreement with our findings [49, 61]. Figure 2(C, F, I) depict the selected area electron diffraction (SAED) patterns of LSTE-, F1-, and F2-AgNPs respectively. The brightly circular patterns indicate that the particles are polycrystalline and can be indexed to the (111), (200), (220), and (311) planes of a face-centred cubic (FCC) structure of silver [51].

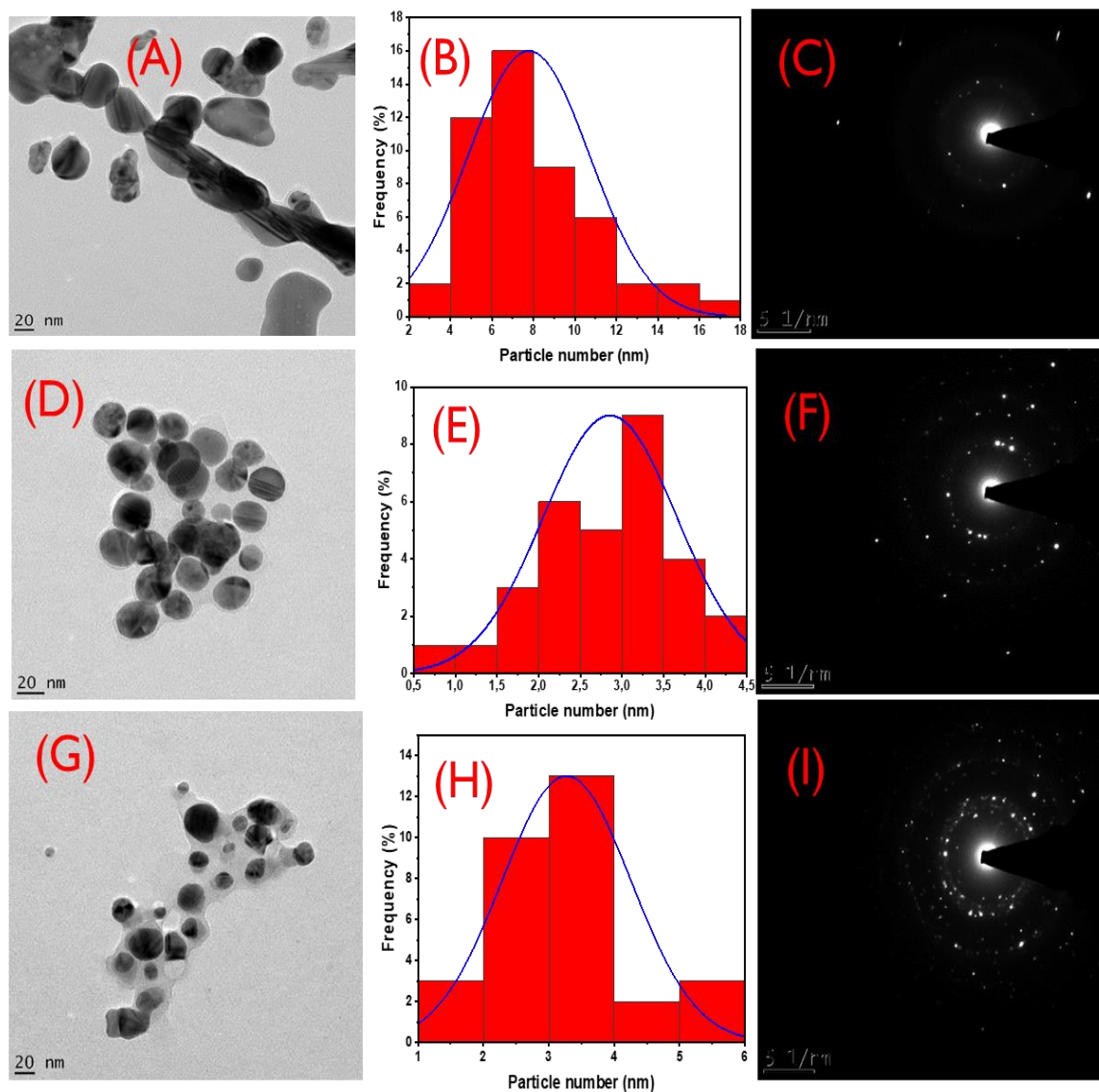


**Figure 4. 2: High-Resolution transmission electron microscopy images for *Leucosidea sericea* total extract -, F1-, and F2-mediated silver nanoparticles are represented as A, D, G and the corresponding particle size distributions as B, E, H respectively. The corresponding selected area electron diffraction pattern of the respective HRTEM images are represented as C, F, I**

#### 4.9.4 XRD Analysis

In order to study the crystal structure of the nanoparticles, XRD analysis was carried out. Figure 4.3 displays the XRD pattern of the AgNPs. The two theta degree values of 38.2, 44.4, 64.6, and 77.5 correlate orderly with the (111), (200), (220), and (311) planes of a face-centred cubic (FCC) silver lattice [62], in comparison with the standard silver structure (JCPDS no. 04-0783). The XRD pattern indicated that the biosynthesized silver nanoparticles are crystalline. Further supporting evidence of crystallinity are given by the



presence of bright spots observed in the selected area electron diffraction patterns as presented in Figure 4.2.

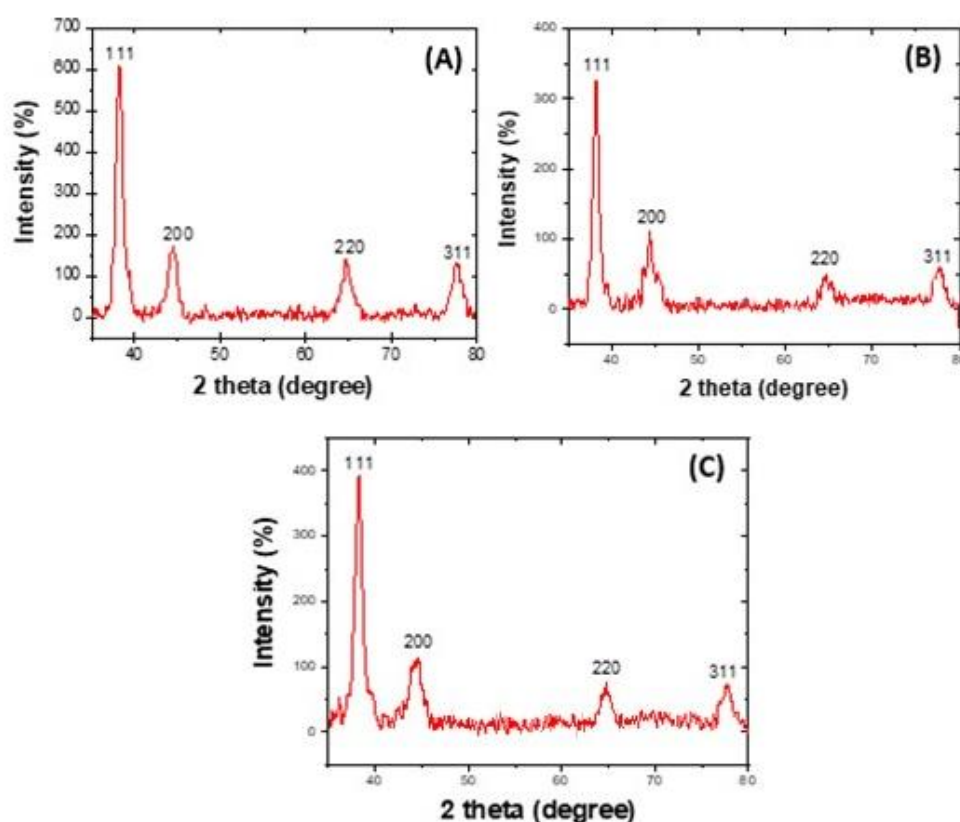


**Figure 4. 3: X-ray Diffraction patterns of the silver nanoparticles formed from *Leucosidea sericea* total extract (A), F1 (B), and F2 (C) showing the crystalline nature of the particles**

#### 4.9.5 DLS measurement

The silver nanoparticles of LSTE-, F1-, and F2 showed hydrodynamic sizes of 148.80, 87.64 and 95.17 nm respectively (Table 4.1). As expected, the agglomerates of silver nanoparticles formed by LSTE gave a high hydrodynamic size above 100 nm, implying aggregation of the particles. The HRTEM images confirms this and a few reasons have been earlier highlighted. Similarly, the size of the other two nanoparticles (F1- and F2-AgNPs) seems to agree with the particle size from TEM analysis. Usually, smaller sizes are recorded by TEM compared to the DLS measurement [63]. Although the size difference is often not more than two-fold, the literature records cases of wider difference. The aggregation of the particles may also be responsible for this wide difference as proper DLS measurements may not be possible with aggregates. Siddiqi and colleagues [64] reported an average hydrodynamic size of 437.1 nm for AgNPs whereas the TEM measurement showed 9.40–11.23 nm.

Additionally, larger particles scatter much more light than the smaller ones. In colloidal suspension, even a small number of large particles can obscure the contribution of the smaller particles. The measured size by the DLS is related to the metallic core of the nanoparticles. The size is also influenced by all the substances surrounding the surface of the nanoparticles such as the capping agents and the thickness of solvation shell, moving along with the particles. The thickness of the solvation shell as well as its influence on the size of measured nanoparticles is, in turn, dependent on the nature of the substances in the colloidal suspension and on the surface of the nanoparticles. All these may contribute to the difference between the measured size by TEM and DLS.

**Table 4.1: Particle size and zeta potential for AgNPs obtained from Dynamic Light Scattering**

Items	Hydrodynamic size (nm)	Polydispersity index	Zeta potential (mV)
LSTE-AgNPs	148.80	0.472	-25.7
F1-AgNPs	87.64	0.398	-29.4
F2-AgNPs	95.17	0.393	-28.8

The polydispersity index (PDI), otherwise called the heterogeneity index, is the degree of non-uniformity of the size distribution of particles. PDI is dimensionless and different size algorithms work with values between 0.05–0.7. According to the standard, PDI values of 0.05 and below are highly monodispersed. On the other hand, values greater than 0.7 shows broad particle size distribution [65]. In this context, the PDI is approximately 0.5, tending towards the extreme of 0.7 and further supporting the aggregation of LSTE-AgNPs. These polydispersity index is corroborated by a relatively lower zeta potential value. Although all the nanoparticles are generally surrounded by negative charges, the value indicates lower stability of LSTE-AgNPs compared to the other two. These results correlate well with hydrodynamic size as well as the TEM suggestion. In addition, the bimodal distribution of LSTE-AgNPs (Appendix K) is an indication that particles of different morphologies or aggregates are present.

The zeta potential (ZP) is associated with charges around nanoparticles. The magnitude of ZP determines the stability of the particles. Thus, the higher the value, the better the stability [66]. The ZP of AgNPs indicates good stability.

#### 4.9.6 In vitro stability study

Different chemical solutions were prepared and added to the silver nanoparticles and their interaction monitored using UV-Vis absorbance reading. As displayed in Appendix H, the UV-Visible measurement was termed 0 h (A1, B1, C1) upon the addition of various solutions to the respective AgNPs. The measurement was repeated at 24 and 48 hr. Aqueous, saline, protein, and buffer solutions interacted with the nanoparticles and caused an increase in the absorption in the long wavelength region. A general observation was the broadening of the absorption peaks. This indicates the formation of a fractal medium where nanoparticles attach to one another in the form of large clusters. The interaction of proteins with nanoparticles has been reported. Bovine serum albumen (BSA), for instance, possesses about 50 lysines on its surface, rendering it to show a high affinity for negative surfaces [67]. Interestingly, the AgNPs in this study are surrounded by negative ions as suggested by negative zeta potential values. Furthermore, it is well known that sodium chloride (NaCl) dissociates into  $\text{Na}^+$  and  $\text{Cl}^-$ . Similarly,  $-\text{COOH}$  and  $-\text{NH}_2$  may also be in solution with the nanoparticles. Thus, this collection of ions interacts with the charges at the surface of nanoparticles. Since the nanoparticles are predominantly surrounded by negative charges, the interaction of cations such as  $\text{Na}^+$  will be higher. When this happens, the Coulomb electrostatic repulsive force between the particles will be reduced. Attraction will then dominate through the Van der Waal's force and this might have resulted in the formation of large aggregates [68]. The significant broadening of the UV-Vis bands over time indicates that the nanoparticles were aggregating as a result of their interaction with solutions. In support of this, previous studies have shown broadening of absorption bands when proteins and other chemicals were employed [69-70]. This indicates formation of aggregates.

#### 4.9.7 Dilution study

Since certain biological applications may require different concentrations of AgNPs, dilution studies are necessary to confirm the retention of properties before future utilization [40]. Figure 4 shows the UV-Visible results of (A) LSTE-, (B) F1-, and (C) F2-AgNPs. The absorption spectra obtained for the different concentrations of the nanoparticles (80, 60, 40, 20, 10, and 5  $\mu\text{g/mL}$ ) suggest that the SPR wavelengths are almost identical for all the solutions. This means that the dilution of nanoparticles does not affect the properties of LSTE-, F1-, and F2-AgNPs. The importance of this dilution study is in the dosage to be used for certain applications. For the prepared nanoparticles to be active at any given concentration, their physicochemical features need to be retained. One of the quickest ways to confirm this is through their absorbance in UV-Visible spectroscopy, a powerful

tool in green synthesis. Thus, if there was no absorbance at the expected region, it may be inferred that the particles have lost their properties and may not be useful at such concentration. This serves as a guide for subsequent applications and consideration of another principle of green chemistry (atom economy).

In support of the above finding, other authors have reported related research work. Nune and colleagues successively diluted tea mediated gold nanoparticles in a previous study. The maximum absorption intensity was monitored and found to be intact even at very diluted conditions [71]. Also, when *acacia gum* mediated gold nanoparticles were diluted, the maximum absorption peak remained the same. They authors further observed that at all the tested concentrations, the absorption peak remained in the same region [72].

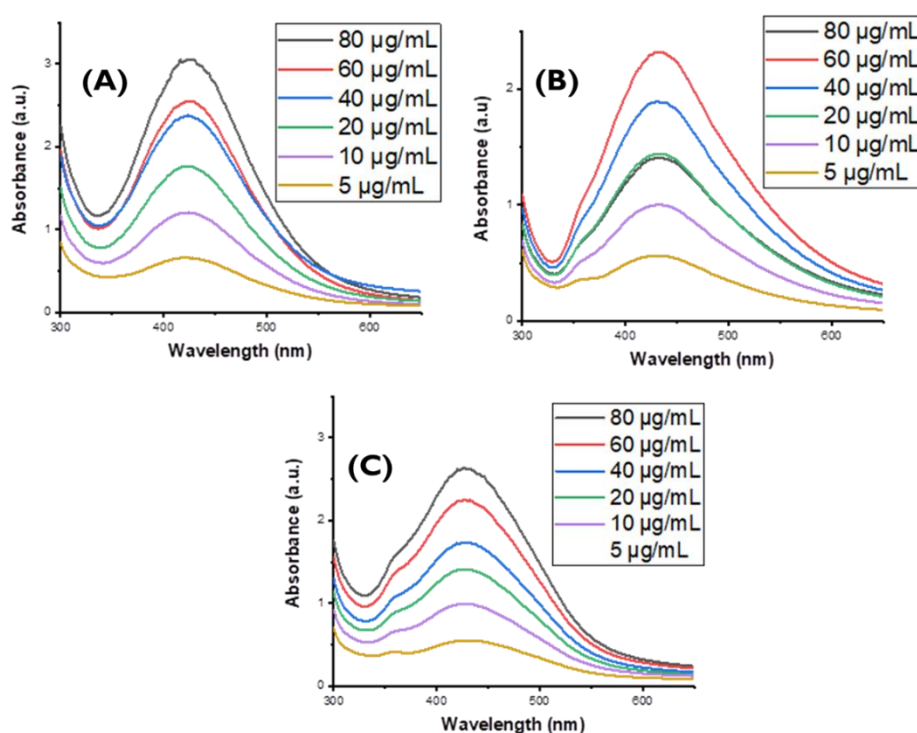


**Figure 4. 4: Surface Plasmon Resonance ( $\lambda$  max) of (A) *Leucosidea sericea* total extract mediated silver nanoparticles, (B) F1-mediated silver nanoparticles, and (C) F2-mediated silver nanoparticles showing the retention of properties by the particles even at low concentrations.**

#### 4.9.8 In-vitro Enzyme inhibition

Although different extract of *Leucosidea sericea* have been safely used to cure many diseases, little is reported about their antidiabetic properties. As a result, a study of the antidiabetic activity of this important plant was presented. Table 4.2 depicts the enzyme inhibitory  $IC_{50}$  values of the three AgNPs alongside their corresponding intact fractions.

Alpha-glucosidase inhibitory  $IC_{50}$  values of 21.48 and 18.76  $\mu\text{g/mL}$  were recorded for LSTE- and F1-AgNPs, respectively. These activities imply that the AgNPs possess potent inhibitory characteristics when compared to the standard drug, acarbose. However, when considering F2-AgNPs, it showed a similar inhibition activity as that of its precursor (F2), perhaps because of the remains of procyanidins on the surface of the nanoparticles as capping agents. On the other hand, LSTE- and F1-AgNPs displayed moderate alpha-amylase inhibitory activity in comparison with acarbose even though LSTE still showed a very high inhibition when compared to its corresponding NPs. Interestingly, F1-AgNPs displayed improved alpha-amylase inhibitory activity when compared to its intact fraction, F1, displaying no inhibition. The percentage inhibition at various concentrations was presented in Figure 4.5.

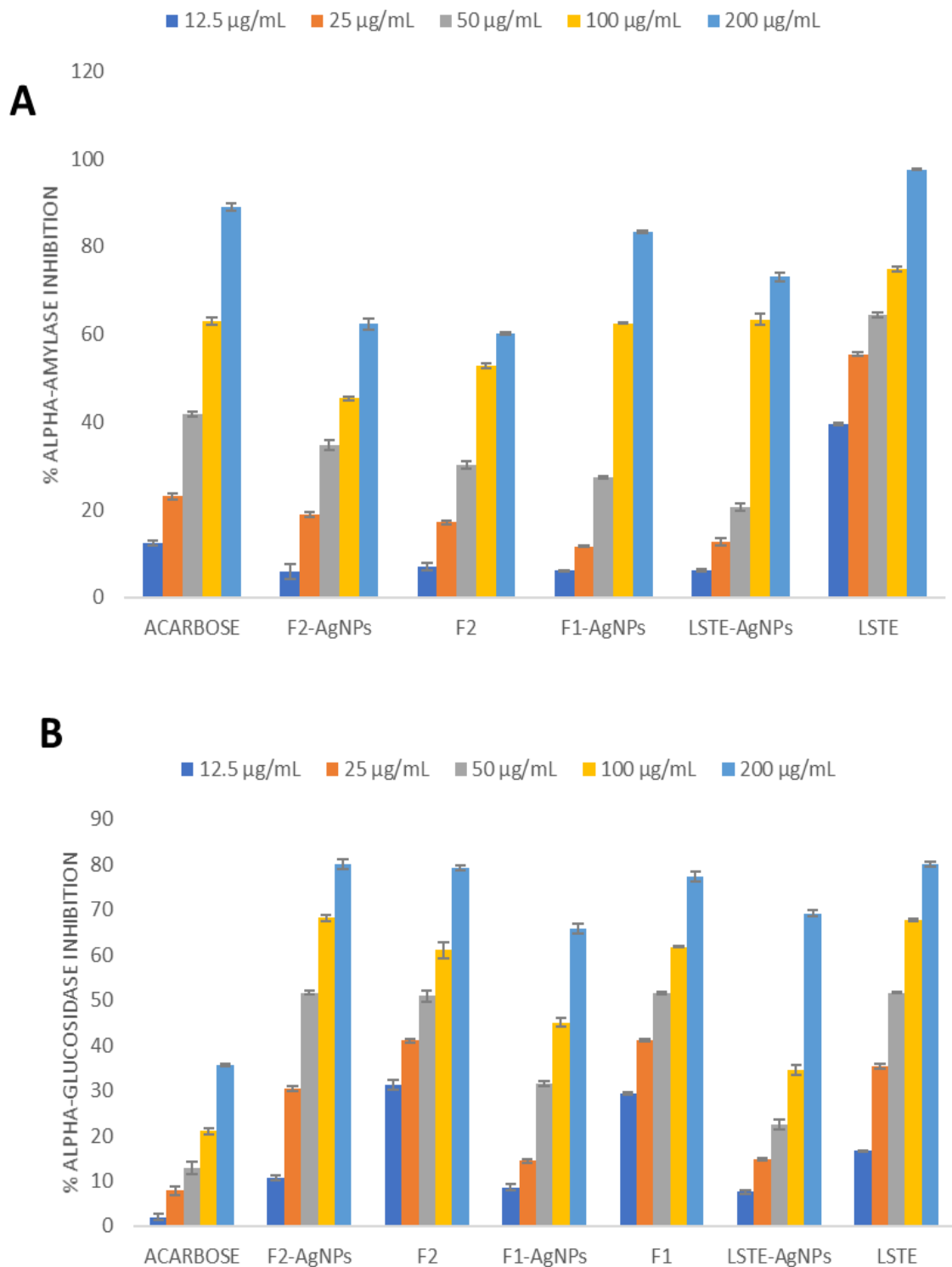


**Figure 4. 5: Antidiabetic activities with regards to alpha-amylase (A) and alpha-glucosidase (B) inhibition by *Leucosidea sericea* total extract (LSTE), procyanidin fractions (F1 and F2), and their respective silver nanoparticles (LSTE-, F1-, and F2-AgNPs)**

**Table 4.2: The enzymatic inhibitory activity, expressed as IC<sub>50</sub> of the *Leucosidea sericea* total extract (LSTE), the intact fractions (F1 and F2), and those of their corresponding silver nanoparticles (LSTE-, F1- and F2-AgNPs) using two assays (µg/mL)**

Items	Alpha-amylase (IC <sub>50</sub> ) (µg/mL)	Alpha-glucosidase (IC <sub>50</sub> ) (µg/mL)
LSTE	3.50±0.70 <sup>a</sup>	8.10±0.60 <sup>a</sup>
LSTE-AgNPs	14.92±1.0 <sup>b</sup>	21.48±0.90 <sup>b</sup>
F1	NA	7.30±0.50 <sup>a</sup>
F1-AgNPs	13.24±0.60 <sup>b</sup>	18.76±1.00 <sup>c</sup>
F2	18.9±0.20 <sup>c</sup>	7.10±0.40 <sup>a</sup>
F2-AgNPs	19.13±0.80 <sup>c</sup>	8.75±0.70 <sup>a</sup>
Acarbose	10.20±0.40 <sup>d</sup>	61.00±1.50 <sup>d</sup>

The results are expressed as mean ± SD of three different independent experiments ( $n = 3$ ). Results not sharing a common superscript alphabet (a, b, c, d, e) are significantly different ( $P < 0.01$ ). Acarbose (standard), NA (not active at the tested concentrations).

As stated earlier for alpha-glucosidase, F2-AgNPs also showed a similar IC<sub>50</sub> value as its precursor (F2) for alpha-amylase. This may be linked to the unique characteristics of these NPs including its morphology. It further shows that the activity may be dependent on size, shape, and other factors such as the type of phytochemical involved as the reductant and capping agent [46]. Previously, AgNPs have displayed alpha-glucosidase inhibition [30]. Our results are also supported by previous antidiabetic studies of AgNPs [30-31, 73]. In summary, the AgNPs in this study demonstrated interesting enzymatic activity, although mostly lower than those of the corresponding precursors, the most important fact is that they showed inhibitory activities.

#### 4.9.9 Antioxidant activity

Antioxidants possess free radical scavenging abilities. Table 4.3 reports the scavenging ability of the three AgNPs biosynthesized from LSTE, F1, and F2 and the respective intact fractions. The antioxidant activities, as measured by the FRAP, ABTS, and FC assays, of the intact fractions were significantly ( $p < 0.01$ ) higher than those of their corresponding AgNPs. For instance, when considering the ABTS assay, all the fractions, roughly showed a doubling of antioxidant activity when compared to the hybrid nanoparticles. This could be ascribed to a change in the functional groups during the nanoparticle formation, rendering them unavailable to participate in the scavenging activity with a subsequent reduction in the antioxidant activity. The antioxidant activity as the equivalence of the standard (Trolox, vitamin C and gallic acid) for ABTS, FRAP, and FC assays respectively, has been shown in Figure 4.6.

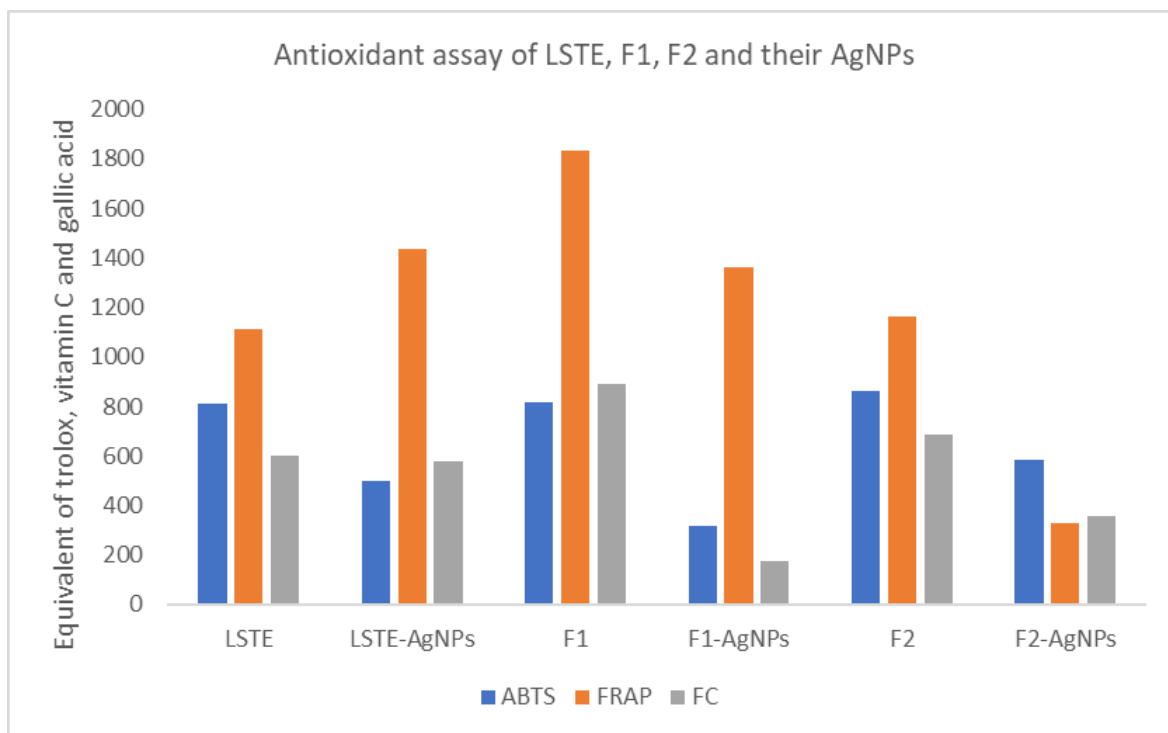


**Figure 4. 6: Antioxidant activity in terms of the ABTS (2,2'-azino-bis-3-ethylbenzotiazolin-6-sulfonic acid), FRAP (Ferric Reducing Antioxidant Power), and FC (Folin–Ciocalteu) scavenging activity by *L. sericea* total extract (LSTE), procyanidin fractions (F1 and F2), and their respective silver nanoparticles (LSTE-, F1- and F2-AgNPs). The antioxidant activities were measured based on the equivalence of standard antioxidants Trolox, vitamin C (ascorbic acid), and gallic acid**

**Table 4.3: The antioxidant activity of the *L. sericea* total extract (LSTE), the intact fractions (F1 and F2), and those of their corresponding silver nanoparticles (LSTE-, F1- and F2-AgNPs) using three assays (ABTS, FRAP, and FC). The percentage phenolic content (FC) of the silver nanoparticles is also presented in the last column of the table**

Items	ABTS (mM TE/g)	FRAP (mM AAE/g)	FC (mM GAE/g)	FC % (AgNPs)
LSTE	814.18±1.80 <sup>a</sup>	1113.20±6.70 <sup>a</sup>	602.60±6.10 <sup>a</sup>	100
LSTE-AgNPs	499.65±1.50 <sup>b</sup>	1438.50±5.60 <sup>b</sup>	578.27±7.70 <sup>b</sup>	57.8
F1	818.20±7.70 <sup>a</sup>	1834.00±4.70 <sup>c</sup>	889.60±6.00 <sup>c</sup>	100
F1-AgNPs	319.18±1.80 <sup>c</sup>	1361.60±6.70 <sup>d</sup>	175.25±2.60 <sup>d</sup>	17.5
F2	861.90±5.30 <sup>d</sup>	1166.00±2.10 <sup>e</sup>	685.70±6.70 <sup>e</sup>	100
F2-AgNPs	583.22±7.30 <sup>e</sup>	326.20±2.20 <sup>f</sup>	357.80±5.30 <sup>f</sup>	35.7

The results are expressed as mean ± SD of three different independent experiments ( $n = 3$ ). Results not sharing a common superscript alphabet (a, b, c, d, e) are significantly different ( $P < 0.01$ ).

When considering the FRAP assay outcomes, a similar trend was observed for the NPs and their corresponding intact fractions, F1 and F2, but not for LSTE, which showed increased antioxidant activity for its corresponding NP. On the other hand, when considering the FC assay outcomes, similar antioxidant activities were observed for LSTE



and its corresponding NP, but for F1 and F2, their corresponding NPs showed a significantly lower antioxidant activity.

The significantly higher antioxidant activity displayed by F2 vs. the F2-AgNPs could be due to low stability, size, and heterogeneity of the latter. Evidently, LSTE-AgNPs displayed better activity than F1- and F2-AgNPs and competes well with the intact fractions. This may be due to the abundance of the phytochemicals surrounding the LSTE nanoparticles as capping agents [49]. Previously, it has been suggested that the activity of nanomaterials may also be a function of the capping agents [46]. Our results were also in agreement with the activity reported by [49]. Reports have linked antioxidants to many deadly diseases including diabetes, hence, materials with dual properties would be of great benefit in reducing these menaces. A herbal formulation [74], the extracts of *Ananas comosus* [30], and *Chamaecostus cuspidatus* [55] were previously employed in synthesizing NPs with encouraging antidiabetic and antioxidant activities. Since certain antioxidants may also be implicated in adverse health-effects, several studies have been done on the antioxidant properties of many biosynthesized nanomaterials in the quest to finding more suitable alternatives [48, 75-76].

#### **4.9.10 The antibacterial assay of AgNPs**

Silver nanoparticles have been in the lead in terms of antibacterial activities [77]. When various plant parts were used for the synthesis, AgNPs have shown potent bactericidal effects on *E. coli* and *S. aureus* [77]. In the current study, the antibacterial activities of the AgNPs were also studied using wild species of both Gram-positive and Gram-negative bacteria. Serially diluted concentrations of the AgNPs were used and the results showed that the MIC values were in the range of 15.63–125 µg/mL [67].

Bacterial growth inhibition varied between the AgNPs tested. Among the three AgNPs, the MIC value of 62.50 µg/mL was most common (Table 4). This was particularly the case with F2-AgNPs except for *B. cereus* where the MIC was at the highest concentration of 125 µg/mL. This was still an improvement as none of the fractions showed any activity even above 1000 µg/mL. Similarly, nanoparticles (NPs) with similar sizes and MICs have been reported [78]. Research has shown that the activity of AgNPs is greatly associated with the concentration, shape, and size of the NPs [77], [79], and that AgNPs of small sizes at low concentrations are often effective antibacterial agents [80]. Various researchers evaluated the activity of these NPs with different sizes and shapes against certain species of bacteria [79, 81-82] and found that 2.5–85 nm-sized AgNPs showed antibacterial activities, while the most effective ones appeared to be between 2.5–20 nm. This implies that smaller silver nanoparticles are highly effective antibacterial agents. In addition, other authors reported that the activities of AgNPs may not only be due to small

size but the overall morphology. While Shao et al. showed that the enhanced antimicrobial activity was due to the small size and spherical shape of their particles, Sahu and colleagues implicated small size and mono-dispersity over large and polydispersed ones [83-84]. From our TEM results, the average size was determined to be in the range of 2.9–7.8 nm. Consequently, LSTE-AgNPs presented the lowest bactericidal activity. Although its MIC falls mostly at 62.50 µg/mL, the percentage inhibitions were only moderate for *P. aeruginosa* and *S. aureus* respectively. The *B. cereus* displayed a mild inhibition whereas *S. marcescens* were completely wiped out at the same concentration. This was, however, not far-fetched as the heavy presence of phenolic content was still observed, evidenced by the values presented in Table 4.3. It should be noted, however, that the intact fractions did not show any activity even at high concentrations (2000 µg/mL). On the other hand, the bactericidal effect of the AgNPs depends on the type of bacteria. In general, the Gram-negative bacterial species responded better to the bactericidal effects of the AgNPs than the Gram-positive species. Previous researchers have also shown this. It has been explained that the Gram-positive bacterial species possess thicker cell walls which makes penetration more difficult. The thinner cell wall of the Gram-negative species may have allowed easier interaction and possible disruption leading to more activity [85]. Overall, the bactericidal effects of our AgNPs appeared to be size-dependent. The smallest AgNPs (2.9 nm) presented more bactericidal effects in four organisms. This includes; *P. aeruginosa*, *B. cereus*, *E. coli*, with MIC of 31.25 µg/mL and even as low as 15.63 µg/mL for *S. aureus*. In a similar study, the antibacterial activity of AgNPs on *S. aureus* at 16.12 µg/mL has been reported [86]. When the particles are smaller, a larger surface area is available for contact with the bacteria, which could possibly lead to greater interaction with the bacteria. Therefore, F1-AgNPs had the largest contact with the bacteria, and might possibly explain the enhanced antibacterial activities observed [87]. Furthermore, previous studies have shown that the antimicrobial activity of a series of AgNPs increased as the size decreased [88]. Our findings, therefore, agree with these studies.

**Table 4.4. The minimum inhibitory concentration (MIC, µg/mL) values of the *L. sericea* total extract (LSTE), the intact fractions (F1 and F2), and their corresponding silver nanoparticles (LSTE-, F1- and F2-AgNPs) using six bacterial species**

Bacteria	LSTE	LSTE-AgNPs	F1	F1-AgNPs	F2	F2-AgNPs	Control*
<i>P. aeruginosa</i>	>2000	62.50	>2000	31.25	>2000	62.50	31.25
<i>S. aureus</i>	>2000	62.50	>2000	15.63	>2000	62.50	15.63
<i>B. cereus</i>	>2000	62.50	>2000	31.25	>2000	125.00	7.81
<i>S. enterica</i>	>2000	31.25	>2000	31.25	>2000	62.50	7.81
<i>E. coli</i>	>2000	62.50	>2000	31.25	>2000	62.50	15.63
<i>S. marcescens</i>	>2000	125.00	>2000	62.50	>2000	62.50	3.90

\*Ampicillin

Finally, extensive research activities are on-going in the field of green nanotechnology. Several authors have reported biosynthesis as a better procedure of forming nanoparticles while maintaining the principles of green chemistry. This study and many others, as mentioned previously, showed the potential of AgNPs as antibacterial agents and can form an important combination with antibiotics against drug-resistant micro-organisms. On the other hand, the previous toxicity measurements indicated marginal toxic effects of AgNPs *in vitro* [32-33]. *In vivo* studies are very limited but indicated toxicity in rats. The toxicity of AgNPs largely depends on the surface charges and the stabilizing (capping) agents which control the cells uptake of the NPs. A changing surface structure of AgNPs may lead to safe AgNPs for human uses and also increase the bioactivity.

Further studies are required to investigate the effects of procyanidins as capping agents and other natural compounds on the activity, cell uptake, and toxicity of the AgNPs. The future *in vivo* studies are highly appreciated in this regard and considered to be essential and helpful to understand the efficiency and safety of the prepared AgNPs utilizing edible, safe, and active compounds such as procyanidins. In addition, investigation of the mechanism of action of AgNPs as a key factor is yet to be established using different *in vitro* studies.

#### **4.10 Conclusions**

To our knowledge, this represents the first scientific research pertaining to the use of *Leucosidea sericea* constituents for AgNPs fabrication and subsequent evaluation of their *in vitro* anti-diabetic, antioxidant, and anti-bacterial activities. Capping agents play important roles in determining the final characteristics of the metal NPs. The procyanidin dimers (type-B) were isolated and employed to synthesise stable and bioactive AgNPs. The results are very encouraging and showed great enhancement in the activities of the intact fractions. The natural products/nanoparticles combination is a new important dimension in the area of drug discovery and the use of natural product compounds, such as procyanidins, that have well-established pharmacological profiles will improve the future usage of the metal NPs in the field of biomedical applications.

#### **Supplementary Materials**

The supplementary documents for this research article have been attached here as Appendix K and L.

## **Author Contributions**

"Conceptualization, A.A.H., S.S.B., and U.M.B.; methodology, J.A.B. and U.M.B.; software, E.I.; validation, S.S.B., J.A.B., and E.I.; formal analysis, U.M.B. and J.L.M.; investigation, U.M.B.; resources, A.A.H., C.W.J.A., and J.L.M.; data curation, S.S.B., E.I., and C.W.J.A.; writing—original draft preparation, U.M.B.; writing—review and editing, U.M.B., S.S.B., and A.A.H.; visualization, U.M.B.; supervision, S.S.B. and A.A.H; project administration, E.I.; funding acquisition, U.M.B. and A.A.H. All authors have read and agreed to the published version of the manuscript.

## **Funding**

TETFund allocation to IBB University, Lapai, Nigeria, and NRF with a grant number (106055) under Professor Ahmed A. Hussein was used for this research work.

## **Acknowledgments**

We would like to thank Charnice Mouton for her assistance in the antibacterial studies. Hamza E. A. Mohamed of iThemba labs, Cape Town, South Africa is also appreciated for XRD analysis.

## **Conflicts of Interest**

The authors declare no conflict of interest.

## References

1. Kumar, A.; Das, N.; Satija, N.K.; Mandrah, K.; Roy, S.K.; Rayavarapu, R.G. A novel approach towards synthesis and characterization of non-cytotoxic gold nanoparticles using taurine as capping agent. *Nanomaterials* **2019**, *10*, 45-63, doi:10.3390/nano10010045.
2. Janas, D.; Koziol, K.K. Carbon nanotube fibers and films: Synthesis, applications and perspectives of the direct-spinning method. *Nanoscale* **2016**, *8*, 19475–19490, doi:10.1039/c6nr07549e.
3. Muneer, I.; Farrukh, M.A.; Javaid, S.; Shahid, M.; Khaleeq-Ur-Rahman, M. Synthesis of Gd<sub>2</sub>O<sub>3</sub>/Sm<sub>2</sub>O<sub>3</sub> nanocomposite via sonication and hydrothermal methods and its optical properties. *Superlattices Microstruct.* **2015**, *77*, 256–266, doi:10.1016/j.spmi.2014.10.006
4. Babu, S.; Kumar, B.; Kumar, K. Environment friendly approach for size controllable synthesis of biocompatible silver nanoparticles using diastase. *Environ. Toxicol. Pharmacol.* **2017**, *49*, 131–136, doi:10.1016/j.etap.2016.11.019
5. Lee, J.; Park, E.Y.; Lee, J. Non-toxic nanoparticles from phytochemicals: Preparation and biomedical application. *Bioprocess. Biosyst. Eng.* **2013**, *37*, 983–989, doi:10.1007/s00449-013-1091-3.
6. Xia, D.-L.; Wang, Y.-F.; Bao, N.; He, H.; Li, X.-D.; Chen, Y.-P.; Gu, H.-Y. Influence of reducing agents on biosafety and biocompatibility of gold nanoparticles. *Appl. Biochem. Biotechnol.* **2014**, *174*, 2458–2470, doi:10.1007/s12010-014-1193-7.
7. Okaiyeto, K.; Hoppe, H.; Okoh, A.I. Plant-based synthesis of silver nanoparticles using aqueous leaf extract of *Salvia officinalis*: characterization and its antiplasmodial activity. *J. Clust. Sci.* **2020**, doi:10.1007/s10876-020-01766-y.
8. Saratale, R.G.; Saratale, G.D.; Shin, H.S.; Jacob, J.M.; Pugazhendhi, A.; Bhisare, M.; Kumar, G. New insights on the green synthesis of metallic nanoparticles using plant and waste biomaterials: Current knowledge, their agricultural and environmental applications. *Environ. Sci. Pollut. Res.* **2017**, *25*, 1–20, doi:10.1007/s11356-017-9912-6.
9. Benelli, G.; Kadaikunnan, S.; Alharbi, N.S.; Govindarajan, M. Biophysical characterization of *Acacia caesia*-fabricated silver nanoparticles: Effectiveness on mosquito vectors of public health relevance and impact on non-target aquatic biocontrol agents. *Environ. Sci. Pollut. Res.* **2017**, *25*, 10228–10242, doi:10.1007/s11356-017-8482-y.
10. Nath, D.; Banerjee, P. Green nanotechnology—A new hope for medical biology. *Environ. Toxicol. Pharmacol.* **2013**, *36*, 997–1014, doi:10.1016/j.etap.2013.09.002.

11. Ovais, M.; Khalil, A.T.; Islam, N.U.; Ahmad, I.; Ayaz, M.; Saravanan, M.; Shinwari, Z.K.; Mukherjee, S. Role of plant phytochemicals and microbial enzymes in biosynthesis of metallic nanoparticles. *Appl. Microbiol. Biotechnol.* **2018**, *102*, 6799–6814, doi:10.1007/s00253-018-9146-7.
12. Chahardoli, A.; Karimi, N.; Fattahi, A. Biosynthesis, characterization, antimicrobial and cytotoxic effects of silver nanoparticles using *Nigella arvensis* seed extract. *Iran. J. Pharm. Res.* **2017**, *16*, 1167–1175.
13. Arassu, R.R.T.; Nambikkairaj, B. *Pelargonium graveolens* plant leaf essential oil mediated green synthesis of silver nanoparticles and its antifungal activity against human pathogenic fungi. *J Pharm. Phytochem* **2018**, *7*, 1778–1784.
14. Ranzoszek-Soliwoda, K.; Tomaszewska, E.; Malek, K.; Celichowski, G.; Orłowski, P.; Krzyzowska, M.; Grobelny, J. The synthesis of monodisperse silver nanoparticles with plant extracts. *Colloids Surf. B: Biointerfaces* **2019**, *177*, 19–24, doi:10.1016/j.colsurfb.2019.01.037.
15. Nayaka, S.; Bhat, M.P.; Chakraborty, B.; Pallavi, S.S.; Airodagi, D.; Muthuraj, R.; Halaswamy, H.M.; Dhanyakumara, S.B.; Shashiraj, K.N.; Kupaneshi, K.N.S.A.C. Seed extract-mediated synthesis of silver nanoparticles from *Putranjiva roxburghii* wall., phytochemical characterization, antibacterial activity and anticancer activity against MCF-7 cell line. *Indian J. Pharm. Sci.* **2020**, *82*, 260–269, doi:10.36468/pharmaceutical-sciences.646.
16. Jemilugba, O.T.; Sakho, E.H.M.; Parani, S.; Mavumengwana, V.; Oluwafemi, O.S. Green synthesis of silver nanoparticles using *Combretum erythrophyllum* leaves and its antibacterial activities. *Colloid Interface Sci. Commun.* **2019**, *31*, 100191, doi:10.1016/j.colcom.2019.100191.
17. Amin, M.; Kouhbanani, J.; Beheshtkhoo, N.; Nasirmoghadas, P. Green synthesis of spherical silver nanoparticles using *Ducrosia anethifolia* aqueous extract and its antibacterial activity. *J. Environ. Treat. Tech.* **2019**, *7*, 461–466.
18. Chahardoli, A.; Karimi, N.; Fattahi, A. *Nigella arvensis* leaf extract mediated green synthesis of silver nanoparticles: Their characteristic properties and biological efficacy. *Adv. Powder Technol.* **2018**, *29*, 202–210, doi:10.1016/j.appt.2017.11.003.
19. Srinivasan, R.; Vigneshwari, L.; Rajavel, T.; Durgadevi, R.; Kannappan, A.; Balamurugan, K.; Devi, K.P.; Ravi, A.V. Biogenic synthesis of silver nanoparticles using *Piper betle* aqueous extract and evaluation of its anti-quorum sensing and antibiofilm potential against uropathogens with cytotoxic effects: An *in vitro* and *in vivo* approach. *Environ. Sci. Pollut. Res.* **2017**, *25*, 10538–10554, doi:10.1007/s11356-017-1049-0.

20. S Khaleel, K.; Govindaraju, R.; Manikandan, J.; Seog, E.Y.; Singaravelu, G. Phytochemical mediated gold nanoparticles and their PTP 1B inhibitory activity. *Colloids Surf. B: Biointerfaces* **2010**, *75*, 405–409.
21. Shah, M.; Nawaz, S.; Jan, H.; Uddin, N.; Ali, A.; Anjum, S.; Giglioli-Guivarc'H, N.; Hano, C.; Abbasi, B.H. Synthesis of bio-mediated silver nanoparticles from *Silybum marianum* and their biological and clinical activities. *Mater. Sci. Eng. C* **2020**, *112*, 110889, doi:10.1016/j.msec.2020.110889.
22. Amini, S.M. Preparation of antimicrobial metallic nanoparticles with bioactive compounds. *Mater. Sci. Eng. C* **2019**, *103*, 109809, doi:10.1016/j.msec.2019.109809
23. Perelshtein, I.; Ruderman, Y.; Francesko, A.; Fernandes, M.M.; Tzanov, T.; Gedanken, A. Tannic acid NPs—Synthesis and immobilization onto a solid surface in a one-step process and their antibacterial and anti-inflammatory properties. *Ultrason. Sonochemistry* **2014**, *21*, 1916–1920, doi:10.1016/j.ultsonch.2013.11.022.
24. Mittal, A.K.; Kumar, S.; Banerjee, U.C. Quercetin and gallic acid mediated synthesis of bimetallic (silver and selenium) nanoparticles and their antitumor and antimicrobial potential. *J. Colloid Interface Sci.* **2014**, *431*, 194–199, doi:10.1016/j.jcis.2014.06.030.
25. Stephen, A.; Seethalakshmi, S. Phytochemical synthesis and preliminary characterization of silver nanoparticles using hesperidin. *J. Nanosci.* **2013**, *2013*, 1–6, doi:10.1155/2013/126564.
26. Safaepour, M.; Shahverdi, A.R.; Shahverdi, H.R.; Khorramizadeh, M.R.; Gohari, A.R. Green synthesis of small silver nanoparticles using geraniol and its cytotoxicity against *fibrosarcoma-wehi* 164. *Avicenna J. Med. Biotechnol.* **2009**, *1*, 111–115.
27. Satsangi, N. Synthesis and characterization of biocompatible silver nanoparticles for anticancer application. *J. Inorg. Organomet. Polym. Mater.* **2019**, *30*, 1907–1914, doi:10.1007/s10904-019-01372-0.
28. Saratale, G.D.; Benelli, G.; Kumar, G.; Kim, D.S. Bio-fabrication of silver nanoparticles using the leaf extract of an ancient herbal medicine, dandelion (*Taraxacum officinale*), evaluation of their antioxidant, anticancer potential, and antimicrobial activity against phytopathogens. *Environ. Sci. Pollut. Res.* **2017**, *25*, 10392–10406, doi:10.1007/s11356-017-9581-5.
29. Bharathi, D.; Bhuvaneshwari, V. Evaluation of the cytotoxic and antioxidant activity of phyto-synthesized silver nanoparticles using *Cassia angustifolia* flowers. *BioNanoScience* **2018**, *9*, 155–163, doi:10.1007/s12668-018-0577-5.
30. Jini, D.; Sharmila, S. Green synthesis of silver nanoparticles from *Allium cepa* and its in vitro antidiabetic activity. *Mater. Today: Proc.* **2020**, *22*, 432–438, doi:10.1016/j.matpr.2019.07.672.
31. Patra, J.K.; Das, G.; Shin, H.-S. Facile green biosynthesis of silver nanoparticles using *Pisum sativum* L. outer peel aqueous extract and its antidiabetic, cytotoxicity,

- antioxidant, and antibacterial activity. *Int. J. Nanomed.* **2019**, *14*, 6679–6690, doi:10.2147/IJN.S212614.
32. Prabhu, S.; Vinodhini, S.; Elenchezhiyan, C.; Rajeswari, D. Evaluation of antidiabetic activity of biologically synthesized silver nanoparticles using *Pouteria sapota* in streptozotocin-induced diabetic rats. *J. Diabetes* **2017**, *10*, 28–42, doi:10.1111/1753-0407.12554.
  33. Saratale, R.G.; Shin, H.S.; Kumar, G.; Benelli, G.; Kim, D.; Saratale, G.D. Exploiting antidiabetic activity of silver nanoparticles synthesized using *Punica granatum* leaves and anticancer potential against human liver cancer cells (HepG2) *Artif. Cells Nanomed. Biotechnol.* **2018**, *46*, 211–222, doi:10.1080/21691401.2017.1337031.
  34. Dong, Y.; Wan, G.; Yan, P.; Qian, C.; Li, F.; Peng, G. Biology fabrication of resveratrol coated gold nanoparticles and investigation of their effect on diabetic retinopathy in streptozotocin induced diabetic rats. *J. Photochem. Photobiol. B Biol.* **2019**, *195*, 51–57, doi:10.1016/j.jphotobiol.2019.04.012.
  35. Ajayi, E.; Afolayan, A.J. Green synthesis, characterization and biological activities of silver nanoparticles from alkalized *Cymbopogon citratus* Stapf. *Adv. Nat. Sci. Nanosci. Nanotechnol.* **2017**, *8*, 015017, doi:10.1088/2043-6254/aa5cf7.
  36. Shanmuganathan, R.; MubarakAli, D.; Prabakar, D.; Muthukumar, H.; Thajuddin, N.; Kumar, S.S.; Pugazhendhi, A. An enhancement of antimicrobial efficacy of biogenic and ceftriaxone-conjugated silver nanoparticles: Green approach. *Environ. Sci. Pollut. Res.* **2017**, *25*, 10362–10370, doi:10.1007/s11356-017-9367-9.
  37. Sharma, R.; Kishore, N.; Hussein, A.A.; Lall, N. The potential of *Leucosidea sericea* against *Propionibacterium acnes*. *Phytochem. Lett.* **2014**, *7*, 124–129, doi:10.1016/j.phytol.2013.11.005.
  38. Nair, J.; Aremu, A.; Van Staden, J. Anti-inflammatory effects of *Leucosidea sericea* (*Rosaceae*) and identification of the active constituents. *S. Afr. J. Bot.* **2012**, *80*, 75–76, doi:10.1016/j.sajb.2012.02.009.
  39. Aremu, A.; Ndhlala, A.; Fawole, O.A.; Light, M.; Finnie, J.; Van Staden, J. *In vitro* pharmacological evaluation and phenolic content of ten South African medicinal plants used as anthelmintics. *S. Afr. J. Bot.* **2010**, *76*, 558–566, doi:10.1016/j.sajb.2010.04.009.
  40. Bosman, A.; Combrinck, S.; Der Merwe, R.R.-V.; Botha, B.; McCrindle, R.; Houghton, P. Isolation of an anthelmintic compound from *Leucosidea sericea*. *S. Afr. J. Bot.* **2004**, *70*, 509–511, doi:10.1016/s0254-6299(15)30189-7.
  41. Adamu, M.; Mukandiwa, L.; Awouafack, M.; Ahmed, A.; Eloff, J.; Naidoo, V. Ultrastructure changes induced by the phloroglucinol derivative agrimol G isolated from *Leucosidea sericea* in *Haemonchus contortus*. *Exp. Parasitol.* **2019**, *207*, 107780, doi:10.1016/j.exppara.2019.107780.



42. Badeggi, U.M.; Isamil, E.; Adeloye, A.O.; Botha, S.; Badmus, J.A.; Marnewick, J.L.; Cupido, C.N.; Hussein, A.A. Green synthesis of gold nanoparticles capped with procyanidins from *Leucosidea sericea* as potential antidiabetic and antioxidant agents. *Biomolecules* **2020**, *10*, 452-475, doi:10.3390/biom10030452.
43. Romeyer, F.M.; Macheix, J.-J.; Sapis, J.-C. Changes and importance of oligomeric procyanidins during maturation of grape seeds. *Phytochem.* **1985**, *25*, 219–221, doi:10.1016/s0031-9422(00)94532-1.
44. Gonthier, M.-P.; Donovan, J.L.; Texier, O.; Felgines, C.; Remesy, C.; Scalbert, A. Metabolism of dietary procyanidins in rats. *Free. Radic. Boil. Med.* **2003**, *35*, 837–844, doi:10.1016/s0891-5849(03)00394-0.
45. Haslam, E. Symmetry and promiscuity in procyanidin biochemistry. *Phytochemistry* **1977**, *16*, 1625–1640, doi:10.1016/0031-9422(71)85060-4.
46. Berké, B.; De Freitas, V. Influence of procyanidin structures on their ability to complex with oenin. *Food Chem.* **2005**, *90*, 453–460, doi:10.1016/j.foodchem.2004.05.009.
47. Granja, A.; Pinheiro, M.; Reis, S. Epigallocatechin gallate nanodelivery systems for cancer therapy. *Nutrients* **2016**, *8*, 307-329, doi:10.3390/nu8050307.
48. Aiello, P.; Consalvi, S.; Poce, G.; Raguzzini, A.; Toti, E.; Palmery, M.; Biava, M.; Bernardi, M.; Kamal, M.A.; Perry, G.; et al. Dietary flavonoids: Nano delivery and nanoparticles for cancer therapy. *Semin. Cancer Boil.* **2019**, *16*, 555-562, doi:10.1016/j.semcancer.2019.08.029.
49. Elbagory, A.M.; Meyer, M.; Cupido, C.N.; Hussein, A.A. Inhibition of bacteria associated with wound infection by biocompatible green synthesized gold nanoparticles from South African plant extracts. *Nanomater.* **2017**, *7*, 417-438, doi:10.3390/nano7120417.
50. Thilagam, E.; Parimaladevi, B.; Kumarappan, C.; Mandal, S.C. Alpha-glucosidase and alpha-amylase inhibitory activity of *Senna surattensis*. *J Acupunct Meridian Stud.* **2013**, *6*, 24–30, doi:10.1016/j.jams.2012.10.005.
51. Pu, S.; Li, J.; Sun, L.; Zhong, L.; Ma, Q. An *in vitro* comparison of the antioxidant activities of chitosan and green synthesized gold nanoparticles. *Carbohydr. Polym.* **2019**, *211*, 161–172, doi:10.1016/j.carbpol.2019.02.007.
52. Salari, S.; Bahabadi, S.E.; Samzadeh-Kermani, A.; Yosefzai, F. *In-vitro* evaluation of antioxidant and antibacterial potential of green synthesized silver nanoparticles using *Prosopis farcta* fruit extract. *Iran. J. Pharm. Res.* **2019**, *18*, 430–455.
53. Gomes, J.F.; Garcia, A.C.; Ferreira, E.B.; Pires, C.; Oliveira, V.L.; Tremiliosi-Filho, G.; Gasparotto, L.H. New insights into the formation mechanism of Ag, Au and Ag/Au nanoparticles in aqueous alkaline media: Alkoxides from alcohols, aldehydes and ketones as universal reducing agents. *Phys. Chem. Chem. Phys.* **2015**, *17*, 21683–21693, doi:10.1039/C5CP02155C.

54. Shamprasad, B.R.; Keerthana, S.; Megarajan, S.; Lotha, R.; Aravind, S.; Veerappan, A.; Anbazhagan, V. Photosynthesized escin stabilized gold nanoparticles exhibit antidiabetic activity in L6 rat skeletal muscle cells. *Mater. Lett.* **2019**, *241*, 198–201, doi:10.1016/j.matlet.2019.01.086.
55. Selvakannan, P.; Swami, A.; Srisathiyanarayanan, D.; Shirude, P.S.; Pasricha, R.; Mandale, A.B.; Sastry, M. Synthesis of aqueous Au core–Ag shell nanoparticles using tyrosine as a pH-dependent reducing agent and assembling phase-transferred silver nanoparticles at the air–water interface. *Langmuir* **2004**, *20*, 7825–7836, doi:10.1021/la049258j.
56. Mendoza-Wilson, A.M.; Balandran, R. Effect of constituent units, type of interflavan bond, and conformation on the antioxidant properties of procyanidin dimers: A computational outlook. *J. Chem.* **2017**, *2017*, 1–11, doi:10.1155/2017/3535148.
57. Ponnaniakamideen, M.; RajeshKumar, S.; Vanaja, M.; Annadurai, G. *In vivo* Type 2 diabetes and wound-healing effects of antioxidant gold nanoparticles synthesized using the insulin plant *Chamaecostus cuspidatus* in albino rats. *Can. J. Diabetes* **2019**, *43*, 82–89.e6, doi:10.1016/j.jcjd.2018.05.006.
58. Amendola, V.; Bakr, O.M.; Stellacci, F. A study of the surface plasmon resonance of silver nanoparticles by the discrete dipole approximation method: effect of shape, size, structure, and assembly. *Plasmonics* **2010**, *5*, 85–97, doi:10.1007/s11468-009-9120-4.
59. Sosa, I.O.; Noguez, C.; Barrera, R.G.; Noguez, C. Optical properties of metal nanoparticles with arbitrary shapes. *J. Phys. Chem. B* **2003**, *107*, 6269–6275, doi:10.1021/jp0274076.
60. Khodashenas, B.; Ghorbani, H.R. Synthesis of silver nanoparticles with different shapes. *Arab. J. Chem.* **2019**, *12*, 1823–1838, doi:10.1016/j.arabjc.2014.12.014.
61. Elbagory, A.M.; Cupido, C.N.; Meyer, M.; Hussein, A.A. Large scale screening of Southern African plant extracts for the green synthesis of gold nanoparticles using microtitre-plate method. *Molecules* **2016**, *21*, 1498, doi:10.3390/molecules21111498.
62. Wang, L.; Zhang, W.; Zhao, Y.; Cao, L. Fabrication of silver nanoparticles loaded flower like CeF<sub>3</sub> architectures and their antibacterial activity. *J. Phys. Chem. Solids* **2018**, *120*, 154–160, doi:10.1016/j.jpcs.2018.04.042.
63. Aarthi, C.; Govindarajan, M.; Rajaraman, P.; Alharbi, N.S.; Kadaikunnan, S.; Khaled, J.M.; Mothana, R.A.; Siddiqui, N.A.; Benelli, G. Eco-friendly and cost-effective Ag nanocrystals fabricated using the leaf extract of *Habenaria plantaginea*: Toxicity on six mosquito vectors and four non-target species. *Environ. Sci. Pollut. Res.* **2017**, *25*, 10317–10327, doi:10.1007/s11356-017-9203-2.
64. Rajarajeshwari, T.; Shivashri, C.; Rajasekar, P. Synthesis and characterization of biocompatible gymnemic acid—gold nanoparticles: A study on glucose uptake

- stimulatory effect in 3T3-L1 adipocytes. *RSC Adv.* **2014**, *4*, 63285–63295, doi:10.1039/c4ra07087a.
65. Siddiqi, K.S.; Rashid, M.; Rahman, A.U.; Husen, A.; Rehman, S. Tajuddin. Biogenic fabrication and characterization of silver nanoparticles using aqueous-ethanolic extract of lichen (*Usnea longissima*) and their antimicrobial activity. *Biomater. Res.* **2018**, *22*, 23, doi:10.1186/s40824-018-0135-9.
  66. Danaei, M.; Dehghankhold, M.; Ataei, S.; Davarani, F.H.; Javanmard, R.; Dokhani, A.; Khorasani, S.; Mozafari, M.R. Impact of particle size and polydispersity index on the clinical applications of lipidic nanocarrier systems. *Pharmaceutics* **2018**, *10*, 57-73, doi:10.3390/pharmaceutics10020057.
  67. Bhumkar, D.R.; Joshi, H.M.; Sastry, M.; Pokharkar, V. Chitosan reduced gold nanoparticles as novel carriers for transmucosal delivery of insulin. *Pharm. Res.* **2007**, *24*, 1415–1426, doi:10.1007/s11095-007-9257-9.
  68. Alzoubi, F. Y.; Bidier, S. A. Characterization and aggregation of silver nanoparticles dispersed in an aqueous solution. *Chinese Journal of Physics*, **2013**, *51*(2), 378-387.
  69. Islam, N. U., Khan, I., Rauf, A., Muhammad, N., Shahid, M., & Shah, M. R. Antinociceptive, muscle relaxant and sedative activities of gold nanoparticles generated by methanolic extract of *Euphorbia milii*. *BMC Complementary and Alternative Medicine*, **2015**, *15*(1), 1-11.
  70. Ikawa, S., Kitano, K., & Hamaguchi, S. Effects of pH on bacterial inactivation in aqueous solutions due to low-temperature atmospheric pressure plasma application. *Plasma Processes and Polymers*, **2010**, *7*(1), 33-42.
  71. Nune, S.K.; Chanda, N.; Shukla, R.; Katti, K.; Kulkarni, R.R.; Thilakavathy, S.; Mekapothula, S.; Kannan, R.; Katti, K.V. Green nanotechnology from tea: phytochemicals in tea as building blocks for production of biocompatible gold nanoparticles. *Journal of materials chemistry*, **2009**, *19*(19), 2912-2920.
  72. Kattumuri, V.; Katti, K.; Bhaskaran, S.; Boote, E.J.; Casteel, S.W.; Fent, G.M.; Robertson, D.J.; Chandrasekhar, M.; Kannan, R.; Katti, K.V. Gum arabic as a phytochemical construct for the stabilization of gold nanoparticles: in vivo pharmacokinetics and X-ray-contrast-imaging studies. *Small*, **2007**, *3*(2), 333-341.
  73. Rani, R.; Sharma, D.; Chaturvedi, M.; Jp, Y. Green synthesis, characterization and antibacterial activity of silver nanoparticles of endophytic fungi *Aspergillus terreus*. *J. Nanomed. Nanotechnol.* **2017**, *8*, 457-464, doi:10.4172/2157-7439.1000457.
  74. Sasidharan J.; Meenakshi, R.V.; Sureshkumar, P. Green synthesis, characterization and evaluation of in-vitro antioxidant & anti-diabetic activity of nanoparticles from a polyherbal formulation-mehani. *J. Environ. Nanotechnol.* **2018**, *7*, 51–59.

75. Patil, M.P.; Seo, Y.B.; Lim, H.K.; Kim, G.-D. Biofabrication of gold nanoparticles using *Agrimonia pilosa* extract and their antioxidant and cytotoxic activity. *Green Chem. Lett. Rev.* **2019**, *12*, 208–216, doi:10.1080/17518253.2019.1623927.
76. Abusahid, Z.; Kandiah, M. *In vitro* green synthesis of *Phoenix dactylifera* silver nanoparticles: assessing their antioxidant and antimicrobial properties. *Int. J. Nanosci.* **2019**, *18*, 1–16, doi:10.1142/s0219581x1850031x.
77. Nyoni, S.; Muzenda, E.; Mukaratirwa-muchanyereyi, N. Characterization and evaluation of antibacterial activity of silver nanoparticles prepared from *Sclerocarya birrea* stem bark and leaf extracts. *Nano Biomed. Eng.* **2019**, *11*, 28–34, doi:10.5101/nbe.v11i1.p28-34
78. Sankar, S.; Kumar, L. Green synthesis of silver nanoparticles using *Givotia moluccana* leaf extract and evaluation of their antimicrobial activity. *Mater. Lett.* **2018**, *226*, 47–51, doi:10.1016/j.matlet.2018.05.009.
79. Dong, Y.; Zhu, H.; Shen, Y.; Zhang, W.; Zhang, L. Antibacterial activity of silver nanoparticles of different particle size against *Vibrio natriegens*. *PLoS ONE* **2019**, *14*, e0222322, doi:10.1371/journal.pone.0222322.
80. Khan, I.; Saeed, K.; Khan, I. Nanoparticles: Properties, applications and toxicities. *Arab. J. Chem.* **2019**, *12*, 908–931, doi:10.1016/j.arabjc.2017.05.011.
81. Mani, N. Evaluation of antimicrobial activity of silver nanoparticle using *Eichhornia crassipes* leaves extract. *J. Pharmacogn. Phytochem.* **2018**, *7*, 1308–1311.
82. Elangovan, M.; Muju, G.; Anantharaman, P. Biosynthesis of silver nanoparticles from platymonas sp. and its antibacterial activity against biofouling causing bacterial strains. *J. Boil. Act. Prod. Nat.* **2019**, *9*, 269–277, doi:10.1080/22311866.2019.1666741.
83. Sahu, N.; Soni, D.; Chandrashekhar, B.; Satpute, D.B.; SaravanaDevi, S.; Sarangi, B.K.; Pandey, R. Synthesis of silver nanoparticles using flavonoids: Hesperidin, naringin and diosmin, and their antibacterial effects and cytotoxicity. *Int. Nano Lett.* **2016**, *6*, 173–181, doi:10.1007/s40089-016-0184-9.
84. Shao, Y.; Wu, C.; Wu, T.; Yuan, C.; Chen, S.; Ding, T.; Ye, X.; Hu, Y. Green synthesis of sodium alginate-silver nanoparticles and their antibacterial activity. *Int. J. Boil. Macromol.* **2018**, *111*, 1281–1292, doi:10.1016/j.ijbiomac.2018.01.012.
85. Saratale, G.D.; Saratale, R.G.; Cho, S.-K.; Ghodake, G.; Bharagava, R.N.; Park, Y.; Mulla, S.I.; Kim, D.S.; Kadam, A.; Nair, S.; et al. Investigation of photocatalytic degradation of reactive textile dyes by *Portulaca oleracea*-functionalized silver nanocomposites and exploration of their antibacterial and antidiabetic potentials. *J. Alloy. Compd.* **2020**, *833*, 155083, doi:10.1016/j.jallcom.2020.155083.
86. Jin, T.; Wang, M. Antibacterial activity of silver nanoparticles from endophytic fungus *Talaromyces purpleogenus*. *Int. J. Nanomed.* **2019**, *14*, 3427–3438.

87. Lu, Z.; Rong, K.; Li, J.; Yang, H.; Chen, R. Size-dependent antibacterial activities of silver nanoparticles against oral anaerobic pathogenic bacteria. *J. Mater. Sci. Mater. Med.* **2013**, *24*, 1465–1471, doi:10.1007/s10856-013-4894-5.
88. Banala, R.R.; Nagati, V.B.; Reddy, K.P. Green synthesis and characterization of *Carica papaya* leaf extract coated silver nanoparticles through X-ray diffraction, electron microscopy and evaluation of bactericidal properties. *Saudi J. Boil. Sci.* **2015**, *22*, 637–644, doi:10.1016/j.sjbs.2015.01.007.

## CHAPTER FIVE

### **Biofabrication, characterization and applications of *Hypoxis hemerocallidea* and hypoxoside mediated silver nanoparticles**

Umar M. Badeggi <sup>1</sup>, Subelia S. Botha <sup>2</sup>, Enas Ismail<sup>1</sup> and Ahmed A. Hussein <sup>2,\*</sup>

<sup>1</sup> Chemistry Department, Cape Peninsula University of Technology, Symphony Rd. Bellville 7535, South Africa; umb2016@gmail.com (U.M.B); enas.ismail4@yahoo.com (E.I.), mohammedam@cput.ac.za (A.A.H.)

<sup>2</sup> Electron Microscope Unit, University of the Western Cape, Bellville, 7535, South Africa; subotha@uwc.ac.za (S.B.)

\* Correspondence: mohammedam@cput.ac.za; Tel.: +27-21-959-6193; Fax: +27-21-959-3055

#### **Abstract**

Medicinal plants contain important phytochemicals believed to be responsible for their biological activities. The plants' reducing potential in the green synthesis of nanoparticles has also been linked to these bioactive ingredients. In this work, hypoxoside was isolated from *Hypoxis hemerocallidea* extract where both were used in the biosynthesis of the corresponding silver nanoparticles (HPX-AgNPs and HHE-AgNPs). The AgNPs were fully characterized using various physicochemical techniques and their antidiabetic, antioxidant, and antimicrobial properties evaluated. TEM revealed sizes of  $24.3 \pm 4$  nm for HHE-AgNPs and  $3.9 \pm 1.6$  nm for HPX-AgNPs. The particles were polycrystalline and showed high stability in the range of -33.3 to -39.8 mV. HHE-AgNPs demonstrated enhanced scavenging properties. HPX-AgNPs displayed better bactericidal effects on *Escherichia coli* and *Salmonella enterica* with MIC value of 1.95 µg/mL, competing well with the standard drug. The study demonstrated the ability of a single phytoconstituent (hypoxoside), not only as the chief bioreductant in the extract but also as a standalone reducing and capping agent, producing ultra-small, spherical and monodispersed AgNPs with enhanced biological properties.

**Keywords:** biofabrication; *Hypoxis hemerocallidea*; characterization; hypoxoside; antimicrobial; antidiabetic; silver nanoparticles; antioxidant

## 5.1 Introduction

The physical and chemical-based synthesis of metallic nanoparticles has limited benefits in biomedical applications due to several disadvantages [1]. Major among them is the use of toxic chemicals like hydrazine. Such hazardous chemicals do not only limit the applicability of the nanoproducts but also have a negative impact on the environment, including a potential threat to aquatic life as the remains are washed down to water bodies [2]. The physical protocols are also faced with demerits like the need for expensive and sophisticated instruments that are unavailable in most laboratories [3]. The biological or green synthesis procedures became a better alternative as environment-friendly solvents are employed, less energy is consumed, simple instruments are sufficient, less time is spent, and small quantities of precursors (plants) are required. In addition, the nanomaterials are biocompatible, and can be applied in various fields including water purification, and biomedical [4]. Interestingly, silver nanoparticles are arguably the most researched metallic nanoparticles. Thousands of studies have been done on biofabrication and characterization of silver nanoparticles (AgNPs). They have been found to possess fascinating antibiofilm [5], anticancer [6], catalytic [7], antioxidant [8], antidiabetic [9], and antimicrobial [10] applications.

Silver nanoparticles have found more biological applications because of the ease of their surface chemistry and biocompatibility. For instance, several silver nanoparticles have demonstrated antioxidant ability when aqueous extracts of *Cassia angustifolia* [8], *Diospyros montana* [11], *Lamprathus coccineus* and *Malephora luteo* [12], *Musa acuminata colla* [13], and *Pisum sativum* [14] were used in their biofabrication. In addition, the alarming rate at which the number of diabetic patients, among the youths, increased, called for renewed attention [15]. Unfortunately, most antidiabetic drugs are not affordable by the common man, necessitating the need for alternatives. Several authors have shown that AgNPs synthesized through the green methods using *Pisum sativum* [14], *Punica granatum* [16], *Tephrosia tinctoria* [17], *Tephrosia tinctorial* [17], *Allium cepa* [18], and *Pouteria sapota* [19] possess antidiabetic properties. Recently, the use of single phytochemicals as reducing/stabilizing agents in the biosynthesis and characterization of metallic nanoparticles (MNPs) with certain bioactivity has gained attention [20-23]. Bacterial infections, which have been with us from time immemorial, is another challenge facing mankind. Although some bacteria are beneficial to humans, the harmful effects on our wellbeing had continued to multiply owing to their resistance to the available antibiotics. Biosynthesized AgNPs using different parts of plants like *Ducrosia anethifolia* [24], *Eulophia herbacea* [10], *Tithonia diversifolia* [25], *Cymbopogon citratus* [26], *Combretum erythrophyllum* [27] and *Diospyros montana* [11], have shown excellent activities against different species of bacteria including the pathogenic types like

*Escherichia coli*, *Staphylococcus aureus*, and *Salmonella typhi* that causes food poisoning and an array of infections.

*Hypoxis Hemerocallidea* (HH) belongs to *Hypoxidaceae*, with a genus of about 90 species out of which 29 are native to South Africa (SA). The plant is widespread in many areas of SA, from the Eastern Cape, through KwaZulu-Natal to Limpopo, Lesotho, and Gauteng. It stretches into Zimbabwe, Mozambique, and parts of eastern Africa [28]. It can be identified by features such as the unique "star-like" yellow flowers. In SA, the plant is locally known as "sterblom" by the Afrikaans community, while the isiZulus call it "inkomfe" and the Sesothos call it "lotsane", while the English name, which is the most popular, is African potato [28]. Extracts of HH have been traditionally employed in the management of diseases like cancer, HIV/AIDS, urinary infections [29], acne, dysentery, dermatitis, wounds, dizziness, testicular tumors, bladder disorders, and high blood pressure [29-30]. The corm is used to treat gall sickness in cattle, psychiatric problems, as a diuretic, and to kill small vermin. The Zulus has used its infusion for many years to cure impotency [32]. HH extracts have also been topically applied to treat skin-related disorders and sexually transmitted diseases such as pimples rash, sunburns, body rashes, sores, boils, gonorrhoea and genital warts [33-36]. The extracts of HH was found to possess anticancer, anti-inflammatory, antineoplastic, anti-infective, antibacterial, antioxidant, antidiabetic, and antifungal activities [30, 35, 37, 40]. To date, only a few compounds have been isolated from this plant. They include sterols and a major constituent, hypoxoside [41-42], that were believed to be responsible for the medicinal properties of the plant.

Despite the huge medicinal value of this plant, little is known about its ability in the modern-day green nanotechnology research. In one instance, a group of researchers have used the constituents of HH in gold nanoparticles synthesis and evaluated their immunomodulatory effects in macrophages and natural killer cells, and their wound healing potential [43-44]. The ability to synthesize other important nanoparticles like platinum and silver have not been studied. Moreover, silver nanoparticles possess superior activities in applications like antimicrobials compared to gold and others [45]. The abundance of its major compound (hypoxoside), that is rather pharmacologically inactive, also calls for its utilization in other forms. Therefore, in this study, biofabrication of AgNPs using HH extract and hypoxoside was undertaken. The resulting AgNPs were fully characterized. A detailed explanation of the involvement of hypoxoside in the green synthesis of the AgNPs was provided for the first time. The variation in the biological activities between the extract- and hypoxoside-mediated AgNPs were also examined.



## 5.2 Materials and Methods

### 5.2.1 Materials and chemicals

Polystyrene 96-well microtitre plates were obtained from Greiner bio-one GmbH (Frickenhausen, Baden-Württemberg, Germany). HPLC grade dichloromethane (DCM), methanol (MeOH), ethyl acetate (EtOAc), and silica gel 60 H (0.040–0.063 mm) particle size were purchased by Merck (Gauteng, Modderfontein, South Africa). Silver nitrate, Iron (III) chloride hexahydrate, 2,4,6-Tris(2-pyridyl)-s-triazine, hydrochloric acid (HCl), alpha-glucosidase (*Saccharomyces cerevisiae*), alpha-amylase (procaïne pancreas), 3,5-dinitro salicylic acid (DNS), p-nitrophenyl- $\alpha$ -D-glucopyranoside (p-NPG), sodium carbonate (Na<sub>2</sub>CO<sub>3</sub>), sodium dihydrogen phosphate, Ceftazidime (CTD), disodium hydrogen phosphate, trolox (6-hydroxyl-2, 5, 7, 8- tetramethylchroman-2-carboxylic acid), 2,2-azino-bis (3-ethylbenzothiazoline-6-sulfonic acid) (ABTS) diammonium salt, Iodonitrotetrazolium chloride (INT), potassium peroxodisulphate, gallic acid, vitamin C, sephadex LH-20, and Sodium Chloride (NaCl) were procured from Sigma-Aldrich (Cape Town, Western Cape, South Africa). Folin-Ciocalteu's phenol reagent was purchased from Boehringer Mannheim GmbH (Mannheim, BW, Germany). Phosphate buffered saline (PBS) was purchased from Lonza (Cape Town, Western Cape, South Africa). Bacterial strains (*Pseudomonas aeruginosa*, *Bacillus cereus*, *Staphylococcus aureus*, *Escherichia coli*, *Serratia marcescens*, and *Salmonella enterica*) were obtained from Microbiology laboratory, Department of Medical Biosciences, University of the Western Cape, South Africa. Brain-Heart infusion broth (BHI) and Muller Hinton Agar were purchased from Biolab (Merck, Modderfontein, South Africa).

### 5.2.2 Isolation of hypoxoside

The HH bulb weighing 374.0 g was rinsed with running tap water to remove the sand after which it was cut into smaller pieces. Using a water bath at 60 °C, the pieces were added to 1L methanol in an extraction bottle and extracted for 48 h. Fresh methanol was added several times and the filtrate pulled together, concentrated under reduced pressure to give 97.20 g of a dark brown methanol extract. About 90.0 g of this was subjected to silica gel column chromatography, collecting batches of fractions in DCM, EtOAc, and MeOH. Subsequent purification of the hypoxoside-containing fraction was achieved when 5.0 g of the EtOAc fraction was subjected to another chromatography on Sephadex LH-20 using methanol and water in a 1:1 (v/v) ratio. The pure hypoxoside was isolated with the aid of preparatory High-Performance Liquid Chromatography (Waters, Milford, MA, USA) equipped with a Quaternary Gradient Module pump (Waters 2535) and a manual injector with variable wavelength detector (Waters 2489). A mixture of methanol and water in the

ratio 1:1 (v/v) was used for elution while the flow rate was set at 5.0 mL/min using a C18 YMC column (5 $\mu$ M, 250 x 30 mm). The structure of the compound was confirmed using NMR spectroscopy and compared with literature.

### **5.2.3 Biofabrication of HHE-AgNPs and HPX-AgNPs**

Before the synthesis, 30 mg each of HHE and HPX was suspended in 3000  $\mu$ L of ultra-pure deionized water and agitated until homogenous brownish and yellowish solutions were obtained respectively. Thereafter, 2000  $\mu$ L of each aqueous solution was added to 100 mL of 1 mM silver nitrate (AgNO<sub>3</sub>) solution and heated at 60 °C with continuous stirring in the dark for 1h. A change of colour to dark brown and pale yellow indicated the formation of HHE- and HPX-AgNPs respectively. The Ultra-violet Visible spectroscopic measurement of the biofabricated AgNPs was carried out with the aid of a plate reader (BMG Labtech, Ortenberg, Germany).

### **5.2.4 Characterisation**

Nuclear Magnetic Resonance (NMR) spectra were obtained using a Bruker spectrometer operating at 400 (for H)/100 (for C) MHz. High-Resolution Transmission Electron Microscopy (FEI Tecnai G2 F20 S-Twin HRTEM, operating at 200 kV) was employed to study the morphology, and crystallinity of the AgNPs. The sizes of the nanoparticles were calculated by counting and measuring the particles using software such as ImageJ. X-ray diffraction (Bruker AXS D8 advance diffractometer with CuK $\alpha$ 1 radiation ( $\lambda$  = 1.5406 Å)) was employed to study the crystal structure of the biofabricated AgNPs. A Malvern Zetasizer Instrument (Malvern Ltd., Worcestershire, United Kingdom) operating at an angle of 25 and 90 degrees was used to obtain information on the hydrodynamic size, polydispersity index, and zeta potential of the AgNPs. Solutions of HHE-AgNPs and HPX-AgNPs were measured in disposable quartz cuvettes upon cooling to room temperature.

### **5.2.5 In-vitro Enzymatic assay**

#### **5.2.5.1 Alpha-amylase inhibitory activity**

A standard protocol was employed where 50  $\mu$ L of phosphate buffer (0.01 M, pH 6.9), 20  $\mu$ L of procaine pancreatic alpha-amylase (2U/mL) solution, and 20  $\mu$ L of the samples were all added in a 96-well plate and incubated for 20 min at room temperature. After this pre-incubation, 20  $\mu$ L of 1% soluble starch was added to the mixture and incubated for an additional 30 min. This was immediately followed by the addition of 100  $\mu$ L of 3,5-dinitro salicylic acid (DNS) which stopped the reaction. The reaction mixture was then incubated

in a boiling water bath for 10 min before the absorbance was read at 540 nm. Acarbose was used as the standard and each experiment was done in triplicate [46]. Equation (1) was used to calculate the percentage inhibition of the alpha-amylase activity.

$$\text{Percentage inhibition (\%)} = \left( C - \frac{T}{C} \right) * 100 \quad (2)$$

where C and T are absorbance readings of the control and the treated sample, respectively.

### **5.2.5.2 Alpha-glucosidase inhibitory activity**

A standard procedure of the alpha-glucosidase assay was followed with slight modification [47]. Briefly, 20 µg/mL of the silver nanoparticles were serially diluted in a 96-well plate using a 100 mM phosphate buffer (PBS) at pH 6.8. The mixture was gently agitated and allowed to stand for 15 min at 25 °C. Thereafter, 20 µL of a 5 mM *p*-nitrophenyl- $\alpha$ -D-glucopyranoside (*p*-NPG) was added as the substrate and the plate was incubated at 37 °C for 20 min. Hereafter, 50 µL of a 0.1 M sodium carbonate (Na<sub>2</sub>CO<sub>3</sub>) solution was added to each well to stop the reaction. With the aid of a plate reader, the absorbance measurement was then taken at 540 nm. The wells with enzyme, buffer, and substrate but without samples served as positive controls and each experiment was conducted in triplicate. The percentage inhibition of the enzymatic property of alpha-glucosidase was determined using Equation (1) in section 5.2.5.1.

### **5.2.6 Antioxidant activity**

#### **5.2.6.1 Ferric Reducing Antioxidant Power (FRAP) assay**

FRAP was conducted according to the procedure of Pu et al. [48] with slight changes using a microtiter plate. Briefly, 10 µL of the sample or standard was added to a well, followed by 300 µL of FRAP reagent. The mixture was allowed to stand for 30 mins at room temperature (25 °C) before the absorbance was measured at 593 nm. Vitamin C was the standard and its curve was used in determining those of the AgNPs.

#### **5.2.6.2 Total Phenolic Content (TPC)**

The TPC of HHE- and HPX-AgNPs were carried out in a 96-well microtiter plate following the modified method described by Nasar et al. [49]. In brief, 25 µL of the sample or standard was added to a well, followed by 125 µL of Folin reagent. Thereafter, 100 µL of

Na<sub>2</sub>CO<sub>3</sub> was added to each well. The mixture was allowed to stand for 2 h at room temperature (25 °C) before the absorbance was measured at 765 nm. Gallic acid (GA) was the standard and its curve was used in quantifying the TPC of the AgNPs, expressed in milligram equivalent of GA.

#### **5.2.6.3 2,2'-azino-bis-3-ethylbenzotiazolin-6- sulfonic acid (ABTS) assay**

The assay was carried out following the slightly modified method of Pu et al. [48]. Briefly, 25 µL of the standard (Trolox) and samples were added to a 96-well plate followed by the ABTS reagent. The reaction mixture was allowed to stand for 30 min before the absorbance was read at 734 nm. The ABTS reagent was prepared 30 min before the experiment at 70 °C. The assay was repeated two more times. The results were expressed as mM Trolox equivalents per Gram sample (mM TE/g).

#### **5.2.7 Antimicrobial activity of silver nanoparticles**

The method described by Shao et al. [50] was used with slight modification. Briefly, Brain-Heart infusion broth (BHI) was employed for serial dilution of both HHE- and HPX-AgNPs into the concentration of 125.00, 62.50, 31.25, 15.63, 7.81, 3.90, and 1.95 µg/mL. Bacterial strains in PBS were standardized to 0.5 McFarland equivalent and further diluted in BHI. Three controls were used; 200 µL of BHI, 200 µL of sterilized deionized water and a mixture of 100 µL of the test organism and 100 µL of sterilized deionized water. After 24 hrs incubation, 40 µL of INT was added and sealed to avoid evaporation and then incubated for 2 hrs after which a colour change took place. A clear BHI-like colouration indicates the death of bacteria whereas a turbid or pinkish colour shows growth. The MIC refers to the lowest concentration of AgNPs that completely inhibits bacterial growth. All tests were done in triplicate. Ceftazidime, which was prepared like the AgNPs, was employed as positive control. The selected bacteria were wild types.

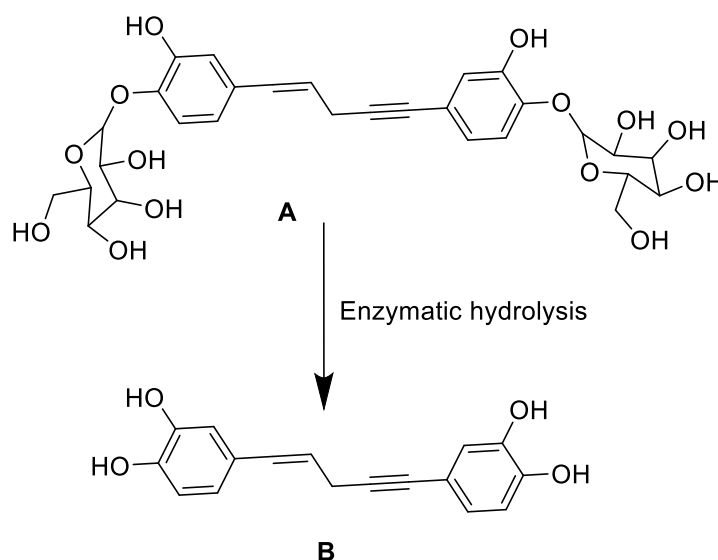
#### **5.2.8 Statistical analysis**

The results of the bioactivities were analysed using two-way ANOVA followed by post hoc Tukey's multiple comparisons test using GraphPad Prism software version 6.05 for Windows (GraphPad Software, La Jolla, CA, USA ([www.graphpad.com](http://www.graphpad.com))).

## 5.3 Results and discussion

### 5.3.1 Isolation, characterization and properties of hypoxoside

Hypoxoside [(E)-1,5-bis(4'- $\beta$ -D-glucopyranosyloxy-3'-hydroxyphenyl) pent-4-en-1-yne] is a glycosylated norlignan that is the major compound found in the corm of HH [37]. Its isolation from HH extract has been reported previously [44, 51] and our spectra correlate with those of previous authors. Hypoxoside has a low toxicity with an uncommon aglycon structure. It is composed of two glucose units at the edges of the two benzene rings in the pentenyne skeleton (Scheme 5.1A) [28]. However, hypoxoside was found to be pharmacologically inactive on its own but is usually converted to its aglycon, rooperol, through hydrolysis of the former by the action of a  $\beta$ -glucosidase enzyme in the human gut (Scheme 5.1) [38]. Rooperol, on the contrary, has fascinating biological activities like anti-inflammatory, anticancer [52] antibacterial, immunomodulatory, antioxidant, antitumor, and anti-convulsant activities [53]. Therefore, there is a need to find other ways by which hypoxoside can be more valuable, especially looking at its quantity from HH extract. One study has utilized hypoxoside in the synthesis of gold nanoparticles [44], but more can be achieved. Hence this study to use the hypoxoside in the green synthesis of AgNPs and to fully characterize it for the first time.



**Scheme 5.1: Chemical structure of hypoxoside (A) and its aglycon, rooperol (B) upon hydrolysis**

### 5.3.2. Biofabrication of HHE-AgNPs and HPX-AgNPs

The success of the biofabrication of HHE-AgNPs and HPX-AgNPs was first observed upon a colour change to brown (Figure 5.1A(i)) and pale yellow (Figure 5.1B (ii)) respectively. While the brownish colour deepens for HHE-AgNPs in the 15 mins of the reaction, the pale yellowish colour remained unchanged for HPX-AgNPs. The stirring of reaction mixture was continued for another 60 mins even as the heat was turned off until it assumed room temperature. The visual difference in colour observed is a result of different phytochemicals serving as the bioreductants in each of the aqueous solutions [54]. The total extract, HHE, composes of many biomolecules, each of which might have participated in the reduction of silver ions to form HHE-AgNPs, while only one participated in HPX, a solution of a single phytochemical (hypoxoside). The development of colour which signifies the formation of a new product is due to the excitation of surface plasmon oscillations in the reduced silver brought about by the bioreductants in the aqueous solutions of HHE and HPX [54].

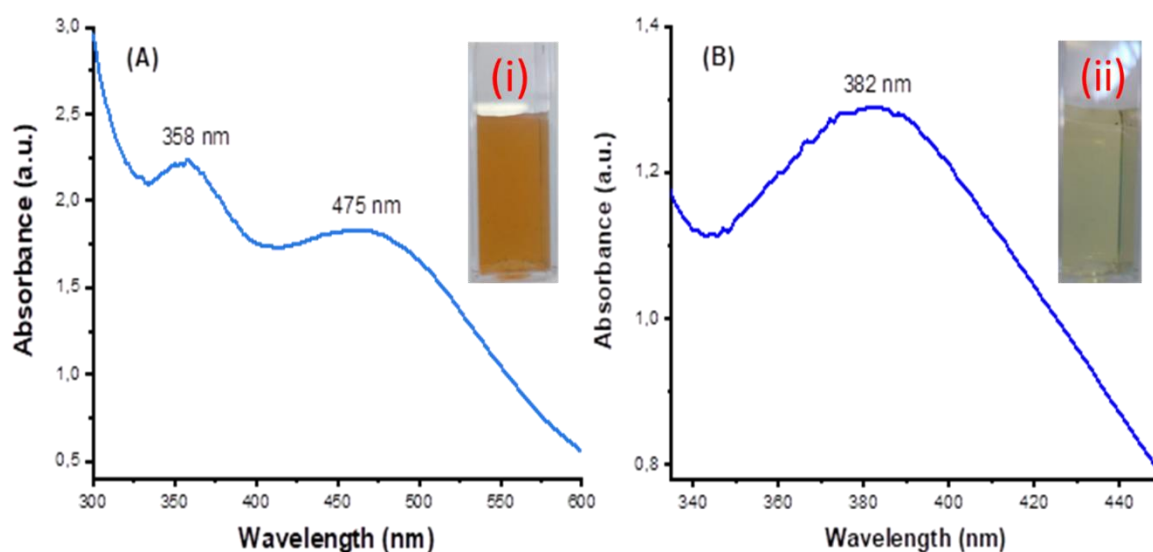


**Figure 5. 1: UV-Vis spectra of (A) HHE-AgNPs and (B) HPX-AgNPs. The insets (i) and (ii) represents the colour of the HHE-AgNPs and HPX-AgNPs respectively.**

The biofabricated HHE-AgNPs showed absorbance at two regions (358 and 475 nm) (Figure 5.1A) whereas HPX-AgNPs displayed its maximum absorption at 382 nm (Figure 5.1B). The plasmonic resonance of AgNPs is sharp and more intense when compared to the other metals like gold because of the difference in the dielectric properties emanating as a result of the slight overlap between the surface plasmon resonance and series of inter-band transitions in silver which begins at 320 nm [55]. Similar plasmonic behaviour to

the HHE-AgNPs shown here was reported by Amendola et al., where two resonance bands appeared at 350 and 450 nm in their studies. Sosa et al. [56] demonstrated the occurrence of two resonance bands between 320 and 500 nm in their work. They added the possibility of a third peak which was referred to as a tail. However, what was not clear was that, while they attributed the bands around 350 nm to spheres, Amendola and colleagues believed it to be due to the presence of cylindrical silver nanoparticles [55-56]. In the present study, the two SPR was due to the presence of both spheres and cylinders and scanty appearance of cones as would be further explained by TEM analysis.

Because of their symmetry, silver nanoparticles with spherical shapes possess only one plasmonic resonance [55, 57]. This appeared to be the case with HPX-AgNPs having a surface plasmon resonance centered at about 382 nm. El-Naggar and colleagues reported AgNPs that absorbs at about the same wavelength to our HPX-AgNPs [58]. Also, using *Elaeagnus umbellata* extract, Ali and co-workers reported AgNPs with absorption at 398 nm [59]. Other researchers have also reported silver nanoparticles whose plasmonic resonance falls between 300-800 nm [60-61]. The above authors showed that the particles were mostly spherical in shape. It is believed that mono or multi-polar excitations may be dependent on certain features like the nature of the material, the geometry, and the size of the nanoparticles being evaluated [56].

### **5.3.3. Morphology and size of HHE-AgNPs and HPX-AgNPs**

In addition to the two SPR observed in the UV-Vis analysis, the TEM micrographs of HHE-AgNPs (Figure 5.2E, G) indicates a mixture of shapes, mainly spheres and a few cylindrical shapes. The nanoparticles also appears to aggregate. Previous studies [43] have reported various shapes when they used an aqueous extract of HH in synthesizing gold nanoparticles. The presence of different phytoconstituents in the aqueous extract of HH might have resulted in the emergence of a mixture of shapes in HHE-AgNPs [62]. When plant extracts are employed in green synthesis of metallic nanoparticles, a strong interactive forces between the bioreductants serving as stabilizing agents and the nanoparticles' surfaces keeps them in solution [63]. Therefore, the appearance of a mixture of shapes in HHE-AgNPs was due to the contribution by other bioreductants that might be adsorbed on the surface of the silver nanoparticles.

The HPX-AgNPs were more monodispersed and mostly spherical (Figure 5.2B, D). This may be because of the purer nature of the reducing agent [64].

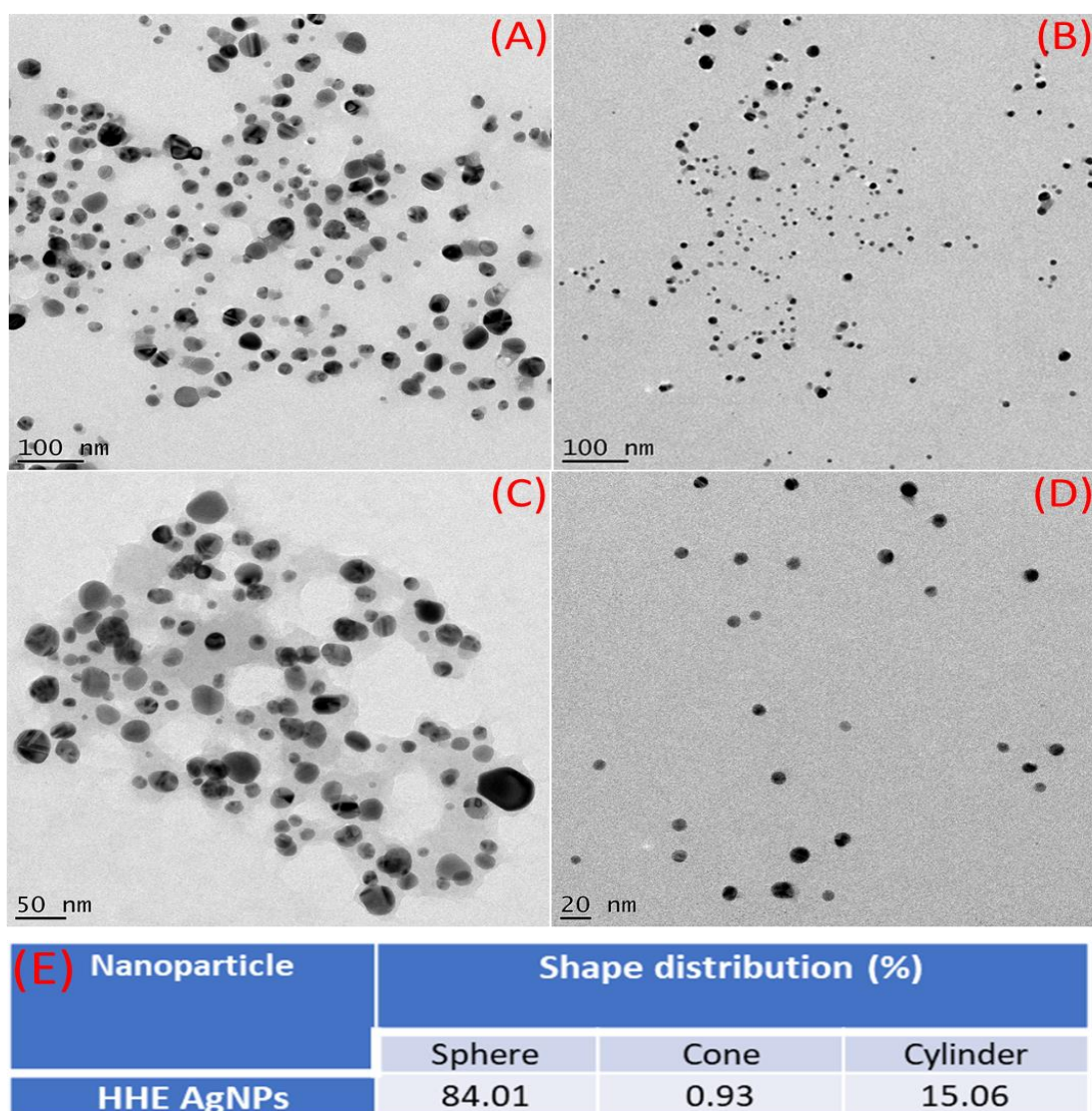


**Figure 5. 2: High-Resolution transmission electron microscopy images showing the morphology of (A, C) HHE-AgNPs and (B, D) HPX-AgNPs. (E) shows that HHE-AgNPs consist of various shapes with spheres dominating as indicated in the table. OTHER HRTEM images used for evaluation of size and shape of HHE-AgNPs was included in Appendix M**

The mean particle sizes of  $24.3 \pm 4$  nm and  $3.9 \pm 1.6$  nm were obtained for HHE-AgNPs and HPX-AgNPs (Figure 5.3A, B) respectively. This is in line with the particles presented in TEM micrograph. More aggregates were observed in the HHE-AgNPs, thereby responsible for the bigger sizes. The UV-Vis analysis earlier suggested that the bigger sizes might be due to mixtures and aggregates. Although the spheres predominate (84.01 %), there was a reasonable percentage (15 %) of the cylindrical shapes. A small fraction of other shape (cone) also made about 0.93 %. The cylinders have a length of 2.26 - 20.58 nm while the diameter ranges from 1.81 to 13.61 nm. Literature has demonstrated that nanoparticles of different sizes and shapes behave differently. In applications like antimicrobials, AgNPs with smaller sizes and other morphologies have been reported by researchers to show



better bactericidal activities over their counterparts [65]. Silver nanoparticles with similar particle size distributions were biosynthesized using the extract of *Litchi chinensis* [66]. Also, using *Sida cordifolia* aqueous extract, Pallela and colleagues have reported a green synthesis of ultra-small, monodispersed silver nanoparticles [67]. Other small sized AgNPs have been reported such as 2.9 nm [68], 3-20 nm [69], 3.1 nm [70], and 4-16 nm [71]. Therefore, the particle size distribution in the present study agrees with the size range earlier reported by other scientists. In addition, it is worthy of note that when single compounds/phytochemicals are employed in MNPs synthesis, small-sized and spherical shaped NPs often results according to several authors [50]. Hypoxoside therefore, successfully mediated the green synthesis of quasi-spherically shaped silver nanoparticles with ultra-small sizes.

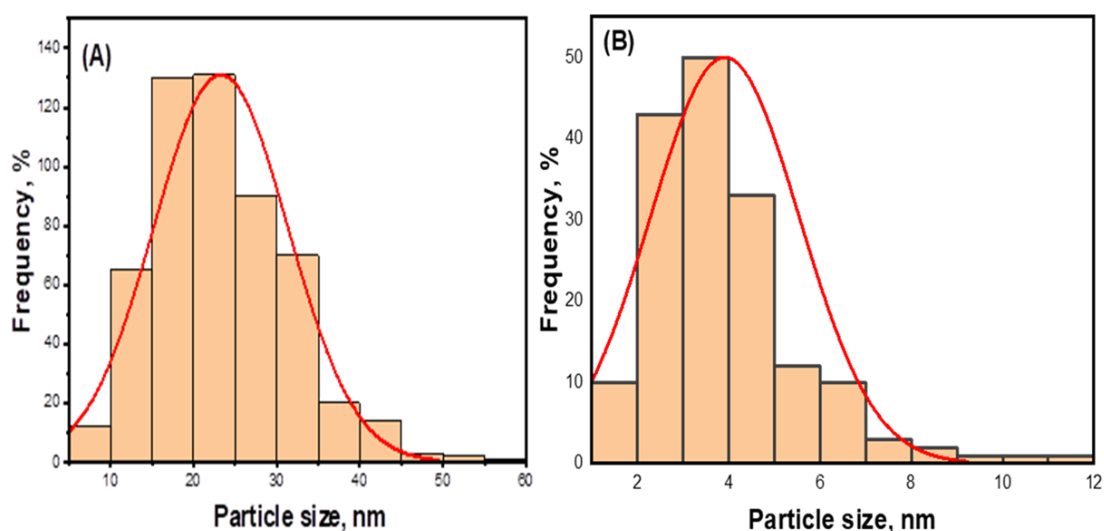


**Figure 5. 3: Histogram displaying the particle size distribution of (A) HHE-AgNPs and (B) HPX-AgNPs**

#### 5.3.4. The crystallinity of HHE-AgNPs and HPX-AgNPs

The x-ray diffraction (XRD) analysis (Figure 5.4) show the approximate 2 theta degree values of 38, 44, 64, and 77 obtained for both HHE-AgNPs (A) and HPX-AgNPs (B), which can be indexed to the (111), (200), (220), and (311) planes of the face-centered cubic structure of silver [72, 73], as per the JCPDS card no. 04-0783, and in agreement with the results from others using aqueous extracts of *Rosa chinensis L.* [73], *Tectona grandis seed* [74], *Sida cordifolia* [67], and *Solanum lycopersicum* [75]. The selected area electron diffraction (as given in figure 5.4 C, D), shows circular rings which corroborate the XRD patterns of the respective silver nanoparticles [74].

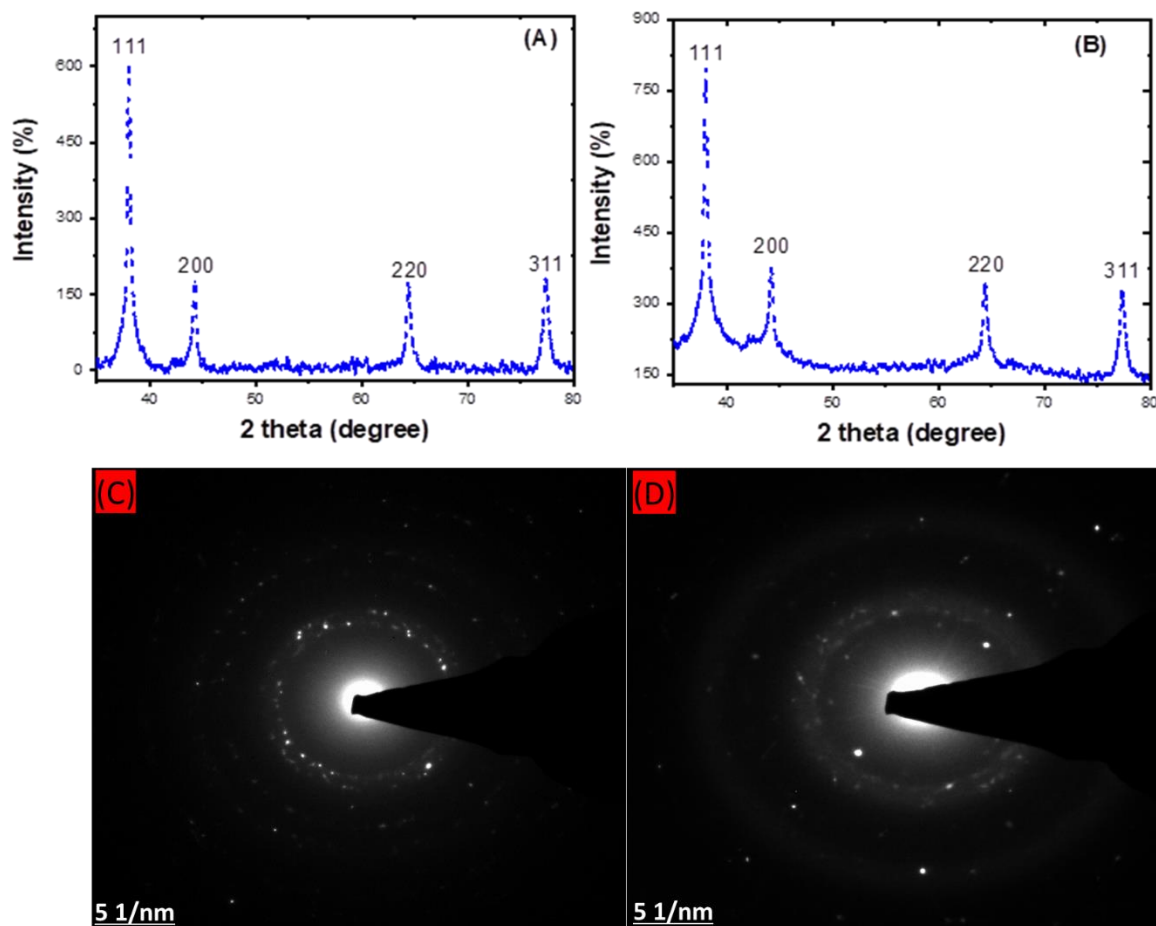


**Figure 5. 4:** X-Ray Diffraction patterns showing the diffraction peaks of (A) HHE-AgNPs (A) and (B) HPX-AgNPs. C and D shows the selected area electron diffraction of the respective HHE-AgNPs and HPX-AgNPs

### 5.3.5. Dynamic Light Scattering

Dynamic Light Scattering (DLS) measures the hydrodynamic size of colloids, which gives a rough estimate of the average size of the particles embedded in the solution. The hydrodynamic size (HDS) was found to be 53.57 nm and 33.94 nm for HHE-AgNPs and HPX-AgNPs (Figure 5.5A, B) respectively. The results implied that the size of the HHE-AgNPs is relatively larger than those in HPX-AgNPs. This might be explained by the number and/or type of constituents present in the reducing agents of HHE-AgNPs and HPX-AgNPs. It is evident that while HHE is a mixture of different phytochemicals, HPX is a solution of hypoxoside bearing different functional groups. The difference in the HDS of the nanoparticles has been supported by both UV-Vis and TEM analysis, showing agreement of results. Additionally, larger particles scatter much more light than the smaller ones. This may account for the bigger HDS possessed by HHE-AgNPs over HPX-AgNPs. In colloidal solutions, larger particles are so dominating that even a small number can obscure the contribution of the smaller particles however their number. However, it is noteworthy that

the size measured by DLS technique is often different from that of TEM [76]. This is because the size relates to the metallic core of the nanoparticles. The size is also influenced by all the substances surrounding the surface of the nanoparticles such as the capping agents and the thickness of solvation shell, moving along with the particles. The thickness of the solvation shell as well as its influence on the size of measured nanoparticles is, in turn, dependent on the nature of the substances in the colloidal suspension and on the surface of the nanoparticles. Hence, the size measured by the DLS technique was bigger than that measured by TEM [77]. Additionally, the difference in size is also due to the instrument used since different instrument uses specific operation techniques.

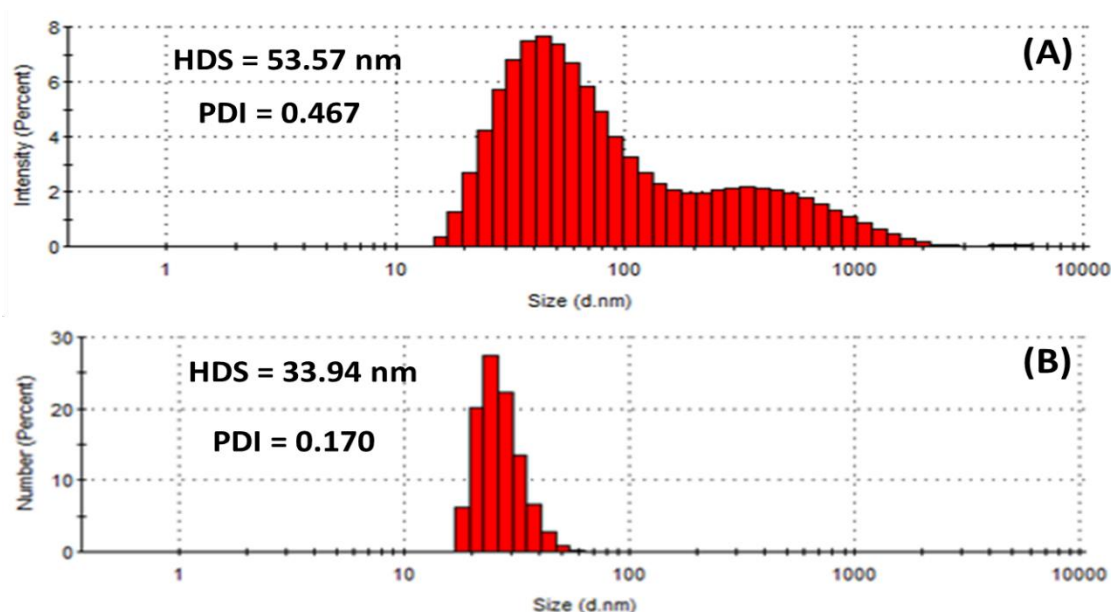


**Figure 5. 5: Hydrodynamic size (HDS) and polydispersity index (PDI) showing the population of particles in (A) HHE-AgNPs, and (B) HPX-AgNPs**

Similarly, the polydispersity index (PDI) of HHE-AgNPs (0.467) differs greatly with that of HPX-AgNPs (0.170) as provided in Figure 5.5. PDI is also known as the heterogeneity index. PDI is unitless. It is a measure of non-uniformity of particles in each colloidal solution. Different algorithms have been used but the standard one considers values between 0.05-0.7 [78]. Colloidal solutions with PDI values close to 0.05 are deemed extremely monodispersed, meaning that almost a hundred percent of the particles are of the same shapes whereas solutions with values close to 0.7 are considered heterogenous, implying that the colloid contains particles of different shapes. In the light of this, it can be observed that an almost 0.5 PDI recorded is tending towards the other end of the standard scale (0.7) which means that HHE-AgNPs contained a good number of particles of various shapes. Additionally, the bimodal nature of the population (Figure 5.5A) also points to this

fact. Conversely, the unimodal population in the case of HPX-AgNPs (Figure 5.5B) is justifiable by the PDI value of 0.170. The above findings are in good agreement with the results of UV-Vis, TEM and HDS (Figure 5.1C, D).

Another key detail of the colloidal solution that can be obtained through DLS measurement is the zeta potential. The zeta potential (ZP) has to do with the charges surrounding the surface of nanoparticles and has been employed by many researchers to evaluate the stability of colloidal suspensions [43, 79]. In this study, ZP values of -39.8 mV and -33.3 mV were obtained for (A) HHE-AgNPs and (B) HPX-AgNPs respectively (Figure 5.6), indicating that highly stable silver nanoparticles were fabricated. Of interest is the fact that external stabilizers were not involved, meaning that the phytochemicals served both the purpose of reducing the silver ions to silver of zero charge as well as stabilizing the silver nanoparticles upon formation. Previous studies have reported similar ZP values for silver nanoparticles [80-83].

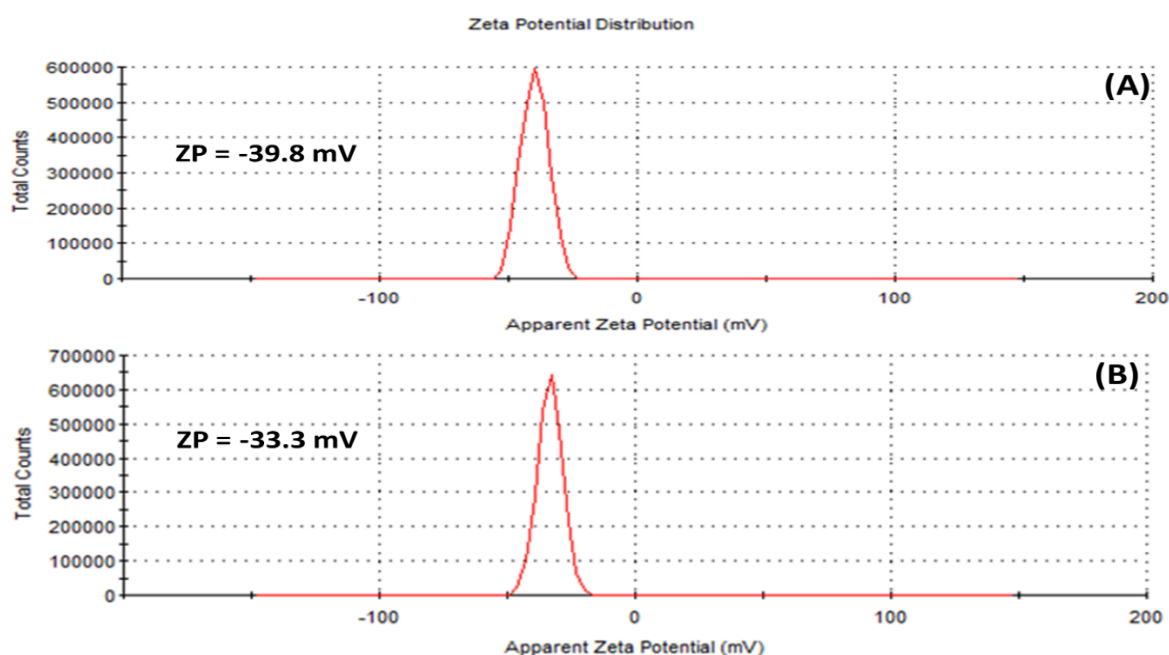


**Figure 5. 6: Zeta potential of (A) HHE-AgNPs, and (B) HPX-AgNPs. The zeta potential values indicate the surface of the nanoparticles were covered with negative ions**

### 5.3.6. Biological activities

#### 5.3.6.1. Antidiabetic activities of HHE-AgNPs and HPX-AgNPs

The inhibition of alpha-glucosidase and alpha-amylase enzymes is one of the ways through which the hypoglycaemic effects of a substance/drug can be tested. As it relates

to diabetes, this *in vitro* studies have been used to show how the glucose level in the body can be affected by the test samples [84]. As shown in Table 5.1, the results imply that alpha-glucosidase was sufficiently inhibited by both HHE-AgNPs and HPX-AgNPs. The high alpha-glucosidase activity displayed by the AgNPs indicates that they possess an antidiabetic potential that may require further investigations. Despite this, it could be observed that the inhibitory activity of HHE-AgNPs was higher than that of HPX-AgNPs against alpha-glucosidase. While no significant inhibition was observed at the test concentrations of HHE-AgNPs against alpha-amylase, interesting inhibition was recorded for HPX-AgNPs. However, it was not as good as that recorded by acarbose. Similar to our findings, Vishnu Kiran and Murugesan reported an IC<sub>50</sub> value of 26.20 for alpha-amylase when AgNPs were biosynthesized using the extract of *Halymenia poryphyroides* [84]. The IC<sub>50</sub> of the alpha-glucosidase was, however, comparatively higher (33.20) than our finding. This may be due to the difference in the mechanism of action. Other similar enzymatic inhibition to those reported here have been documented in previous studies of AgNPs biosynthesized from plants [9, 16, 19, 85-86]. MNPs formed from single phytochemicals with potential antidiabetic activities have also been reported [20-21, 23]. Previous studies have also reported the antidiabetic potential of methanol extract of *Hypoxis hemerocallidea*. It showed a potent antidiabetic activity as it inhibits alpha-amylase enzyme to about 90% [87]. This further supports the activity reported in the present trial. Overall, the AgNPs possess the ability to inhibit the enzymes suggesting them as good candidates for diabetes management.

**Table 5.1: The IC<sub>50</sub> values of the antidiabetic activities of *Hypoxis hemerocallidea* extract, hypoxoside, HHE-AgNPs and HPX-AgNPs in micro gram per litre (µg/mL).**

<i>Antidiabetic activities of silver nanoparticles</i>		
<i>Items</i>	<i>Alpha-glucosidase</i>	<i>Alpha-amylase</i>
<i>HHE</i>	26.86 ± 0.7	19.43 ± 0.8
<i>HHE-AgNPs</i>	51.42 ± 0.8	46.34 ± 1.2
<i>HPX</i>	62.01 ± 1.5	55.43 ± 0.9
<i>HPX-AgNPs</i>	29.27 ± 0.7	26.06 ± 1.1
<i>Acarbose</i>	18.58 ± 1.5	10.20 ± 0.4

Acarbose: positive control. The results are expressed as mean ± SD for *n* = 3.

### 5.3.6.2. Antioxidant activities of HHE-AgNPs and HPX-AgNPs

Materials with both antioxidant and other potential activities are of great benefit, necessitating the need to search for antioxidants with enhanced reducing abilities [88-89]. Antioxidants are substances that can inhibit or delay the oxidation of a substrate when present in low concentrations. To evaluate the antioxidant potential of a given material,

standard methods such as FRAP, TPC, and ABTS are among the assays often employed. Different reaction mechanisms are involved. FRAP operates by a mechanism known as single electron transfer (SET), whereby an antioxidant transfers an electron to the corresponding cation which would neutralize it, whereas ABTS is largely operating on hydrogen atom transfer (HAT) [90]. TPC measures the antioxidant powers of materials based on their phenolic content. Like the metal-reducing ability of plant extracts, the antioxidant activity has been associated with the plants' phenolics [91]. Pu and colleagues argued that antioxidants possess free radical scavenging properties; hence, they play a role in promoting health and preventing diseases [48]. The antioxidant activities of the AgNPs in this study has been presented in Table 5.2.

**Table 5.2: The antioxidant activities of HHE-AgNPs and HPX-AgNPs. The three assays compared the antioxidant properties of the two silver nanoparticles**

Antioxidant activities of silver nanoparticles			
ITEMS	FRAP ( $\mu\text{M AAE/g}$ )	ABTS ( $\mu\text{M TE/g}$ )	TPC ( $\mu\text{M GAE/g}$ )
HHE	1123.6 $\pm$ 4.2	818.6 $\pm$ 2.5	650.8 $\pm$ 6.3
HHE-AgNPs	4711.6 $\pm$ 6.7	635.1 $\pm$ 3.2	134.2 $\pm$ 7.7
HPX	860.1 $\pm$ 3.4	817.8 $\pm$ 4.7	414.5 $\pm$ 5.6
HPX-AgNPs	2497.3 $\pm$ 8.4	580.6 $\pm$ 6.4	120.8 $\pm$ 1.8
Standard	3976.8 $\pm$ 3.8	7525.0 $\pm$ 4.9	2367 $\pm$ 4.2

From the table, interesting activities were recorded for the two AgNPs. However, across the different methods, the HHE-AgNPs displayed more scavenging ability; HHE-AgNPs showed about a 2-fold scavenging potential over HPX-AgNPs for FRAP, and slightly higher activities could be observed for ABTS and TPC. This is expected as the antioxidant activities are believed to be associated with the functional groups of phytoconstituents, mostly the polyphenols, that are equally largely involved in the reduction and subsequent stabilization of the biofabricated AgNPs [92-93]. The many other phytoconstituents present in HHE-AgNPs compared to the single phytoconstituent present in HPX-AgNPs, could explain the higher antioxidant activities observed in the former. To further support our findings, Mittal and colleagues have shown that, in their antioxidant studies of silver/selenium nanoparticles using quercetin and gallic acid, the antioxidant activities of pure quercetin and gallic acid were higher than those of the corresponding nanoparticles from the two assays (ABTS and DPPH). It means that the functional groups in those compounds have participated in the nanoparticle formation thereby leaving only fewer

ones [92]. In addition, green synthesized nanoparticles of *Cassia angustifolia*, *Alcea rosea*, and *Chamaecostus cuspidatus* have demonstrated potent antioxidant activities [8, 91, 94].

### 5.3.6.3. Antimicrobial studies of HHE-AgNPs and HPX-AgNPs

Common pathogenic bacteria such as *Escherichia coli* and *Salmonella enterica* are known to cause food poisoning, whereas *Staphylococcus aureus* causes a series of infections like pneumonia, boils, wound infections, and cellulitis. Bacterial infections are contagious and can be complicated in some instances, especially with individuals having a compromised immune system due to diabetes, and other deadly diseases. Antibiotic resistance has become a global challenge for a long time, affecting both the health and economy of the world [49]. Therefore, in the search for alternatives, green nanotechnology has drawn attention as MNPs have displayed fascinating inhibitory activities against many pathogenic bacterial strains [95]. Silver NPs have been used as a top antibacterial agent against various bacterial strains because of its unique characteristics [27, 45]. In this study, both Gram-positive and Gram-negative bacteria were employed to evaluate the inhibitory ability of the synthesized AgNPs. From Table 5.3, the inhibitory ability of both HHE- and HPX-AgNPs followed a similar pattern for gram-positive bacteria since they inhibited *P. aeruginosa* and *S. aureus* at the same MICs. A similar trend could be observed for *B. cereus* except that HPX-AgNPs showed a one-fold higher activity compared to HHE-AgNPs. In general, their activities against this set of organisms was at higher MIC compared to the MIC of the standard. Singh and colleagues [96] explained that AgNPs demonstrated more inhibition on the gram-negative strains of bacteria than the gram-positive counterpart which may make it difficult for the particles to penetrate due to the thicker cell walls of the latter. On the other hand, of the three gram-negative bacteria tested, only *S. marcescens* demonstrated weak activities (125.00 µg/mL) for HHE- and HPX-AgNPs when compared to the standard drug. Similar activity was displayed by HHE-AgNPs against *S. enterica*, while HPX-AgNPs showed a distinct inhibitory activity to the equivalent MIC of the standard (1.95 µg/mL). As for the *E. coli*, HHE-AgNPs showed moderate inhibition with MIC of 31.25 µg/mL, which was also the best activity of the HHE-AgNPs in the study. However, its counterpart, HPX-AgNPs displayed a very high inhibition on *E. coli* with the same MIC of the standard drug.

**Table 5.3: Minimum inhibitory concentration of the antimicrobial activities of AgNPs using six bacterial species. The activity of Ceftazidime as the standard was also included ( $\mu\text{g/mL}$ )**

Antimicrobial activities of silver nanoparticles			
Bacteria species	HHE-AgNPs	HPX-AgNPs	CTD
<i>P. aeruginosa</i>	62.50	62.50	1.95
<i>S. aureus</i>	125.00	125.00	1.95
<i>B. cereus</i>	62.50	31.35	1.95
<i>S. enterica</i>	125.00	1.95**	1.95
<i>S. marcescens</i>	125.00	125.00	1.95
<i>E. coli</i>	31.25	1.95**	1.95

CTD: Ceftazidime, HHE-AgNPs: Hypoxis hemerocallidea extract mediated silver nanoparticles, HPX-AgNPs: Hypoxoside mediated silver nanoparticles. \*\*: MIC values equal to those of the standard drug used

Overall, the best activity from both HHE-AgNPs and HPX-AgNPs was displayed against *E. coli*. This behaviour has literature backing from previous studies [49]. The 3-fold enhanced activity of HPX-AgNPs over HHE-AgNPs, in this case, might be due to the difference in size and morphology between the two. Previous evaluations have shown that AgNPs with smaller sizes possess better antibacterial activities when compared to those of bigger sizes [50, 65]. Alginate-mediated silver nanoparticles displayed distinct antimicrobial activity against *E. coli* with a very low MIC value. The authors attributed these activities to the small size and spherical nature of the AgNPs [50]. When three polyphenols namely naringin, hesperidin, and diosmin were employed in silver nanoparticle formation, the naringin-AgNPs displayed better antibacterial activity than others which was linked to the small size and monodispersed nature of naringin-AgNPs compared to the large and polydispersed form of the AgNPs from hesperidin and diosmin [97]. Other researchers also showed that AgNPs between the sizes of 1-12 nm disrupted the external cell membrane of *E. coli* and caused cell death [98-99]. Hence, the smaller HPX-AgNPs shows predominantly higher activity than the HHE-AgNPs. The smaller the size, the more the particles can penetrate the cell wall, which leads to more cell death.

#### 5.4 Conclusions

A facile, cost-effective, and eco-friendly protocol led to the biofabrication of HHE- and HPX-AgNPs. The AgNPs were fully characterized using UV-Vis, TEM, SAED, HDS, PDI, ZP, and XRD. The silver nanoparticles were found to possess antioxidant, antidiabetic, and antimicrobial activities. The study demonstrated, for the first time, that the constituents of HHE possess the required functionality that aided the successful green synthesis of silver nanoparticles. The study also shows the involvement of hypoxoside as a single



phytochemical serving as the bio-reductant and stabilizer in both HHE- and HPX-AgNPs. Because of its unique characteristics, the smaller, spherical, monodispersed and stable HPX-AgNPs displayed enhanced antimicrobial activities against *E. coli* and *S. enterica* while HHE-AgNPs showed more scavenging abilities. A pharmacologically inactive hypoxoside may be a useful ingredient in the preparation of future antimicrobials. Further studies are, however, recommended.

### **Author Contributions**

Conceptualization, A.A.H, S.S.B. and U.M.B.; methodology, U.M.B.; software, U.M.B. and S.S.B.; investigation, U.M.B.; resources, A.A.H.; data curation, S.S.B.; writing—original draft preparation, U.M.B.; writing—review and editing, U.M.B, S.S.B. and A.A.H.; visualization, U.M.B.; supervision, S.S.B. and A.A.H; project administration, A.A.H.; funding acquisition, U.M.B. and A.A.H. All authors have read and agreed to the published version of the manuscript.

### **Funding**

A 2016 Tertiary Education Fund (TETFUND) intervention awarded to U.M.B in Ibrahim Badamasi Babangida University, Lapai, Nigeria was used for the research. It was also supported by a research fund (106055) awarded to Professor Ahmed Mohammed of Cape Peninsula University of Technology by National Research Foundation.

### **Acknowledgments**

We would like to thank Profs Jeanine L. Marnewick and Charlene W.J. Africa for space and resources, Dr Jelili A. Badmus, Fanie Rautenbasch, Charnice Mouton, Keith and Luzell for assistance during biological activities.

### **Conflicts of Interest**

The authors declare no conflict of interest.

## References

- [1] S. A. Aromal, V. K. Vidhu, and D. Philip, 'Green synthesis of well-dispersed gold nanoparticles using *Macrotyloma uniflorum*', *Spectrochim. Acta - Part A Mol. Biomol. Spectrosc.*, 85, pp. 99-104, 2012.
- [2] J. Lee, E. Y. Park, and J. Lee, 'Non-toxic nanoparticles from phytochemicals: Preparation and biomedical application', *Bioprocess Biosyst. Eng.*, 37(6), pp. 983–989, 2014.
- [3] S. Babu, B. Kumar, and K. Kumar, 'Environment friendly approach for size controllable synthesis of biocompatible silver nanoparticles using diastase', *Environ. Toxicol. Pharmacol.*, 49 pp. 131–136, 2017.
- [4] H. Duan, D. Wang, and Y. Li, 'Green chemistry for nanoparticle synthesis', *Chem. Soc. Rev.*, 44(16), pp. 5778–5792, 2015.
- [5] S. Hamedi, S. A. Shojaosadati, and A. Mohammadi, 'Evaluation of the catalytic, antibacterial and anti-biofilm activities of the *Convolvulus arvensis* extract functionalized silver nanoparticles', *J. Photochem. Photobiol. B Biol.*, 167, pp. 36–44, 2017.
- [6] M. Safaepour, A. R. Shahverdi, H. R. Shahverdi, M. R. Khorramizadeh, and A. R. Gohari, 'Green synthesis of small silver nanoparticles using geraniol and its cytotoxicity against fibrosarcoma-wehi 164.', *Avicenna J. Med. Biotechnol.*, 1(2), pp. 111–5, 2009.
- [7] M. Gondwal and G. Joshi Nee Pant, 'Synthesis and catalytic and biological activities of silver and copper nanoparticles using *Cassia occidentalis*', *Int. J. Biomater.*, 6735426, 2018.
- [8] D. Bharathi and V. Bhuvaneshwari, 'Evaluation of the cytotoxic and antioxidant activity of phyto-synthesized silver nanoparticles using *Cassia angustifolia* flowers', *Bionanoscience*, 9(1), pp. 155–163, 2019.
- [9] G. Das, J. K. Patra, N. Basavegowda, C. N. Vishnuprasad, and H. S. Shin, 'Comparative study on antidiabetic, cytotoxicity, antioxidant and antibacterial properties of biosynthesized silver nanoparticles using outer peels of two varieties of *Ipomoea batatas* (L.) lam', *Int. J. Nanomedicine*, 14, pp. 4741–4754, 2019.
- [10] J. S. Pawar and R. H. Patil, 'Green synthesis of silver nanoparticles using *Eulophia herbacea* (Lindl.) tuber extract and evaluation of its biological and catalytic activity', *SN Appl. Sci.*, 2(1), pp. 1–12, 2020.
- [11] D. Bharathi, M. Diviya Josebin, S. Vasantharaj, and V. Bhuvaneshwari, 'Biosynthesis of silver nanoparticles using stem bark extracts of *Diospyros montana* and their antioxidant and antibacterial activities', *J. Nanostructure Chem.*, 8(1), pp. 83–92, 2018.
- [12] E. G. Haggag *et al.*, 'Antiviral potential of green synthesized silver nanoparticles of *Lampranthus coccineus* and *Malephora lutea*', *Int. J. Nanomedicine*, 14, pp. 6217–6229, 2019.
- [13] S. Valsalam *et al.*, 'Journal of Photochemistry & Photobiology , B: Biology Rapid biosynthesis and characterization of silver nanoparticles from the leaf extract of *Tropaeolum majus* L. and its enhanced *in-vitro* antibacterial , antifungal , antioxidant and anticancer properti', *J. Photochem. Photobiol. B Biol.*, 191, pp. 65–74, 2019.
- [14] J. K. Patra, G. Das, and H. Shin, 'Facile green biosynthesis of silver nanoparticles using *Pisum sativum* L. outer peel aqueous extract and its antidiabetic, cytotoxicity, antioxidant, and antibacterial activity', *Int. J. Nanomedicine*, pp. 6679–6690, 2019.

- [15] S. Renner *et al.*, 'Porcine models for studying complications and organ crosstalk in diabetes mellitus', *Cell Tissue Res.*, 380(2), pp. 341–378, 2020.
- [16] R. G. Saratale, H. S. Shin, G. Kumar, G. Benelli, D. Kim, and G. D. Saratale, 'Exploiting antidiabetic activity of silver nanoparticles synthesized using *Punica granatum* leaves and anticancer potential against human liver cancer cells (HepG2)', *Artif. Cells, Nanomedicine, Biotechnol.*, 46(1), pp. 211–222, 2018.
- [17] K. Rajaram, D. C. Aiswarya, and P. Sureshkumar, 'Green synthesis of silver nanoparticle using *Tephrosia tinctoria* and its antidiabetic activity', *Mater. Lett.*, 138, pp. 251–254, 2015.
- [18] D. Jini and S. Sharmila, 'Green synthesis of silver nanoparticles from *Allium cepa* and its in vitro antidiabetic activity', *Mater. Today Proc.*, 22, pp. 432–438, 2020.
- [19] S. Prabhu, S. Vinodhini, C. Elanchezhiyan, and D. Rajeswari, 'Evaluation of antidiabetic activity of biologically synthesized silver nanoparticles using *Pouteria sapota* in streptozotocin-induced diabetic rats', *Int. J. Nanomedicine*, 14, pp. 4741–4754, 2018.
- [20] B. R. Shamprasad, S. Keerthana, S. Megarajan, R. Lotha, S. Aravind, and A. Veerappan, 'Photosynthesized escin stabilized gold nanoparticles exhibit antidiabetic activity in L6 rat skeletal muscle cells', *Mater. Lett.*, 241, pp. 198–201, 2019.
- [21] T. Rajarajeshwari, C. Shivashri, and P. Rajasekar, 'Synthesis and characterization of biocompatible gymnemic acid – gold nanoparticles : a study on glucose uptake stimulatory effect in 3T3-L1 adipocytes', *RSC Adv.*, 4, pp. 63285–63295, 2014.
- [22] Y. Dong, G. Wan, P. Yan, C. Qian, F. Li, and G. Peng, 'Fabrication of resveratrol coated gold nanoparticles and investigation of their effect on diabetic retinopathy in streptozotocin induced diabetic rats', *J. Photochem. Photobiol. B Biol.*, 195(1), pp. 51–57, 2019.
- [23] J. N. Payne *et al.*, 'Development of dihydrochalcone-functionalized gold nanoparticles for augmented antineoplastic activity', *Int. J. Nanomed.*, 13, pp. 1917–1926, 2018.
- [24] M. A. J. Kouhbanani *et al.*, 'Green synthesis of spherical silver nanoparticles using *Ducrosia anethifolia* aqueous extract and its antibacterial activity', *J. Environ. Treat. Tech.*, 7(3), pp. 461–466, 2019.
- [25] A. O. Dada *et al.*, 'Effect of operational parameters, characterization and antibacterial studies of green synthesis of silver nanoparticles using *Tithonia diversifolia*', *PeerJ*, 6, pp. 1–17, 2018.
- [26] E. Ajayi and A. Afolayan, 'Green synthesis, characterization and biological activities of silver nanoparticles from alkalized *Cymbopogon citratus* Stapf', *Adv. Nat. Sci. Nanosci. Nanotechnol.*, 8, 015017, 2017.
- [27] O. T. Jemilugba, E. H. M. Sakho, S. Parani, V. Mavumengwana, and O. S. Oluwafemi, 'Green synthesis of silver nanoparticles using *Combretum erythrophyllum* leaves and its antibacterial activities', *Colloids Interface Sci. Commun.*, 31, pp. 100191, 2019.
- [28] S. E. Drewes, E. Elliot, F. Khan, J. T. B. Dhlamini, and M. S. S. Gcumisa, '*Hypoxis hemerocallidea*- Not merely a cure for benign prostate hyperplasia', *J. Ethnopharmacol.*, 119(3), pp. 593–598, 2008.
- [29] D. Naidoo, S. F. Van Vuuren, R. L. Van Zyl, and H. De Wet, 'Plants traditionally used individually and in combination to treat sexually transmitted infections in

- northern Maputaland, South Africa: Antimicrobial activity and cytotoxicity', *J. Ethnopharmacol.*, 149(3), pp. 656–667, 2013.
- [30] V. Steenkamp, M. C. Gouws, M. Gulumian, E. E. Elgorashi, and J. Van Staden, 'Studies on antibacterial, anti-inflammatory and antioxidant activity of herbal remedies used in the treatment of benign prostatic hyperplasia and prostatitis', *J. Ethnopharmacol.*, 103(1), pp. 71–75, 2006.
- [31] B. Ncube, A. R. Ndhlala, A. Okem, and J. Van Staden, '*Hypoxis (Hypoxidaceae)* in African traditional medicine', *J. Ethnopharmacol.*, 150(3), pp. 818–827, 2013.
- [32] A. K. Jäger, A. Hutchings, and J. Van Staden, 'Screening of Zulu medicinal plants for prostaglandin-synthesis inhibitors', *J. Ethnopharmacol.*, 52(2), pp. 95–100, 1996.
- [33] H. De Wet, V. N. Nzama, and S. F. Van Vuuren, 'Medicinal plants used for the treatment of sexually transmitted infections by lay people in northern Maputaland, KwaZulu-Natal Province, South Africa', *South African J. Bot.*, 78, pp. 12–20, 2012.
- [34] K. Bassey, A. Viljoen, S. Combrinck, and Y. H. Choi, 'New phytochemicals from the corms of medicinally important South African *Hypoxis* species', *Phytochem. Lett.*, 10, pp. lxi–lxxv, 2015.
- [35] J. L. Mwinga *et al.*, '*In vitro* antimicrobial effects of *Hypoxis hemerocallidea* against six pathogens with dermatological relevance and its phytochemical characterization and cytotoxicity evaluation', *J. Ethnopharmacol.*, 242, pp. 112048, 2019.
- [36] J. A. Asong, P. T. Ndhlovu, N. S. Khosana, A. O. Aremu, and W. Otang-Mbeng, 'Medicinal plants used for skin-related diseases among the Batswanas in Ngaka Modiri Molema District Municipality, South Africa', *South African J. Bot.*, 126, pp. 11–20, 2019.
- [37] O. Laporta, L. Pérez-Fons, R. Mallavia, N. Caturla, and V. Micol, 'Isolation, characterization and antioxidant capacity assessment of the bioactive compounds derived from *Hypoxis rooperi* corm extract (African potato)', *Food Chem.*, 101(4), pp. 1425–1437, 2007.
- [38] P. M. O. Owira and J. A. O. Ojewole, "'African potato" (*Hypoxis hemerocallidea* corm): A plant-medicine for modern and 21st century diseases of mankind? – A Review', 152, pp. 147–152, 2009.
- [39] Shaik, S., Govender, K. & Leanya M, 'Ga<sub>3</sub>-mediated dormancy alleviation in the reputed African potato, *Hypoxis hemerocallidea*'. *A. J. Tradit and C. Altern*, 11(2), pp. 330-333, 2014.
- [40] M. Keneilwe, G. Saramma, and C. Kelvin, 'An *in-vitro* antioxidant and antidiabetic evaluation of traditional medicinal plants of Botswana', *J. Pharm. Res. Int.*, 22(6), pp. 1–12, 2018.
- [41] G. J. Boukes, M. Van De Venter, and V. Oosthuizen, 'Quantitative and qualitative analysis of sterols/sterolins and hypoxoside contents of three *Hypoxis* (African potato) spp.' *Afr. J. Biotech.*, 7(11), pp. 1624–1629, 2008.
- [42] V. D. P. Nair and I. Kanfer, 'Sterols and sterolins in *Hypoxis hemerocallidea* (African potato)', *S. Afr. J. Sci.*, 104(7–8), pp. 323–324, 2008.
- [43] Elbagory, A.M., Meyer, M., Cupido, C.N. & Hussein, A.A., 'Inhibition of bacteria associated with wound infection by biocompatible green synthesized gold nanoparticles from South African plant extracts'. *Nanomaterials*, 7, pp.417, 2017.
- [44] A. M. Elbagory, A. A. Hussein, and M. Meyer, 'The *in vitro* immunomodulatory effects of gold nanoparticles synthesized from *Hypoxis hemerocallidea* aqueous extract and hypoxoside on macrophage and natural killer cells', *Int. J.*

*Nanomedicine*, 14, pp. 9007–9018, 2019.

- [45] M. Shah *et al.*, 'Synthesis of bio-mediated silver nanoparticles from *Silybum marianum* and their biological and clinical activities', *Mater. Sci. Eng. C*, 112, p. 110889, 2020.
- [46] U. M. Badeggi *et al.*, 'Green synthesis of gold nanoparticles capped with procyanidins from *Leucosidea sericea* as potential antidiabetic and antioxidant agents', *Biomolecules*, 10(3), pp. 452-475, 2020.
- [47] A. O. Ademiluyi and G. Oboh, 'Experimental and toxicologic pathology soybean phenolic-rich extracts inhibit key-enzymes linked to type 2 diabetes ( $\alpha$ -amylase and  $\alpha$ -glucosidase) and hypertension (angiotensin I converting enzyme) *in vitro*', *Exp. Toxicol. Pathol.*, 65(3), pp. 305–309, 2013.
- [48] S. Pu, J. Li, L. Sun, L. Zhong, and Q. Ma, 'An *in vitro* comparison of the antioxidant activities of chitosan and green synthesized gold nanoparticles', *Carbohydr. Polym.*, 211, pp. 161–172, 2019.
- [49] M. Q. Nasar, A. T. Khalil, M. Ali, M. Shah, M. Ayaz, and Z. K. Shinwari, 'Phytochemical analysis, ephedra procera C. A. Mey. mediated green synthesis of silver nanoparticles, their cytotoxic and antimicrobial potentials', *Med.*, 55(7), pp. 1–18, 2019.
- [50] Y. Shao *et al.*, 'Green synthesis of sodium alginate-silver nanoparticles and their antibacterial activity', *Int. J. Biol. Macromol.*, 111, pp. 1281–1292, 2018.
- [51] V. D. P. Nair and I. Kanfer, 'High-performance liquid chromatographic method for the quantitative determination of hypoxoside in African potato (*Hypoxis hemerocallidea*) and in commercial products containing the plant material and/or its extracts', *J. Agric. Food Chem.*, 54(8), pp. 2816–2821, 2006.
- [52] G. J. Boukes and M. Van De Venter, 'Rooperol as an antioxidant and its role in the innate immune system: An *in vitro* study', *J. Ethnopharmacol.*, 144(3), pp. 692–699, 2012.
- [53] M. M. Kabanda, 'Antioxidant activity of rooperol investigated through Cu (I and II) chelation ability and the hydrogen transfer mechanism: A DFT study', *Chem. Res. Toxicol.*, 25(10), pp. 2153–2166, 2012.
- [54] A. E. Adebayo *et al.*, 'Biosynthesis of silver, gold and silver–gold alloy nanoparticles using *Persea americana* fruit peel aqueous extract for their biomedical properties', *Nanotechnol. Environ. Eng.*, 4(1), pp. 1–15, 2019.
- [55] V. Amendola, O. M. Bakr, and F. Stellacci, 'A study of the surface plasmon resonance of silver nanoparticles by the discrete dipole approximation method: Effect of shape, size, structure, and assembly', *Plasmonics*, 5(1), pp. 85–97, 2010.
- [56] I. O. Sosa, C. Noguez, and R. G. Barrera, 'Optical properties of metal nanoparticles with arbitrary shapes', *J. Phys. Chem. B*, 107(26), pp. 6269–6275, 2003.
- [57] F. Göl, A. Aygün, A. Seyrankaya, T. Gür, C. Yenikaya, and F. Şen, 'Green synthesis and characterization of *Camellia sinensis* mediated silver nanoparticles for antibacterial ceramic applications', *Mater. Chem. Phys.*, 250, p. 123037, 2020.
- [58] M. Y. El-Naggar, W. Ramadan, and R. A. El-Hamamsy, 'The application of mediated biosynthesized green silver nanoparticles by *Streptomyces griseorubens* in water treatment', *J. Pure Appl. Microbiol.*, 11(2), pp. 685–694, 2017.
- [59] S. Ali *et al.*, 'Bioinspired morphology-controlled silver nanoparticles for antimicrobial application', *Mater. Sci. Eng. C*, 108, p. 110421, 2020.

- [60] S. Sarwar, S. Islam, T. Hosain, H. Sarwar, and M. J. Rashid, 'A comparison of the absorbed power for periodic, disordered and deterministic aperiodic arrays of silver nanoparticles', *J. Phys. Conf. Ser.*, 1086(1), 012008, 2018.
- [61] Z. Gün Gök, K. Günay, M. Arslan, M. Yiğitoğlu, and İ. Vargel, 'Coating of modified poly(ethylene terephthalate) fibers with sericin-capped silver nanoparticles for antimicrobial application', *Polym. Bull.*, 77(4), pp. 1649–1665, 2020.
- [62] A. M. Elbagory, C. N. Cupido, M. Meyer, and A. A. Hussein, 'Large scale screening of southern African plant extracts for the green synthesis of gold nanoparticles using microtitre-plate method', *Molecules*, 21(11), 2016.
- [63] M. V. Sujitha and S. Kannan, 'Green synthesis of gold nanoparticles using citrus fruits (*Citrus limon*, *Citrus reticulata* and *Citrus sinensis*) aqueous extract and its characterization', *Spectrochim. Acta - Part A Mol. Biomol. Spectrosc.*, 102, pp. 15–23, 2013.
- [64] A. Aygün *et al.*, 'Biological synthesis of silver nanoparticles using *Rheum ribes* and evaluation of their anticarcinogenic and antimicrobial potential: A novel approach in phytonanotechnology', *J. Pharm. Biomed. Anal.*, 179, 2020.
- [65] Z. Lu, K. Rong, J. Li, H. Yang, and R. Chen, 'Size-dependent antibacterial activities of silver nanoparticles against oral anaerobic pathogenic bacteria', *J Mater Sci: Mater Med*, 24, pp. 1465–1471, 2013.
- [66] N. Tehri *et al.*, 'Biosynthesis, characterization, bactericidal and sporicidal activity of silver nanoparticles using the leaves extract of *Litchi chinensis*', *Prep. Biochem. Biotechnol.*, pp. 1–9, 2020.
- [67] P. N. V. K. Pallela, S. Ummey, L. K. Ruddaraju, S. V. N. Pammi, and S. G. Yoon, 'Ultra Small, mono dispersed green synthesized silver nanoparticles using aqueous extract of *Sida cordifolia* plant and investigation of antibacterial activity', *Microb. Pathog.*, 124, pp. 63–69, 2018.
- [68] S. Yin *et al.*, 'Si/Ag/C nanohybrids with *in situ* incorporation of super-small silver nanoparticles: Tiny amount, huge impact', *ACS Nano*, 12(1), pp. 861–875, 2018.
- [69] L. Korösi *et al.*, 'Ultrasml, ligand-free ag nanoparticles with high antibacterial activity prepared by pulsed laser ablation in liquid', *J. Chem.*, 2016.
- [70] C. Kästner, D. Lichtenstein, A. Lampen, and A. F. Thünemann, 'Monitoring the fate of small silver nanoparticles during artificial digestion', *Colloids Surfaces A Physicochem. Eng. Asp.*, 526, pp. 76–81, 2017.
- [71] Y. Feng, Q. Yao, J. Li, N. Goswami, J. Xie, and J. Yang, 'Converting ultrafine silver nanoclusters to monodisperse silver sulfide nanoparticles via a reversible phase transfer protocol', *Nano Res.*, 9(4), pp. 942–950, 2016.
- [72] S. Singh, R. Vyas, A. Chaturvedi, and R. Sisodia, 'Rapid phytosynthesis of silver nanoparticles using *Chlorophytum borivillianum* root extract and its antimicrobial activity', 7(5), pp. 1738–1744, 2018.
- [73] S. Bangale and S. Ghotekar, 'Bio-fabrication of Silver nanoparticles using *Rosa Chinensis L.* extract for antibacterial activities', *Int. J. Nano Dimens.*, 10(2), pp. 217–224, 2019.
- [74] A. Rautela, J. Rani, and M. Debnath (Das), 'Green synthesis of silver nanoparticles from *Tectona grandis* seeds extract: characterization and mechanism of antimicrobial action on different microorganisms', *J. Anal. Sci. Technol.*, 10(1), 2019.
- [75] M. F. Baran and H. Açay, 'Antimicrobial activity of silver nanoparticles synthesized

- with extract of tomato plant against bacterial and fungal pathogens', *Middle Black Sea J. Heal. Sci.*, 5, pp. 67–73, 2019.
- [76] J. Singh, T. Dutta, K. H. Kim, M. Rawat, P. Samddar, and P. Kumar, "Green" synthesis of metals and their oxide nanoparticles: Applications for environmental remediation', *J. Nanobiotechnology*, 16(84), pp. 1–24, 2018.
- [77] Tomaszewska, E.; Soliwoda, K.; Kadziola K.; Tkacz-Szczesna B.; Celichowski, G.; Cichomski, M; Szmaja, W.; Grobelny, J. Determination limits of DLS and UV-Vis spectroscopy in characterization of polydisperse nanoparticles colloids. *Journal of Nanomaterials*, **2013**.
- [78] S. A. Cumberland and J. R. Lead, 'Particle size distributions of silver nanoparticles at environmentally relevant conditions', *J. Chromatogr. A*, 216(52), pp. 9099–9105, 2009.
- [79] M. Danaei *et al.*, 'Impact of particle size and polydispersity index on the clinical applications of lipidic nanocarrier systems', *Pharmaceutics*, 10(2), pp. 1–17, 2018.
- [80] Y. Agrawal and V. Patel, 'Nanosuspension: An approach to enhance solubility of drugs', *J. Adv. Pharm. Technol. Res.*, 2(2), pp. 81, 2011.
- [81] M. Zahran, M. El-Kemary, S. Khalifa, and H. El-Seedi, 'Spectral studies of silver nanoparticles biosynthesized by *Origanum majorana*', *Green Process. Synth.*, 7(2), pp. 100–105, 2018.
- [82] M. M. Nadzir, F. N. Idris, and K. Hat, 'Green synthesis of silver nanoparticle using *Gynura procumbens* aqueous extracts', *AIP Conf. Proc.*, 2124, 2019.
- [83] R. Tantra, P. Schulze, and P. Quincey, 'Effect of nanoparticle concentration on zeta-potential measurement results and reproducibility', *Particuology*, 8(3), pp. 279–285, 2010.
- [84] U. Pyell, A. H. Jalil, C. Pfeiffer, B. Pelaz, and W. J. Parak, 'Characterization of gold nanoparticles with different hydrophilic coatings via capillary electrophoresis and Taylor dispersion analysis. Part I: Determination of the zeta potential employing a modified analytic approximation', *J. Colloid Interface Sci.*, 450, pp. 288–300, 2015.
- [85] M. Vishnu Kiran and S. Murugesan, 'Biogenic silver nanoparticles by *Halymenia poryphyroides* and its *in vitro* anti-diabetic efficacy', *J. Chem. Pharm. Res.*, 5(12), pp. 1001–1008, 2013.
- [86] C. Dhand *et al.*, 'Methods and strategies for the synthesis of diverse nanoparticles and their applications: A comprehensive overview', *RSC Adv.*, 5(127), pp. 105003–105037, 2015.
- [87] D. Jini and S. Sharmila, 'Green synthesis of silver nanoparticles from *Allium cepa* and its *in vitro* antidiabetic activity', *Mater. Today Proc.*, 22, pp. 432–438, 2020.
- [88] Castellano, J.M.; Guinda, A.; Delgado, T.; Rada, M.; Cayuela, J.A. Biochemical Basis of the Antidiabetic Activity of Oleanolic Acid and Related Pentacyclic Triterpenes. *Diabetes* **2013**, 62, 1791–1799.
- [89] P. F. Laura, M. T. Garzón, and M. Vicente, 'Relationship between the antioxidant capacity and effect of rosemary (*Rosmarinus officinalis* L.) polyphenols on membrane phospholipid order', *J. Agric. Food Chem.*, 58(1), pp. 161–171, 2010.
- [90] H. Sies, 'Oxidative stress: A concept in redox biology and medicine', *Redox Biol.*, 4, pp. 180–183, 2015.
- [91] S. Duletić-Laušević *et al.*, 'Antineurodegenerative, antioxidant and antibacterial activities and phenolic components of *Origanum majorana* L. (Lamiaceae) extracts',

- J. Appl. Bot. Food Qual.*, 91, pp. 126–134, 2018.
- [92] M. Khoshnamvand, C. Huo, and J. Liu, 'Silver nanoparticles synthesized using *Allium ampeloprasum* L. leaf extract : Characterization and performance in catalytic reduction of 4-nitrophenol and antioxidant activity', *J. Mol. Struct.*, 1175, pp. 90–96, 2019.
- [93] A. K. Mittal, Y. Chisti, and U. C. Banerjee, 'Synthesis of metallic nanoparticles using plant extracts', *Biotechnol. Adv.*, 31(2), pp. 346–356, 2013.
- [94] A. K. Mittal, J. Bhaumik, S. Kumar, and U. C. Banerjee, 'Biosynthesis of silver nanoparticles: Elucidation of prospective mechanism and therapeutic potential', *J. Colloid Interface Sci.*, 415, pp. 39–47, 2014.
- [95] M. Ponnaniakamideen and S. Rajeshkumar, '*In vivo* type 2 diabetes and wound-healing effects of antioxidant gold nanoparticles synthesized using the insulin plant *Chamaecostus cuspidatus* in albino rats', *Can. J. Diabetes*, 43(2), pp. 82-89, 2019.
- [96] A. J. Huh and Y. J. Kwon, "'Nanoantibiotics": A new paradigm for treating infectious diseases using nanomaterials in the antibiotics resistant era', *J. Control. Release*, 156(2), pp. 128–145, 2011.
- [97] J. Singh, A. S. Dhaliwal, and R. Extract, 'Novel green synthesis and characterization of the antioxidant activity of silver nanoparticles prepared from *Nepeta leucophylla* root extract novel green synthesis and characterization of the antioxidant activity of silver nanoparticles prepared from', *Anal. Lett.*, pp. 1–18, 2018.
- [98] N. Sahu *et al.*, 'Synthesis of silver nanoparticles using flavonoids: hesperidin, naringin and diosmin, and their antibacterial effects and cytotoxicity', *Int. Nano Lett.*, 6(3), pp. 173–181, 2016.
- [99] D. Swolana *et al.*, 'The antibacterial effect of silver nanoparticles on *Staphylococcus epidermidis* strains with different biofilm-forming ability', *Nanomaterials*, 10(5), pp. 1–12, 2020.



## CHAPTER SIX

### General discussion

This study investigated the ability to synthesize gold and silver nanoparticles using the chemical constituents of *Leucosidea sericea* and *Hypoxis hemerocallidea* through the green synthesis route. The study also entails the characterization and applications of the biosynthesized gold and silver nanoparticles.

The aerial parts of *L. sericea* and the corm of *H. hemerocallidea* were extracted in aqueous methanol exhaustively. The total extract (TE) in each case was then partitioned into different fractions of butanol, ethyl acetate, dichloromethane and hexane. Preliminary studies indicated that only the butanol, ethyl acetate and total extracts possessed the ability to synthesize MNPs. This was an indication that polar compounds possess better abilities, that is, have the required functional groups capable of reducing metals to their zero valence states. Efforts made to purify the extracts led to the identification of a mixture of procyanidins from *L. sericea* extracts and isolation of hypoxoside which is a major compound from the *H. hemerocallidea*. Thereafter, fractions containing a mixture of procyanidins from *L. sericea*, the pure hypoxoside as well as their respective TEs were employed in the green synthesis of the MNPs.

For proper identification of the procyanidins, both Nuclear Magnetic Resonance (NMR) spectroscopy and Liquid Chromatography-Mass Spectrometry (LC-MS) were used after purification of the fractions through several silica gel and Sephadex column chromatography.  $^1\text{H}$ ,  $^{13}\text{C}$ , and DEPT 135 NMR initially showed F1 and F2 as dimers and trimers of procyanidins respectively until more sensitive LC-MS showed that both are mixtures of B-type procyanidin series in different proportions. Overall, F1 and F2 were constituents of *L. sericea* that were majorly procyanidins (Badeggi et al., 2020).

The *L. sericea* total extract (LSTE), F1, and F2 were then employed in the green synthesis of gold nanoparticles (AuNPs). The method was simple and eco-friendly, resulting in bioactive AuNPs. The nanoparticles (NPs) were characterized using UV-Vis, DLS, TEM, SAED, EDS and XRD. The ruby-red coloration of the colloidal solutions first confirmed the successful synthesis followed by the absorbance of about 500 nm, which is the typical region for the surface plasmon resonance of AuNPs (Nune et al., 2009). The EDS analysis also supported the confirmation of NPs. From the TEM micrographs, various shape such as sphere, rod-like and triangle were found. The spherical shapes predominated others in all the nanoparticles. Thus, the nanoparticles composed mixture of shapes which is a characteristic of a green synthesis using plant material. The information on the dynamic

size was also provided by DLS in addition to their high stability. Then, SAED and XRD showed that the AuNPs were crystalline.

From the combined spectroscopic and microscopic analysis, it is evident that procyanidins were actively involved in the biosynthesis of the LSTE-AuNPs. This was substantiated when similar particles were formed for LSTE- and F2 AuNPs. This involvement was illustrated in the proposed mechanism.

Because these NPs may have biomedical potential, their biocompatibility in physiological conditions was evaluated *in vitro* and the results showed that they were stable in different biological buffers and media except for the F1-AuNPs which showed evidence of slow aggregation with time. Its stability was, therefore, short-lived compared to those of LSTE- and F2-AuNPs. Also, some biomedical applications may require NPs at different concentrations. Therefore, dilution studies demonstrated that the properties of the NPs remained intact even at diluted concentrations.

As a measure of the antidiabetic potential, the AuNPs displayed better inhibition for alpha-amylase and alpha-glucosidase enzymes when compared to the respective extract and fractions. However, the extracts and fractions demonstrated more scavenging abilities which were largely due to the dependence of the assays on the phenolic content of the materials (Badeggi et al., 2020). The relatively higher percentage phenolic content in F2-AuNPs than F1-AuNPs was explained in terms of the extent of the homogeneity of the fraction as well as its high packing power. Thus, the green synthesized AuNPs showed promising biomedical potential.

Silver nanoparticles were also biosynthesized for the first time using the constituents of *L. sericea*. The total extract (LSTE), and the procyanidin rich fractions (F1 and F2) were employed in the green synthesis that resulted in the corresponding LSTF-, F1-, and F2-AgNPs. The AgNPs were fully characterized like the AuNPs counterparts. UV-Vis spectra analysis revealed particles with SPR of about 400 nm. The plasmonic resonance of AgNPs is sharp and more intense relative to AuNPs due to the difference in the dielectric properties caused by the overlap between the SPR and series of inter-band transitions in silver which begins at about 320 nm. The mean particle size of AgNPs was relatively smaller when compared to their corresponding AuNPs. This has been established according to some authors when extracts and single phytochemicals like resveratrol were employed in the green synthesis of both gold and silver NPs in the same study (Amendola et al., 2010; Park et al., 2016). However, aggregates of silver nanoparticles were formed suggesting that the gold counterparts were more stable. This may be due to inertness of gold which would have kept the particles in solution as a result of electrostatic forces.

Like their gold counterparts, the results of SAED and XRD for the three AgNPs also showed that the particles were crystalline. This could be argued to be due to the participation of similar chemical constituents in the TEs as well as the fractions in the two cases of gold and silver NPs. Also, the dilution studies equally affirmed that the AgNPs retained their properties at diluted concentrations like the AuNPs (Nune et al., 2009; Park et al., 2016; Sahu et al., 2016).

The AgNPs were tested for their scavenging potential and found to demonstrate lower activities than the extracts and fractions. When compared to their gold counterparts, the variation was dependent on the type of assay. While the antioxidant activity through ABTS was generally higher in AuNPs than AgNPs of the same precursor constituents, the opposite was the case in the FRAP technique except for F1-AgNPs, which displayed lower activity than the corresponding gold form. The pattern of activity is similar to what was obtainable in AuNPs for the total phenolic content assay where the activity of the NPs was generally lower than those of the corresponding extracts and fractions due to obvious reasons. However, the average percentage of phenolic content was higher in AuNPs.

The alpha-amylase and alpha-glucosidase enzymatic activities demonstrated by AgNPs were lower than those of the corresponding AuNPs in general. Literature had recorded more antidiabetic activities of AuNPs synthesized from plant extracts and pure compounds compared to AgNPs probably due to better biocompatibility of the former (Elahi et al., 2018). Also, the antimicrobial activities of the AgNPs showed interesting bactericidal activities which may be because of their small sizes. The smallest F1-AgNPs displayed the highest inhibition against *S. aureus*. This inhibition was better than what has been previously reported (Shao et al., 2018). Silver nanoparticles with smaller sizes have been reported to show better bactericidal effects due to their large surface area to volume ratio (Shao et al., 2018). On the other hand, no significant inhibitory activities were shown by the AuNPs counterparts at the test concentrations. It is suggested that AgNPs possess superior antimicrobial activities than AuNPs.

Similarly, the aqueous solutions of *H. hemerocallidea* extract (HHE), as well as hypoxoside (HPX), were employed in the green synthesis of silver NPs. The gold counterparts have already been reported in literature. The AgNPs of HHE and HPX was synthesized using a green procedure that is simple, fast and inexpensive. Microscopic and spectroscopic analysis were used to characterize the particles. The techniques revealed several variations between HHE- and HPX-AgNPs. From the analysis, ultra-small, spherical, monodispersed, and stable AgNPs were obtained for HPX-AgNPs whereas a mixture of shapes were recorded for HHE-AgNPs. Spherical and cylindrical particles were found with sizes relatively bigger than those of HPX. Occurrence of these type of shapes have

been reported elsewhere (Amendola et al., 2010). It also showed that the AgNPs were crystalline as revealed by SAED and XRD. ZP results showed that HHE-AgNPs are relatively more stable than HPX-AgNPs owing to a variety of chemical constituents involved in capping the NPs (Badeggi et al., 2020). PDI on the other hand showed that HPX-AgNPs are more homogenous, meaning that the particles were more uniformly shaped compared to the different shapes obtained in HHE-AgNPs. This was also shown in the UV-Vis spectra where two plasmonic resonance appeared for HHE-AgNPs while only one was observed for HPX-AgNPs. The two plasmonic resonance was due to particles of different morphologies. This was further confirmed by the presence of spheres and cylinders according to TEM evaluation. AgNPs with spherical shapes often possess one plasmonic resonance due to their symmetry (Amendola et al., 2010). Furthermore, the bimodal appearance of HHE-AgNPs as depicted by HDS in DLS measurement gave additional evidence on the presence of a mixture of shapes in the colloidal solution. All these variations come from the different chemical constituents in the precursors of the AgNPs. More importantly, is the clear involvement of the hypoxoside in the reduction and subsequent capping of the NPs. The TEM results revealed the capability of HPX as the chief reducing and capping agent in HHE-AgNPs, being solely responsible for the formation of spherical and monodispersed HPX-AgNPs. These results further emphasized the importance in finding the phytochemicals truly responsible for the reduction and stabilization of gold and silver nanoparticles in green synthesis.

The antidiabetic, antioxidant and antimicrobial activity of HHE- and HPX-AgNPs were then evaluated. Although both showed encouraging antidiabetic potential, the HHE-AgNPs displayed enhanced activity against alpha-glucosidase over HPX-AgNPs while the latter demonstrated better inhibition against alpha-amylase. Similarly, HHE-AgNPs showed better scavenging abilities over the HPX-AgNP counterparts possibly due to the difference in the number of phytoconstituents that may be serving as capping agents. As for the antimicrobial properties, the general trend was such that the AgNPs demonstrated more activity on the Gram-negative bacteria strains which may be because of the difference in their cell walls. The Gram-positive types were believed to have thicker cell walls that are difficult to penetrate by the particles. Moreover, the HPX-AgNPs displayed more bactericidal activities than the HHE-AgNPs which may be because of the size difference. AgNPs with small sizes often show good antibacterial activities against relatively bigger ones. This activity might have been enhanced because of the ultra-small size coupled with the spherical nature of the monodispersed HPX-AgNPs (Lu et al., 2013). From the six bacterial species employed, HPX-AgNPs displayed the highest inhibitory activities against *E. coli* and *S. enterica* while HHE-AgNPs showed moderate inhibition against *E. coli*. The

AgNPs demonstrated interesting biological activities that could make them good candidates in applications like biomedical and food processing industries.

## Conclusion

In this study, the aqueous extract of *Leucosidea sericea* and *Hypoxis hemerocallidea* demonstrated the ability to form gold and silver nanoparticles. The study showed the involvement of polyphenols as the chief reducing and capping agents in the extracts. Further, it affirmed the use of a single phytochemical in forming biostable and bioactive metal nanoparticles. Cleaner nanoparticles were obtained. Among the importance of this is the potential application in biomedical. The single compound-nanoparticles conjugate may be useful in the formulation of nano-drugs with specific functional groups. The study represents a fundamental model to be further explored in the design of effective antidiabetic, antioxidant and antibacterial therapeutics.

## Recommendations

This study was centered on the ability application of chemical constituents (extracts, fractions and compounds) of *L. sericea* and the corm of *H. hemerocallidea* in the biosynthesis of gold and silver NPs. NMR and LC-MS were used to determine the composition of the constituents or to identify the compounds and/or their functional groups before use in the green synthesis. However, the mechanism by which the NPs are formed, and the involvement of the functional groups still need to be further understood. Therefore, more spectroscopic and microscopic techniques may need to be involved for better understanding of the process. This may be done by solid state NMR of the powdered nanoparticles and biology TEM. Subsequent studies should also include, for instance, LC-MS analyses of the synthesized gold and silver nanoparticles to compare with those of the starting materials.

The use of more sophisticated separation techniques such as a combination of NMR, Quadrupole Time-of-Flight Mass Spectrometry, and an ultra-High Performance Liquid Chromatography that may be coupled with Mass Spectrometry for easier and better separation of compounds, especially with regards to procyanidins that are highly difficult to separate from one another. This will then make their involvement in the MNPs synthesis and the discussion of their behaviour much more informative. Better information on the chemistry of MNPs synthesis is of immense significance as this can pave way for future conjugation studies that are highly needed for the drug delivery potential of the NPs.

Hypoxoside is largely abundant in the corm of *H. hemerocallidea* and pharmacologically inactive. However, up till now, it has only been used to synthesize gold and silver NPs,

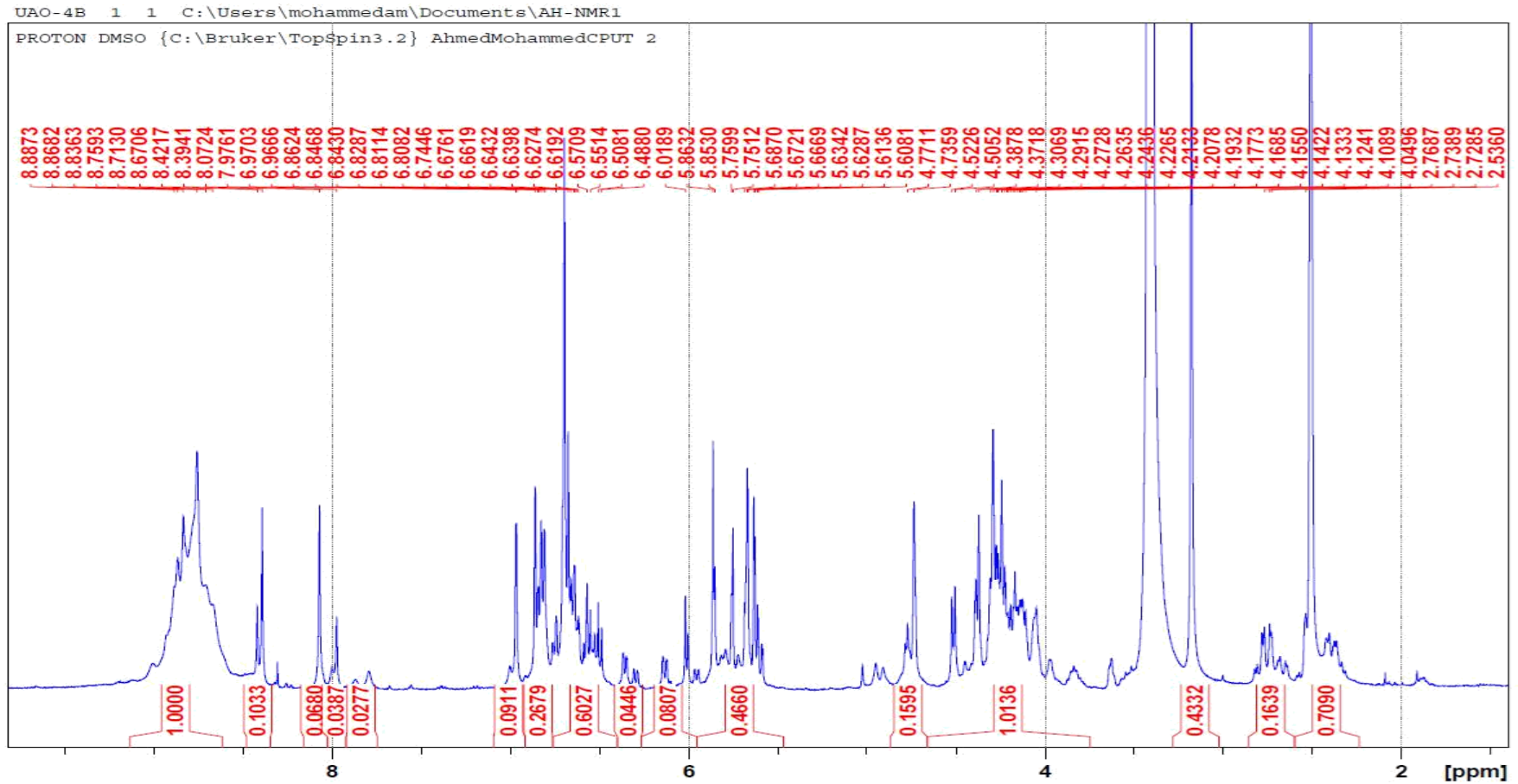
which have demonstrated brilliant biological activities. Therefore, it is suggested that more metals such as platinum and copper be studied using hypoxoside because some NPs of these precious metals have shown interesting biomedical potentials including anticancer (Sunderam et al., 2019), an indication that HPX-PtNPs and HPX-CuNPs may have promising biomedical applications yet to be explored.

The search for more bioactive compounds from South African Flora with specific biological activities, further in-depth biological activities of the compounds and testing the bioactive NPs against different biological targets is also recommended.

## References

- Amendola, V., Bakr, O.M. & Stellacci, F. 2010. A study of the surface plasmon resonance of silver nanoparticles by the discrete dipole approximation method: Effect of shape, size, structure, and assembly. *Plasmonics*, 5(1): 85–97.
- Badeggi, U.M., Ismail, E., Adeloye, A.O., Botha, S., Badmus, J.A., Marnewick, J.L., Cupido, C.N. & Hussein, A.A. 2020. Green synthesis of gold nanoparticles capped with procyanidins from *Leucosidea sericea* as potential antidiabetic and antioxidant agents. *Biomolecules*, 10(3), 452-475.
- Elahi, N., Kamali, M. & Baghersad, M.H. 2018. Recent biomedical applications of gold nanoparticles: A review. *Talanta*, 184: 537–556.
- Lee, Y.J. & Park, Y. 2019. Green synthetic nanoarchitectonics of gold and silver nanoparticles prepared using quercetin and their cytotoxicity and catalytic applications. *Journal of Nanoscience and Nanotechnology*, 20(5): 2781–2790.
- Lu, Z., Rong, K., Li, J., Yang, H. & Chen, R. 2013. Size-dependent antibacterial activities of silver nanoparticles against oral anaerobic pathogenic bacteria. *Journal of Material Science: Materials in Medicine*, 24:1465–1471.
- Nune, S.K., Chanda, N., Shukla, R., Katti, Kavita, Kulkarni, R.R., Thilakavathy, S., Mekapothula, S., Kannan, R. & Katti, Kattesh V. 2009. Green nanotechnology from tea: Phytochemicals in tea as building blocks for production of biocompatible gold nanoparticles. *Journal of Materials Chemistry*, 19(19): 2912–2920.
- Park, Sohyun, Cha, S.H., Cho, I., Park, Soomin, Park, Yohan, Cho, S. & Park, Youmie. 2016. Antibacterial nanocarriers of resveratrol with gold and silver nanoparticles. *Materials Science and Engineering C*, 58: 1160–1169.
- Sahu, N., Soni, D., Chandrashekhar, B., Satpute, D.B., Saravanadevi, S., Sarangi, B.K. & Pandey, R.A. 2016. Synthesis of silver nanoparticles using flavonoids: Hesperidin, naringin and diosmin, and their antibacterial effects and cytotoxicity. *International Nano Letters*, 6(3): 173–181.
- Shao, Y., Wu, C., Wu, T., Yuan, C., Chen, S., Ding, T., Ye, X. & Hu, Y. 2018. Green synthesis of sodium alginate-silver nanoparticles and their antibacterial activity. *International Journal of Biological Macromolecules*, 111: 1281–1292.
- Sunderam, V., Thiyagarajan, D., Lawrence, A.V., Mohammed, S.S.S. & Selvaraj, A. 2019. *In-vitro* antimicrobial and anticancer properties of green synthesized gold nanoparticles using *Anacardium occidentale* leaves extract. *Saudi Journal of Biological Sciences*, 26(3): 455–459.

## APPENDICES

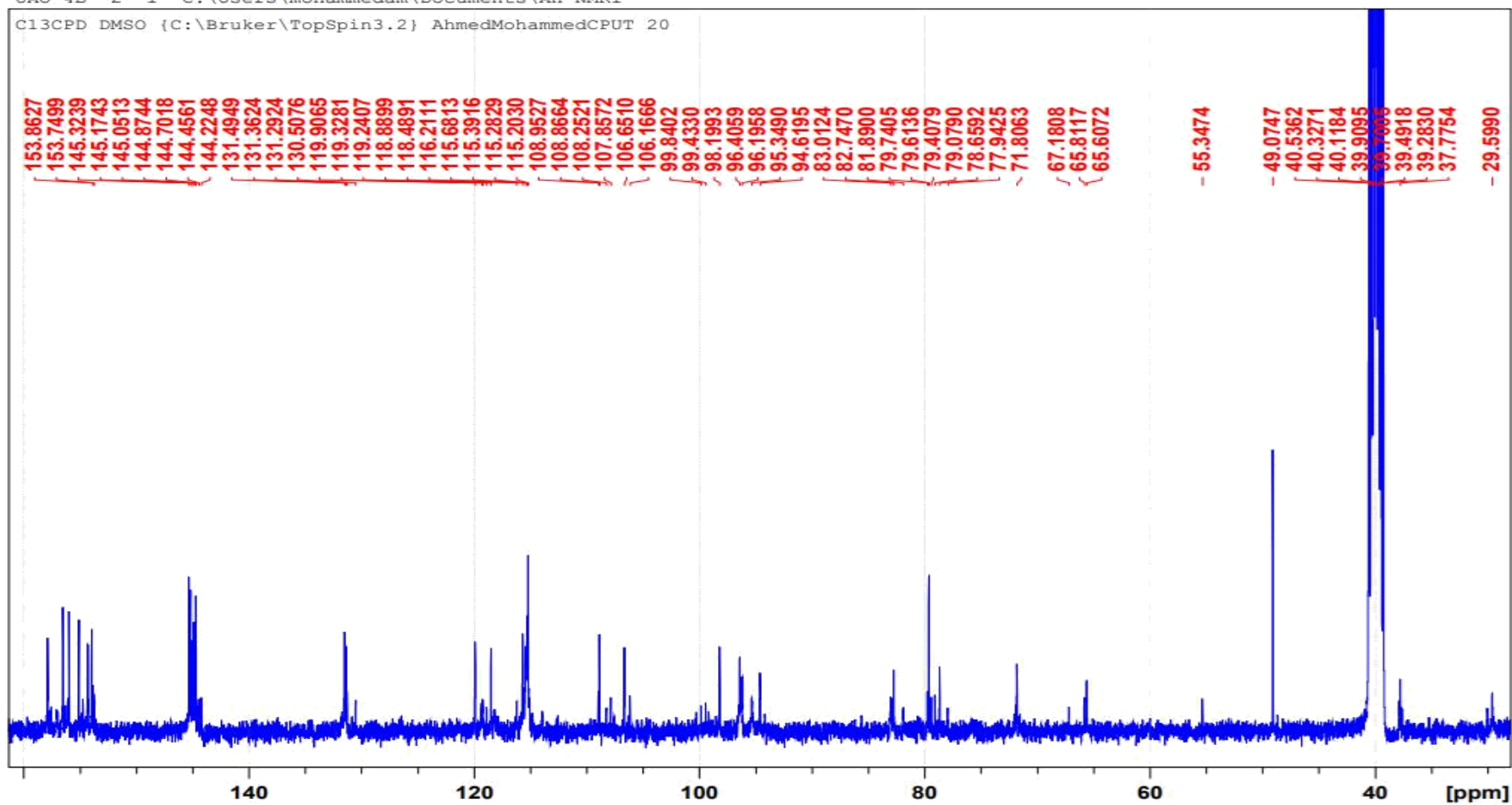


Appendix A: The proton ( $^1\text{H}$ ) Nuclear Magnetic Resonance spectra of Fraction F1

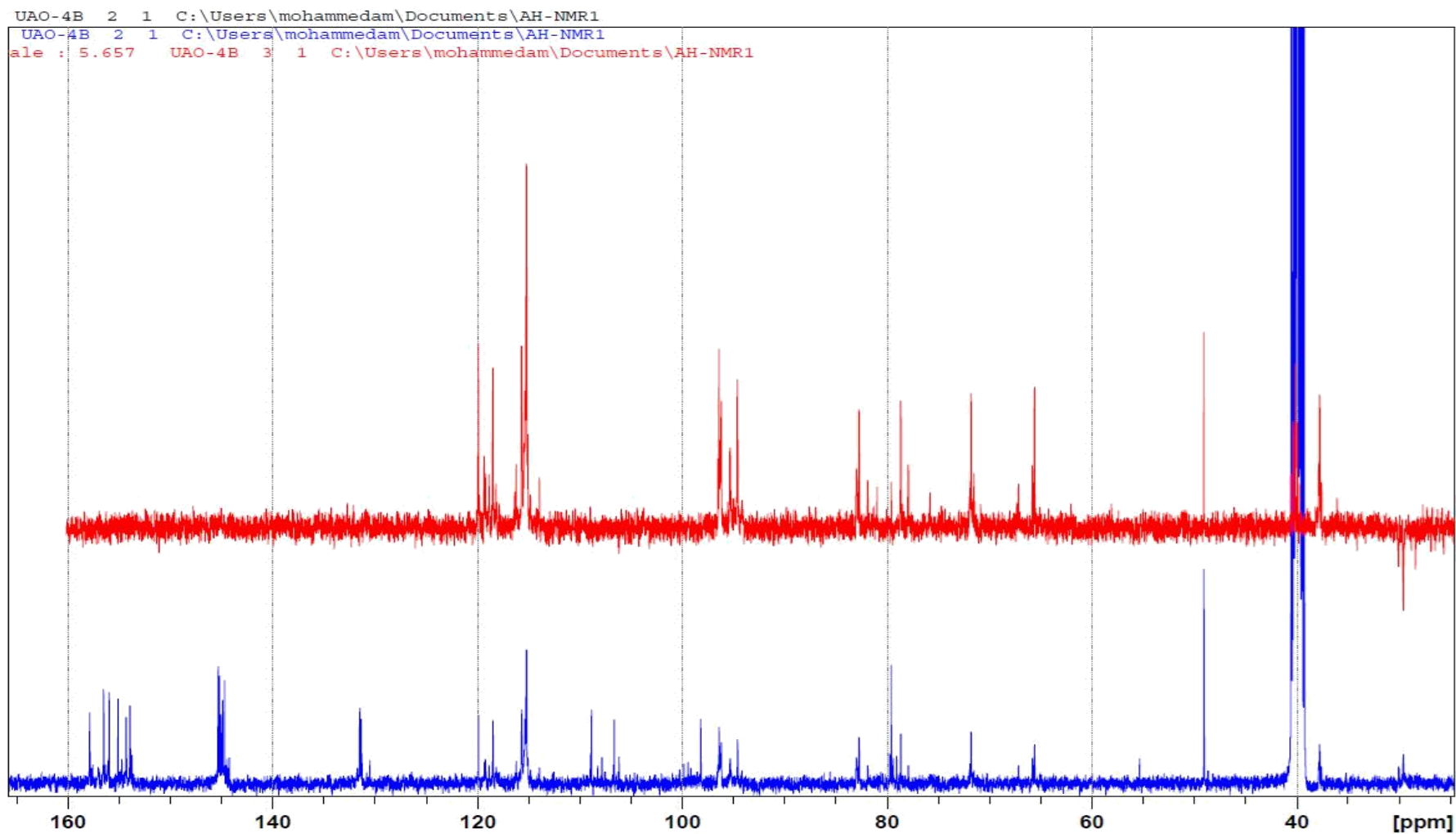


UAO-4B 2 1 C:\Users\mohammedam\Documents\AH-NMR1

C13CPD DMSO {C:\Bruker\TopSpin3.2} AhmedMohammedCPUT 20



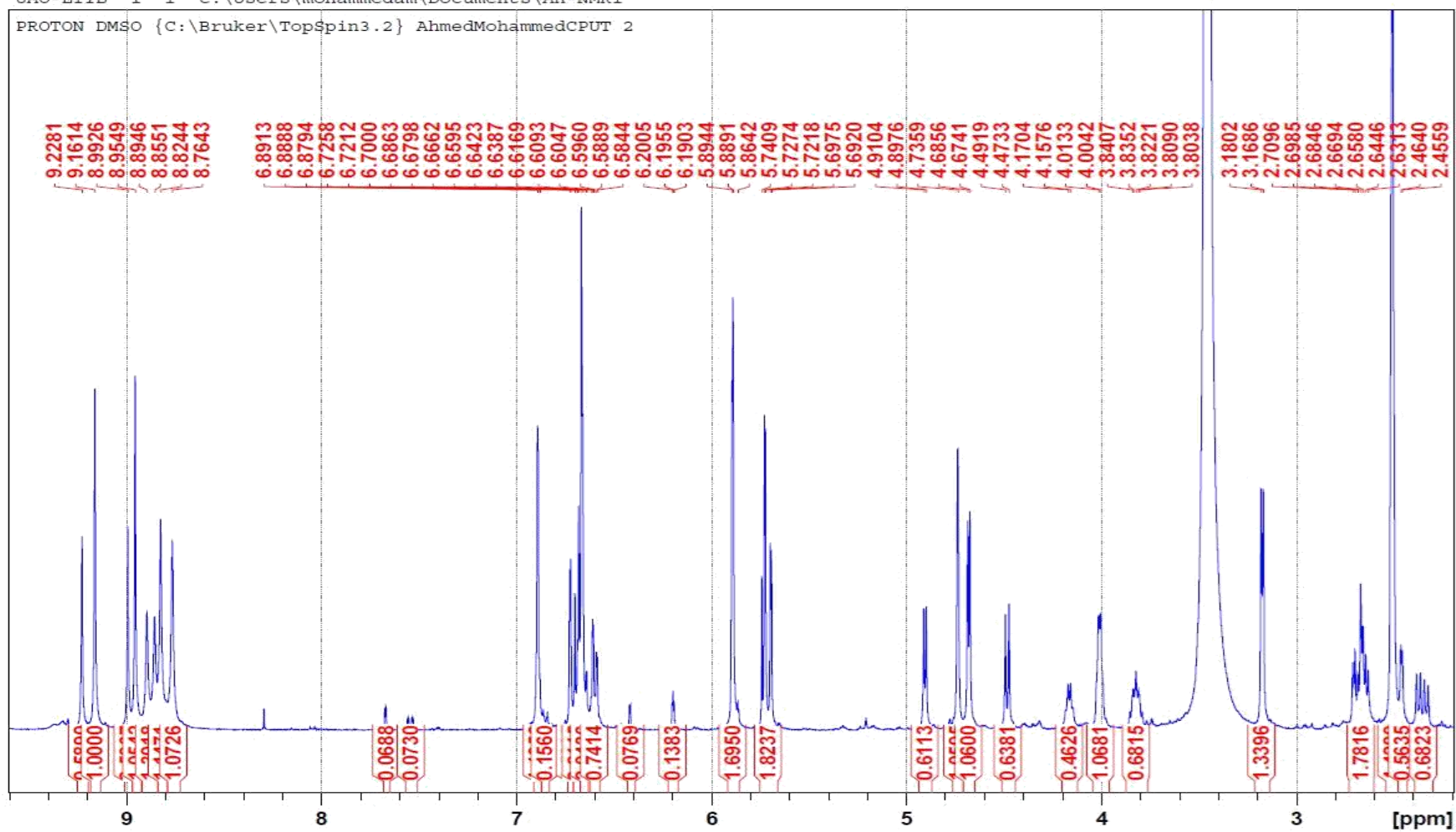
Appendix B: The carbon 13 (<sup>13</sup>C) Nuclear Magnetic Resonance spectra of Fraction F1



Appendix C: The carbon 13 (DEPT-135) Nuclear Magnetic Resonance spectra of Fraction F1

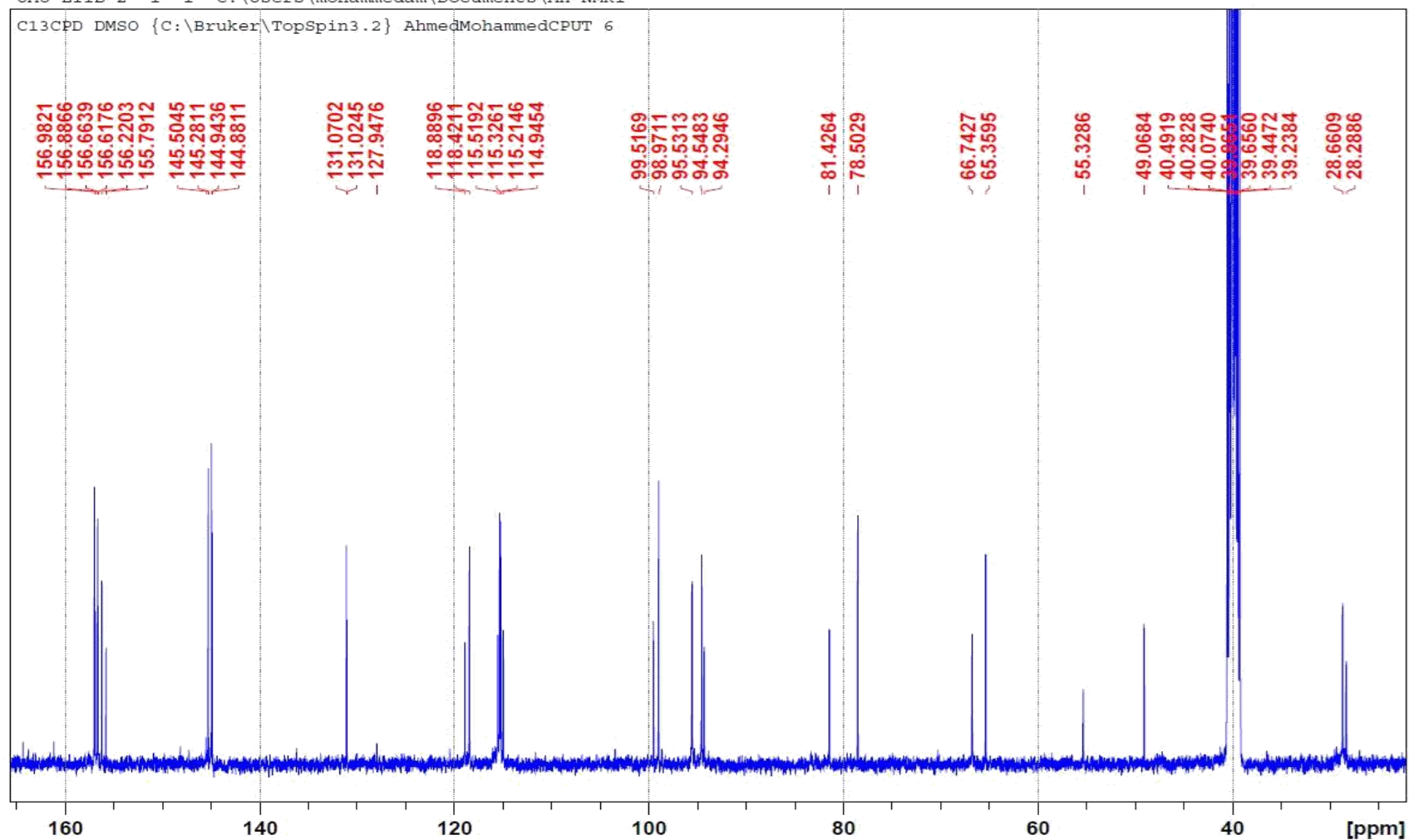
UAO-EIIB 1 1 C:\Users\mohammedam\Documents\AH-NMR1

PROTON DMSO {C:\Bruker\TopSpin3.2} AhmedMohammedCPUT 2

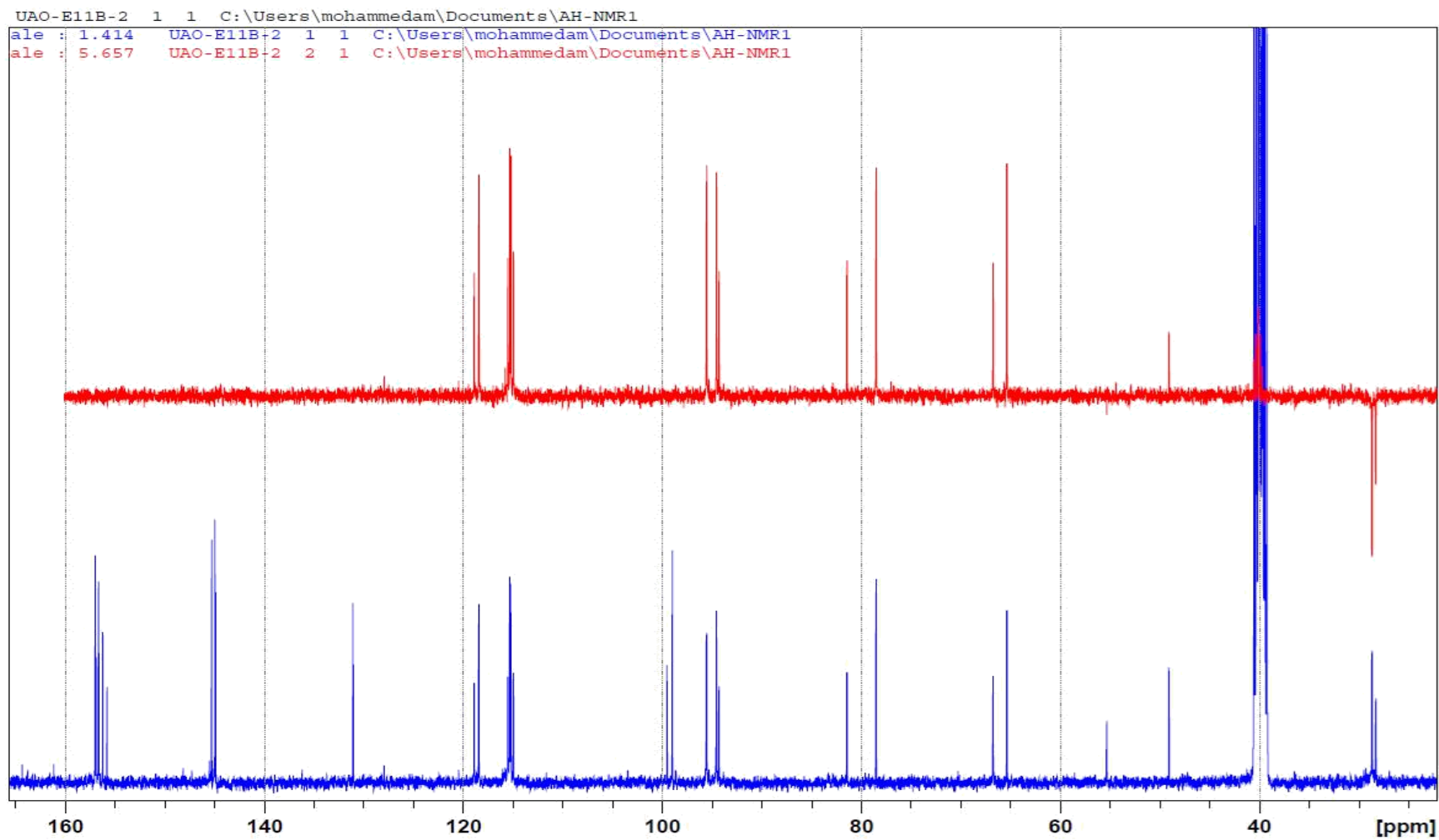


Appendix D: The proton (<sup>1</sup>H) Nuclear Magnetic Resonance spectra of Fraction F2

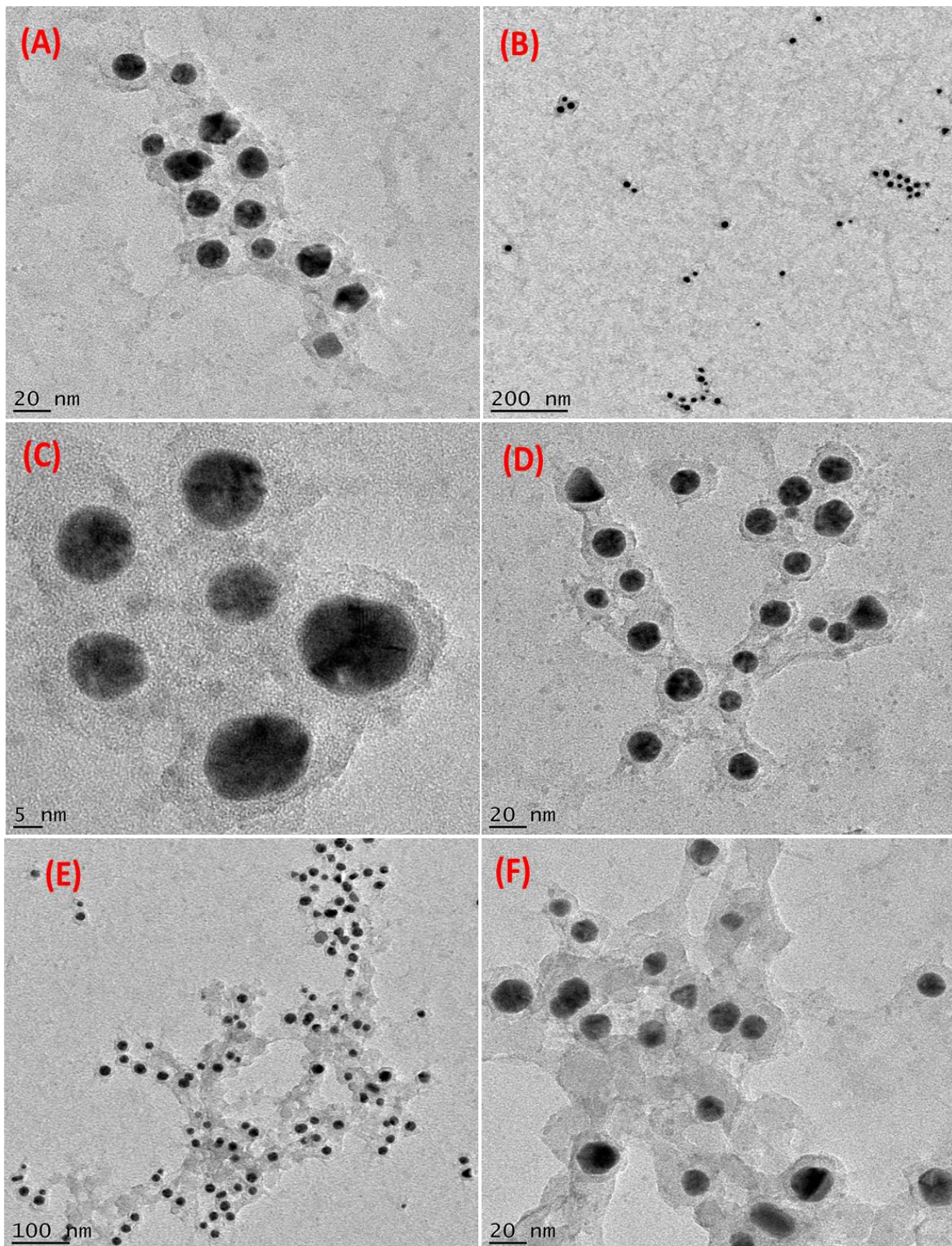
UAO-E11B-2 1 1 C:\Users\mohammedam\Documents\AH-NMR1  
C13CPD DMSO {C:\Bruker\TopSpin3.2} AhmedMohammedCPUT 6



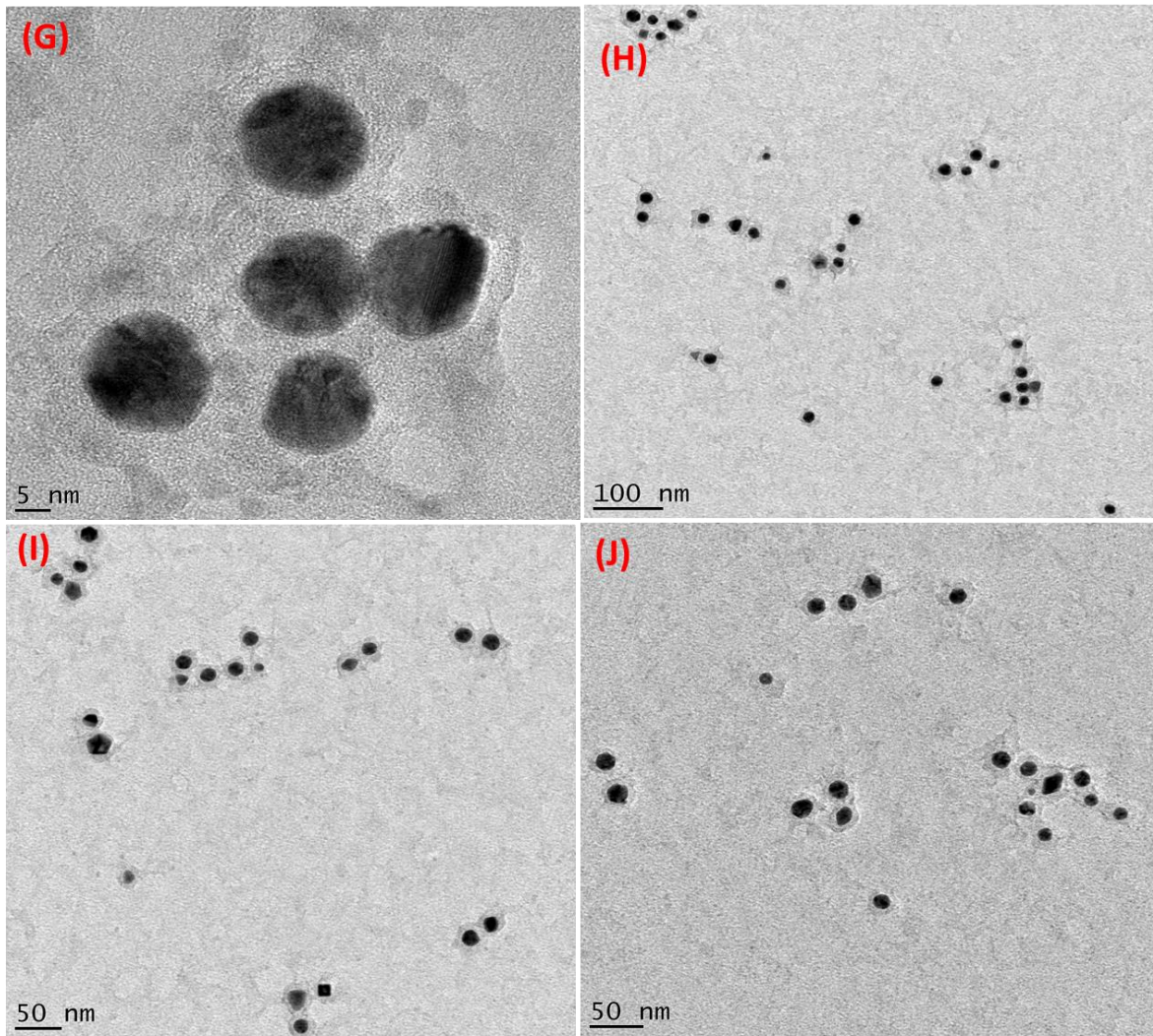
Appendix E: The carbon 13 (<sup>13</sup>C) Nuclear Magnetic Resonance spectra of Fraction F2



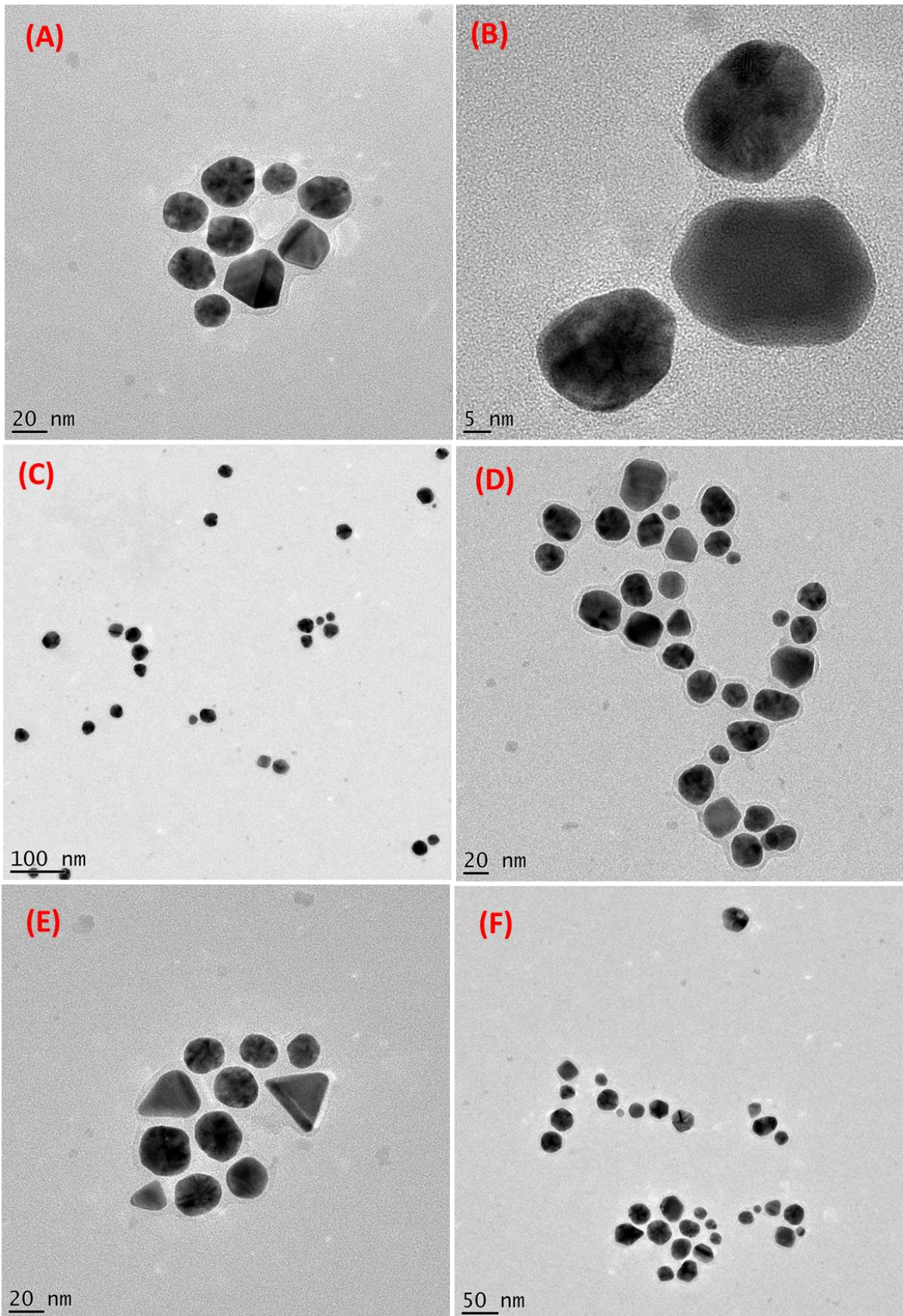
Appendix F: The carbon 13 (DEPT-135) Nuclear Magnetic Resonance spectra of Fraction F2



**Appendix G: Other HRTEM images (A-F) of the *Leucosidea sericea* total extract-mediated gold nanoparticles. The images were taken at various points on the gold coated carbon grid.**

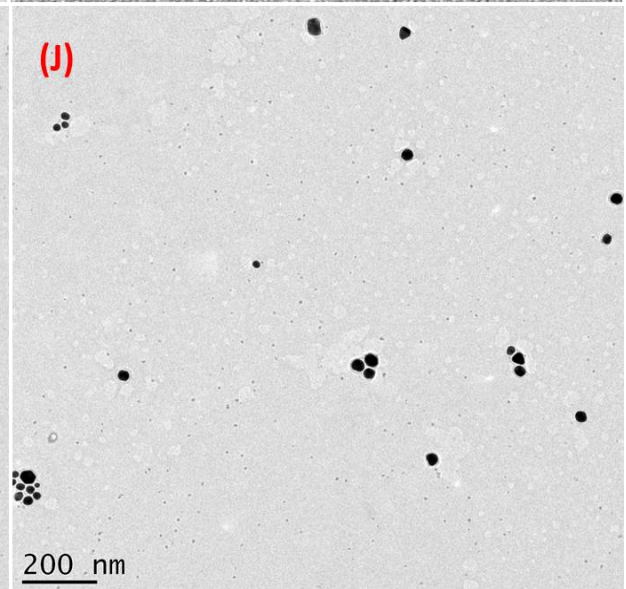
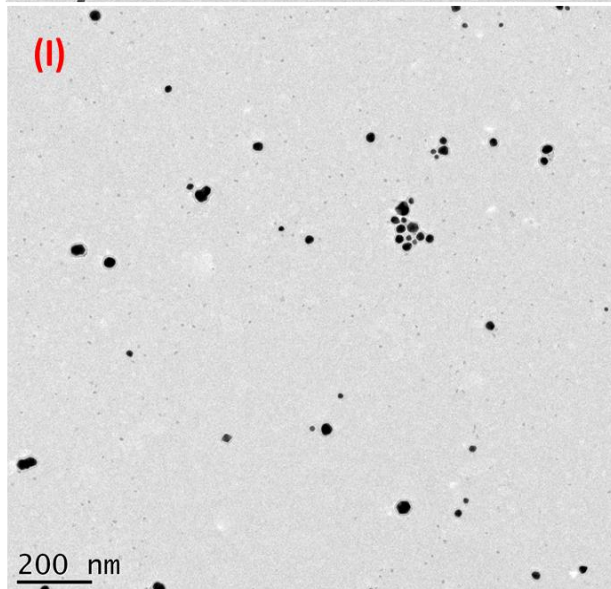
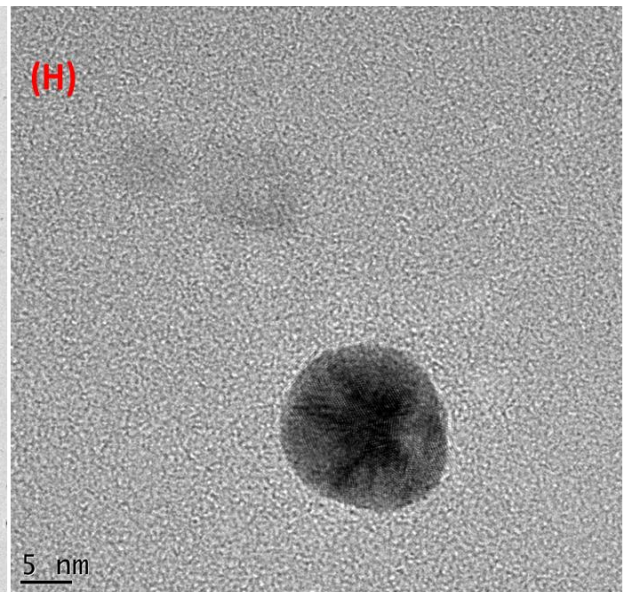
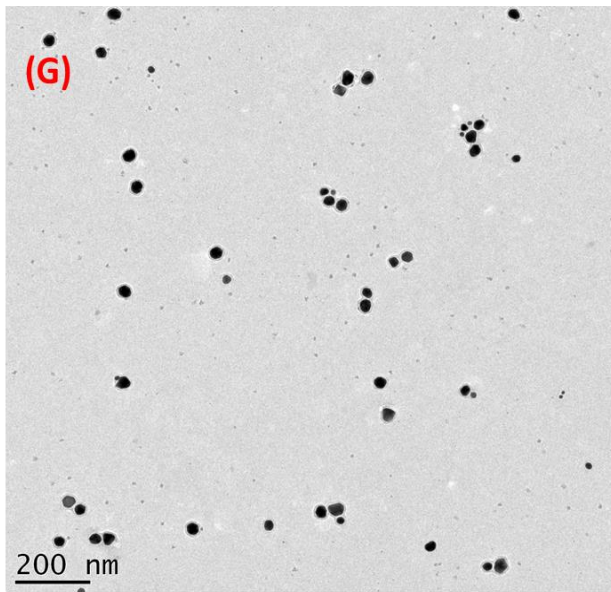


Appendix G: Continued with other HRTEM images (G-J)

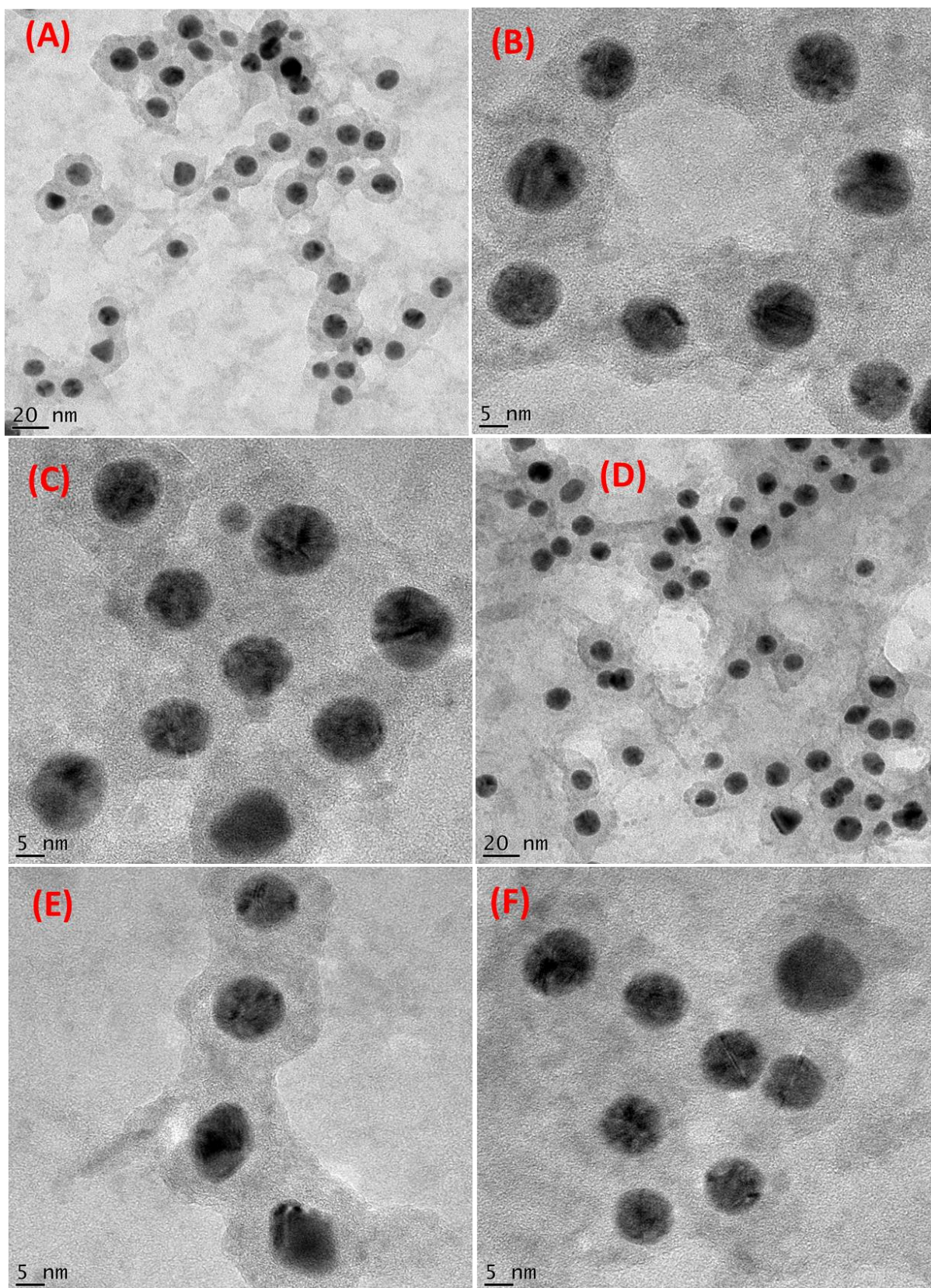


**Appendix H: Other HRTEM images (A-F) of the F1-mediated gold nanoparticles. The images were taken at various points on the gold coated carbon grid**

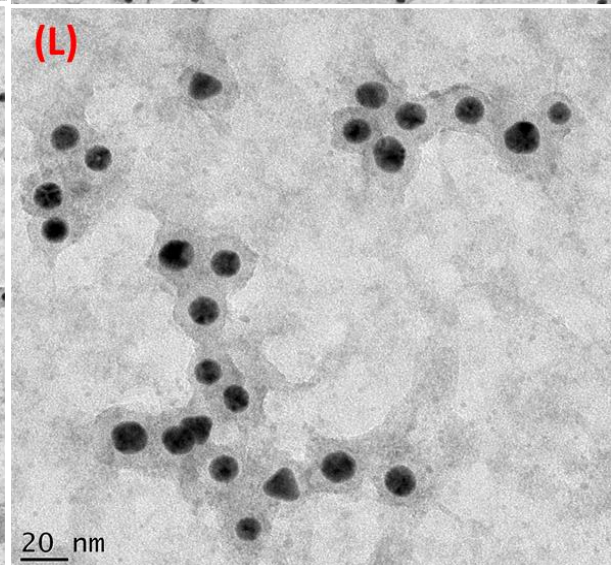
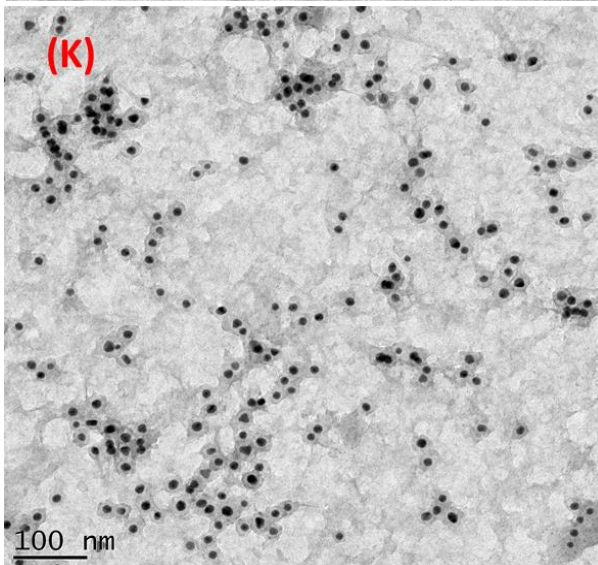
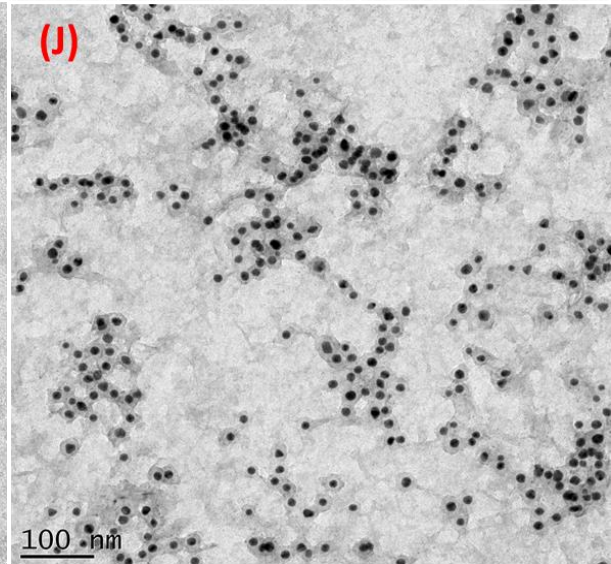
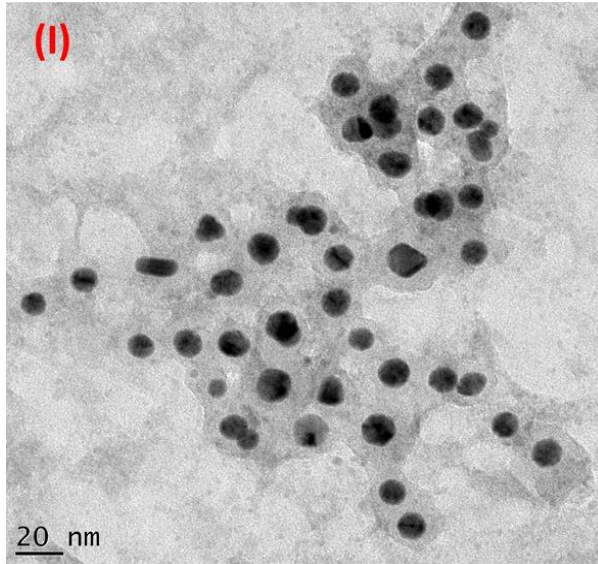
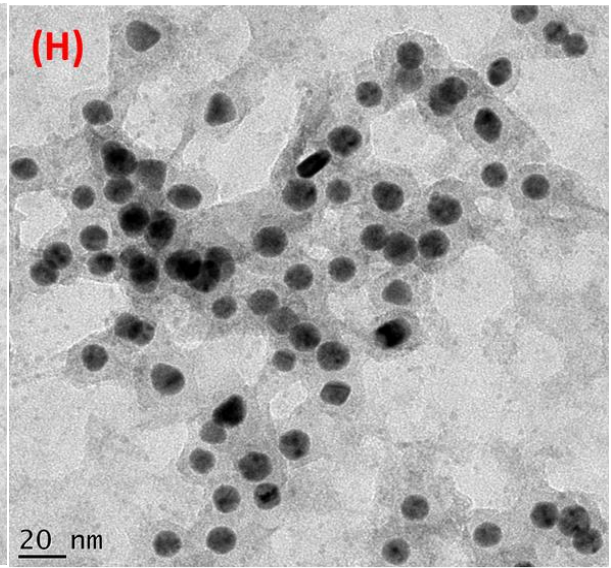
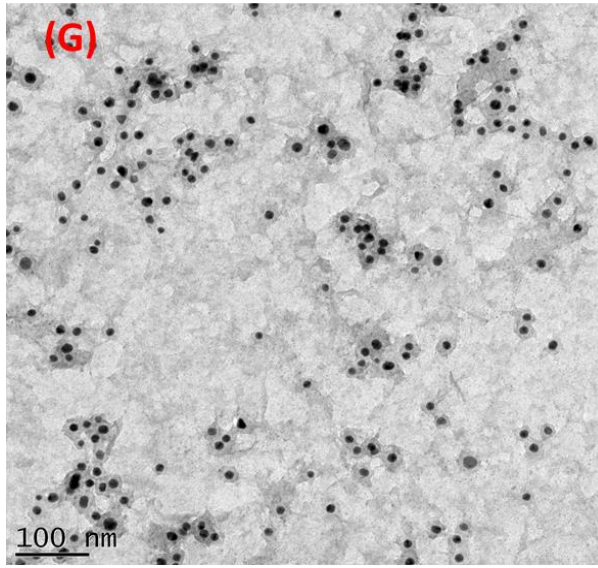




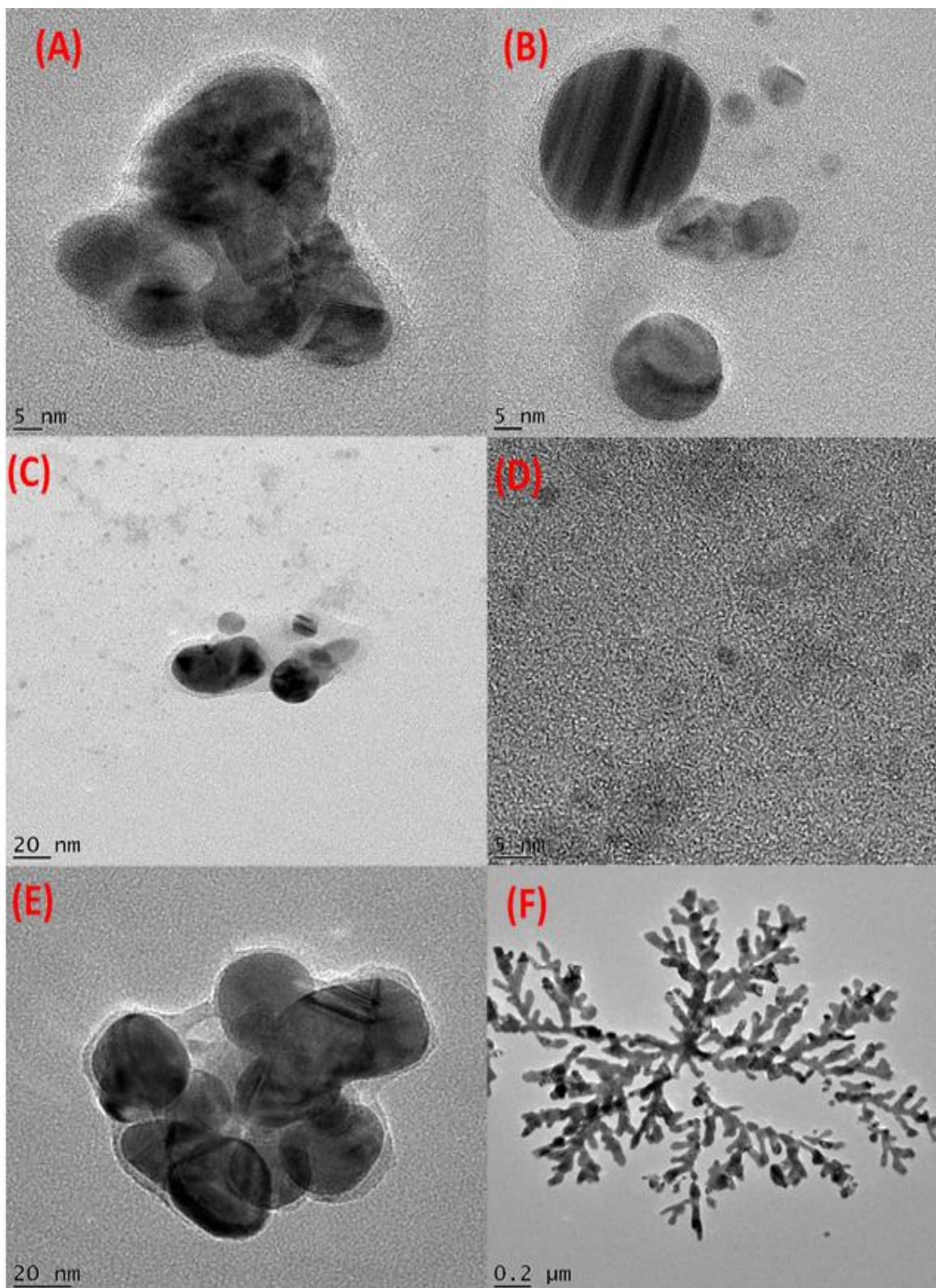
Appendix H: Continued with HRTEM images (G-J)



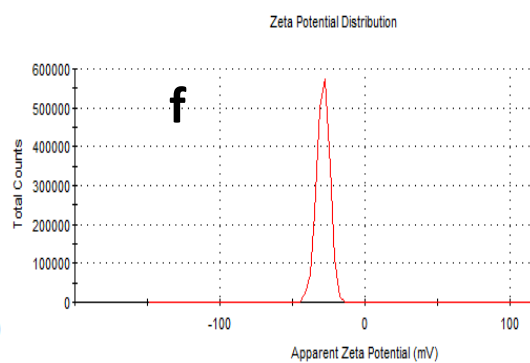
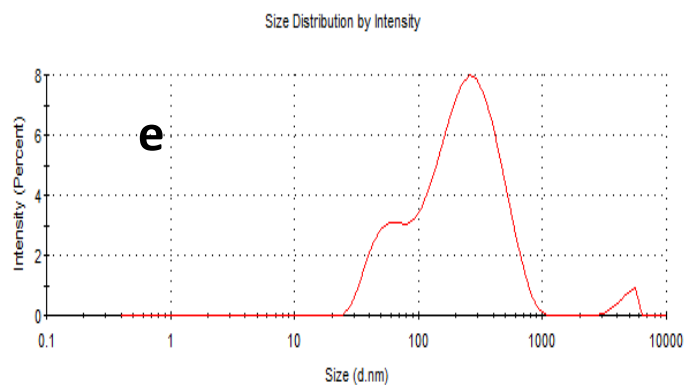
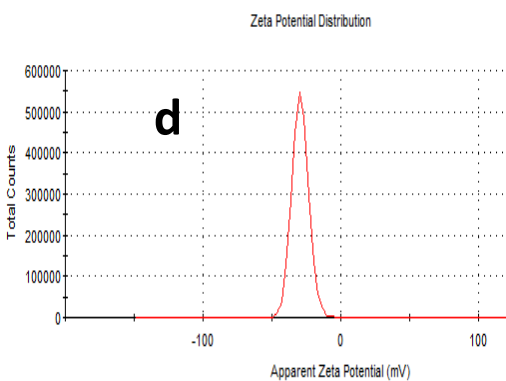
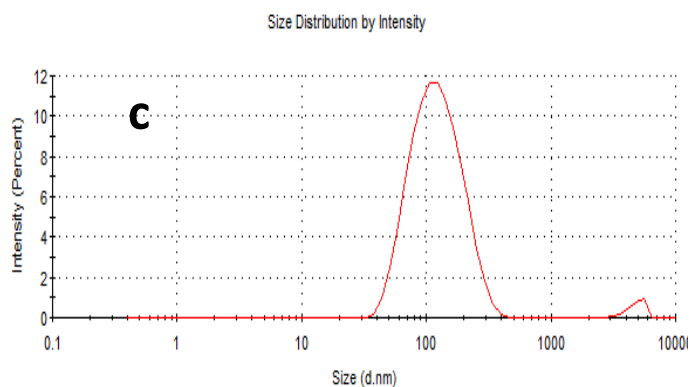
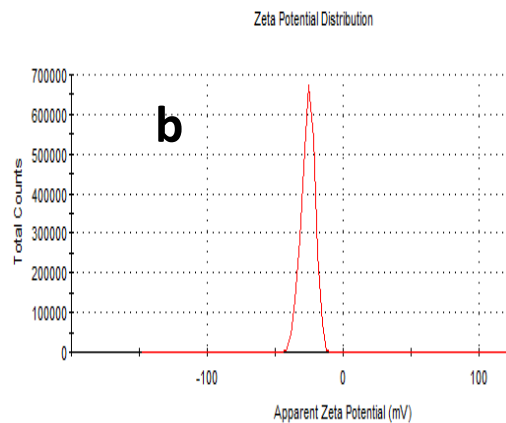
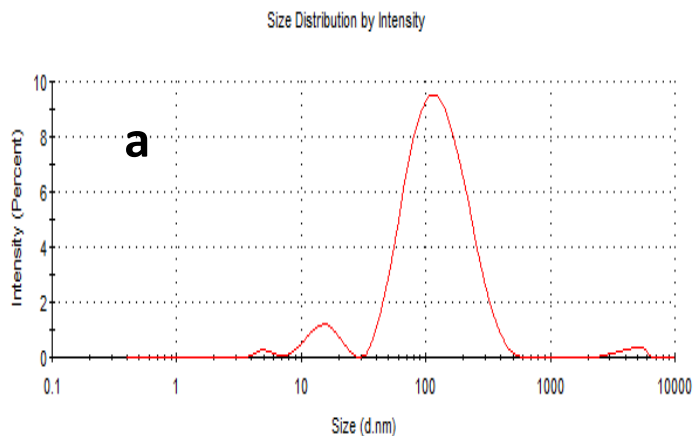
**Appendix I: Other HRTEM images (A-F) of the F2-mediated gold nanoparticles. The images were taken at various points on the gold coated carbon grid**



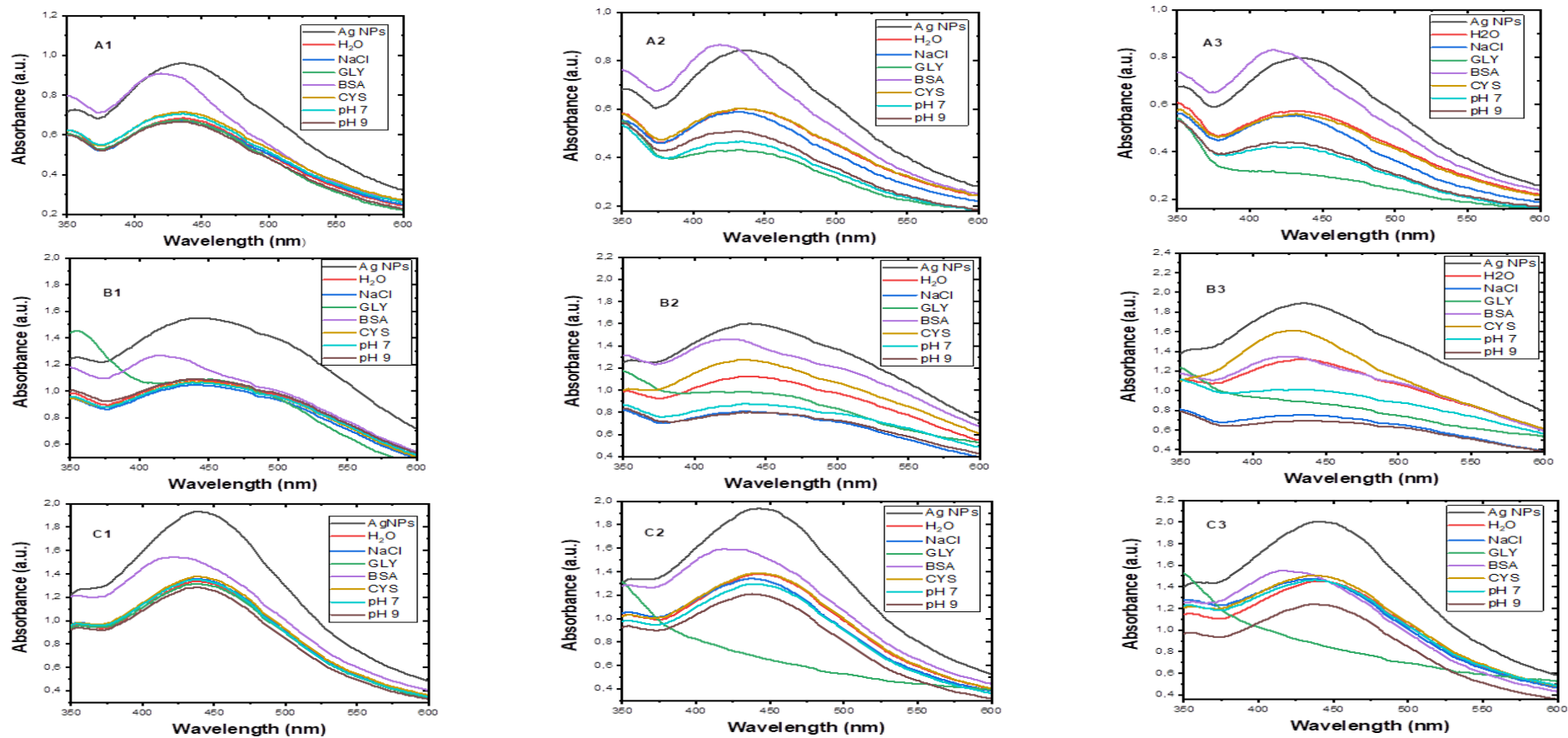
**Appendix I: Continued with other HRTEM images (G-L)**



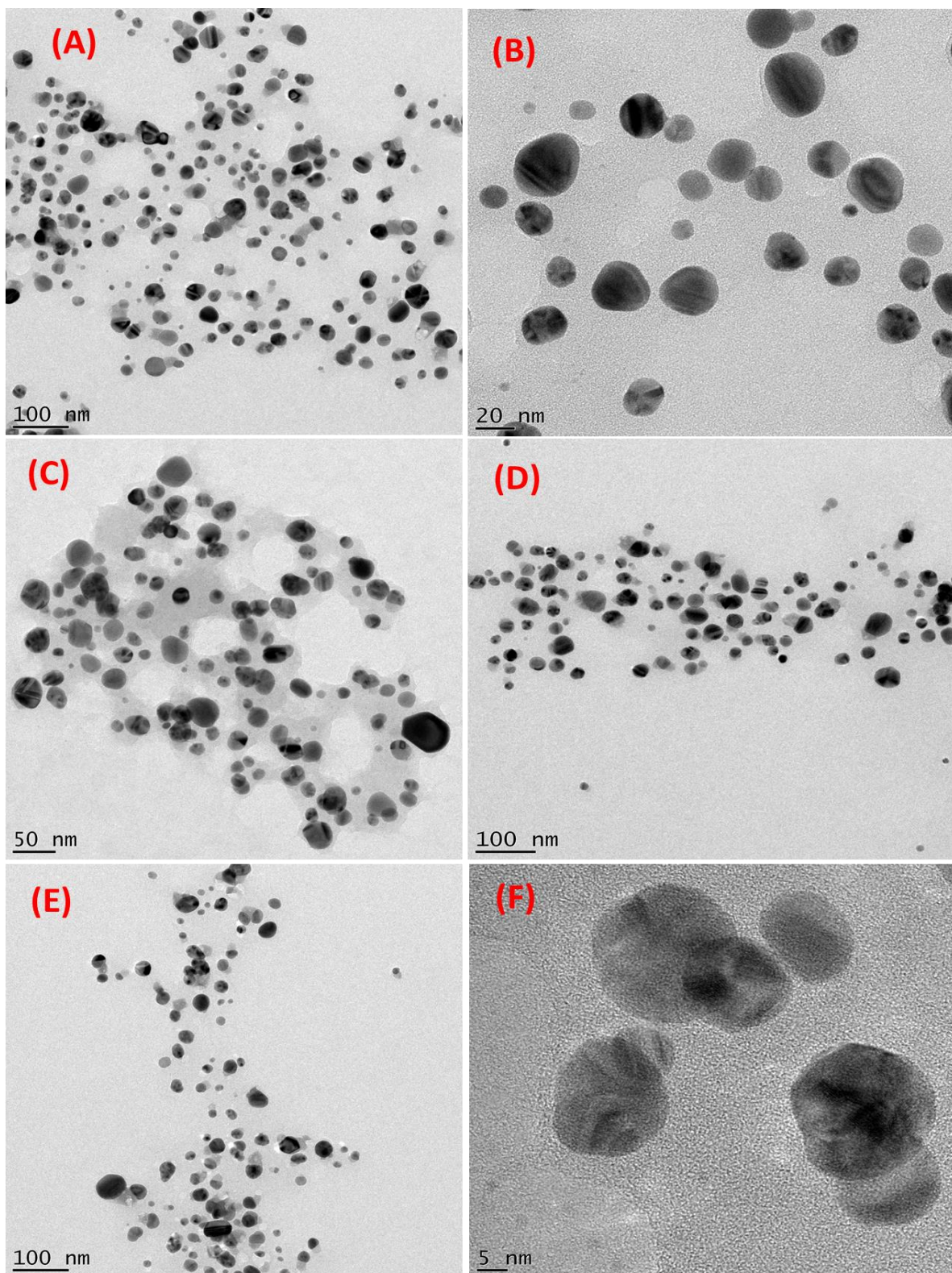
**Appendix J: Other HRTEM images (A-F) of the *Leucosidea sericea* total extract-mediated silver nanoparticles. The images were taken at various points on the silver coated carbon grid indicating agglomerates of the nanoparticles. These were taken alongside the image represented in figure 4.2 A**



**Appendix K: Hydrodynamic size of (a) F1, (c) F2-, (e) *Leucosidea sericea* total extract-mediated silver nanoparticles and zeta potential of (b) F1, (d) F2- and (f) *Leucosidea sericea* total extract-mediated silver nanoparticles as measured by Dynamic Light Scattering technique**



**Appendix L: Stability of *Leucosidea sericea* total extract-mediated silver nanoparticles for (A1) 0 h, (A2) 24 h, (A3) 48 h, F1- mediated silver nanoparticles for (B1) 0 h, (B2) 24 h and (B3) 48 h and F2- mediated silver nanoparticles for (C1) 0 h, (C2) 24 h, (C3) 48 h in different solutions and buffers**



**Appendix M: HRTEM images used in evaluating the size and shape of HHE-AgNPs. The images were taken at various points of the nanoparticles on the carbon grid**

## Appendix N: ADDENDUM

### ADDENDUM I: RESEARCH OUTPUTS

**Badeggi, Umar M.**, Enas Ismail, Adewale O. Adeloye, Subelia Botha, Jelili A. Badmus, Jeanine L. Marnewick, Christopher N. Cupido, and Ahmed A. Hussein. "Green synthesis of gold nanoparticles capped with procyanidins from *Leucosidea sericea* as potential antidiabetic and antioxidant agents." *Biomolecules* 10(3), (2020): 452.

**Badeggi, Umar M.**, Jelili A. Badmus, Subelia Botha, Enas Ismail, Jeanine L. Marnewick, Charlene W. J. Africa and Ahmed A. Hussein. "Biosynthesis, characterization, and biological activities of procyanidin capped silver nanoparticles" *Journal of functional biomaterials* 11(66), 2020.

**Badeggi, Umar M.**, Subelia Botha, Enas Ismail and Ahmed A. Hussein. "Biofabrication, characterization and applications of *Hypoxis hemerocallidea* and hypoxoside mediated silver nanoparticles" (manuscript under submission).

**Badeggi, Umar M.**, Subelia Botha, and Ahmed A. Hussein. A review article "Uni-capped metal nanoparticles: Synthesis, mechanism and applications" (**manuscript in preparation**).

### ADDENDUM II: CONFERENCES

- The South African Chemical Institute/Royal Society of Chemistry; "Western Cape Young Chemists' Symposium" 6th April, 2018 University of Cape Town, Cape Town, South Africa. "Preliminary investigations of the role of plant extracts on the stability of gold nanoparticles" **Badeggi U. M.**, Subelia Botha, Ahmed Mohammed (Oral presentation).
- International conference on Surfaces, Coatings and Nanostructured Materials (NANOSMAT-AFRICA 2018 Western Cape), Cape Town, South Africa, 19-23 November 2018. "The role of glycosides in the green synthesis of gold nanoparticles" **Badeggi U. M.**, Subelia Botha, Ahmed Mohammed (Poster presentation).
- Enabling the commercialisation of nanotechnological innovation (NANOAFRICA, 2020). "Green synthesis, characterization and enzymatic activity of gold nanoparticles using procyanidins from *Leucosidea sericea*" **Badeggi U. M.**, Subelia Botha, Enas Ismail, Ahmed Mohammed (Abstract accepted for oral presentation).